

JOHANNES  
**GUTENBERG**  
UNIVERSITÄT  
MAINZ



**The role of Dendritic cells (DC) in  
Friend Retrovirus-induced  
immunosuppression and immunotherapeutic  
applications of functionalized nanoparticles**

**Limei Shen**

**The role of Dendritic cells in  
Friend Retrovirus-induced  
immunosuppression and tumorigenesis and  
immunotherapeutic applications of functionalized  
nanoparticles**

Doctorial Dissertation  
to achieve the degree of  
“Doktor der Naturwissenschaften”  
at the Faculty of Biology,  
Johannes Gutenberg University, Mainz

**Limei Shen**

born 28<sup>th</sup> October.1975 in Beijing.P.R.China

Mainz, 28<sup>th</sup> June 2013  
Department of Dermatology,  
University Medical Center  
Johannes Gutenberg University Mainz



***Du Jun***

***&***

***Shen Jianping***

***&***

***Yan Wang***

## **Commitment**

Herewith I confirm that the present work was composed by myself and that all used resources are mentioned in the text. Parts corresponding to other authors are marked as references. This also applies to the Figs.

## **Erklärung**

Ich erkläre, dass ich die vorgelegte Promotionsarbeit selbständig, ohne unerlaubte fremde Hilfe und nur mit den Hilfen angefertigt habe, die ich in der Thesis angegeben habe. Alle Textstellen, die wörtlich oder sinngemäß aus veröffentlichten oder nicht veröffentlichten Schriften entnommen sind, und alle Angaben, die auf mündlichen Auskünften beruhen, sind als solche kenntlich gemacht. Bei den von mir durchgeführten Untersuchungen habe ich die Grundsätze guter wissenschaftlicher Praxis eingehalten, wie sie in der Satzung der Johannes Gutenberg - Universität Mainz zur Sicherung guter wissenschaftlicher Praxis niedergelegt sind.

---

Limei Shen

Mainz, 28, June, 2013

Acknowledgements.....	7
Abbreviations.....	8
1. Summary.....	11
2. Introduction.....	14
2.1. Immune system.....	14
2.2. Biology of Dendritic cells (DC).....	15
2.2.1. DC are the most potent professional APC.....	15
2.2.2. DC subsets.....	15
2.2.3. The origin and development of DC.....	21
2.2.4. Ag and Pathogen recognizing receptor expressed by DC.....	25
2.2.5. Antigen uptake, processing and presentation of derived peptides by DC .....	30
2.2.6. Maturation of DC.....	32
2.2.7. Immune stimulation and tolerance induced by DC.....	32
2.2.8. Myeloid-derived suppressor cells (MDSC).....	33
2.3. Cellular and humoral immune responses induced by DC.....	34
2.3.1. CD4 <sup>+</sup> and CD8 <sup>+</sup> T cell response.....	34
2.3.2. DC- induced humoral immune response.....	36
2.4. DC in cancer.....	37
2.5. DC vaccination for the induction of antitumor responses.....	38
2.6. Cancer immunotherapy.....	41
2.7. Nanoparticles for delivery of cancer vaccines.....	42
2.8. Friend virus infection.....	42
2.8.1. Friend gamma retrovirus.....	42
2.8.2. Molecular mechanisms of FV-induced disease.....	43
2.8.3. Host genetic factors involved in FV infection.....	44
2.9. Asthma and Anaphylaxis.....	45

2.10. Aim of the PhD study.....	46
3. Results.....	47
3.1. Friend virus-induced alterations of myeloid DC.....	47
3.1.1. Analysis of FV-infected DC <i>ex vivo</i> and generation of FV-infected myeloid BMDC <i>in vitro</i> .....	47
3.1.2. FV infection interferes with the DC immunophenotype.....	49
3.1.3. FV infected BMDC induce reduced T cell proliferation compare to uninfected BMDC.....	52
3.1.4. FV-infected BMDC induce an altered cytokine profile in DC/T cell cocultures.....	54
3.1.5. FV-infected BMDC induce lower CD4 <sup>+</sup> T cells proliferation than uninfected BMDC <i>in vivo</i> in a genotype-independent manner.....	56
3.1.6. FV infected BMDC are weaker inducers of CD8 <sup>+</sup> T cell proliferation <i>in vivo</i> .....	58
3.1.7. FV-infected BMDC display an altered proteome profile.....	60
3.1.8. FV-infected BMDC of either genotype show an increased endocytotic capability.....	60
3.1.9. FV-infected BMDC are characterized by a higher content of F-actin in a mouse strain-specific manner.....	62
3.1.10. S100A9 expression is upregulated in FV-infected BMDC in a genotype-dependent manner.....	64
3.1.11. S100A9 may contribute to prevent cellular FV infection.....	66
3.2. Dextran-based nanoparticles induce strong antigen-specific cellular and humoral responses.....	71
3.2.1. Shape and size of OVA-containing dextran-based nanoparticles.....	71
3.2.2. OVA-containing DEX nanoparticles are engulfed by BMDC in a mannose receptor-dependent manner.....	72
3.2.3. BMDC incubated with particulate OVA induce robust antigen-specific CD4 <sup>+</sup> T cell proliferation.....	75
3.2.4. DEX-based nanovaccines induce strong CD8 <sup>+</sup> T cell activation and strong cytotoxic activity of CD8 <sup>+</sup> T cells <i>in vivo</i> .....	78

3.2.5. DEXparticles which codeliver OVA and LPS induce a Th2-biased humoral response.....	80
3.3. Ferro-magnetic solid-core nanoparticles (NP) targeting DC induce antigen-specific cellular and humoral immune responses.....	82
3.3.1. NP functionalized with a DC-targeting antibody are engulfed by BMDC .....	82
3.3.2. DC-targeting NP coated with OVA protein induce robust antigen-specific T cell proliferation <i>in vitro</i> .....	84
3.3.3. OVA-coated NP evoke stronger CD4 <sup>+</sup> T cell proliferation <i>in vivo</i> when addressing DC via DEC205.....	85
3.3.4. p(CpG) induce stronger DC activation than soluble CpG <i>in vitro</i> .....	86
3.3.5. p(CpG) induce stronger CD4 <sup>+</sup> and CD8 <sup>+</sup> T cell proliferation <i>in vivo</i> .....	87
3.3.6. Efficient <i>in vivo</i> CTL activation by vaccination with a trifunctional NP, conjugated with OVA, CpG, and anti-DEC-205.....	89
3.3.7. TrifunctionalNP inducepotent therapeutic anti-tumor immunity.....	91
3.4. Nanoparticles induce an antigen-specific humoral response.....	95
3.4.1. DEX-coated ferromagnetic NP colocalize with CD19 <sup>+</sup> B cells irrespective of their targeting moiety.....	95
3.4.2. Binding of DEX-coated ferromagnetic NP to B cells <i>in vitro</i> requires serum.....	95
3.4.3. Preincubation of DEX-coated ferromagnetic NP with heat labile serum components is necessary for B cell-specific binding.....	96
3.4.4. Serum-coated NP bind to the B cell complement receptor (CD21/CD35) .....	97
3.4.5. NP contained with CpG are engulfed by B cell <i>in vitro</i> and in a serum-independent manner.....	98
3.4.6. Functionalized NP induce an antigen-specific Th1-biased humoral response.....	100
3.4.7. Complement-dependent binding of NP to B cells is conserved between mouse and human.....	101
3.5. B cell-based immunotherapy with nanoparticles.....	102
3.5.1. Anaphylaxis model.....	102



3.5.2. Acute asthma model.....	106
4. Discussion.....	114
4.1. The impact of FV-infection on DC phenotype and functions.....	114
4.1.1. Alterations of the phenotype of BMDC induced by FV infection occur both in a genotype-dependent and -independent manner.....	114
4.1.2. FV infected BMDC induce alteration of T cell response in genotype independent manner.....	116
4.1.3. FV-induced alterations in protein expression in DC in genotype dependent manner.....	118
4.2. Dextran nanoparticles.....	122
4.3. Solid core nanoparticles induce an effective antitumor response.....	126
4.4. Fe-NP that co-deliver antigen and a TLR9 ligand induce a potent humoral response.....	130
4.5. Scavenger receptor mediated nanoparticle uptake.....	133
5. Materials and Equipments.....	135
5.1. Expendable materials.....	135
5.2. Buffers and Solution.....	136
5.2.1. Cell Culture Medium for Mouse Experiment.....	136
5.2.2 Cell Culture Medium for Human PBMC Experiments.....	136
5.2.3. Buffers.....	137
5.2.4. Reagents and chemicals.....	137
5.3. Antibodies.....	139
5.4. Friend retrovirus.....	140
5.5. Cell culture.....	140
5.6. B16-OVA melanoma cell line.....	140
5.7. Animals.....	141
5.8. Electronic Equipments.....	142
6. Experimental procedures.....	143
6.1 Cell biology methods.....	143

6.1.1 Generation of murine bone marrow-derived dendritic cells.....	143
6.1.2 Isolation of human PBMCs from whole blood.....	143
6.1.3. Detection of Friend virus infected murine BMDC.....	143
6.1.4. DC isolation from the spleen.....	144
6.1.5. Endocytosis Assay <i>in vitro</i> .....	145
6.1.6. BMDC migration within 3D collagen Gels.....	145
6.1.7. Isolation and proliferation of T-lymphocytes.....	146
6.1.8. <i>In vivo</i> killing assay.....	147
6.1.9. Isolation of B-lymphocytes.....	148
6.1.10. Cytospins.....	148
6.1.11. Laser Scanning Microscopy (LSM).....	148
6.2. Immunological methods.....	149
6.2.1. Magnetic cell sorting (MACS).....	149
6.2.2. Fluorescence Activated Cell Sorting (FACS).....	149
6.2.3. Cytokine measurement.....	150
6.2.4. Bicinchoninic Acid (BCA) Protein Assay.....	151
6.3. Nanoparticle Experiments.....	151
6.3.1. Preparation of dextran nanospheres.....	151
6.3.2. Iron oxide solid core nanoparticle.....	152
6.3.4. BMDC viability.....	152
6.3.5. Cellular uptake of Nanoparticles by BMDC <i>in vitro</i> .....	153
6.4. Tumor therapeutic models (Melanoma model).....	153
6.5. Anaphylaxis model.....	154
6.6. Acute Asthma model.....	154
6.6.1. Invasive measurement of AHR to MCh in mice.....	155
6.6.2. Serum collection and detection of OVA specific IgE.....	156
6.6.3. Bronchoalveolar lavage (BAL).....	156

6.6.4. Lung histology.....	156
6.7. Statistical analysis and software.....	157
7. Reference.....	158

## Acknowledgements

As another beautiful summer is coming, I have finished my final words for my PhD thesis. I would like to express my gratitude to all those who have given me the possibility to complete this thesis.

First of all, I am deeply indebted to my supervisor Prof. Dr. S. Grabbe whose help, stimulating suggestions and encouragement helped me all of the time, both during my studies and while writing this thesis. Prof. Dr. Stephan Grabbe, thank you so much for giving me the chance to begin my PhD work in your lab and working on these interesting topics. I want to say thanks to Dr. Bros, thank you for your help and all the advice you have given me. Without your help I could not finish my studies so smoothly. I also want to thank Prof. Dr. Markl for his willingness to co-supervise my thesis work. Thanks to Ingrid for your help during these three years. You were always there when I had a problem or when I needed help. I really learned a lot of techniques from you. With your devotion, now I can finish writing my thesis. Moreover, I am so lucky to be in a group with Steffi, Nicole, Monika, Bärbel, and Anita. I want to thank them for all their help, support, interest and valuable hints. I am so happy that I could finish my PhD thesis and at the same time got good friends like you. I really want to say thanks to everybody in the research groups of the Department of Dermatology. Thanks to all the members of the laboratory for scientific advice and friendship. Finally, I want to say thanks to my love Yan whose patient love enabled me to complete this work. You always have been supporting me silently with your love. Especially, I would like to give my special thanks to my parents, they are my biggest motivation. Without them, I could not have finished my studies in Germany.

## Abbreviations

1x	onefold
4x	fourfold
10x	tenfold
20x	twentyfold
100x	hundredfold
$\alpha$ -	anti
AB	antibody
AC	apoptotic (tumor) cells
ADCC	Antibody-dependent cell-mediated cytotoxicity
AHR	airway hyperresponsiveness
APC	antigen presenting cell
Ag	antigen
A3	APOBEC3
BMDC	bone marrow-derived dendritic cell
BSA	bovine serum albumin
CD	cluster of differentiation
CDP	Common DC precursor
CFSE	carboxylfluorescein diacetate succinimidyl ester
cDC	Conventional DC
CTL	Cytotoxic T lymphocyte
DC	dendritic cell
dLN	draining lymph node
DEX	Dextran based nanoparticle
DMEM	Dulbecco Mod's Eagle Medium
DMSO	dimethylsulfoxide

<i>et al.</i>	et alii (and others)
FACS	fluorescent activated cell sorting
FCS	fetal calf serum
FV	Friend virus
FITC	fluorescein isothiocyanate
Flt3	FMS-like tyrosine kinase 3
GM-CSF	granulocyte macrophage colony stimulating factor
h	hours
HEPES	4-(2-hydroxyethyl)-1-piperazineethanesulfonic acid
i.d.	intradermal
i.p.	intraperitoneal
i.v.	intravenous
IgE	immunoglobulin class E
IgG	immunoglobulin class G
IL	interleukin
IFN $\gamma$	interferon gamma
KO	knockout
LC	Langerhans cells
LN	lymph node
LPS	lipopolysaccharide
$\mu$ g	microgram
$\mu$ l	microliter
$\mu$ m	micrometer
M	molar
MACS	magnetic cell sorting
M-CSF	macrophage colony-stimulating factor

mAb	monoclonal antibody
MDSC	myeloid derived suppressor cell
MFI	mean fluorescence intensity
mg	milligram
MHC	major histocompatibility complex
min	minute
ml	milliliter
MR	mannose receptor
mM	millimolar
n	numbers
nm	nanometer
ng	nanogram
NP	nanoparticle
OVA	ovalbumin
o.n.	overnight
p	p-value
p.a.	per analysis
pDC	plasmacytoid DC
PBS	phosphate buffered saline
PE	phycoerythrin
PFA	paraformaldehyde
pg	pictogram
pOVA	particulate ovalbumin
qPCR	QuantitativeReal time PCR
rpm	revolutions per minute
RT	room temperature
RC system	Four-chamber resistance and compliance (RC) system

---

s.c.	subcutaneous
SEM	standard error of the mean
SIT	Antigen-specific immunootherapy
SSC	side scatter
TCR	T cell receptor
Th	T helper cell
Treg	regulatory T cell
TLR	toll like receptor
vs.	<i>versus</i>
wt	wild type



## 1. Summary

Friend murine leukemia Virus (FV) infection of immunocompetent mice is a well-established model to acquire further knowledge about viral immune suppression mechanisms, with the aim to develop therapeutics against retrovirus-induced diseases. Interestingly, BALB/c mice are infected by low doses of FV and die from FV-induced erythroleukemia, while C57/BL6 mice are infected by FV only at high viral dose, and remain persistently infected for their whole life. Due to the central role of dendritic cells (DC) in the induction of anti-viral responses, we asked for their functional role in the genotype-dependent sensitivity towards FV infection. In my PhD study I showed that bone marrow (BM)-derived DC differentiated from FV-infected BM cells obtained from FV-inoculated BALB/c (FV susceptible) and C57BL/6 (FV resistant) mice showed an increased endocytotic activity and lowered expression of MHCII and of costimulatory receptors as compared with non-infected control BMDC. FV-infected BMDC from either mouse strain were partially resistant towards stimulation-induced upregulation of MHCII and costimulators, and accordingly were poor T cell stimulators *in vitro* and *in vivo*. In addition, FV-infected BMDC displayed an altered expression profile of proinflammator cytokines and favoured Th2 polarization.

Ongoing work is focussed on elucidating the functional role of proteins identified as differentially expressed in FV-infected DC in a genotype-dependent manner, which therefore may contribute to the differential course of FV infection *in vivo* in BALB/c versus C57BL/6 mice. So far, more than 300 proteins have been identified which are differently regulated in FV-infected vs. uninfected DC from both mouse strains. One of these proteins, S100A9, was strongly upregulated specifically in BMDC derived from FV-infected C57BL/6 BM cells. S100A9<sup>-/-</sup> mice were more sensitive towards inoculation with FV than corresponding wild type (WT) mice (both C57BL/6 background), which suggests a decisive role of this factor for anti-viral defense. In addition, FV-infected S100A9<sup>-/-</sup> BMDC showed lower motility than WT DC. The future work is aimed to further elucidate the functional importance of S100A9 for DC functions.

To exploit the potential of DC for immunotherapeutic applications, in another project of this PhD study the usability of different types of functionalized

nanoparticles, based on either dextran molecules or a ferromagnetic solid core, to induce potent immune responses was assessed.

We tested nano-sized dextran (DEX) particles to serve as a DC-addressing nanocarrier platform. Non-functionalized DEX particles had no immunomodulatory effect on bone marrow (BM)-derived DC *in vitro*. However, when adsorbed with ovalbumine (OVA), DEX particles were efficiently engulfed by DC in a mannose receptor-dependent manner. A DEX-based nanovaccine containing OVA and lipopolysaccharide (LPS) as a DC stimulus induced strong OVA peptide-specific CD4<sup>+</sup> and CD8<sup>+</sup> T cell proliferation both *in vitro* and *in vivo*, as well as a robust OVA-specific humoral immune response (IgG1>IgG2a) *in vivo*. Accordingly, this nanovaccine raised a stronger induction of cytotoxic CD8<sup>+</sup> T cells than obtained upon administration of OVA and LPS in soluble form. Therefore, DEX-based nanoparticles constitute a potent, versatile and easy to prepare nanovaccine platform for immunotherapeutic approaches.

In order to enhance tumor antigen-specific immune responses by *in vivo* delivery of antigen and adjuvant specifically to DC, three issues were considered for the ferromagnetic solid core nanoparticle: Due to the inherent capability of CD8<sup>+</sup>DEC205<sup>+</sup> DC to efficiently cross-present antigens and thereby prime CD8<sup>+</sup> T cells, solid core nanoparticles (NP) were conjugated with a DEC205-specific antibody ( $\alpha$ DEC205). In addition, NP were coated with the model antigen ovalbumin (OVA), constitutively expressed by a OVA-transduced B16 melanoma subline (B16/OVA) used for subcutaneous tumor inoculation. NPs were coupled in addition with the TLR9 ligand CpG as an adjuvant to activate DC. *In vivo* studies revealed superior efficacy of this trifunctional NP formulation (NP[OVA+CpG+ $\alpha$ DEC205]) to evoke antigen-specific T cell (CD4<sup>+</sup>,CD8<sup>+</sup>) proliferation, and induction of cytotoxic T lymphocyte responses, as compared with other types of NPs (NP[OVA], NP[OVA+CpG]). Accordingly, in a therapeutic B16/OVA melanoma model, only tumor-burdened mice vaccinated with trifunctional NP showed a pronounced anti-tumor response as reflected by an arrested tumor growth and significantly higher survival rate as compared with groups of mice left untreated or vaccinated with either of the other NP formulations.

Interestingly, *in vivo* these solid core NP were found to bind specifically to B cells due to opsonization with heat-labile serum components as confirmed by *in vitro*

studies. Furthermore, NP that codelivered with ovalbumin (OVA) and CpG mounted OVA-specific antibody production. Additional conjugation with aDEC205 antibody, known to enhance antigen uptake by dendritic cells (DC) and subsequent induction of T cell helper cells (see above) which provide B cell activation in an antigen-specific manner, indeed enhanced OVA-specific antibody production, with a strong Th1 bias. Therefore, the efficacy of these Fe-NP for the B cell based immunotherapy was analysed. In therapeutic OVA-based anaphylaxis model, the particles conjugated with OVA and CpG inhibited significant IgE production, and the survival in the group which immunized with p(OVA-CpG) and p(OVA-CpG-aDEC205) was increased. In a model of OVA-based acute asthma, administration of NP conjugated with OVA+CpG was effective to attenuate bronchial hyper responsiveness, and inflammation of the lung was reduced.

Taken together, Fe-NP nanoparticles constitute a well available nanoform most suitable for the induction of strong cellular and humoral immune responses, essential for the therapy of infectious diseases and supportive of anti-tumor.

## 2. Introduction

### 2.1. Immune system

Successful immunity of an organism against pathogens as well as malignant cells is based on a complex interplay between the innate and the adaptive immune system. The cells of innate immune system, among them antigen presenting cells (APC), recognize and respond to pathogens in a generic way, but do not confer immunological memory. The innate immune response acts in an antigen-unspecific manner, since cells recognize invading pathogens by conserved pattern recognition receptors (e.g., lectin receptors, Toll-like receptors [TLR], and NOD-like receptors [NLRs]).

In contrast to the innate immune response, T cells and B cells constitute the cellular part of the adaptive immune system, and use clonal receptors (T cell receptors and B cell receptors, respectively) that recognize antigens in a highly specific manner. The combined activity of the innate and adaptive immune system is required for the development of protective immune responses.

The innate immune response serves as an initial defense against pathogens by providing a local and immediate response. Moreover, APC which engulf and process pathogen-derived antigen are required to initiate antigen-specific, B and T cell-based adaptive immune responses. For most types of pathogens, adaptive immune responses are required for complete pathogen clearance and the generation of immunologic memory. APCs, which consist of macrophages, B cells and dendritic cells (DC), are central to this system. After four decades of research, it is now generally acknowledged that DC provide an essential link between the innate and adaptive immune response due to their potency to act as sensors for pathogen invasion and tissue damage, as well as their potential to induce primary antigen-specific immune responses (Mercedes *et al.*,2011).

## **2.2. Biology of Dendritic cells (DC)**

### **2.2.1. DC are the most potent professional APC**

DC are bone marrow-derived cells that are seeded in all tissues (Banchereau and Steinman 1998). They capture endogenous antigens or pathogens and transmit the gathered information to cells of the adaptive immune system (T cells and B cells). DC initiate an immune response by presenting captured antigens, which after their processing are complexed with major histocompatibility complex (MHC) molecules, to be presented to T cells in lymphoid tissues. As compared with the other professional APC populations, such as macrophages and B cells, DC are very efficient APC and are considered to constitute the only APC population that is able to activate naive antigen-specific T cells. In contrast, the main purpose for antigen presentation of B cells to T cells is to receive help from preactivated T helper cells to initiate antibody secretion. The primary function of macrophages is to clear tissues from cellular debris and invading pathogens. Although they are poorly able to prime naïve T cells, B cells and macrophages are efficient to induce secondary immune responses.

### **2.2.2. DC subsets**

Since their first description in 1973 (Steinman & Cohn, 1973) as an adherent cell type with fine dendrites, DC are now considered as a heterogeneous population within the mononuclear phagocyte system (MPS) that derives from bone marrow precursors (Auffray C, 2009). Different DC subtypes have been identified, which are characterized by differential functional abilities and their distinct patterns of cell-surface molecule expression (Fig. 1; Tab 1). The four major subsets of DC are conventional DC (cDC, also known as myeloid DC), found in the steady state, plasmacytoid DC (pDC), monocyte-derived DC, which are induced in the response to inflammation (Heath WR, 2009), and Langerhans cells (LCs).

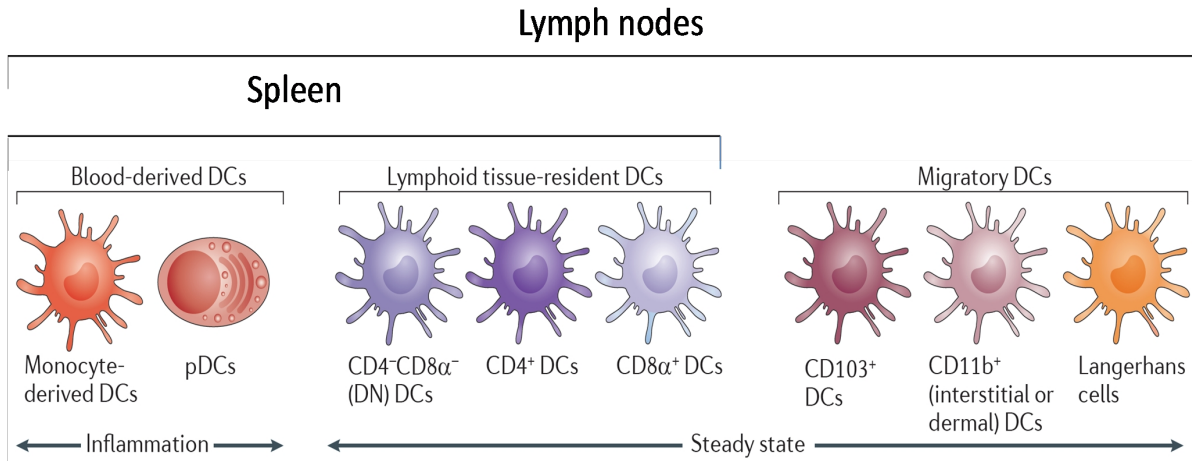


**Fig. 1: Overview of DC subsets.** The figure shows key surface phenotype markers of different DC subsets, which are delineated on the basis of their localization in secondary lymphoid tissues. Inflammatory monocyte-derived DC are rapidly recruited to sites of inflammation, whereas other DC subsets are normally present in the steady state. The relationship between inflammatory and steady-state DC remains an open issue. (Modified from Gabrielle T. Belz and Stephen L. Nutt NATURE REVIEWS Immunology 2013).

DC subset	DC type	CD8α	CD103	CD205	EPCAM (CD326)	CD11b	B220 or CD45R	DC-SIGN	Langerin (CD207)
CD8α <sup>+</sup> DC	Lymphoid resident DCs	+	low	+	-	+	-	-	+
CD4 <sup>+</sup> DCs	Lymphoid resident DCs	-	-	-	-	+	-	-	-
CD4-CD8-DCs	Lymphoid resident DCs	-	-	-	-	+	-	-	-
CD11b <sup>+</sup> DCs	Migratory DCs	-	+/-	+	-	+	-	-	-
CD103 <sup>+</sup> DCs	Migratory DCs	-	+	+	+/-	-/+	-	-	+
Langerhans cells	Migratory DCs	-	-	+	+	+	-	-	+
pDCs	Lymphoid resident DCs	+/-	-	-	-	-	+	+	-
Monocyte-derived DCs	Induced by inflammation	-	-	-	-	+	-	+	-

**Tab. 1: Phenotypic markers of DC subsets.**

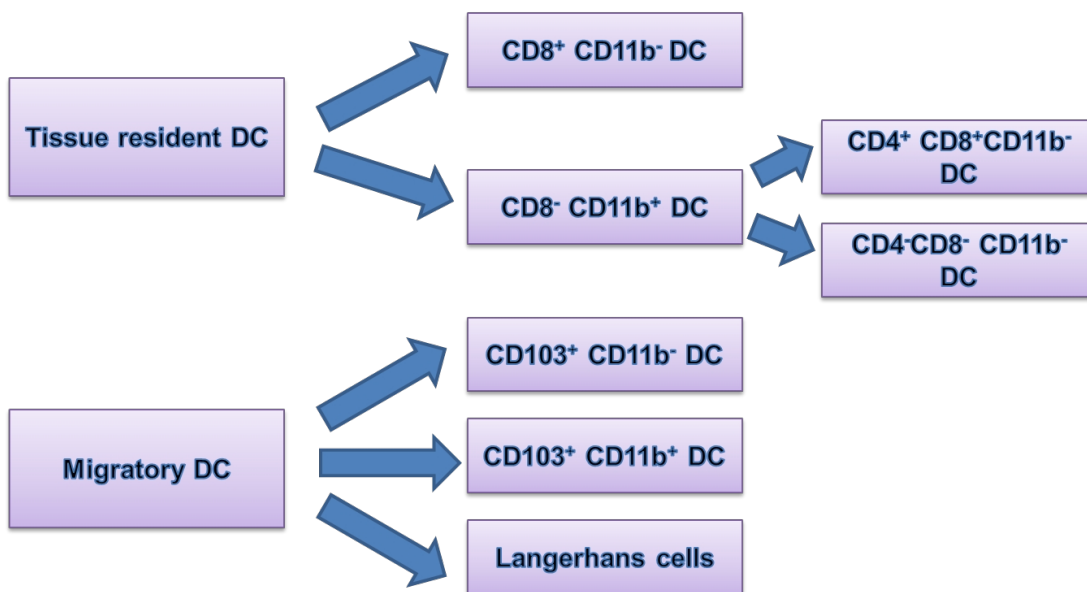
### **Conventional DC**

The mouse conventional DC population includes lymphoid organ resident DC and migratory DC (Belz GT & Nutt S, 2013). As shown in Fig. 1, all DC express the CD11c  $\beta$ 2-integrin and MHC class-II (MHC-II) molecules at varying amounts, and they are further distinguished phenotypically by their differential expression of CD8 $\alpha$ , CD4, CD11b, Langerin, and PDCA-1, as well as a growing list of other markers (Belz & Nutt, 2013). Tissue resident DC and migratory DC populations can be further divided into several subsets on the based of their phenotype (Tab. 2).

CD8<sup>+</sup>CD11b<sup>+</sup> and CD8<sup>-</sup>CD11b<sup>+</sup> DC are the two main types of resident DC, which are found in the spleen, lymph nodes and thymus (see Tab. 2). CD8<sup>+</sup> DC were shown to be more efficient in cross-presentation (see chapter 2.2.5) than CD8<sup>-</sup> DC in the steady state (Joffre *et al.*, 2012) and accordingly play a major role in priming cytotoxic CD8<sup>+</sup> T cell responses (Allan *et al.*, 2003). CD8<sup>-</sup> DC can be further subdivided in CD4<sup>+</sup>CD8<sup>-</sup> and CD4<sup>-</sup>CD8<sup>-</sup> subsets that differ in their cytokine secretion pattern (Reis e Sousa *et al.*, 1997). The CD8<sup>+</sup> and CD8<sup>-</sup> cDC also differ in cytokine production and the presentation of antigens on MHC I molecules (Heath *et al.*, 2004). CD8<sup>+</sup> and CD8<sup>-</sup> DC populations are thought to be functionally and developmentally distinct. Lymphoid tissue resident DC are in an immature state, characterized by a high endocytotic capacity and low MHC II expression as compared with activated DC.

### **Migratory DC**

Migratory DC are found in most non-lymphoid organs and migrate to draining lymph nodes after activation (Bell *et al.*, 1999). They comprise two main subpopulations: CD103<sup>+</sup>CD11b<sup>-</sup> and CD103<sup>+</sup>CD11b<sup>+</sup>DC. These DC subsets are equivalent to lymphoid tissue CD8<sup>+</sup>DC. CD103<sup>+</sup>CD11b<sup>-</sup>DC share the same differentiation requirements as CD8<sup>+</sup>DC (see chapter 2.2.3.2). Among migratory DC, CD103<sup>+</sup>DC are the most efficient in terms of cross-presentation (Tab. 2).



**Tab. 2: Subsets of murine myeloid DC populations.** Based on Hashimoto *et al.*, 2011, Liu, 2001, Ueno *et al.*, 2007, Geissmann *et al.*, 2010)

### **Langerhans Cells (LC)**

Langerhans cells are resident in the skin and are the only DC population of the epidermis. LC constitute the first immunological barrier against pathogens and external stress. This DC population is derived from a local LY6C<sup>+</sup> myelomonocytic precursor cell population in the skin (Ginhoux and Merad *et al.*, 2007). LCs are equipped to capture antigens present in the skin and migrate to the draining lymph node both in steady-state and inflammatory conditions (Kripke *et al.*, 1990) After activation, LCs increase their expression of major histocompatibility complex (MHC) class II and costimulatory molecules and migrate to the T cell areas of draining lymph nodes where they secrete different chemokines and interact with antigen-specific T cells (Kripke *et al.*, 1990).

### **Plasmacytoid DC (pDC)**

Another recognized member of DC family is the plasmacytoid DC (pDC), which is different enough from the rest of the DC to be included in a subgroup of its own, distinct from the other subtypes of “conventional DC”. pDC differ from mDC in that they are relatively long-lived and a proportion of them carries characteristic immunoglobulin rearrangements (Corcorlan *et al.*, 2003). pDC are primarily found



in blood and lymphoid organs such as the thymus, bone marrow, spleen and lymph nodes. pDC are the principal producers of type I interferons (IFNs) in response to microbial and viral infection, with the ability to produce up to 1,000-fold more type I IFNs in response to viral infections than any other cell type (Colonna 2004 & McKenna, 2005). pDC express several characteristic markers, including sialic acid-binding immunoglobulin-like lectin H (SIGLEC-H) and bone marrow stromal antigen 2 (BST2) in mouse, and blood DC antigen 2 (BDCA2; also known as CLEC4C) and leukocyte immunoglobulin-like receptor, subfamily A, member 4 (LILRA4; also known as ILT7) in humans (Belz and Nutt, 2013).

Like mDC subsets, pDC may also be involved in immune responses against tumors. For example, pDC may contribute to the priming of melanoma-specific CD8<sup>+</sup> T cell responses (Colonna, 2004). Compared to mDC, pDC express different TLRs: pDC in human recognize viral components through TLR7/8 and TLR9, which leads to the secretion of large amounts of IFN. Murine pDC express TLR7 and TLR9. Unlike mDC, pDC do not express TLR2, TLR4, TLR5, or TLR3, which may explain why pDC do not respond to bacterial products such as peptidoglycans, lipopolysaccharide and flagellin, or poly(I:C), which mimics viral double-stranded RNA (Iwasaki & Medzhitov, 2004).

### ***Inflammatory DC (monocyte derived DC)***

Finally, there is an additional subset of DC, known as inflammatory DC, which differentiate from monocytes during inflammation. These DC are not present in the steady state, but appear in peripheral non-lymphoid tissues in the course of inflammation. These monocyte-derived inflammatory DC can be distinguished from steady-state splenic DC by their intermediate expression of expression of CD11c and by their high level expression of CD11b. Monocyte-derived DC express MAC3 (CD107b, LAMP2). In addition as compared with steady-state splenic cDC they lack CD4, and CD8 expression, respectively, (Naik & Shortman *et al.*, 2006), and lose the expression of LY6C as compare with monocyte and DC (Cheong *et al.*, 2010). It is currently thought that their main function is to elicit secondary immune responses at sites of acute inflammation (Cheong *et al.*, 2010). It is yet unclear whether this DC subset shares a common progenitor with

inflammatory macrophages or myeloid-derived suppressor cells (MDSC), and which cytokines or transcription factors drive their differentiation *in situ* (see chapter 2.2.3.2). GM-CSF is thought to be critical for the differentiation of inflammatory DC, but the definite evidence of the role of this cytokine remains unclear so far (Shortman and Naik, 2007).

### Human DC

In contrast to the many studies on mouse DC, there are relatively few studies on the nature of human DC. Blood is the only available source for iDC and pDC. As depicted in Fig.2, subsets of human DC in the blood can be distinguished by the differential expression of three cell surface markers: CD303 (also known as BDCA2 and CLEC4C), CD1c (BDCA1), and CD141 (BDCA3). CD303<sup>+</sup> DC are plasmacytoid DC (Palucka *et al.*, 2012). While CD1c and CD141<sup>+</sup> are cDC (Fig.2), CD141<sup>+</sup> DC share with mouse CD8<sup>+</sup> DC the high capacity to capture exogenous antigens for presentation on MHC I molecules (known as cross presentation) than CD1c DC (Haniffa *et al.*, 2012). The human skin hosts two main subsets of mDC: epidermal Langerhans cells (LCs) and dermal interstitial DC (Merad *et al.*, 2008). The dermal DC population can be subdivided into CD1a<sup>+</sup> DC and CD14<sup>+</sup> DC. LCs and CD1a<sup>+</sup> DC are known to be more efficient in cross presentation, and may prime the differentiation of CD8<sup>+</sup> T cells into CTLs, whereas CD14<sup>+</sup> DC are less efficient in that regard (Bedoui *et al.*, 2009 & Merad *et al.*, 2008 )

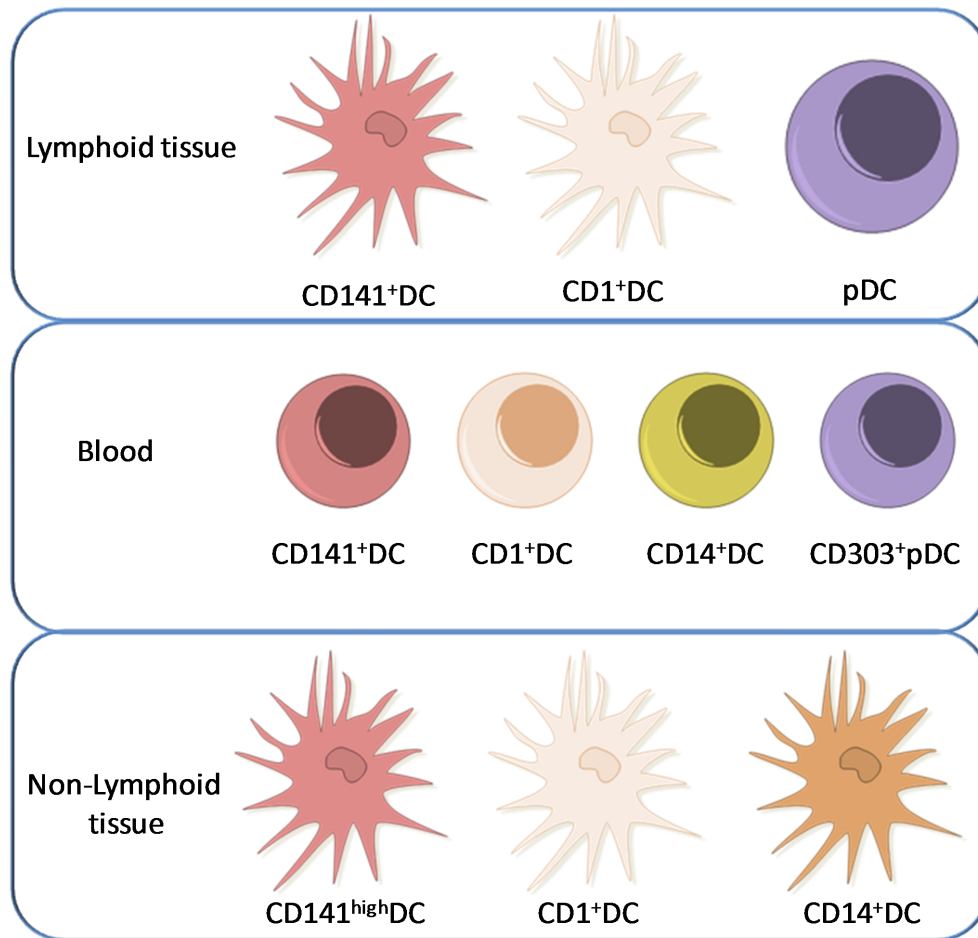


**Fig. 2: Human DC subsets.** Human tissues contain CD1c<sup>+</sup> DC, CD14<sup>+</sup> DC, CD303<sup>+</sup> DC (pDC) and a CD141<sup>hi</sup> cross-presenting DC subset. CD141<sup>hi</sup> DC migrate to draining lymph nodes after activation and probably arise from blood CD141<sup>+</sup> DCs. Human tissue CD141<sup>hi</sup> DC are homologous to mouse CD103<sup>+</sup> or CD8<sup>+</sup> DC. Human tissue CD1c<sup>+</sup> DC correspond to mouse CD4<sup>+</sup> DC (Modified from Haniffa *et al.*, 2012, Bedoui *et al.*, 2009 and Merad *et al.*, 2008).

## 2.2.3. The origin and development of DC

### 2.2.3.1 Cytokines for DC development

Many studies have shown that different precursor-cell populations and different cytokines are usable to generate DC in several culture systems. The differentiation of different DC subsets from hematopoietic progenitor cells relies on the activity of several cytokines (Fig. 3), for example most prominently, FMS-related tyrosine kinase 3 ligand (Flt3L), granulocyte/macrophage colony-stimulating factor (GM-CSF), and macrophage colony-stimulating factor (M-CSF).

A study from Onai *et al.*, (2008) indicated that activation of the Flt3 ligand (Flt3L) and signal transducer and activator of transcription 3 (STAT3, a signaling molecule downstream of FLT3) signaling pathways are key transcription factors for DC development in lymphoid organs. *In vitro*, Flt3L as a single cytokine can drive the generation of pDC and cDC from bone marrow progenitors (Naik *et al.*, 2005). Flt3 ligand deficient mice have strongly reduced pools of both CD8<sup>+</sup> and CD8<sup>-</sup> DC in spleen, lymph node and thymus (Satpathy *et al.*, 2011). Two studies from Maraskovsky and his coworkers (1996, 2000) have shown that administration of Flt3L to mice (1996) or humans (2000) results in high level generation of CD11c<sup>+</sup> MHC II<sup>+</sup> DEC205<sup>+</sup> DC. Flt3 expression is maintained in lymphoid DC, and Flt3L has been shown to control the proliferation and homeostasis of DC in lymphoid organs (Liu *et al.*, 2007), and is crucial for the development of steady-state cDC and pDC. Flt3 is also very important for the development of migratory DC, since the numbers of both pre-DC and CD103<sup>+</sup> DC were significantly reduced in a range of tissues from mice deficient for Flt3L or STAT3 as compared with the numbers in wild type mice (Waskow *et al.*, 2008).

M-CSF is the major cytokine involved in the differentiation of macrophages and monocytes. Recent studies have shown that mice lacking the M-CSF receptor are deficient in both monocytes and skin Langerhans cells (Ginhoux *et al.*, 2006). Therefore, M-CSF could be critical for the development of migratory DC. However, some studies have indicated that M-CSF is also required for the development of CD103<sup>-</sup>CD11b<sup>+</sup>DC in non-lymphoid tissues (Bogunovic *et al.*, 2009), and may compensate for cDC and pDC differentiation in cell culture in the absence of Flt3 (Fancke *et al.*, 2008).

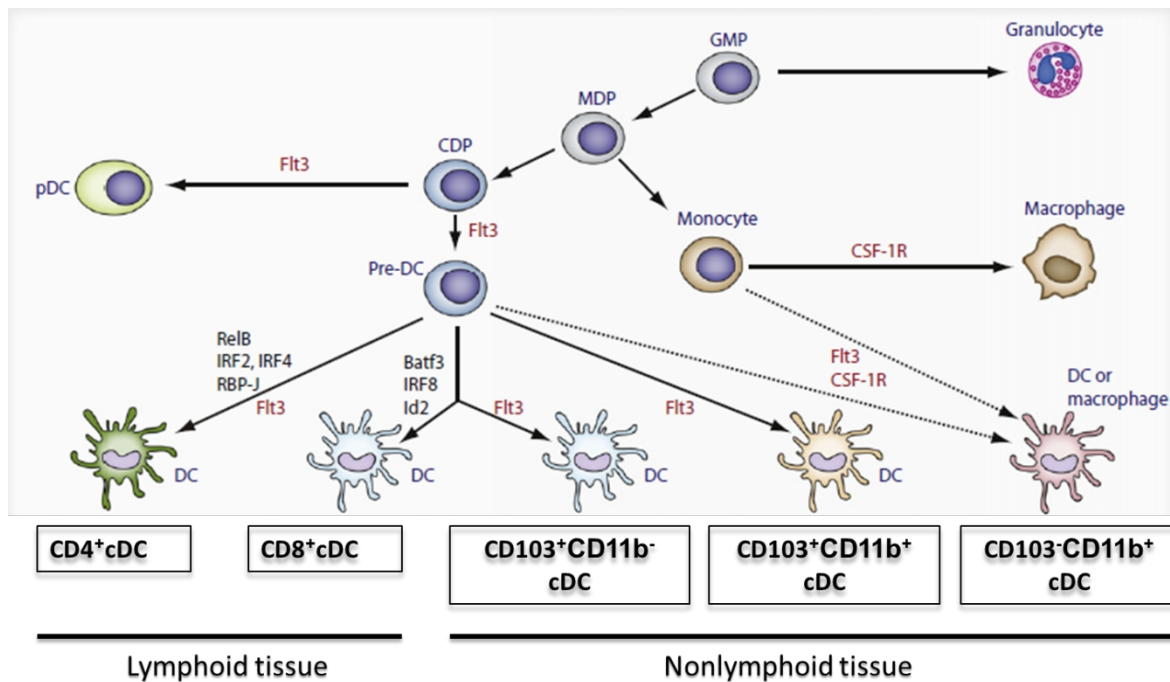
A study of Bogunovic *et al.* (2009) has demonstrated that GM-CSF is important for the differentiation of CD103<sup>+</sup>CD11b<sup>+</sup>DC in the lamina propria. Other studies have shown that the addition of GM-CSF to bone marrow culture promotes the development of cells which resemble monocyte-derived DC (Schuler & Steinman, 1985).

### 2.2.3.2. Transcription factors for DC development

In general, cell fate specification occurs through the action of transcription factors, which can be induced or inhibited by initiating extracellular cues. More recently, in several studies a number of transcription factors that control the commitment, specification, and survival of DC has been identified (Fig. 3).

Studies on interferon-regulatory factor 8 (IRF8, also known as ICSBP, [Interferon consensus sequence-binding protein]) deficient mice have shown that the development and activation of CD8 $\alpha$ <sup>+</sup>, CD103<sup>+</sup>DC and pDC relies on this transcription factor (Schiavoni *et al.*, 2002, Tsujimura *et al.*, 2003). Conversely, mice deficient in IRF4 were characterized by a selective deficiency of CD4<sup>+</sup> cDC (Suzuki *et al.*, 2004). Mice deficient in RelB, a member of the NF-kappaB family of transcription factors, showed a significant decrease in the CD4<sup>+</sup> cDC population, while CD8<sup>+</sup> cDC and pDC appeared to be unaffected (Wu *et al.*, 1998). The inhibitor of DNA protein (Id2) also contributes to the development of CD8<sup>+</sup> cDC and of LCs (Hacker *et al.*, 2003). In addition, the signaling pathways as activated by engagement of FLT3 and CSF-1(GM-CSF) receptors, and the corresponding downstream transcription factors STAT3 and STAT5, respectively, play a role in DC differentiation. The transcription factor BATF3 (also known as *Jun dimerization protein p21SNFT*) is required for many aspects of murine DC differentiation including the development of CD8 $\alpha$ <sup>+</sup> DC (Hildner *et al.*, 2008). In a study from Hildner *et al.* (2008) was observed a selective loss of CD8 $\alpha$ <sup>+</sup> cDC in spleens of *Batf3*<sup>-/-</sup> mice.

In addition, a study from Carotta (2010) and his colleague showed that the ETS-family transcription factor PU.1 is absolutely important for the generation of all cDC populations and of pDC both *in vivo* and *in vitro* (Guerriero *et al.*, 2000), and regulates the expression of the cytokine receptors Flt3, M-CSFR and GM-CSFR (Belz *et al.*, 2012).



Modified from Hashimoto et al., *Immunity* 2011

**Fig. 3: Cytokines and transcription factors involved in DC development.** The development of CD8 $\alpha$ <sup>+</sup> and CD103<sup>+</sup> DC relies on the stepwise activity of interferon-regulatory factor 8 (IRF8), inhibitor of DNA binding 2 (ID2), E4 promoter-binding protein 4 (E4BP4), and basic leucine zipper transcription factor, ATF-like 3 (BATF3), as well as on FLT3 signaling. CD11b<sup>+</sup> DC depend on a unique set of transcription factors, including RELB (one of the members of the nuclear factor (NF)- $\kappa$ B family of transcription factors), IRF2, IRF4 and Ikaros, and to some extent on the cytokines M-CSF and GM-CSF (also known as CSF-1, colony stimulating factor-1). The plasmacytoid DC (pDC) lineage requires IRF8, a low level of PU.1, and absence of ID2. The differentiation of pDC from an immature precursor requires E2-2 and Ikaros, with induced loss of E2-2 converting pDC into cells that closely resemble CD8 $\alpha$ <sup>+</sup> conventional DC. CDP, common DC progenitor; CLP, common lymphoid progenitor; CMP, common myeloid progenitor; FLT3L, FLT3 ligand; GF11, growth factor independent 1; LMPP, lymphoid-primed multipotent progenitor; MDP, macrophage and DC progenitor (Modified from Hashimoto et al., *Immunity* 2011).

### 2.2.3.3 Origin of DC

All leukocytes including DC develop from BM-derived hematopoietic stem cells. Lymphoid and myeloid lineage divergence is an early event in hematopoiesis. As we know by now, monocytes, macrophages, granulocytes and erythrocytes differentiate from a common myeloid progenitor (CMP) (Liu & Nussenzweig, 2010). CMP are thought to differentiate into macrophage and DC progenitors (MDP), which are the direct precursors of common DC progenitors (CDP). MDP and CDP reside in the bone marrow and express Flt3 and M-CSFR. CDP can differentiate

into precursors of cDC subsets and pDC, termed pre-DC (Fig. 4). Pre-cDC leave the bone marrow to arrive in blood, and secondary lymphoid organs, where they differentiate into cDC subsets. The LC population is derived from a local LY6C myelomonocytic precursor cell population in the skin (Shortman *et al.*, 1997).

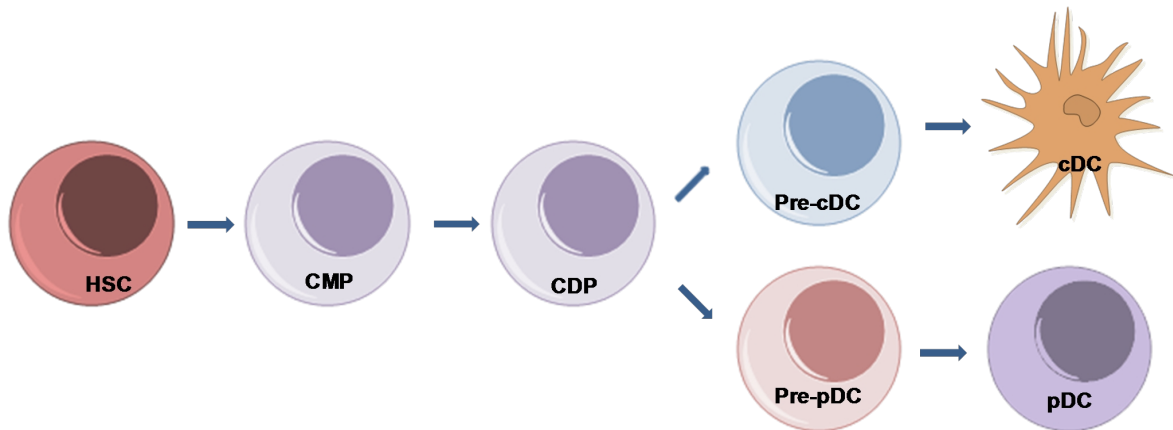


**Fig. 4: Dendritic cells development from haematopoietic stem cells.** HSC, hematopoietic stem cell; CMP, common myeloid progenitor; CDP, common DC progenitors; pre-pDC, pre-plasmacytoid DC; cDC, conventional DC; pDC, plasmacytoid DC. (Modified from Liu and Nussenzweig 2010).

#### 2.2.4. Ag and Pathogen recognizing receptor expressed by DC

As described above (chapter 2.2.2), DC encompass distinct subsets with both common and unique functions. Different subsets may mediate distinct functions in response to the encounter of pathogen-derived antigens and activation signals. All DC responses depend on the expression of surface receptors of DC and the integration of intracellular signals induced by these (Fig. 5). DC engulf antigens through phagocytosis, macropinocytosis, and receptor-mediated endocytosis via different groups of receptor families, such as Fc receptors (Fc- $\gamma$  receptors CD32 and CD64), which bind antigen/antibody complexes, integrins ( $\alpha\beta 2$ ,  $\alpha\beta 3$  or  $\alpha\beta 5$ ) that bind apoptotic cells, C-type lectin receptors (CLRs) that recognize glycoproteins, pattern recognition receptors, such like scavenger receptors which

bind microbial products (Mukhopadhyay *et al.*, 2004). Due to their relevance for the work presented here, TLRs and CLR are discussed in more detail below.

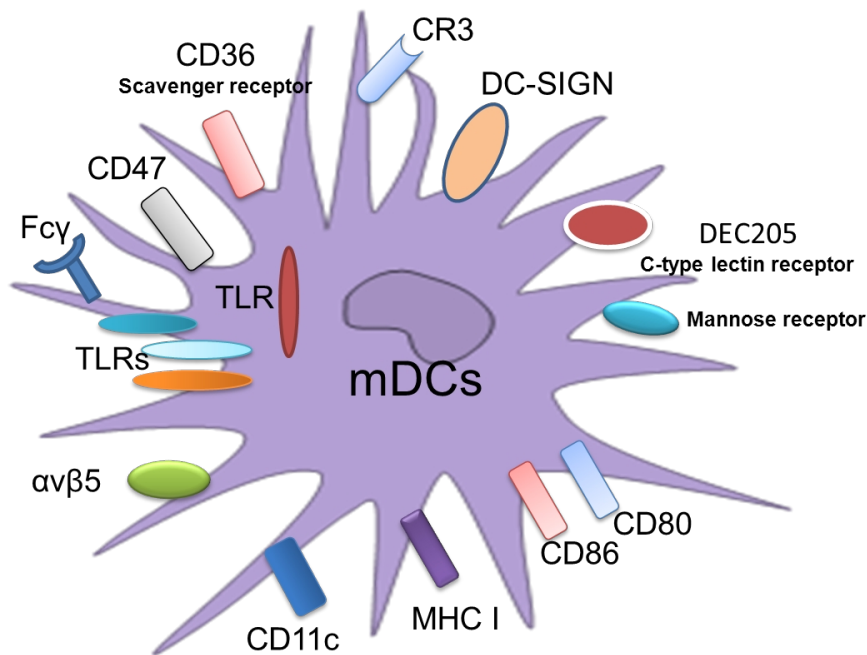


**Fig. 5: Subset of receptors expressed by DC.** DC sense their environment through both surface and intracellular receptors, which comprise several families, including cells surface CLR (e.g., DEC205, mannose receptor, DC-SIGN), surface and intracellular TLRs, scavenger receptors (e.g., CD36). Engulfment of pathogens results in the maturation and subsequently migration of DC, which is orchestrated by certain adhesion molecules like  $\alpha\beta 5$ , chemokine receptor like CCR7, MHCII, and results in enhanced expression of co-stimulatory molecules (CD80, CD86).

#### 2.2.4.1. Role of Toll-like receptors (TLRs)

TLRs are known best for their ability to recognize conserved microbial structures, termed PAMPs (pathogen-associated molecular patterns) by Janeway (Janeway, 1989). Any TLR constitutes a type I transmembrane protein with leucine-rich repeats in the extracellular domain and a cytoplasmic Toll/interleukin (IL)-1 receptor homology (TIR) domain (Takeda *et al* 2003). TLRs are expressed on the cell surface or intracellularly in endo/lysosomes (TLRs 3, 7/8, and 9), predominantly by APC of the innate immune system, for example macrophages, B cells and DC (Fig. 6). By now, 10 TLRs have been identified in human and 13 TLRs in mouse.



The recognition of PAMPs by TLRs induces the secretion of inflammatory cytokines like IL-1 $\beta$ , IL-6, and TNF- $\alpha$  by macrophages and DC (Hou *et al.*, 2008). Many studies have shown that stimulation with TLR ligands induces the maturation of DC, which thereby enhances their antigen presenting capability.

TLRs detect multiple PAMPs, including bacterial lipopolysaccharide (LPS) (detected by TLR4), lipoproteins and lipoteichoic acids (TLR2), unmethylated CpG DNA of bacteria and viruses (TLR9), double-stranded (TLR3) and single-strand viral RNA (TLR7/8). TLR2 can recognize lipoproteins by cooperation with TLR1 and TLR6. Therefore, TLR1, 2, 4, and 6 are specialized in the recognition of molecules that are unique to pathogens.

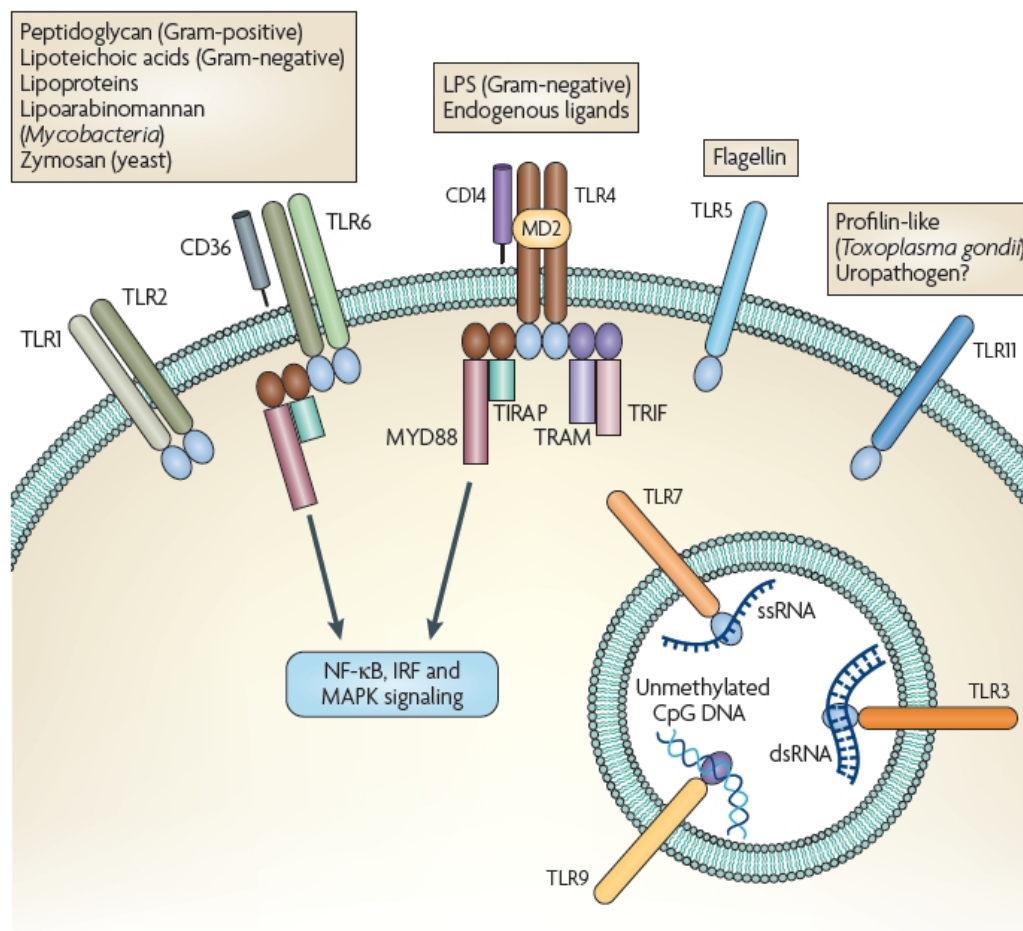
TLR7 and TLR8 are located on the X chromosome and are highly homologous. TLR7/8 recognizes single-stranded RNAs (ssRNA) or ssRNA viruses, such like influenza virus and vascular stomatitis virus (Heil *et al.*, 2004). TLR9 mediates immune responses to immunostimulatory DNA containing unmethylated CpG motifs, such as bacterial genomic DNA, and synthetic oligodeoxynucleotides (ODN). CpG ODN can induce effective production of inflammatory cytokines and T helper (Th)-1 polarizing immune responses, and are classified into three types according to their structures, sequences, and biological activities: A-type CpG are especially potent in activating NK cells and induce high amounts of IFN- $\alpha$  production by pDC (Rothenfusser *et al.*, 2004), whereas B-type CpG induce pDC maturation and potently activate B cells, but evoke only limited productions of IFN- $\alpha$  and IFN- $\beta$  (Rothenfusser *et al.*, 2004 & Krieg, 2002). Taken together, TLRs 3, 7/8, and 9 are specialized in the detection of virus and bacteria due to the recognition of pathogen-derived nucleic acids (Medzhitov, 2004).

TLRs play an important role not only for the recognition of pathogens, thereafter inducing inflammatory responses. As described above, TLRs are expressed by DC, and the activation of TLRs enhances the antigen presenting activity of DC, which initiate antigen-specific T cell responses. Naïve CD4<sup>+</sup> T cells can differentiate into T helper 1, T helper 2 cells, Th3 and Th17 helper cells. The differentiation of Th cells is controlled by DC, and different TLR ligands exert distinct effects on Th cell differentiation. For example, infection with gram-negative bacteria activates DC via LPS-mediated stimulation of TLR4, which results in the production of Th1-inducing cytokines like IL-12 (Hou *et al.*, 2008). In contrast, a study from Le Bon *et al.* (2001)

has demonstrated that DC stimulated with the TLR3 agonist Poly I:C evoked a mixed Th1/Th2 immune response. Thus, TLR signaling in DC controls in part the character of DC-induced T cell effector responses.

Interestingly, different subsets of DC express different TLRs: In mouse, all splenic DC express TLR-1, -2, -4, -6, -8, and -9. CD8<sup>+</sup> DC lack TLR5 and TLR7 expression. Some studies have shown that freshly isolated splenic DC versus *in vitro* generated DC are characterized by a differential TLR expression pattern: For example, TLR4 is expressed at very low amounts on splenic DC *in situ*. Therefore, freshly isolated mouse splenic DC do not respond to LPS stimulation (Boonstra *et al.*, 2003).

Freshly isolated human pDC express TLR7 and TLR9 only, whereas CD11c<sup>+</sup> human myeloid DC show expression of TLR-1, -2, -3, -5, -6 and -8 (Iwasaki and Medzhitov, 2004).



Seth Rakoff-Nahoum & Ruslan Medzhitov *Nature Reviews Cancer* 2009

**Fig. 6: TLRs are involved in the recognition of microbial and endogenously derived molecular patterns.** This occurs both at the plasma membrane and within intracellular compartments. After ligation of TLR ligands either directly or with the help of accessory molecules such as CD14, MD2 (also known as LY96) and CD36, TLRs dimerize and transmit signals throughout the cell by means of adaptor molecules, such as myeloid differentiation factor 88 (MYD88), and TRIF (TIR-domain-containing adapter-inducing interferon- $\beta$ ). This leads to the activation of multiple cellular signaling pathways, including NF- $\kappa$  B, MAPKs and IRFs. TLR activation regulates innate and adaptive immune responses, inflammation and tissue repair. LPS, lipopolysaccharide (from Rakoff-Nahoum & Medzhitov, *Nature Reviews Cancer* 2009).

#### 2.2.4.2. Role of C type lectin receptors (CLRs)

CLRs represent a family of calcium-dependent lectin receptors that share primary structural homologies in their carbohydrate recognition domains (Robinson, 2006). CLRs bind to self and non-self sugars. Several CLRs have been found to act as pathogen recognition receptors, and many CLR family members are expressed on myeloid cells, including cDC. Immature human monocyte-derived DC and murine DC express a panel of distinct CLRs, which are often downregulated upon maturation. The expression of CLRs on immature DC is linked to their function to capture and process antigen, and present derived peptides via MHC class I and II molecules. The mannose receptor (CD206), DEC205 (CD205), DC-SIGN (CD209), Dectin-1, 3, BDCA-2, and C-CLEC constitute important CLRs (Colonna *et al.*, 2000). LCs express Langerin (CD207) and DEC205, whereas pDC express BDCA-2 and DEC205. Many CLRs are not exclusively expressed by DC, but also by other APC like macrophages. However, some CLRs are rather DC-specific, like DC-SIGN (Steinman *et al.*, 2000), DEC205 on murine CD8<sup>+</sup> DC, Langerin by human LCs, and by a subset of dermal DC (Valladeau *et al.*, 2000).

The intracellular signaling pathways activated in response to ligand-mediated engagement of these CLRs are still poorly defined. However, the functional effects of targeting antigens to the aforementioned CLRs have been analyzed in a number of studies, aimed to assess the potential of derived immunotherapeutic applications (Sancho *et al.*, 2008). For example, when anti-DEC-205 mAb is conjugated to a model antigen and is co-administered *in vivo* with DC-maturation agents such as anti-CD40 mAb, efficient cellular and humoral immune responses were induced (Bonifaz and Steinman, 2002). In the absence of adjuvants, antigen targeting to DEC-205 resulted in T cell tolerance (Mahnke *et al.*, 2002). Similarly,

other CLRs like the MR (He *et al.*, 2007), Clec9A (Caminschi *et al.*, 2008) and DC-SIGN (Kretz-Rommel *et al.*, 2007) have been assessed for their suitability to serve as antigen targeting structures. Moreover, other surface receptors, largely restricted in expression to DC, like CD11c have been tested in this regard, with the aim to elicit anti-tumor responses (van Broekhoven *et al.*, 2004).

### **2.2.5. Antigen uptake, processing and presentation of derived peptides by DC**

In peripheral tissues, DC take up self and non-self antigens (Geijtenbeek *et al.*, 2004). Internalized antigens are processed into small peptides (8-11 amino acids long), and these peptides are loaded on MHC class I and II molecules for presentation to T cells. These MHC-peptide complexes have only very short half-lives of <1 h and are rapidly recycled. Upon encounter of a maturation stimulus, DC rapidly down-modulate their Ag uptake and stop recycling surface MHC-peptide complexes, which now remain present on the DC surface for >24 h. The process of antigen uptake, degradation and loading onto MHC molecules is termed antigen presentation (Guermonprez *et al.*, 2002).

Endogenous antigens are degraded into small peptides by the proteasome in the cytosol. These self-peptides are subsequently transported into the endoplasmic reticulum (ER) by specialized peptide transporters for antigen presentation molecules (TAP), and then are loaded on MHC class I molecules (Guermonprez *et al.*, 2003 & Burgdorf *et al.*, 2008). These complexes are transported out of the ER through the Golgi apparatus, and then onto the cell surface for presentation to CD8<sup>+</sup> T cells. This MHC class I antigen presentation pathway enables the immune system to detect transformed or infected cells, which display peptides from modified self or pathogen-encoded proteins. Naive antigen specific CD8<sup>+</sup> T cells cannot eliminate transformed or infected cells directly. In order to become effector cytotoxic T lymphocytes (CTL), naive CD8<sup>+</sup> T cells need to be activated by stimulated APC like DC (Heath *et al.*, 2004). When APC are not directly infected, they need to acquire exogenous antigen from the infectious agent or infected

(apoptotic) cells, and cross-present them to MHC class I molecules, termed cross presentation (Heath *et al.*, 2002). CD8<sup>+</sup>DC were shown to be more efficient in cross-presentation than CD8<sup>-</sup>DC (Shortman & Heath, 2010). CD103<sup>+</sup> DC are the most efficient DC population, for antigens captured in peripheral tissues in terms of cross-presentation in the lymph nodes (Bedoui, *et al.*, 2009, del Rio *et al.*, 2007). Many types of antigen have been reported to be cross-presented, including immune complexes, soluble proteins, intracellular bacteria, parasites, and cellular antigens from infected cells (Heath *et al.*, 2002). In general, exogenous protein antigens are engulfed and are subsequently processed in endosomes. Endosomes contain proteases which degrade proteins into oligopeptides before they are loaded onto MHC class II molecules. The peptide-loaded MHC II complexes are then transported to the cell surface for presentation to CD4<sup>+</sup> T cells (Guermonprez *et al.*, 2002).

#### **2.2.6. Maturation of DC**

Under homeostatic conditions, DC are in an immature state and serve to establish peripheral tolerance against self and non-dangerous environmental antigens (Mahnke *et al.*, 2002). In a state of danger such as a microbial invasion, immature DC receive activation signals through the binding of conserved pathogen-derived molecular motifs to pattern recognition receptors (PRRS), such as TLRs (see chapter 2.2.4). This results in DC maturation and migration to the secondary lymphoid tissues.

The maturation of DC is characterized by a shutdown of phagocytic capacity, but enhanced antigen processing during the early phase of activation, an enhanced ability to migrate to lymphoid organs, and an increased ability to activate T cells and B cells due to high level antigen presentation.

On the molecular level, DC maturation is accompanied by an increased expression of chemokine receptors (CCR-7) and adhesion molecules (e.g. ICAM-1) that are involved in the directed migration of DC to lymphoid tissues, and of costimulatory molecules (CD40, CD80, CD86), which serve as the second signal

that is required for the activation of T cells and of B cells (Sabado and Bhardwaj 2010). Moreover, the maturation of DC also involves the production of cytokines, which play a very important role in differentiating subsets of CD4<sup>+</sup> T cells such as T helper (Th) 1, Th2, Th9, Th17 and various types of regulatory T cells (Treg).

### **2.2.7. Immune stimulation and tolerance induced by DC**

Many studies have demonstrated that DC are involved in the initiation of both immunity and immunological tolerance (Moser *et al.*, 2003 & Steinman *et al.*, 2003): In steady state, the immune system must be able to prevent self-destructive autoimmunity and unnecessary immune activation. Two safety strategies have evolved to ensure this: central and peripheral tolerance (Lewis *et al.*, 2012). Many studies have evidenced that, in addition to their role in the induction of effector T cell responses, DC have an important role in peripheral tolerance. Under steady state conditions, DC recognize and capture apoptotic cells using different receptors, including the scavenger receptor CD36, integrins  $\alpha V\beta 3$  and  $\alpha V\beta 5$ , and the complement receptors (CRs) CR3 and CR4 to mediate peripheral tolerance to self-antigens (Steinbrink *et al.*, 2007). Several studies have shown that under non-infectious conditions DC, which have internalized apoptotic cells, the MHC and costimulatory molecules are not upregulated. In addition, the ability to secrete proinflammatory cytokines of these DC was reduced, and the production of immunosuppressive cytokines like IL-10 and TGF- $\beta$  was increased (Morelli *et al.*, 2006 & Adler and Steinbrink, 2007).

A study from Steinman and his colleagues (2003) demonstrated that in steady state, targeting of DC via the DEC205 receptor with antigen at low dose leads to the deletion of antigen-specific naive T cells and unresponsiveness to antigenic challenge in combination with strong adjuvants. In contrast, if a stimulus for DC maturation is coadministered with the antigen in the course of initial administration, mice develop immunity, including the induction of IFN $\gamma$  secreting effector T cells and memory T cells.

### 2.2.8. Myeloid-derived suppressor cells (MDSC)

Myeloid-derived suppressor cells (MDSC) are a heterogeneous population of myeloid progenitor cells which can differentiate to DC, macrophages and neutrophils *in vitro* (Gabrilovich und Nagaraj, 2009). Murine MDSC are characterized by co-expression of Gr-1 and CD11b, and can be further subdivided into two major groups: granulocytic MDSC (which can also be identified as CD11b<sup>+</sup> Ly-6G<sup>+</sup> Ly6C<sup>low</sup> MDSC) and monocytic MDSC (which can also be identified as CD11b<sup>+</sup> Ly-6G<sup>-</sup> Ly6C<sup>high</sup> MDSC (Gabrilovich und Nagaraj, 2009).

MDSC constitute 2 to 4% of splenocytes from naive mice (Gabrilovich und Nagaraj, 2009), but markedly expand during cancer (Almand *et al.*, 2001 & Ochoa *et al.*, 2007), and infection (Vollbrecht *et al.*, 2012) due to tumor-secreted proinflammatory factors like IL-6 (Xiang *et al.* 2009), IL-1 $\beta$  (Elkabets *et al.*, 2010) or tumor derived the bioactive lipid prostaglandin E2 (PGE 2) (Obermajer *et al.*, 2012). The expansion of MDSC is also associated with autoimmunity (Meyer *et al.*, 2011) and inflammation (Gabrilovich und Nagaraj, 2009). Cheng and his coworkers (2008) have shown that S100A9, a TLR4 ligand can also induce the upregulation of MDSC and therefore inhibit the differentiation of myeloid progenitor cells.

MDSC-dependent mechanisms of immune suppression have been described in detail and can be divided into mechanisms either dependent or independent on L-arginine metabolism (Marigo *et al.*, 2008). A substantial part of MDSC-induced immune suppression is associated with the activity of two enzymes: ARG and NOS. ARG1 and NOS2, the main immune-related isoforms, share the common substrate L-arginine, which is metabolized to produce, respectively, either urea and L-ornithine or NO and L-citrulline (NOS2) (Bogdan, 2001). By this, T cell functions were inhibited and MDSC-derived cytokines like IL-10 and TGF- $\beta$  were produced (Gabrilovich *et al.*, 2009).

## 2.3. Cellular and humoral immune responses induced by DC

### 2.3.1. CD4<sup>+</sup> and CD8<sup>+</sup> T cell response

T lymphocytes (T cells) are important CD3<sup>+</sup> immune cells which express a clonal-specific T cell receptor (TCR) that enables specific binding to MHCII/peptide complexes. Most of the T cells in the body belong to one of two subsets: CD4<sup>+</sup> or CD8<sup>+</sup> cells. Naïve CD4<sup>+</sup> and CD8<sup>+</sup> T cells develop in the thymus. After infection or immunization, naïve T cells recognize antigenic peptides presented on the surface of APC (1st signal)(Alberts *et al.*,2002) along with appropriate costimulatory molecules such as CD80/CD86, which interact with CD28 to initiate T cell activation (2nd signal) (Alberts *et al.*, 2002). Activated T cells undergo a phase of clonal expansion and differentiation into effector or memory T cells, which in concert with antibody responses form the basis for protective immunity against infection and disease (Seder and Ahmed, 2003 ).

CD4<sup>+</sup> effector T cells can be grouped into different functional subsets based on their function and cytokine secretion patterns as shown in Fig. 7. IL-12 initiates the differentiation of Th1 cells that are characterized by high IFN $\gamma$  production, which in turn activates mononuclear phagocytes, thus protecting against intracellular microbes (O'Garra, 1998).Furthermore, productionof cytokines by Th1 cells promote the differentiation of CD8 T cells into cytotoxic cells and the activation of neutrophils and NK cells, further supporting a cellular response (London *et al.*,1998).In contrast, the differentiation of Th2 cells is triggered by IL-4. Th2 cells produce interleukin 4 (IL-4) and IL-5, IL-10, and IL-13 (O'Garra, 1998 ). They exert a key function in organizing host defense against extracellular pathogens, and are involved in responses dominated by IgG1 and IgE, and innate immune cells like mast cells, eosinophils and basophils. Th17 cells are a subset of CD4<sup>+</sup> effector T, which produce IL-17 and exhibit effector functions distinct from Th1 and Th2 cellscells (Korn *et al.*,2009). The primary function of Th17 cells appears to be the clearance of pathogens that are not adequately handled by Th1 or Th2 cells. Accordingly, IL-17 is important in the host defense against extracellular bacteria (Chung *et al.*, 2003) and against fungi such as *Candida albicans* (Huang ,2004). However, Th17 cells are potent inducers of tissue inflammation and have been



associated with the pathogenesis of experimental autoimmune diseases and human inflammatory conditions.

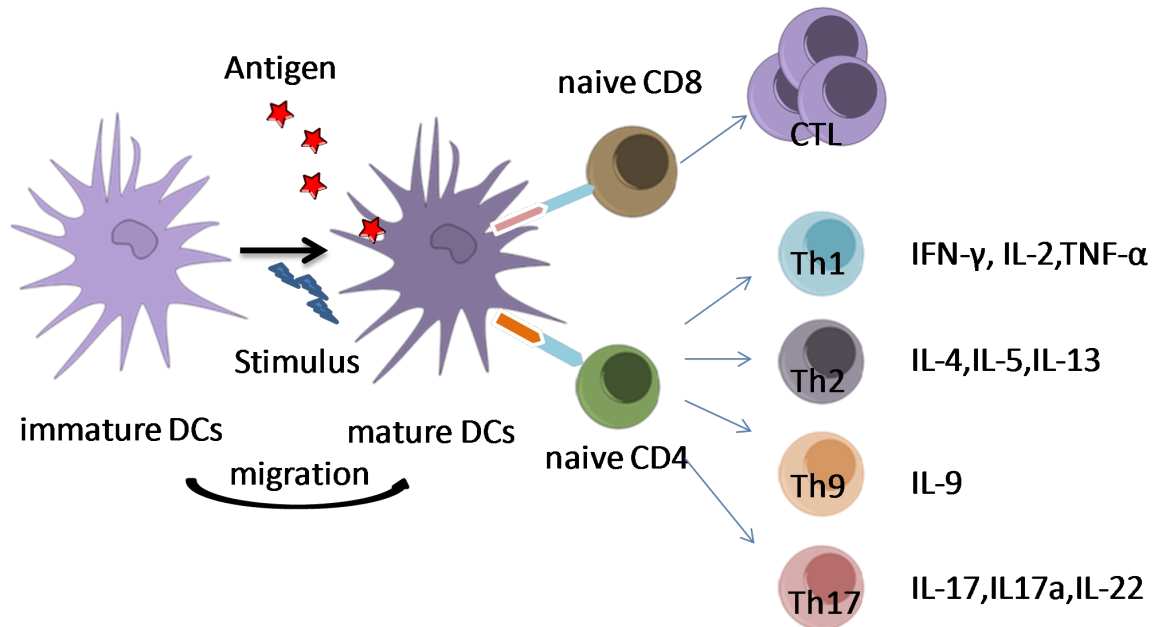


**Fig. 7: CD4<sup>+</sup> T-cell subsets develop from naive CD4 T cells after antigen-dependent T-cell activation.**

T cells that express CD8 on their cell surface are selected in the thymus to recognize and respond to peptides that are presented in the groove of MHC class I molecules. When activated, they become potent, cytotoxic T lymphocyte (CTL), also referred to as CD8<sup>+</sup>effector or killer cells, which can enter any tissue to destroy their targets, like cancer cells or virus-infected cells (Bevan, 2004 ). CD8<sup>+</sup> effector cells mediate their functions through the production of cytokines such as IFN-γ, tumor necrosis factor (TNF)-α, perforin and granzymes. Many studies have confirmed that help from CD4<sup>+</sup> cells is required to fully activate CD8<sup>+</sup> T cells to exert effective killing function (Bevan, 2004 ).

### 2.3.2. DC- induced humoral immune response

The humoral immune response is mediated by circulating antibodies (Abs), structurally conserved proteins that bind specifically to other proteins and other molecules. These Abs are produced by B lymphocytes which differentiate in the

bone marrow. Following engagement of the B cell receptor (BCR) by binding of foreign naive antigen, B cell activation is initiated. B cells can recognize soluble and membrane-associated antigen. Following activation, B cells process and present antigens associated with MHC II molecules. If the antigen is recognized by CD4<sup>+</sup> T effector cells, they release cytokines which support B cell activation to result in the production of antibodies specific for the native protein bound to the B cell receptor. On one hand, B cells can differentiate to extrafollicular plasmablasts that are essential for rapid antibody production and early protective immune responses (Batista and Harwood 2009). On the other hand, activated B cells can enter germinal centers, where they can differentiate into plasma cells that secrete high-affinity Abs following affinity maturation, or memory B cells, which confer long-lasting protection from secondary challenge with antigen (Batista *et al.*, 2009, Depoil *et al.*, 2008).

## 2.4. DC in cancer

Many studies have demonstrated that the immune system serves to prevent the appearance of tumors by killing malignant cells (Finn *et al.*, 2008). Cellular effector mechanisms are considered the most important mediators of antitumor immunity. In murine cancer models it has been thoroughly shown that DC can capture tumor antigens released from alive and dying tumor cells, and cross-present these antigens to T cells in tumor-draining lymph nodes. This process results in the generation of tumor-specific CTL, which contribute to tumor elimination (Diamond *et al.*, 2011). As another mechanism of tumor killing, antibody-dependent cellular cytotoxicity (ADCC) occurs when antibodies bind to antigens on tumor cells and the antibody Fc domains engage Fc receptors on the surface of immune effector cells (NK cells, macrophages), which promotes tumor cell killing (Scott *et al.*, 2012). Both CTL and antibody induced tumor killing are initiated by DC, and the immunological memory to control tumor relapse is induced by DC as well. Therefore, DC represent critical targets for therapeutic interventions in cancer.

Numerous studies have demonstrated that the generation of protective anti-tumor immunity depends on the presentation of tumor antigens by DC. DC can present tumor antigens through the capture of dying tumor cells. Apoptotic (tumor) cells (AC) mobilize three signals when interacting with DC: 1) find me, 2) eat me, and 3) don't eat me (Ravichandran, 2011). "Find me" signals are soluble factors with chemoattracting function, such as lysophosphatidylcholine (LPC), sphingosine 1-phosphate (S1P), CX3CL1, and the nucleotides ATP and UTP. "Find me" signals induce migration of phagocytic cells to apoptotic cells. "Eat me" signals are usually membrane-bound factors that serve as markers for phagocytes to recognize an AC. A number of receptors expressed on immature DC such as  $\alpha$ V $\beta$ 5 integrin, complement receptors and CD36 are thought to be involved in AC uptake. The "don't eat me" signals serve as negative regulators for the capture of cancer cells by DC. They are critical to prevent the uptake of living cells. These signals include lactoferrin and CD47, the interaction of which with signal-regulatory protein- $\alpha$  on phagocytes provide inhibitory signals that prevent phagocytosis (Palucka and Banchereau, 2012 ).

Tumors can prevent antigen presentation and the establishment of tumor-specific immune responses by various means (Mellmann *et al.*,2011). In this regard, tumors interfere with the differentiation and maturation of DC: First, by promoting the differentiation of monocytes to macrophages, which is mediated by the interplay of IL-6 and macrophage colony-stimulating factor (M-CSF), rather than DC. Due to the expansion of MDSC, tumors can prevent the priming of tumor-specific T cells by DC(Chomarat *et al.*,2000). Second, tumors inhibit the maturation of DC through the secretion of IL-10 (Fiorentino *et al.*,1991 & Steinbrink *et al.*,1997), which leads to antigen-specific anergy and thereby indirectly promotes tumor growth (Aspord *et al.*,2007). Tumor antigens can also interfere with the DC antigen-capture, processing and antigen presenting pathway. For example, tumor glycoproteins such as CEA and mucin-1(MUC-1), overexpressed and secreted by breast cancer cells, are endocytosed by DC via DC-SIGN, but are retained in early endosomes, leading to its inefficient processing and presentation to T cells, thus resulting in low numbers of MUC-1-specific effector cells (Hiltbold *et al.*,2000).In addition, paracrine mediators derived from the tumor, such as adenosine, prostaglandin E2 (PGE2), TGF- $\beta$  and VEGF-A exert multiple direct and indirect immunosuppressive activities (Mellman *et al.*,2011). These mediators contribute to

suppress the function of DC, indirectly inhibit effector T-cell migration into the tumour or directly suppress effector T-cell activation while enhancing the function of Tregs.

## 2.5. DC vaccination for the induction of antitumor responses

Because of their capacity to modulate immune responses, DC are an attractive target for vaccine development (Palucka & Banchereau, 2012). A major goal of a DC-focused cancer vaccine is to induce tumor-specific CD8<sup>+</sup> T cells, which mediate immune responses, at best sufficiently robust and long-lasting to generate durable tumor regression and eradication. Two distinct approaches for DC-based vaccination have been developed: antigen-loading and stimulation of *ex vivo*-generated DC, reinfused into the patient, and direct *in vivo* application of antigen and adjuvants with the ultimate aim to specifically target DC.

Cancer vaccination strategies based on the isolation of DC progenitors from peripheral blood, and the culture of large numbers of DC *in vitro*, have so far failed to demonstrate reliable clinical effectiveness (Tacke *et al.*, 2007). In these strategies, monocytes (CD14<sup>+</sup>) are isolated from peripheral blood and cultured in the presence of granulocyte-macrophage colony stimulating factor (GM-CSF) and IL-4 to generate immature DC. Immature DC are subsequently loaded with tumor antigens (peptides or tumor lysates) that are added to the DC culture medium. To ensure sufficient co-stimulatory capacity to induce potent antigen-specific immune response, antigen-loaded DC are treated with different kinds of maturation stimuli such as TLR ligands, CD40L or proinflammatory cytokines such as IL-1 TNF- $\alpha$  and IL-6 (Figdor *et al.*, 2004). Afterwards, antigen-loaded mature DC are injected into the patient through intravenous, subcutaneous, intradermal or intralymphatic routes of administration. Except for prostate cancer, where a DC vaccine has shown to prolong survival and has thus been approved for therapeutic use (Provenge®), the majority of clinical trials that used *ex vivo*-generated DC for immunotherapy provided no clear-cut therapeutic benefit, mostly due to problems in yielding standardized DC preparations of reliable quality and quantity (Dougan *et al.*, 2009).

The alternative strategy is to load DC directly with tumor antigens and adjuvants *in vivo*: here, antigens are directly delivered to DC *in vivo* using e.g. chimeric proteins that are comprised of an antibody which is specific for a DC receptor, and is fused to a selected antigen (Bonifaz *et al.*, 2002). Such vaccines codeliver antigens and maturation stimuli to the DC, to exploit the intricate migratory capacity of DC in their natural environment. Ralph Steinman and his group (2004) demonstrated that specific targeting of antigens to DC *in vivo* elicits effective antigen-specific CD4<sup>+</sup> and CTL responses. As antigen uptake is their natural function, DC express several receptors as described in chapter 2.2.4 that mediate Ag uptake and presentation. These receptors can be used to target an Ag of choice to DC *in vivo*. For example, DEC-205 (CD205) is an endocytosis-mediating receptor that belongs to the C-type lectin receptor family. Mouse studies have proven that targeting DEC205 with antigens led to Ag-specific immune responses. And this type of targeting not only resulted in MHC II-dependent presentation of antigen, but also in antigen loading to MHC I and subsequent cross presentation to CD8<sup>+</sup> T cells. Some other C-type lectin receptors, e.g. the mannose receptor or DC-SIGN, which facilitate binding and endocytosis of ligands that have a terminal sugar residue such as mannose and fucose, resp., have also been used as DC targeting structures for vaccination (Figdor *et al.*, 2013).

To efficiently mature DC *in vivo* after loading with antigens and mABs, DC maturation stimuli, such as pathogen-derived TLR ligands, are usually applied for the vaccination. TLR triggering has been demonstrated to be one of the most potent inducers of DC maturation *in vivo*. Several studies have demonstrated the suitability of the TLR 3 ligand poly I:C to increase the number and function of antigen-specific CD8<sup>+</sup> T cells in murine disease models, which resulted in protection from a subsequent challenge with tumor cells (Salem *et al.*, 2005). Although many TLR ligands are currently under study as tools for *in vivo* activation of DC, in recent years there has been a particular focus on CpG-rich oligonucleotides (ODNs), which act as TLR9 ligands. Unmethylated CpG ODNs stimulate DC to express costimulatory molecules and to increase antigen presentation. CpG-ODNs also can improve the MHC I peptide-processing pathway, leading to an increased number of cross-presented epitopes on the DC surface

(Krieg *et al.*, 2004). These effects render CpG-ODN a promising adjuvant for *in vivo* DC activation (Klinman *et al.*, 2004). There are at least three structurally distinct classes of synthetic CpG ODNs have been described that are capable to stimulate cells that express TLR9 (Tab. 4). A-type CpG ODNs directly induce the secretion of IFN- $\alpha$  from pDC, which indirectly supports the subsequent maturation of APC (Krug *et al.*, 2001). B type CpG (CpG-B) encode multiple CpG motifs on a phosphorothioate backbone, and trigger the differentiation of APC and the activation and proliferation of B cells (Verthelyi *et al.*, 2001). C type CpG can stimulate B cells to secrete IL-6 and pDCs to produce IFN- $\alpha$  (Klinman *et al.*, 2004).

CpG-ODN type	Example	Immunomodulatory activity
CpG-A	GGTGCATCGATGCAGGGGGG	APC maturation, mediated by ) Preferentially stimulates pDCs to CpG flanking region forms a palindrome (red) secrete IFN- $\alpha$
CpG-B	TCCATGGACGTTCTGAGCGTT	pDC maturation and production Triggers B-cell proliferation, and IgM and IL-6 production
CpG-C	TCGTCGTTCGAACGACGTTGAT	Stimulates B cells to produce Multiple CpG motifs (blue) IgM and IL-6 Activates pDCs to secrete IFN- $\alpha$

.....Modified from Klinman *et al.*, 2004 Nature Review

**Tab. 3: Comparison of ‘A’-, ‘B’- and ‘C’-type oligodeoxynucleotides.**

## 2.6. Cancer immunotherapy

Cancer represents one of the leading causes of death worldwide. Cancer accounts for about 30% of deaths in the European population. With more than 3 million new cases and 1.7 million deaths each year, cancer is the most important cause of death and morbidity in Europe after cardiovascular diseases (Statistic from WHO). Great progress has been made in cancer therapy in the past decades: tumor patients are treated with a combination of surgery, radiotherapy, and chemotherapy in most cases. As a standard therapy, the primary tumor is to be removed first. However, micro-metastases of disseminated tumor cells may cause tumor relapse and therapeutic failure. On the other hand, chemotherapy and radiotherapy are nonspecific, and healthy cells are invariably destroyed in addition. This is one of the major reasons why cancer patients suffer from devastating side

effects of treatment and have a poor quality of life throughout therapy. In order to overcome these obstacles, tumor immunotherapy has come into the focus of tumor immunology (Xiang *et al.*, 2004).

Immunotherapy refers to therapeutic strategies which support the immune system to kill tumor cells / malignant cells (Mellman *et al.*, 2011). The main focus of immunotherapeutic strategies is not only aimed to target and kill tumor cells, but also to active the immune system in a sustained manner in order to induce a long term anti-tumor response. One strategy is aimed at nonspecific activation of the immune system, by supplying high amounts of effector molecules, such as tumor-specific monoclonal antibodies (mAbs). Another immunotherapy strategy is directed on activation of the patient's immune system to target and kill cancer cells. The latter strategy may result in overlapping immune responses, i.e. simultaneous activation of innate immune cells, e.g. granulocytes and natural killer (NK) cells as well as of APC, and thereby also of CD4<sup>+</sup> T cells, CD 8<sup>+</sup> T cells, as well as B cells to coordinately eradicate tumor cells.

## **2.7. Nanoparticles for delivery of cancer vaccines**

In the past 20 years, several therapeutics based on particles with a size in the 10–500 nm dimension range, hence termed nanoparticles, have been introduced for

cancer therapy and the treatment of infectious diseases (Petros and DeSimone, 2010). Nanoparticle-based therapeutics are typically comprised of different therapeutic entities, such as small-molecule drugs, peptides, proteins and nucleic acids, and components that assemble with these, such as lipids and polymers, to form nanoparticles (Davis *et al.*, 2008). A stronger immune response is elicited when an antigen is associated with nanoparticles as compared with soluble antigen. Some clinical trials suggest that nanoparticle-based therapeutics can show enhanced anticancer effects as compared with direct application of the therapeutic

entities they contain, while simultaneously exerting less side effects, due to direct cellular targeting (Peer *et al.*, 2007).

## **2.8. Friend virus infection**

### **2.8.1. Friend gamma retrovirus**

Scientific knowledge of human retroviral infections is relatively well established, but the mechanisms of retrovirus-associated immunosuppression are still not fully understood. However, such knowledge is extremely valuable for the development of immunotherapeutic strategies and the design of vaccines (Miyazaw *et al.*, 2008). In this regard, Friend retrovirus (FV) constitutes an important model due to the availability of immuno-competent mouse strains which survive FV infection, as well as mouse strains, which show a lethal course of infection based on the development of acute erythroleukemia.

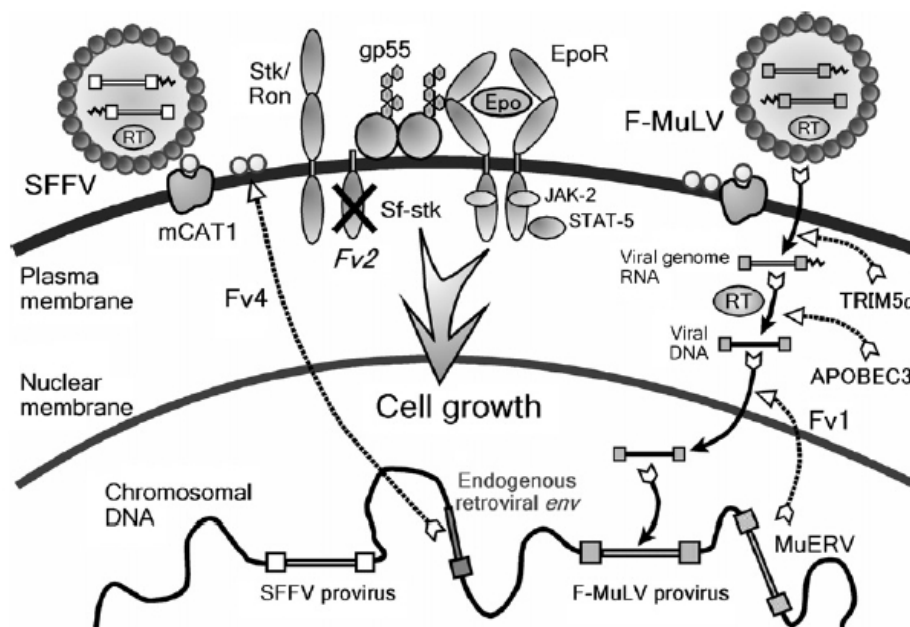
FV is a gamma retrovirus, isolated from leukemic mice by Charlotte Friend (Friend, 1957), and has been studied as a virus model to identify viral genes that control both susceptibility towards viral infection and virus-induced tumorigenesis (Chesebro, 1990). FV is a retroviral complex comprised of Friend murine leukemia virus (F-MuLV), a non-pathogenic, replication-competent helper virus, and of spleen focus-forming virus (SFFV), a replication-defective virus, which is responsible for pathogenesis (Kabat, 1989). Therefore, SFFV can spread only as cargo of F-MuLV-encoded viral particles. In susceptible mouse strains like BALB/c, FV induces lethal erythroleukemia (Chesebro, 1990). Mice of resistant strains (e.g. C57BL/6) are unable to clear the virus completely, and remain persistently infected (Chesebro, 1990).

When adult mice of susceptible strains are infected with FV, their spleens rapidly enlarge because of virus-induced polyclonal proliferation of erythroid precursor cells. Subsequent proviral integration at the Spi-1(ets) oncogene locus, combined with inactivation or mutation of the p53 tumor suppressor gene, produces fully malignant erythroleukemias. This process results in splenomegaly at 7-9 days post infection.



### 2.8.2. Molecular mechanisms of FV-induced disease

After inoculation with FV, the product of the SFFV env gene, gp55, forms a complex with the erythropoietin receptor (EpoR) (Ben-David and Bernstein, 1991). This interaction induces the proliferation and differentiation of erythroid progenitor cells (Tab. 7; Masaaki *et al* 2008). EpoR is expressed by erythroid progenitor cells at stages later than burst-forming unit, and is mainly effective in the growth regulation of the colony-forming unit of erythroid (CFU-e) (Kabat, 1989). The first cellular target of FV infection is the CFU-e in the bone marrow, and infected CFU-e migrate into the spleen, where they continue to divide and differentiate. This process is the reason for the development of splenomegaly. The transduction of growth signals from the gp55-EpoR complex also requires the involvement of another molecule, sf-STK (a short form of a kinase-type hematopoietic growth factor receptor). Mice of C57BL/6 background lack expression of sf-STK, and thus are resistant to the development of massive splenomegaly (Masaaki *et al.*, 2008).



Masaaki Miyazawa *et al.*, Vaccine\_2008

**Fig. 8: Mechanisms of FV-induced erythroid cell growth potentiation and cellular factors that interfere with FV infection (Masaaki Miyazawa *et al.*, 2008).**

### 2.8.3. Host genetic factors involved in FV infection

Many genes are involved in conferring immunological resistance to FV-induced disease. The induction of erythroleukemia is affected by many host genes, including major histocompatibility complex (MHC) (H-2) and non-MHC genes (Fv1, Fv2, Fv4, Rfv3 and others) (Chesebro *et al.*, 1990). The H-2b haplotype as carried by C57BL/6 is usually associated with relative resistance to FV, whereas H-2d (BALB/c), H-2q (FVB/N), H-2a and H-2k (C3H) are associated with susceptibility (Hasenkrug *et al.*, 1997).

Recent work has shown that APOBEC3 (mA3, apolipoprotein B mRNA-editing complex), which exerts antiviral activities against exogenous and endogenous viruses, as well as retrotransposons, also restricts infection by murine leukemia virus (MuLV), porcine endogenous retrovirus, and foamy viruses (Delebecque *et al.*, 2006 & Harris *et al.*, 2003). Mouse retroviruses escapes from the host's APOBEC3 activity in two ways: by the exclusion of mouse APOBEC3 from the virions and by the cleavage of incorporated mouse APOBEC3 with viral protease after virion maturation (Abudu *et al.*, 2006). In different inbred mouse strains polymorphic APOBEC3 alleles have been found (Takeda *et al.*, 2008). For example, C57BL/6 mice, which are resistant to F-MuLV, express an APOBEC3 isoform different from that encoded by F-MuLV-susceptible BALB/c mice. The predominant Apobec3-mRNA produced by cells of C57BL/6 mice lacks exon 5 (mA3-5) and encodes a protein with 15 polymorphic amino acids (Takeda *et al.*, 2008). It has also been reported that BALB/c mice produce only a APOBEC3 mRNA variant that lacks exon 2 (mA3-2).

## 2.9. Asthma and Anaphylaxis

Asthma is a multifactorial and complex chronic obstructive disease of the lower airways (Bochner *et al.*, 1994). It is characterized by exacerbations of partially reversible airflow limitation, along with bronchial hyperreactivity and chronic airway inflammation (Bochner *et al.*, 1994). Asthma is one of the most common chronic inflammatory diseases, according to the report from the WHO. In the past 20 years,

the prevalence of asthma has almost doubled, and currently about 300 million people suffer from asthma (Wang *et al.*, 2012). One of the hallmarks of asthma is the infiltration of the airway wall by Th2 cells, eosinophils and mast cells. Priming of allergen-specific CD4<sup>+</sup> T cells results in the increased production of Th2 cytokines (such as IL-4, IL-5 and IL-13). These cytokines are responsible for class-switching to the  $\epsilon$  immunoglobulin heavy chain, which results in IgE production by B cells. IgE binds with the Fc $\epsilon$ RI, which is expressed on the surface of mast cells and basophils (Hamid *et al.*, 2009). Crosslinking of IgE-Fc $\epsilon$ RI complexes by allergen results in the degranulation of mast cells and basophils, which thereby release histamine, lipid mediators, chemokines and other cytokines, and induce the first allergic reaction.

Anaphylaxis is a severe, potentially life-threatening, systemic allergic reaction, which generally happens unexpectedly in healthy individuals (Rietschel *et al.*, 2013). Studies in mouse OVA models demonstrated 2 pathways for the systemic anaphylaxis. One is the classical pathway mediated by IgE, Fc $\epsilon$ RI (high-affinity Fc receptor for IgE), mast cells, histamine and platelet-activating factor (PAF). The other pathway is mediated by IgG, Fc $\gamma$ RIII, macrophages and PAF (Finkelman 2007).

## 2.10. Aim of the PhD study

The aim of the work presented here was to study how retroviral infection alters DC-T cell immunity, whether these effects are important for the generation of retrovirus-induced immunosuppression, and how suppression of antigen presentation may contribute to tumorigenesis and tumor formation are related. In a second series of experiments, the usability of functionalized, nano-sized, dextran-based and solid core particles to induce potent antitumor immune responses was assessed both *in vitro* and *in vivo* in different therapeutic disease models, including a melanoma model, allergic asthma, and anaphylaxis.

### 3. Results

#### 3.1. Friend virus-induced alterations of myeloid DC

Due to the central role of dendritic cells (DCs) in the induction of anti-viral responses, we asked for their functional role in the genotype-dependent sensitivity towards FV infection. A study from our group (Balkow *et al.*, 2007) showed that formation of the immunological synapse between dendritic cells (DCs) and T cells differed when FV-infected DCs were used as stimulators. MyPhD study was focussed on elucidating the functional role of proteins identified as differentially expressed in FV-infected DC in a genotype-dependent manner, which therefore may contribute to the differential course of FV infection *in vivo* in BALB/c versus C57BL/6 mice.

##### 3.1.1. Analysis of FV-infected DC *ex vivo* and generation of FV-infected myeloid BMDC *in vitro*

###### 3.1.1.1. In FV-susceptible BALB/c mice the frequency of FV-infected splenic DC is higher than in FV-resistant C57BL/6 mice

To determine whether DC generated *in vitro* from FV-infected progenitor cells exhibited similar characteristics as DC in FV-infected mice, we stained splenic DC derived from acutely FV-infected mice of either genotype with an antibody against FV encoded protein for expression of the FV-glycosylated Gag protein on CD11c<sup>+</sup> splenic DC. In FV-susceptible BALB/c mice, 7 days after inoculation with FV around 25.29 % splenic DC were positive for FV Gag protein, but only 6.2 % of splenic DC derived from FV-inoculated C57BL/6 mice expressed this viral protein (Fig. 9).

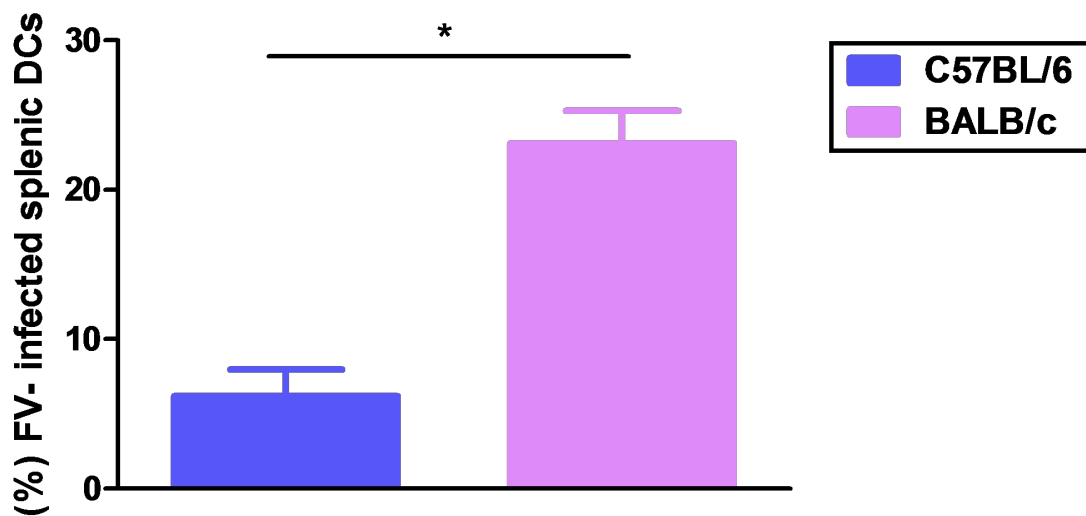


**Fig. 9: Frequencies of FV-infected splenic DC in BALB/c and C57BL/6 mice.** Myeloid DC were isolated from the spleen of FV-infected mice 7 days after infection and were immunosorted by CD8<sup>+</sup>CD11c<sup>+</sup> positive selection. The frequencies of splenic DC expressing a FV-encoded protein (p34) on their surface were assessed by FACS analysis. Data represent the mean±SEM of 5 independent experiments. Statistically significant differences between C57BL/6 versus BALB/c are indicated (\* p<0.05).

### 3.1.1.2. The frequency of FV-infected BM cells is higher in BALB/c than in C57BL/6 mice

To study the properties of FV-infected DC with a genotype of FV-susceptible versus resistant mice side-by-side, C57BL/6 and BALB/c mice were left untreated or were inoculated with FV, and their bone marrow (BM) was isolated one week later to generate BM-derived DC. Fig. 10 shows that the frequency of FV-infected BM cells was higher in case of BALB/c mice than of C57BL/6 mice.

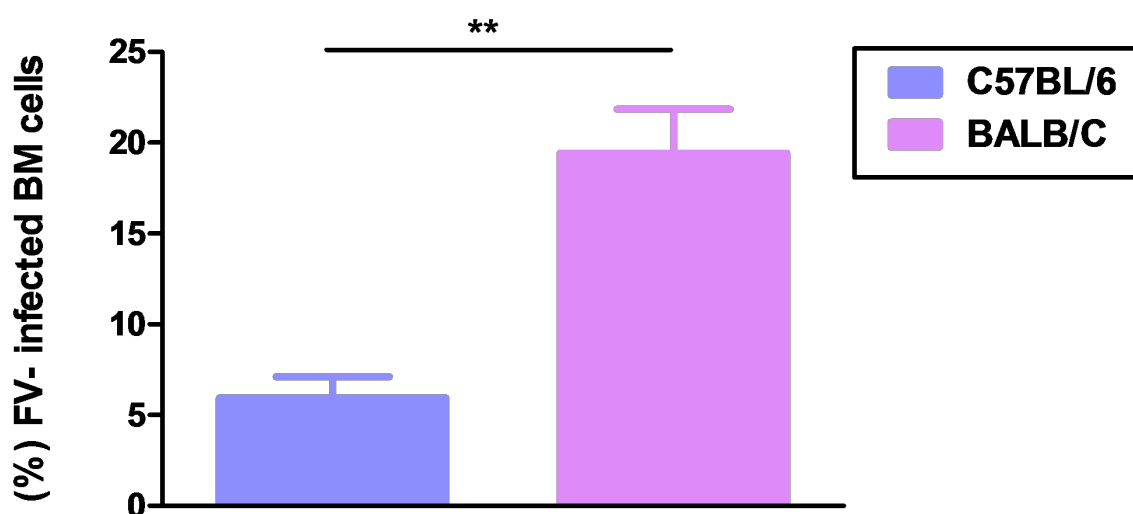


**Fig. 10: Frequencies of FV-infected Bone Marrow (BM) cells derived from FV-infected BALB/c and C57BL/6 mice.** 7 days post infection with FV, BM was isolated from the femurs of mice. The frequencies of BM cells expressing a FV-encoded protein (mAb34) on their surface were assessed by FACS analysis. FV-infected BM cells were separated by immunomagnetic positive selection using a p34-specific antibody. Data represent the mean±SEM of 15 independent experiments. Statistical significant differences between C57BL/6 versus BALB/c are indicated (\*\*  $p < 0.01$ , \*\*\*).

### 3.1.2. FV infection interferes with the DC immunophenotype

#### 3.1.2.1. The expression of MHCII and of costimulatory markers is impaired in BMDC derived from FV-infected BM cells in a strain-independent manner

To assess the consequences of FV infection of DC for their immuno-phenotype, the expression of cell surface markers was determined. The maturation of DC was associated with increased expression of MHC II and costimulatory molecules. After 6 days of differentiation, the expression of MHCII and costimulatory molecules in BMDC derived from uninfected and FV-infected BM cells of either mouse strain was analysed by FACS. Fig.11 shows that BMDC derived from FV-infected BM cells displayed a lower expression of MHC II, and of CD40, CD80 and CD86 than observed for the corresponding control group. These results indicate that FV infection establishes an immature immunophenotype in BMDC in a genotype-independent manner. Interestingly, however, MHC II expression by DC was diminished to a

significantly greater extent in BALB/c mice, whereas the expression of CD80 and CD86 molecules was affected more prominently in C57BL/6 mice.

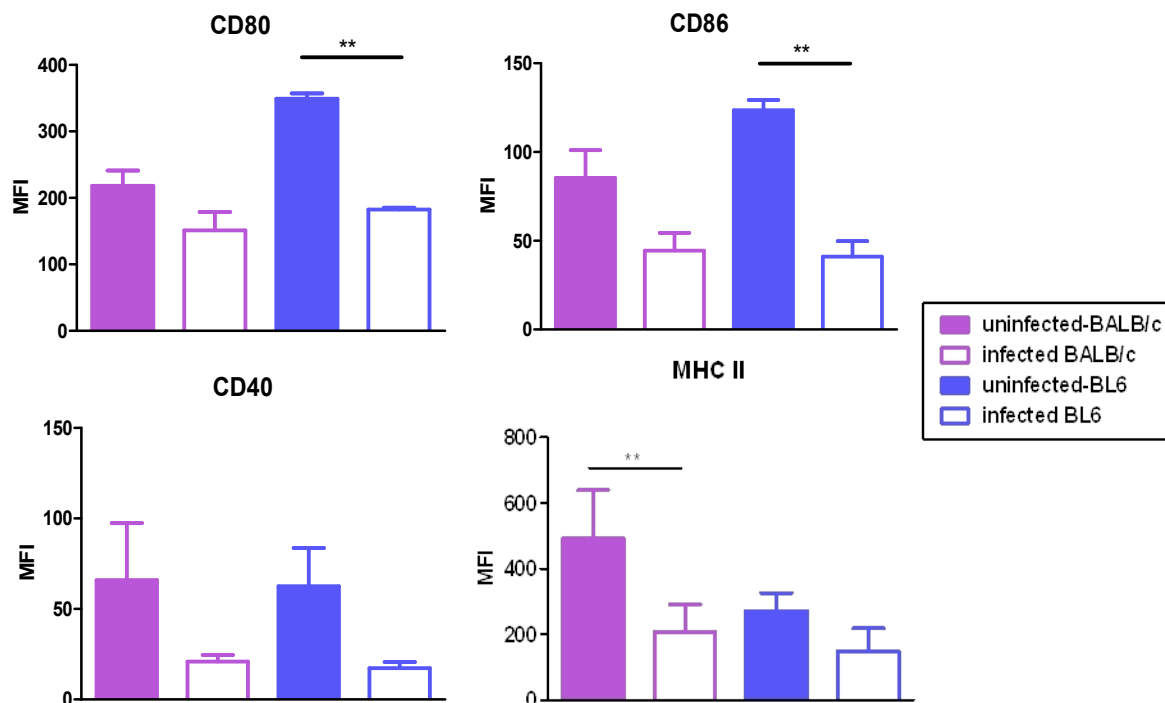


**Fig. 11: FV-infected and uninfected BMDC from both mouse strains show differences in the expression of DC activation markers.** 7 days post FV infection, BM was isolated from the femurs of mice. FV-infected BM cells were separated by immunomagnetic positive selection using a p34-specific antibody. FV-infected and uninfected BM cells were incubated in parallel cultures with GM-CSF for 6 days. On day 6, immature DC were harvested and subsequently analysed by FACS for the expression of CD11c, MHCII, CD40, CD80, and CD86. Data represent the mean $\pm$ SEM of 5 independent experiments. Statistically significant differences between uninfected versus FV-infected DC are indicated (\*\*  $p < 0.05$ )

### 3.1.2.2 FV-infected BMDC display unaltered cytokine secretion pattern

In addition to the phenotypic characterization of FV-infected DC from either genotype, we studied their ability to produce cytokine. IL-12 and IL-10 are important cytokines required for activation and differentiation of T cells upon DC–T-cell contact. As shown in Fig. 12, after stimulation of LPS, FV-infected BMDC driven from BALB/c mice showed enhanced production of IFN $\gamma$ , TNF- $\alpha$ , IL-6 and IL-12 but no clearly difference of IL-10 production. In FV-infected BMDC driven from C57BL/6 mice no difference of cytokine productions were observed.

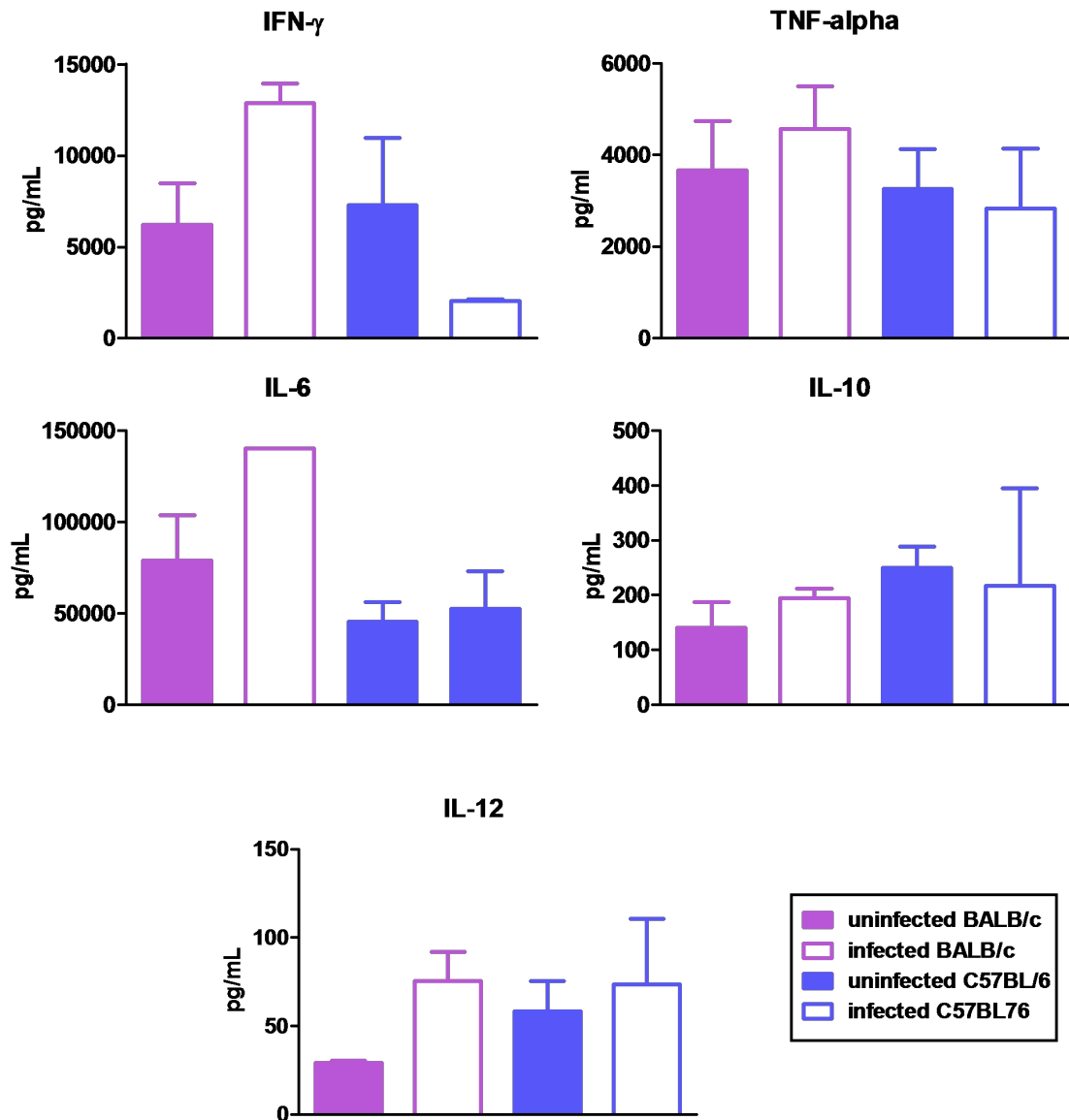


**Fig. 12: FV-infected BMDC are not affected in their cytokine production.** 7 days post FV infection, FV-infected BM cells were separated by immunomagnetic positive selection using a p34-specific antibody. FV-infected and uninfected BM cells were incubated with GM-CSF for 6 days. On day 6, immature BMDC were harvested and stimulated *in vitro* with LPS (100ng/ml). After 24 hours, supernatants from BMDC cultures were analyzed by CBA for concentrations of IFN $\gamma$ , TNF- $\alpha$ , IL-6, IL-10 and IL-12. Data represent mean $\pm$ SEM of three independent experiments. Cumulative data from 3 independent experiments are shown.



### **3.1.3. FV infected BMDC induce reduced T cell proliferation compare to uninfected BMDC**

#### **3.1.3.1. FV infected BMDC are poor CD4<sup>+</sup>T cell stimulators *in vitro***

So far, the results show that FV infection of DC progenitors resulted in impaired expression of MHCII and costimulatory markers by BM-derived DC without affecting their cytokine production by BMDC to a significant extent. Next, the functional properties of FV-infected BMDC were analyzed. In a previous study, time lapse microscopy revealed that FV-infected BALB/c BMDC had more prolonged contacts with syngeneic DO11.10 T cells than uninfected DC, and favored the expansion of CD4<sup>+</sup>Foxp3<sup>+</sup> T cells (Balkow *et al.*, 2007). Therefore, it was of interest to analyze to which extent FV-infected C57BL/6 BMDC could stimulate antigen-specific T cell proliferation. To test this, uninfected and FV-infected BMDC of either genotype were pulsed with OVA peptide, and subsequently used to stimulate the proliferation of OVA peptide-specific CD4<sup>+</sup> T cells (BALB/c: DO11.10, C57BL/6: OT-II). As shown in Fig. 13, unstimulated BMDC (uninfected and FV-infected) of both strains mediated low T cell proliferation. When stimulated with LPS, uninfected BMDC mounted significantly higher T cell proliferation than FV-infected BMDC in a genotype-independent manner.

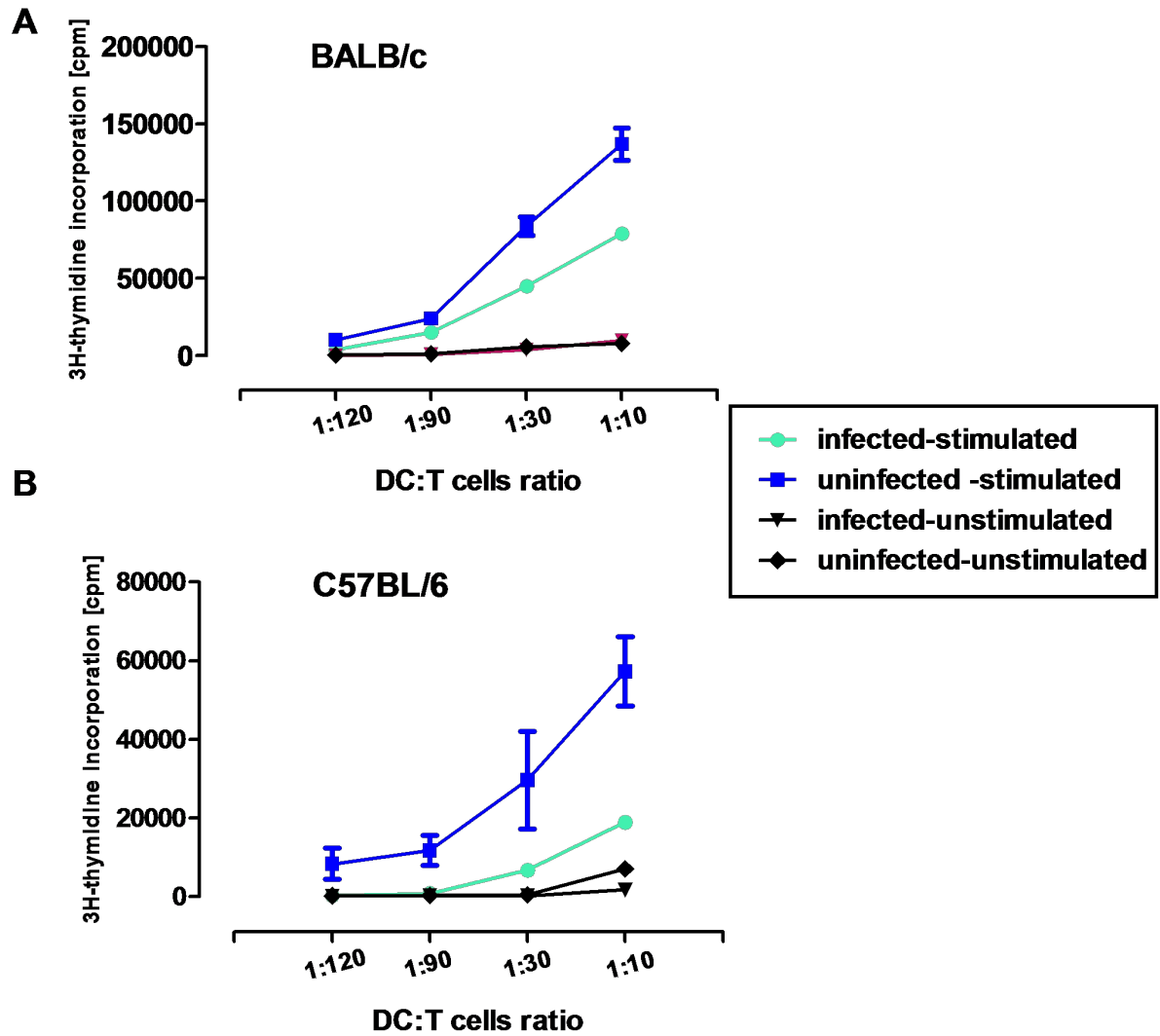


**Fig. 13: BALB/c and C57BL/6 BMDCat stimulated state show an impaired T cell stimulatory capacity when infected with FV.** 7 days after FV infection, BM cells were separated by immunomagnetic positive selection using a p34-specific antibody, and both FV infected and uninfected BM cells were incubated with GM-CSF for DC differentiation. On day 6, immature BMDC were harvested and aliquots were stimulated with LPS (100ng/ml) over night. BMDC were pulsed with OVA<sub>323-329</sub> for 2h. Afterwards, titrated numbers of harvested BMDC were cocultured with OVA peptide-specific CD4<sup>+</sup> (DO11.10 [A], OT-II [B]) T cells in triplicates for 72 h. T cell proliferation was assessed by uptake of <sup>3</sup>H-thymidine during the last 16 h of culture. Data represent mean±SEM of triplicates. Results from one representative out of three independent experiments are shown.

### 3.1.4. FV-infected BMDC induce an altered cytokine profile in DC/T cell cocultures

#### 3.1.4.1. FV-infected BMDC induce lower Th1 and Th17 responses

To investigate alterations of the cellular immune response induced by FV-infected DC, FV-infected and uninfected OVA<sub>323-329</sub>-pulsed and LPS-stimulated BMDC of either genotype were cocultured with corresponding OVA peptide-specific CD4<sup>+</sup> T cells (DO11.10 for BALB/c and OT-II for C57BL/6 DC/T cell coculture). Three days later, the supernatants of these cocultures were assessed for cytokine contents. As shown in Fig.14, in general FV-infected BMDC evoked a significantly reduced production of the Th1 cytokine IFN $\gamma$ , and of the Th17 marker IL-17 as compared with uninfected BMDC. In contrast, FV-infected BMDC mounted a stronger IL-2 production than the corresponding control BMDC.

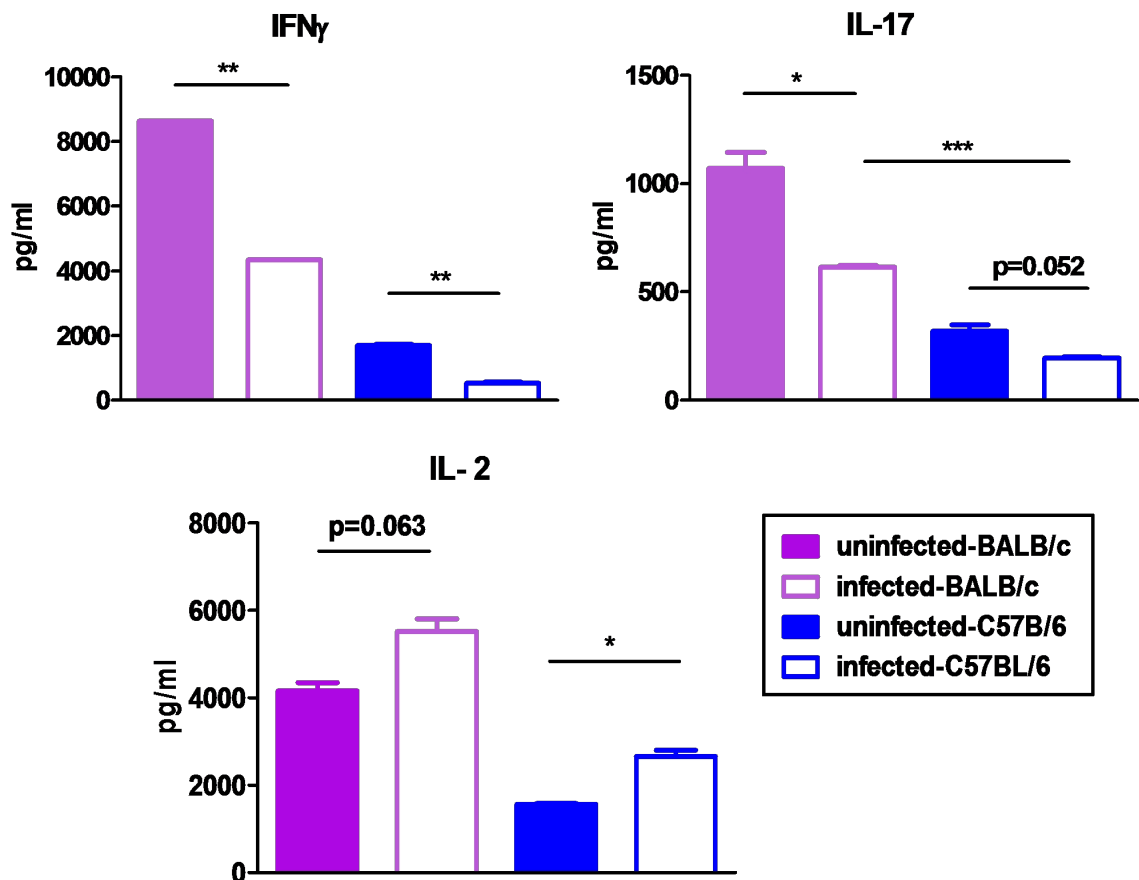


**Fig. 14: Th1 and Th17 cytokine levels were altered in FV-infected-DC/CD4<sup>+</sup> T cell cocultures.** 7 days post FV infection BM was isolated from the femurs of mice. The frequencies of BM cells expressing a FV-encoded protein (p34) on their surface were assessed by FACS analysis. FV-infected BM cells were separated by immunomagnetic positive selection using a p34-specific antibody. FV infected and uninfected BM cells were incubated with GM-CSF. Both uninfected and FV-infected BMDC (BALB/c and C57BL/6) were harvested on day 6 of culture, were pulsed with OVA<sub>323-329</sub>. Two hours later, LPS (100 ng/ml) was added. One day later, BMDC (each 5,000) were cocultured with CD4<sup>+</sup> DO11.10 or OT-II T cells (50,000) for 72 h. Cytokines contents of DC/T cell coculture supernatants were analyzed by CBA. Data represent mean±SEM of three independent experiments. Statistically significant differences between uninfected versus infected DC/T cell cocultures are indicated (\* p<0.05, \*\* p<0.01, \*\*\* p<0.001).

### 3.1.4.2. FV-infected BMDC amplify the Th2 response

The immunological resistance of a host against viral infections is strongly affected by cytokines such as IL-4, IL-5 and IL-13, which promote T helper type 2 responses and thereby may evoke an enhanced antiviral humoral immune response. As depicted in Fig. 15, FV infected BMDC of either genotype induced a stronger production of the Th2 cytokines IL-4, IL-5 and IL-13 than the corresponding control BMDC population.

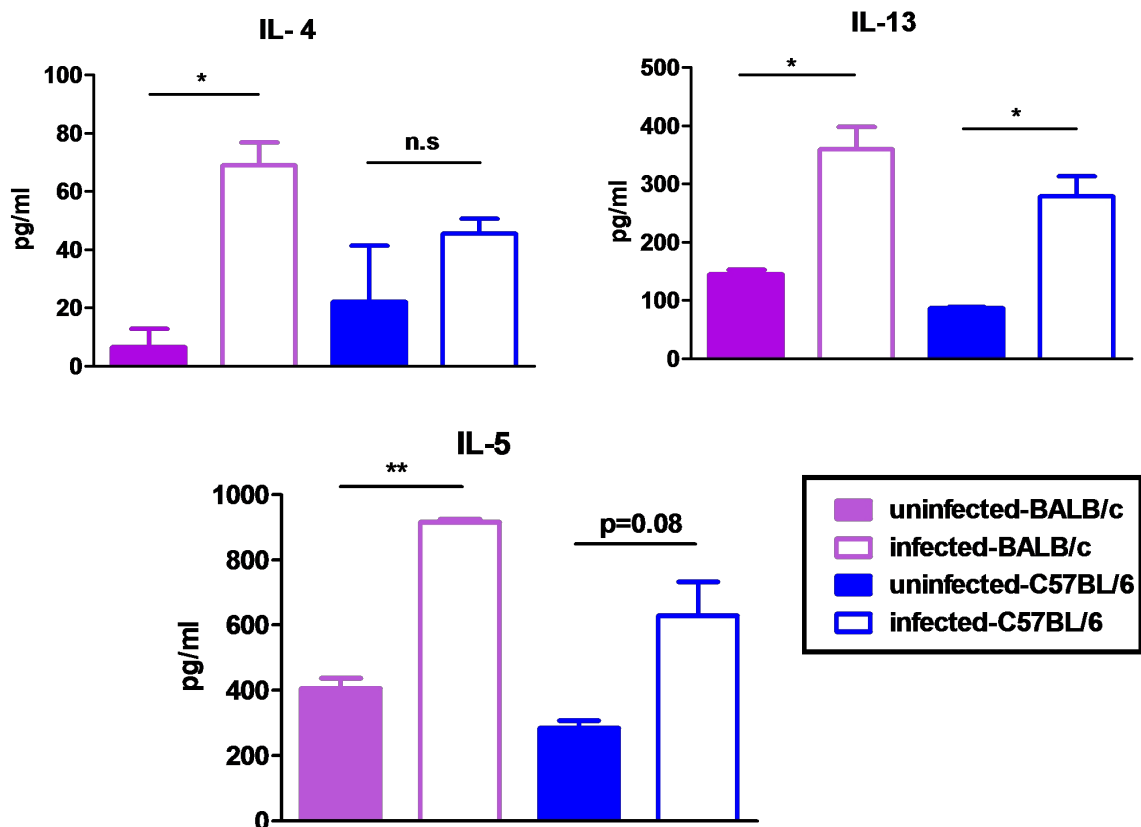


**Fig. 15: Th2 cytokine levels were increased in FV infected-DC/CD4<sup>+</sup> T cell coculture supernatants.** 7 days post FV infection BM was isolated from femurs of mice. The frequencies of BM cells expressing a FV-encoded protein (p34) on their surface were assessed by FACS analysis. FV-infected BM cells were separated by immunomagnetic positive selection using a p34-specific antibody. FV infected and uninfected BM cells were incubated with GM-CSF. Both uninfected and FV-infected BMDC (BALB/c and C57BL/6) were harvested on day 6 of culture and were pulsed with OVA<sub>323-329</sub>. Two hours later, LPS (100 ng/ml) was added. One day later, BMDC (5,000) were cocultured with CD4<sup>+</sup> DO11.10 or OT-II T cells (each 50,000) for 72 h. Cytokines contents of DC/T cell coculture supernatants were analyzed by CBA. Data represent mean±SEM of three independent experiments. Statistically significant differences between uninfected versus infected DC/ T cell cocultures are indicated (\* p<0.05, \*\* p<0.01,).

### **3.1.5. FV-infected BMDC induce lower CD4<sup>+</sup> T cells proliferation than uninfected BMDC *in vivo* in a genotype-independent manner**

Due to the impaired ability of FV-infected BMDC to stimulate antigen-specific CD4<sup>+</sup> T cells *in vitro*, next their ability to mount OVA-specific CD4<sup>+</sup> T cell responses *in vivo* was tested. To this end, DO11.10 (BALB/c background) or OT-II (C57BL/6 background) T cells were labeled with CFSE and were injected *i.v.* into syngeneic BALB/c or C57BL/6 mice, respectively. Two days later, FV-infected and uninfected BMDC were pulsed with OVA peptide and were injected *i.v.* into corresponding recipient mice. Three days later, the extent of OVA-dependent proliferation of CFSE-labeled OT-II T cells of spleen cells was analyzed by flow cytometry.

In case of the mice that had been immunized with FV-infected DC, the *in vivo* proliferation of DO11.10 (Fig. 16A) and OT-II T cells (Fig. 16B) was significantly lower as compared with T cells derived from mice immunized with uninfected DC. In accordance with the finding of reduced IFN $\gamma$  contents in DC/T cell coculture supernatants containing FV-infected BMDC as stimulators, the frequency of IFN $\gamma$ <sup>+</sup>OT-II T cells was significantly lower in mice immunized with FV-infected BMDC (Fig. 16C).

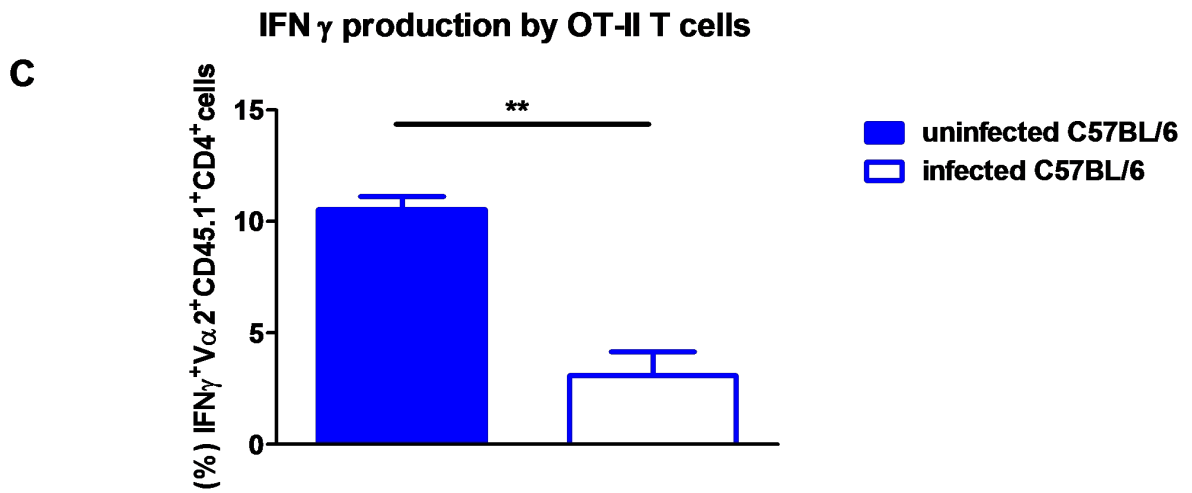
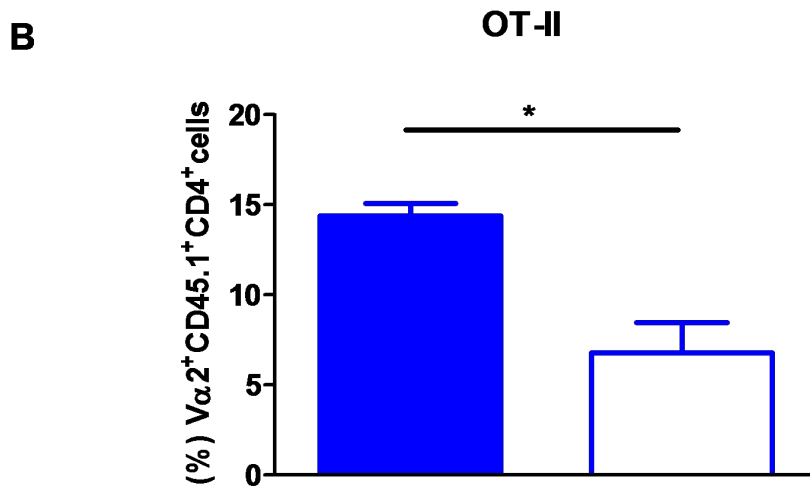
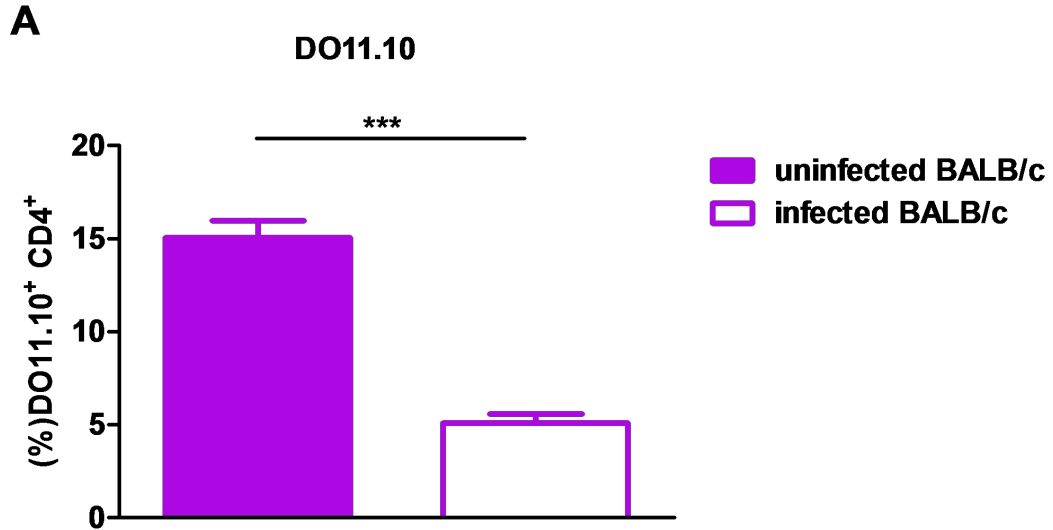


**Fig. 16: The *in vivo* proliferation of transgenic CD4<sup>+</sup> T cells is reduced when FV-infected BMDC are used as stimulators.** Splenocytes derived from OT-II transgenic mice were labeled with 0.5  $\mu$ mol CFSE. 10<sup>7</sup> T cells (OT-II, DO11.10) were injected *i.v.* into syngenic C57BL/6 mice or BALB/c mice. After 2 days, recipients were immunized with uninfected or FV-infected BMDC (each 3x10<sup>6</sup>) pulsed with OVA peptide, and stimulated with LPS (100 ng/ml) prior to transfer. Three days later, the frequencies of CFSE-labeled CD4<sup>+</sup> T cells within the spleen cell suspensions were assessed by flow cytometry. (A) Compared to uninfected BMDC, FV-infected (A) BALB/c and (B) C57BL/6 BMDC exerted a reduced capacity to stimulate the proliferation of CFSE-labeled CD4<sup>+</sup> T cells (A: DO11.10, CFSE<sup>+</sup>CD4<sup>+</sup>DO11.10<sup>+</sup>; B: OT-II, CFSE<sup>+</sup>CD4<sup>+</sup> CD45.1<sup>+</sup> V $\alpha$ 2<sup>+</sup>) *in vivo*. Results from one out of three independent experiments are shown. (C) Stimulated FV-infected C57BL/6 BMDC induced less secretion of IFN $\gamma$  from CFSE-labeled OVA-reactive CD4<sup>+</sup> OT-II T cells than uninfected BMDC. (A-C) Data represent the mean  $\pm$  SEM of 3 independent experiments. Statistically significant differences between groups are indicated (\* p<0.05, \*\* p<0.01, \*\*\* p<0.001).

### 3.1.6. FV infected BMDC are weaker inducers of CD8<sup>+</sup> T cell proliferation *in vivo*

Due to the reduced proliferation and lowered frequency of IFN $\gamma$  production of CD4<sup>+</sup> antigen-specific T cells stimulated by FV-infected BMDC, the suitability of FV-infected BMDC to evoke CD8<sup>+</sup> T cell responses was assessed. To this end, splenocytes derived from OT-I mice bearing OVA peptide-specific CD8<sup>+</sup> T cells were labeled with CFSE and were injected *i.v.* into C57BL/6 mice. After two days, groups of mice were treated with uninfected or FV-infected BMDC. Four days later, the *in vivo* proliferation of CFSE<sup>+</sup> OT-I T cells was assessed in spleen cell suspensions.

When mice had been immunized with FV-infected BMDC, CD8<sup>+</sup> OT-I T cells proliferated at a significantly lower extent than in mice immunized with uninfected control BMDC (Fig. 17A). Similar to the findings for CD4<sup>+</sup>OT-II T cells, the frequency of OT-I T cells producing the Th1 cytokine IFN $\gamma$  was lower in mice immunized with FV-infected BMDC than after treatment with control DC (Fig. 17B).

IFN $\gamma$  secreting Th1 cells are likely to be critical for effective and long-lasting anti-tumor immunity. First we hypothesized that in C57BL/6 mice, their ability to mount a stronger Th1 response might contribute to their FV resistance. However, FV-infected DC displayed a reduced ability to induce proliferation of CD8<sup>+</sup> T cells, and the frequency of IFN $\gamma$  producing OT-I T cells is decreased.

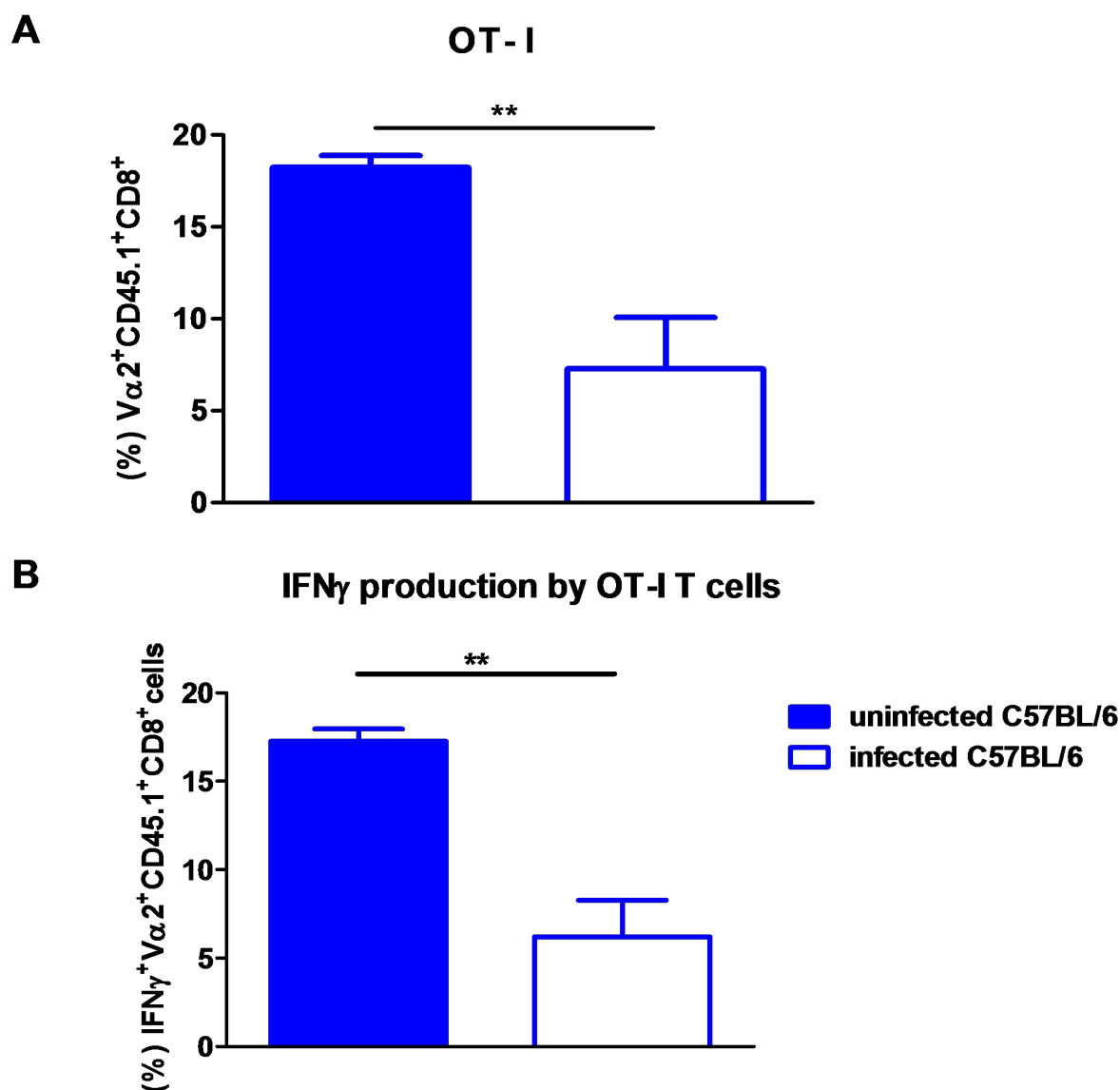


**Fig. 17: The *in vivo* proliferation of antigen-specific CD8<sup>+</sup> T cells is reduced when employing FV-infected BMDC as stimulators.** Splenocytes derived from OT-I transgenic mice were labeled with 0.5  $\mu$ mol CFSE. 10<sup>7</sup> OT-I cells were injected i.v. into syngenic C57BL/6 mice. After 2 days, recipients were immunized with uninfected or FV-infected BMDC which pulsed with OVA peptide. Three days later, the frequencies of CFSE<sup>+</sup>CD8<sup>+</sup> CD45.1<sup>+</sup> V $\alpha$ 2<sup>+</sup> cells within the spleen cell suspensions were assessed by flow cytometry. **(A)** Compared to uninfected BMDC, FV-infected C57BL/6 BMDC pulsed with OVA<sub>257-264</sub> mediated a less proliferation of CFSE-labeled CD8<sup>+</sup> T cells (OTI) *in vivo* **(B)** Stimulated FV-infected C57BL/6 BMDC induced a lower frequency of IFN $\gamma$  produce by CFSE-labeled CD8<sup>+</sup> T cells than uninfected BMDC. Data represent the mean $\pm$ SEM of 3 independent experiments. Statistically significant differences between groups are indicated (\* p<0.05, \*\* p<0.01, \*\*\* p<0.001).



### **3.1.7. FV-infected BMDC display an altered proteome profile**

Taken together, FV-infected BMDC displayed an impaired T cell stimulatory, but Th2-biased capacity, irrespective of their genotype. Thus, no overt functional difference was detectable between BMDC of FV-susceptible and FV-resistant mouse strains. However, since BALB/c mice are susceptible to FV infection, in contrast to C57BL/6 mice, a proteome analysis of FV-infected versus uninfected BMDC at unstimulated states was undertaken in order to identify strain-specifically FV-regulated proteins, which may affect DC functions.

On day 6 of culture, BMDC ( $3 \times 10^6$ ) per group were analyzed by protein mass spectrometry for three times (by Dr. Stefan Tenzer; Institute of Immunology, University Medical Center Mainz). By these analyses, more than 300 significantly differentially expressed proteins were identified in infected versus uninfected BMDC, which were regulated either similarly in BMDC of either genotype or in a genotype-specific manner. For some of these FV-regulated proteins more detailed analyses have been performed in order to determine their impact on DC functions.

### **3.1.8. FV-infected BMDC of either genotype show an increased endocytotic capability**

DC regulate antigen uptake by controlling their endocytotic capacity. Immature DC actively internalize antigen, while mature DC display poor endocytotic activity. It is known that endocytotic activity is controlled by Rho family GTPases (Bokoch, 2005). Protein-mass fingerprinting of FV-infected versus uninfected BMDC revealed that some small G-proteins, including RHO and proteins involved in antigen processing (cathepsins), were stronger differentially regulated (Tab. 4) in both FV-infected BMDC populations as compared with their uninfected counter parts.

	C57BL/6	BALB/c
GDIR-1 (Rho inhib. 1)	↓	○
GDIR-2 (Rho inhib. 2)	↑	○
RAC-2	○	↓
RHO-A	○	↓
Cathepsin B	↑	↑
Cathepsin D	↑↑	↑↑

Tab. 4: Rho proteins and Cathepsin are differentially expressed in FV-infected versus uninfected BMDC in a genotype-dependent - or -independent manner (↑ upregulated, ↑↑ strongly upregulated, ↓ downregulated).

Due to these results, the endocytotic activity of FV-infected BMDC was analyzed in more detail. Fig. 18 shows that upon FV infection, the endocytotic activity of BMDC was significantly increased.

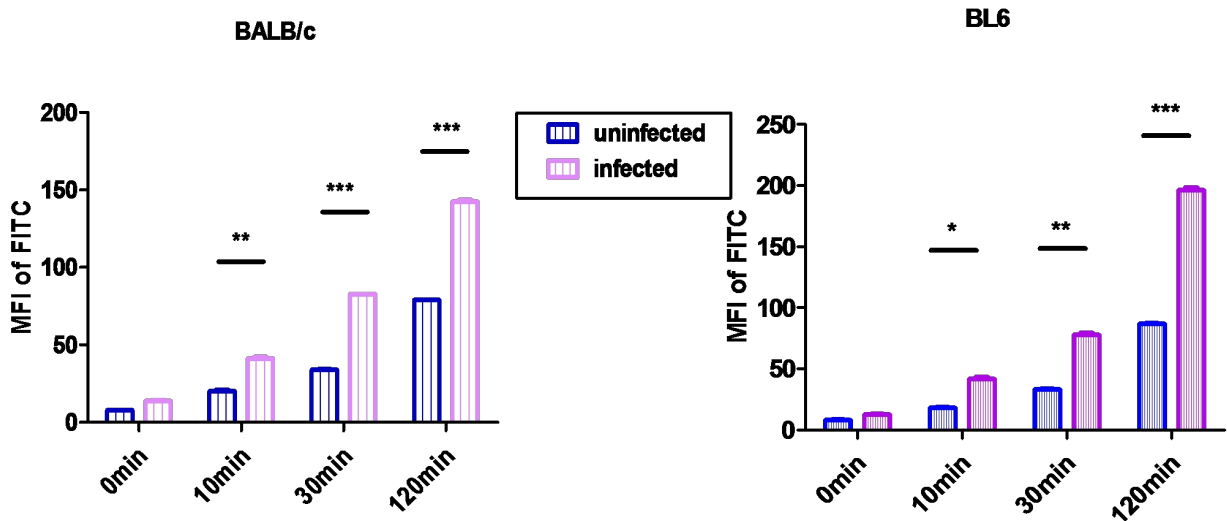


Fig. 18: FV-infected and uninfected BMDC show differences in endocytosis in a genotype-independent manner. 7 days post FV infection, BM was isolated from femurs of mice. FV-infected BM cells were separated by immunomagnetic positive selection using a p34-specific antibody. FV-infected and uninfected BM cells were incubated with GM-CSF to induce DC differentiation. Both uninfected and FV-infected BMDC (BALB/c and C57BL/6) were harvested on day 6 of culture. Uninfected and FV-infected BMDC were incubated with FITC-OVA at either 37°C or 4°C as a control. After 10, 30, and 120 minutes endocytotic uptake of FITC-OVA was stopped, cells were counterstained with anti-CD11c, and was examined by FACS. Data represent mean±SEM of five independent

experiments. Statistically significant differences between groups are indicated (\*  $p < 0.05$ , \*\*  $p < 0.01$ , \*\*\*  $p < 0.001$ ).

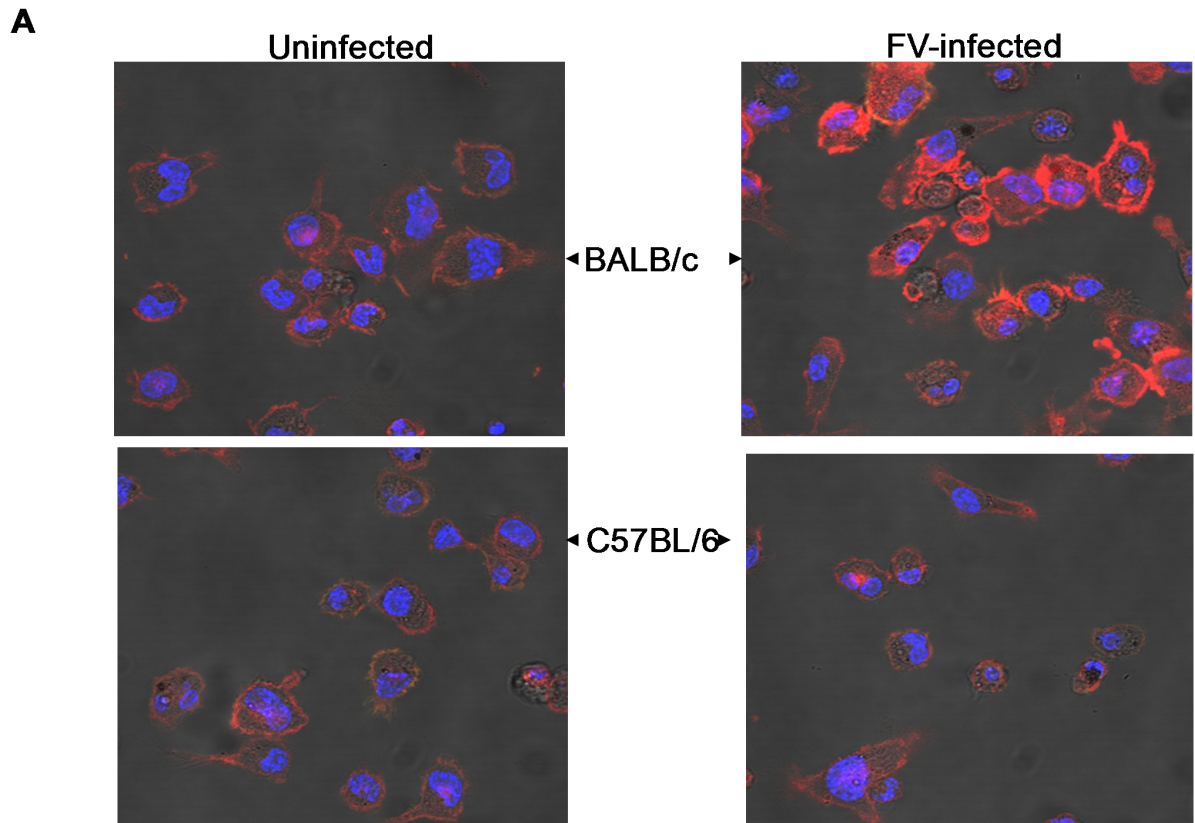
### 3.1.9. FV-infected BMDC are characterized by a higher content of F-actin in a mouse strain-specific manner

In general, the concerted activity of cytoskeletal proteins is critical for numerous physical cellular processes, including cell adhesion and migration. The function of DC critically depends on a coordinated cytoskeletal activity, which is essential not only for DC migration from peripheral tissues to lymphatic organs, but also for Ag uptake and formation of the immunological synapse during Ag presentation. Tab. 5 shows FV-induced alterations of cytoskeletal proteins in BMDC of BALB/C and C57BL/6 background mice as detected by proteome analysis.

	<b>C57BL/6</b>	<b>BALB/c</b>
Myosin 10	↑	↑↑
Filamin A	↑↑	↑
ARPC4	↑	○
Tubulin A8	○	↑
Tubulin B2B	↑	○
Tubulin B6	○	↑
Talin 1	○	↑
Tropomyosin A3	↑	○

**Tab. 5: Cytoskeletal proteins are differentially expressed in FV-infected versus uninfected BMDC in a genotype-dependent or -independent manner (↑ upregulated, ↑↑ strongly upregulated, ↓ downregulated).**

Due to the differential regulation of a number of proteins known to affect the actin cytoskeleton in BMDC infected with FV, as a more general readout we monitored the F-actin content in unstimulated BMDC populations. Fig. 19 (A, B) shows that in FV-infected BMDC of BALB/c genotype the content of F-actin was higher than in uninfected BMDC. However, in case of C57BL/6 BMDC the F-actin content was not affected by FV infection in.



### F-actin mean intensity (CLSM)

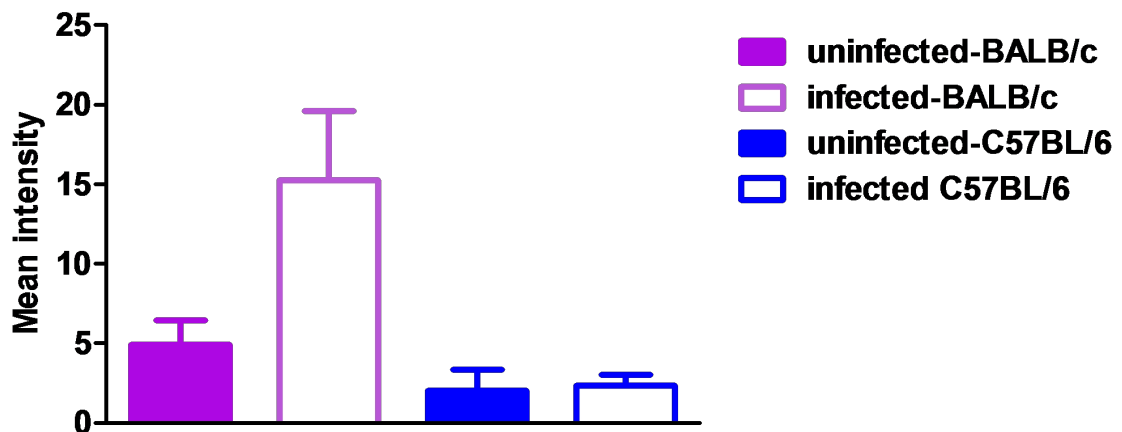
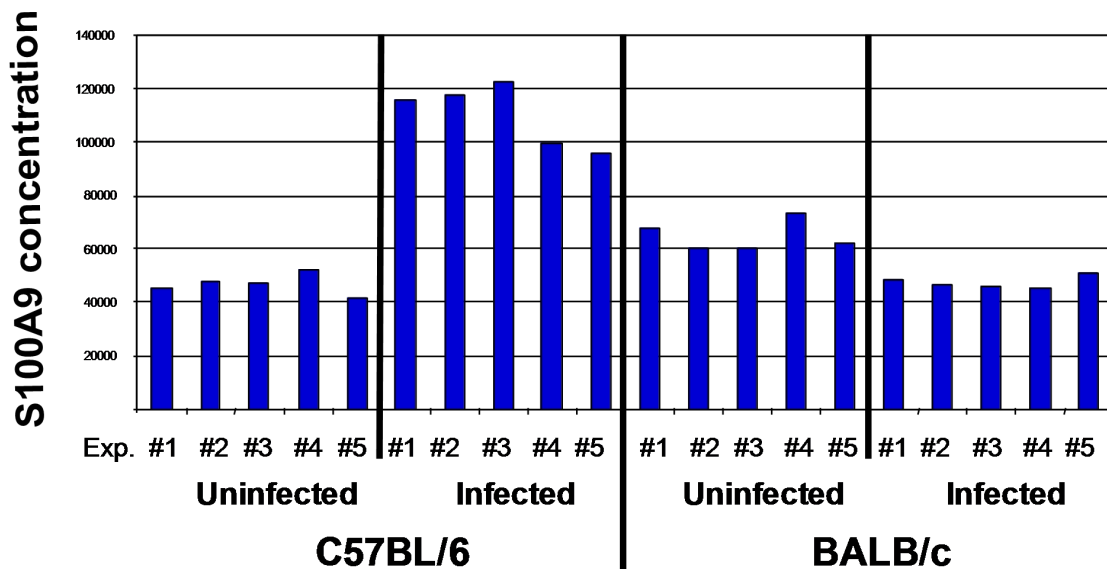


**Fig. 19: The F-actin content of BMDC is affected by FV infection in a genotype-dependent manner.** 7 days post FV infection, BM was isolated from femurs of mice. FV-infected BM cells were separated by immunomagnetic positive selection using a p34-specific antibody. Uninfected and FV infected BM cells were incubated with GM-CSF for 6 days to generate BMDC. On day 6, immature BMDC were harvested. **(A)** Uninfected and FV-infected DC ( $5 \times 10^5$ ) were seeded into cell chambers and stained with anti-F-actin antibody (red) and DAPI (blue), and were analyzed by CLSM. **(B)** The expression levels of F-actin in DC were quantified by measuring the mean relative fluorescent intensities of the images. Data represents mean  $\pm$  SEM of  $5 \times 10^4$  DC).

### 3.1.10. S100A9 expression is upregulated in FV-infected BMDC in a genotype-dependent manner

Besides a differential expression of molecules that control endocytosis and cytoskeletal activity, the protein mass array analysis also revealed an enhanced content of S100A9 in FV-infected versus uninfected BMDC of C57BL/6, but not of BALB/c genotype (Fig. 20A). In accordance, qPCR analysis showed that S100A9 mRNA levels were enhanced in unstimulated FV-infected BMDC of C57BL/6 genotype only (Fig. 20B). After stimulation of DC with LPS, S100A9 mRNA expression decreased in all DC populations.

**A**



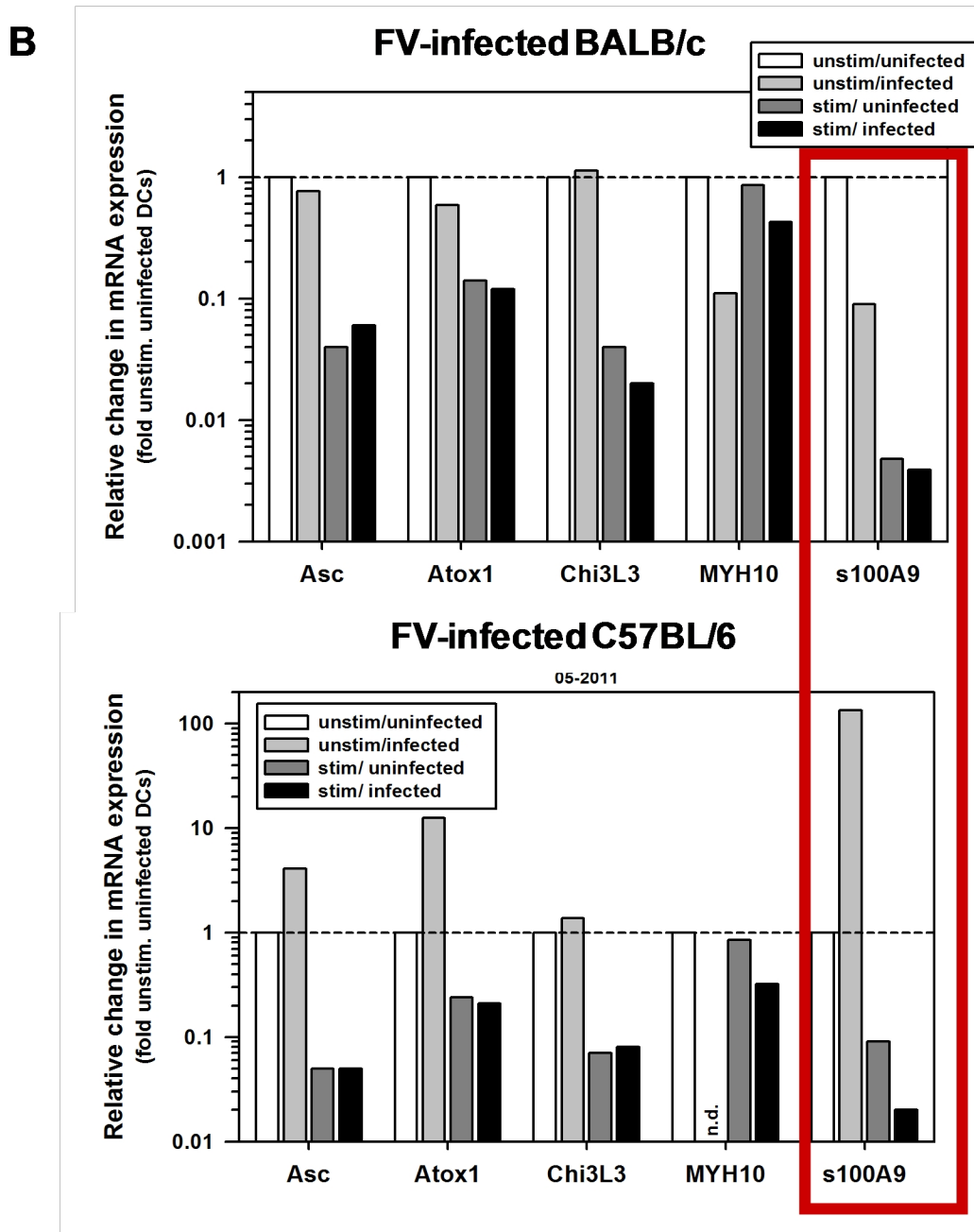


**Fig. 20: S100A9 is differentially expressed in FV-infected BMDC in a genotype-dependent manner.** 7 days post FV infection, BM was isolated from femurs of mice. FV-infected BM cells were separated by immunomagnetic positive selection using a p34-specific antibody. Uninfected and FV infected BM cells were incubated with GM-CSF for 6 days to generate BMDC. On day 6, immature BMDC were harvested. **(A)** S100A9 protein content in BMDC samples as assessed by protein mass array analysis. **(B)** S100A9 mRNA levels in unstimulated and LPS-stimulated BMDC populations of either genotype (upper part: C57BL/6, lower part: BALB/c) were monitored by qPCR analysis.

### **3.1.11. S100A9 may contribute to prevent cellular FV infection**

#### **3.1.11.1. More FV infected BMDC were detected in S100A9 KO mice after FV infection**

S100A8 and S100A9 are two members of the S100 family calcium-binding proteins that form a heterodimer termed calreticulin, which was originally discovered as a protein that highly expressed and secreted by granulocytes, monocytes, and early differentiation states of macrophages (Gebhardt, 2006). Subsequently, calreticulin has emerged as an important pro-inflammatory mediator in acute and chronic inflammation (Ehrchen *et al.*, 2009). Moreover, increased S100A8 and S100A9 levels were also detected in various human cancers, abundantly expressed in neoplastic tumor cells as well as infiltrating immune cells (Arai *et al.*, 2008). So far, many functions have been proposed for S100A8/A9 (Gebhardt, 2006), but to a large extent its biological role still remains to be defined. In this study, significant alterations in the expression of S100A9 in BMDC of FV- susceptible and resistant mouse strains were detected (Fig. 20A, Fig. 20B), which raised the hypothesis that S100A8/S100A9 may play a role in FV-induced immune responses.

For this, friend virus complex was injected *i.v.* into S100A9 knockout mice (C57BL/6 background). Seven days after infection, FV-BM was isolated and FV-glycosylated Gag positive BM cells were sorted for the generation of infected BMDC. On day 6, immature BMDC were stained as well as for the expression of FV-glycosylated Gag. As shown in Fig. 21, S100A9<sup>-/-</sup>BMDC were characterized by a higher frequency of FV-infected cells as compared with WT BMDC.

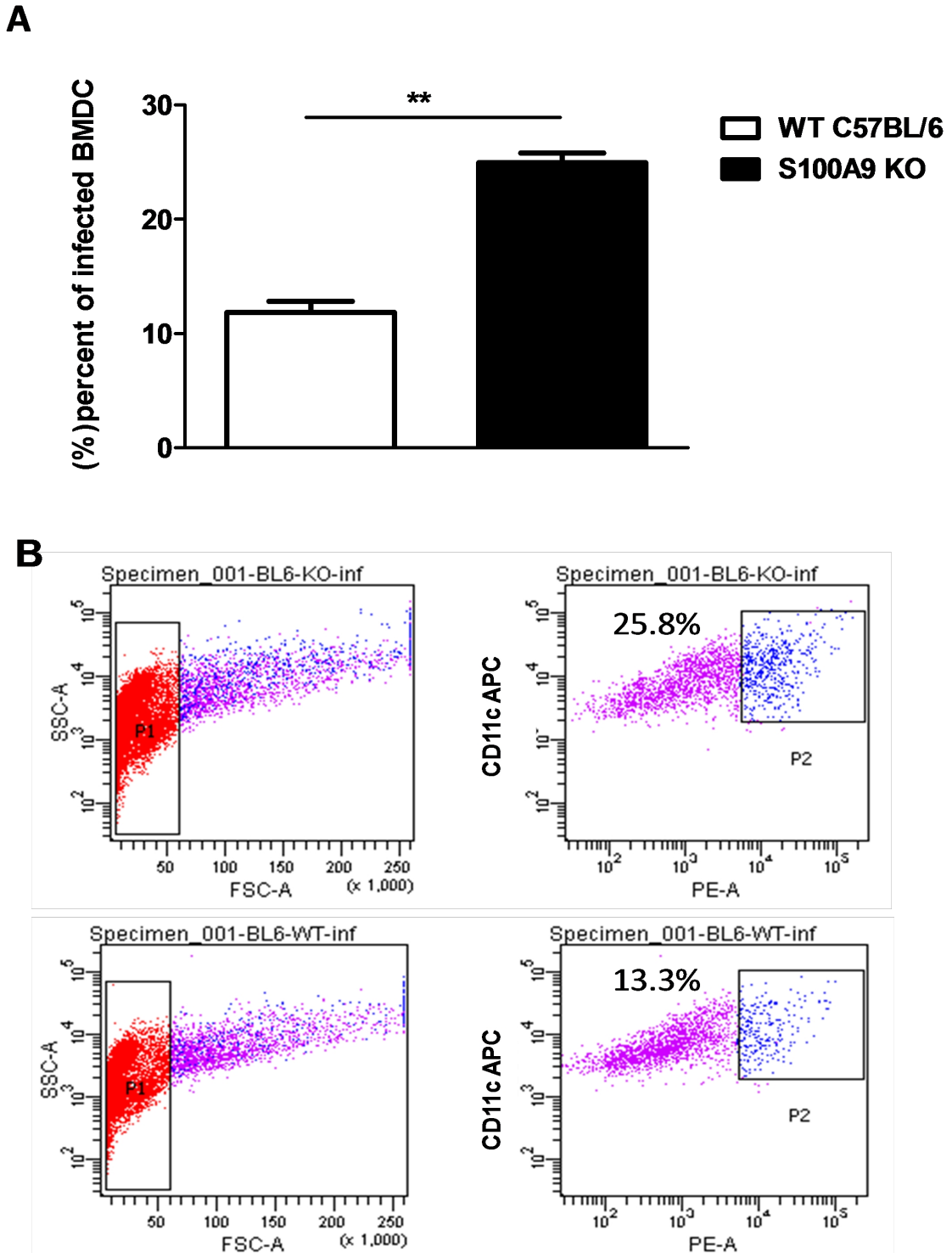


**Fig. 21: S100A9<sup>-/-</sup> BMDC are infected by FV at higher frequency than WT BMDC.** Seven days post infection with FV, BM was isolated from the femur of mice (9 mice per group). FV-infected BM cells were separated by positive selection using an antibody against a FV encoded protein (anti-mAb 34 and PE conjugated secondary AB). FV infected BM cells were incubated with GM-CSF for 6 days. On day 6 of culture, BMDC were costained with anti-mAb34 antibody against the FV encoded protein and anti-CD11c antibody. **(A)** Data represent mean $\pm$ SEM of frequencies of double positive cells obtained from each 9 mice per group of 2 experiments. Statistically significant differences between groups are indicated (\*\*  $p < 0.01$ ). **(B)** Raw FACS original data. Results from one out of 2 independent experiments (9 mice per group) are shown.



### 3.1.11.2. S100A9 is required for the acquisition of enhanced motility of FV-infected C57BL/6 BMDC

Migration of DC to draining LNs is a key step in the initiation of immune responses. Therefore, the motility of FV-infected BMDC with C57BL/6 background derived from WT and S100A9<sup>-/-</sup> mice was assessed. The result shown in Fig. 22 indicates that FV-infected WT BMDC showed a statistically significant increase in their motility compared to control DC. This infection-associated effect was abrogated in S100A9<sup>-/-</sup> BMDC.

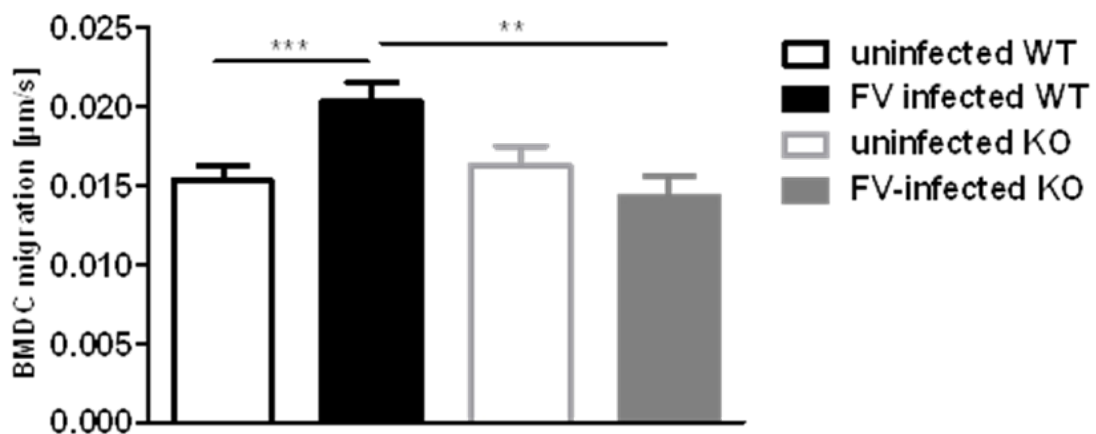


**Fig. 22: FV-infected S100A9<sup>-/-</sup>BMDC from S100A9 KO mice fail to increased motility.** Seven days post FV infection, BM was isolated from the femur of FV-infected WT and S100A9<sup>-/-</sup> mice, and BMDC were differentiated from sorted FV-infected BM cells. FV-infected BM cells were incubated with GM-CSF for 6 days. On days 6 of DC culture, BMDC were harvested and their spontaneous migratory speed was analyzed. Data represent mean±SEM of 30 DC per group. Statistically significant differences between groups are indicated (\*\* p<0.01, \*\*\* p<0.001).

### 3.1.11.3. The expression of APOBEC3 is reduced in S100A9<sup>-/-</sup>BMDC

As described in 2.5.3, several groups have shown that mA3 restricts infection of Friend murine leukemia virus. The results presented in this study( in 3.1.10.1 and 3.1.10.2 ) showed that S100A9 KO mice were more susceptible towards FV infection on cellular level as reflected by higher frequencies of FV-infected BM cells and derived BMDC. Therefore, we investigated the expression of mA3 in BMDC derived from S100A9<sup>-/-</sup> mice by. The result showed in Fig. 23 suggests that S100A9<sup>-/-</sup>BMDC express lower level of mA3 than WT BMDC.

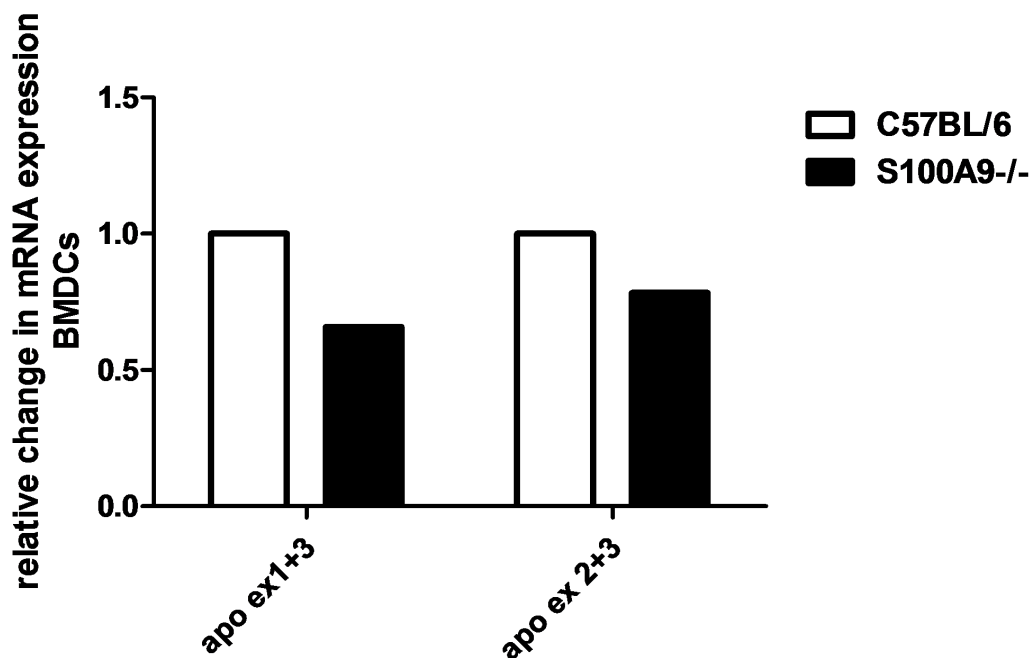


**Fig. 23: mA3 RNA is expressed at lower levels in S100A9<sup>-/-</sup>BMDC.** BM cells were isolated from the femur of each on WT and S100A9<sup>-/-</sup> mouse, and incubated with GM-CSF for 6 days to differentiate DC. On day 7 of culture, BMDC were harvested, and expression of mA3 mRNA was monitored by qPCR analysis. Data represent mean $\pm$ SEM of 1 experiment performed in duplicate.

### 3.1.11.4. Recombinant S100A8/9 enhances the expression of APOBEC3 in C57BL/6 BMDC

A study from Okeoma *et al.*(2009) has shown that the bacterial TLR ligand LPS induced mA3 expression in BMDC, and virus restriction in different inbred mouse strains upon *in vivo* application. S100A8/9 constitutes an alternative TLR4 ligand. Therefore, effects of exogenous S100A8 and S100A9 homo- and heterodimers on mA3 expression in BMDC were monitored. As shown in Fig. 24, the level of total mA3 and its isoforms  $\delta$  ex2 and  $\delta$  ex5 were significantly increased when S100A8/9 was used for BMDC stimulation. In contrast, neither LPS nor S100A8 and S100A9 homodimers, respectively, exerted any stimulatory effect on mA3 expression.

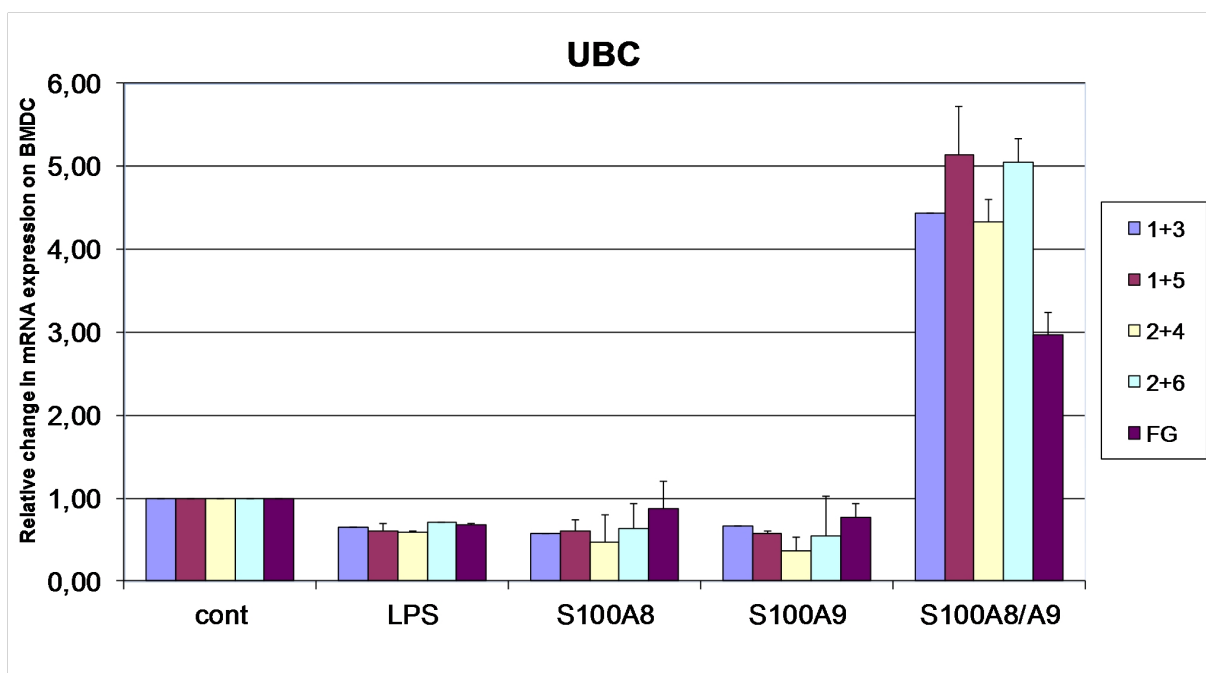


**Fig. 24:** The expression of mA3 in C57BL/6 BMDC was increased upon stimulation with S100A8/9. BM cells were isolated from femurs of C57BL/6 mice, and incubated with GM-CSF to differentiate DC. On day 7 BMDC were harvested, reseeded ( $10^6$ /ml in 1 ml) and either left untreated or incubated with LPS or either of the S100 proteins indicated (each 1  $\mu$ g/ml) for 24h. Afterwards, mRNA expression of total APOBEC3 and its isoforms was monitored by real time PCR analysis. Data represent mean  $\pm$  SEM of two independent experiments performed in duplicate.

### 3.2. Dextran-based nanoparticles induce strong antigen-specific cellular and humoral responses

To exploit the potential of DC for immunotherapeutic applications, in another project of this PhD study the usability of different types of functionalized nanoparticles to serve as a DC-addressing nanocarrier platform was tested.

#### 3.2.1. Shape and size of OVA-containing dextran-based nanoparticles

Dextran (DEX)-based nanoparticles containing OVA protein, LPS, or both compounds in combination, were generated as described in the experiments procedures. After preparation, the different types of DEX-based particles were resuspended in PBS for subsequent analysis. To determine concentrations of DEX-encapsulated OVA protein, particles were disrupted by ultrasonication, and analyzed by BCA Assay. By this assay, OVA-containing DEX particles were shown to contain about 200  $\mu\text{g}$  of OVA/ $\mu\text{l}$  of undiluted DEX particles. By LAL assay, DEX(LPS) were determined to contain about 13 pg of surface accessible LPS per  $\mu\text{l}$  of undiluted DEX particles, while control DEX particles (DEX[-]) were devoid of LPS.

As assessed by electron microscopy, DEX[-] were of spherical shape and rather uniform in size (Fig. 25A). DEX formulations containing OVA and LPS either alone or in combination were comparable in terms of appearance and size (data not shown). Their actual size in solution was analyzed by dynamic light scattering (experiments were performed by Prof. Schmidt, Institute of Physical Chemistry, Johannes Gutenberg University). The angular dependency of the hydrodynamic radius of DEX[-] is shown in Fig. 25B. Extrapolation to  $q=0$  resulted in the z-average value of the hydrodynamic radius of the DEX particles  $\langle R_h^{-1} \rangle_z^{-1} = 23 \text{ nm}$ .

Next, we monitored potential cytotoxic effects of different DEX formulations. For this, BMDC were incubated with DEX[-] at amounts as indicated, and BMDC viability was assessed one day later. In the range of concentrations tested, neither DEX formulation affected BMDC viability to a significant extent (data not shown).

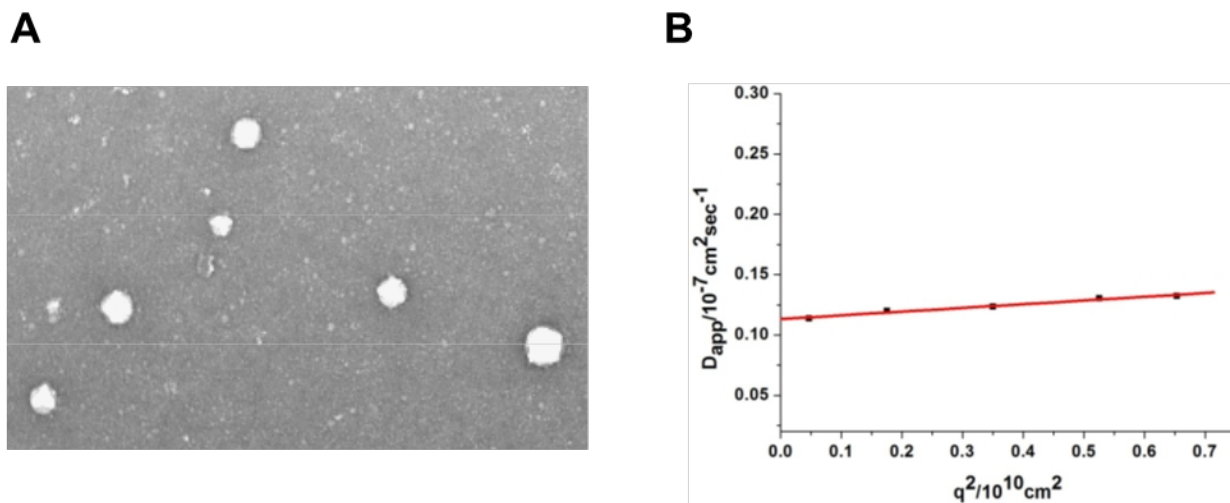


**Fig. 25: DEX particles are of spherical appearance and uniform in size. Left:** Shape distribution of DEX[-] dispersed in PBS were studied by electron microscopy. **Right :**Hydrodynamic radii of Dextran T500 and derived DEX particle formulations as function of  $q^2$  in DPBS buffer (0.33 mg/ml) were determined by DLS (see Methods). Graphs denote the angular dependency of the apparent diffusion coefficient of the different dextran solutions in buffer solution.

### 3.2.2. OVA-containing DEX nanoparticles are engulfed by BMDC in a mannose receptor-dependent manner

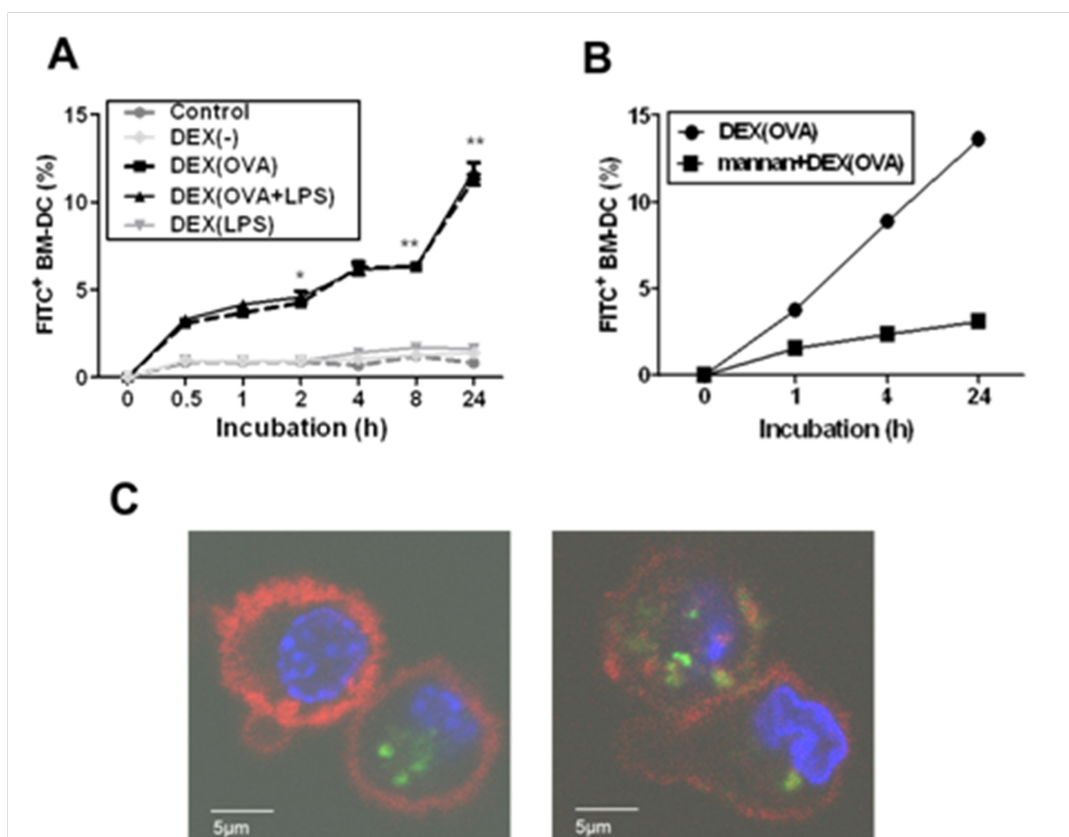
In order to monitor intracellular uptake of DEX-based particles by BMDC, unstimulated BMDC were coincubated with FITC-labeled DEX particles, and the frequency of FITC<sup>+</sup> CD11<sup>+</sup>BMDC was determined by FACS analysis over time. DEX formulations devoid of OVA protein showed very little uptake by BMDC over 24 hr of coincubation (Fig. 26A). In contrast, incubation with OVA-containing DEX formulations resulted in a steadily increasing frequency of FITC<sup>+</sup>BMDC over the period of time monitored. Confocal microscopy confirmed cellular uptake of OVA-containing DEX particles by BMDC (Fig. 26C) as assessed at 4 hr (left panel) and 24 hr (right panel) after the onset of coincubation.

In several reports, OVA protein has been shown to constitute a mannose receptor (MR) ligand due to its mannosylated state. In light of the OVA-dependent uptake of DEX particles by BMDC, we determined the functional relevance of this receptor for OVA uptake. In competition experiments, preincubation of BMDC with the prototypic MR ligand mannan at high concentration significantly reduced cellular binding of

subsequently applied DEX(OVA) as reflected by lower frequencies of FITC<sup>+</sup>BMDC (Fig. 26B).

Based on the result of MR-dependent cellular binding of DEX, next we evaluated the suitability of OVA-containing DEX to specifically target primary APC as well, an important prerequisite for their intended application *in vivo*. For this, isolated spleen cells were coincubated with FITC-labeled DEX formulations for 24 hr, and for different immune cell types the frequencies of FITC<sup>+</sup> cells were assessed afterwards. As shown in Fig. 26D, only CD11c<sup>+</sup>DC and F4/80<sup>+</sup> macrophages efficiently bound FITC<sup>+</sup> DEX(OVA+LPS), but not control DEX particles. In contrast, both CD19<sup>+</sup> B cells and CD3<sup>+</sup> T cells, known to lack MR expression, showed no efficient binding of either DEX formulation.

These results show that DEX particles were not incorporated efficiently by any cell type tested *per se*, but may require binding of OVA to the MR for efficient receptor-mediated uptake. Interestingly, as shown for BMDC, the TLR4 ligand LPS had no influence on the engulfment of OVA-containing DEX particles. Moreover, in agreement with the expression pattern of the MR *in vivo*, largely confined to myeloid APC, only DC and macrophages efficiently bound an OVA-containing DEX formulation, thereby confirming its general suitability for APC-targeted vaccination *in vivo*.



**D**

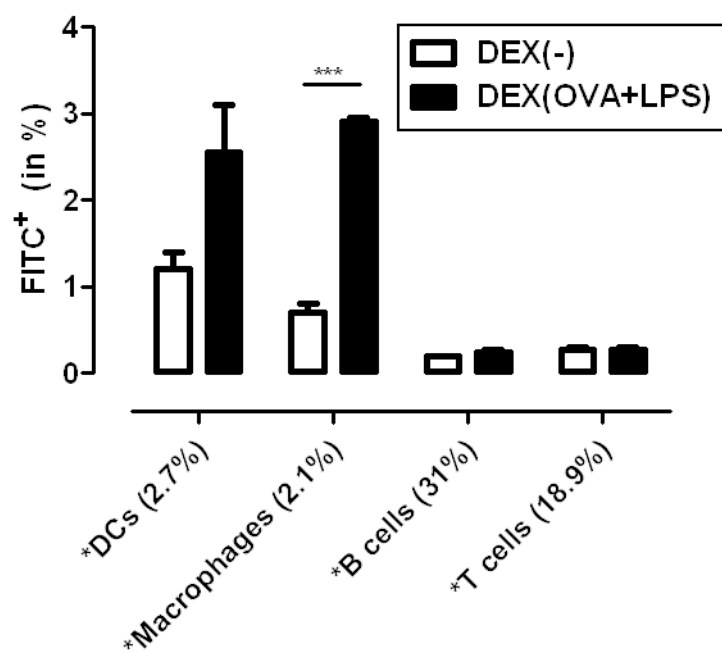


**Fig. 26: BMDC engulf DEX particle formulations in an OVA-dependent manner, mainly via the MR (A-C).** Aliquots of unstimulated day 6 BMDC ( $5 \times 10^5$  cells; C57BL/6) were left untreated [control] or were coincubated with FITC-labeled DEX formulations in duplicates as indicated (each 50  $\mu$ l). **(A)** Aliquots were removed after the indicated period of time, and the frequencies of FITC<sup>+</sup>CD11c<sup>+</sup>BMDC were assessed by flow cytometry. Data represent mean $\pm$ SEM of duplicates and are representative of three independent experiments. Statistically significant differences between OVA-containing DEX formulations (DEX[OVA], DEX[OVA+LPS]) and the corresponding control group (DEX[-], DEX[LPS]) are indicated for each time point (\*  $p < 0.05$ , \*\*  $p < 0.01$ ). **(B)** In parallel cultures, aliquots of BMDC were left untreated or were incubated with mannan at high dose (200  $\mu$ g/ml) for 30 min. Afterwards, DEX(OVA+LPS) was added to either group. Aliquots of BMDC were harvested at the indicated time points, stained for CD11c, and analyzed by flow cytometry. **(C)** Cellular uptake of FITC-labeled DEX(OVA) by BMDC, stained with anti-CD11c antibody (red) and DAPI(blue), was assessed by confocal laser scanning microscopy 4 h (left panel) and 24 h (right panel) after onset of coincubation. Data represent mean $\pm$ SEM of duplicates and are representative of three independent experiments.**(D)**Spleen cells derived from C57BL/6 mice ( $2 \times 10^6$  cells/200 $\mu$ l) were left untreated (data not shown) or were coincubated with FITC-labeled DEX formulations as indicated (each 30  $\mu$ l) for 24h. Afterwards, the cells were stained with either of the indicated cell lineage markers (DC: CD11c-PE-Cy7, macrophages: F4/80-eFlour405, B cells: CD19-APC, T cells: CD3-PE), and the frequencies of FITC<sup>+</sup> populations of either group were assessed by flow cytometry. Data represent mean $\pm$ SEM of three independent experiments. Numbers in brackets indicate the overall frequency of either cell lineage within the spleen cell suspension.

### 3.2.3. BMDC incubated with particulate OVA induce robust antigen-specific CD4<sup>+</sup> T cell proliferation

Exogenous proteins engulfed by DC are degraded in the late endosomal/lysosomal compartment. Oligopeptides derived from this compartment are loaded onto MHCII molecules for presentation to CD4<sup>+</sup> T cells. In order to assess the efficacy of DEX to cross present OVA protein after intracellular uptake, BMDC were incubated with equal amounts of OVA, which was applied either in soluble form or as DEX-based formulations, in either case either alone or in combination with LPS. One day later, BMDC were incubated with OVA-peptide specific OT-II CD4<sup>+</sup> T cells, and their proliferation was assessed after three days of DC/T cell coculture (Fig. 27A).

BMDC preincubated with soluble OVA protein alone induced no marked T cell proliferation. Only BMDC treated with soluble OVA plus soluble LPS induced considerable OT-II proliferation. On the other hand, incubation of BMDC with DEX(OVA) at a equimolar dose as soluble OVA facilitated T cell activation, which was further enhanced by application of DEX containing both OVA and LPS (DEX[OVA+LPS]).



Due to the strong bioactivity of OVA when applied as a particulate formulation, we asked for the suitability of DEX particles to mount an OVA-specific CD4<sup>+</sup> T cell response when applied directly *in vivo*, which requires targeting of MR-expressing APC. To this end, OT-II T cells were labeled with CFSE and were injected i.v. into C57BL/6 mice. Two days later, groups were treated with soluble OVA plus LPS, or with DEX formulations containing either OVA alone, or in combination with LPS (DEX[OVA]+LPS), or with DEX particles loaded with both compounds (DEX[OVA+LPS]). All groups received equimolar amounts of OVA. Four days later, the extent of OVA-dependent proliferation of CFSE-labeled OT-II T cells was analyzed by flow cytometry. As shown in Fig. 27B, in all groups of mice which had received OVA plus LPS, strong proliferation of OT-II T cells was detected.

These data confirm that coadministration of particulate OVA plus LPS resulted in antigen specific T cell proliferation also when applied *in vivo*. Therefore, DEX-based formulations may qualify as nanovaccines suitable for APC-focused delivery of antigen and adjuvant *in vivo*.

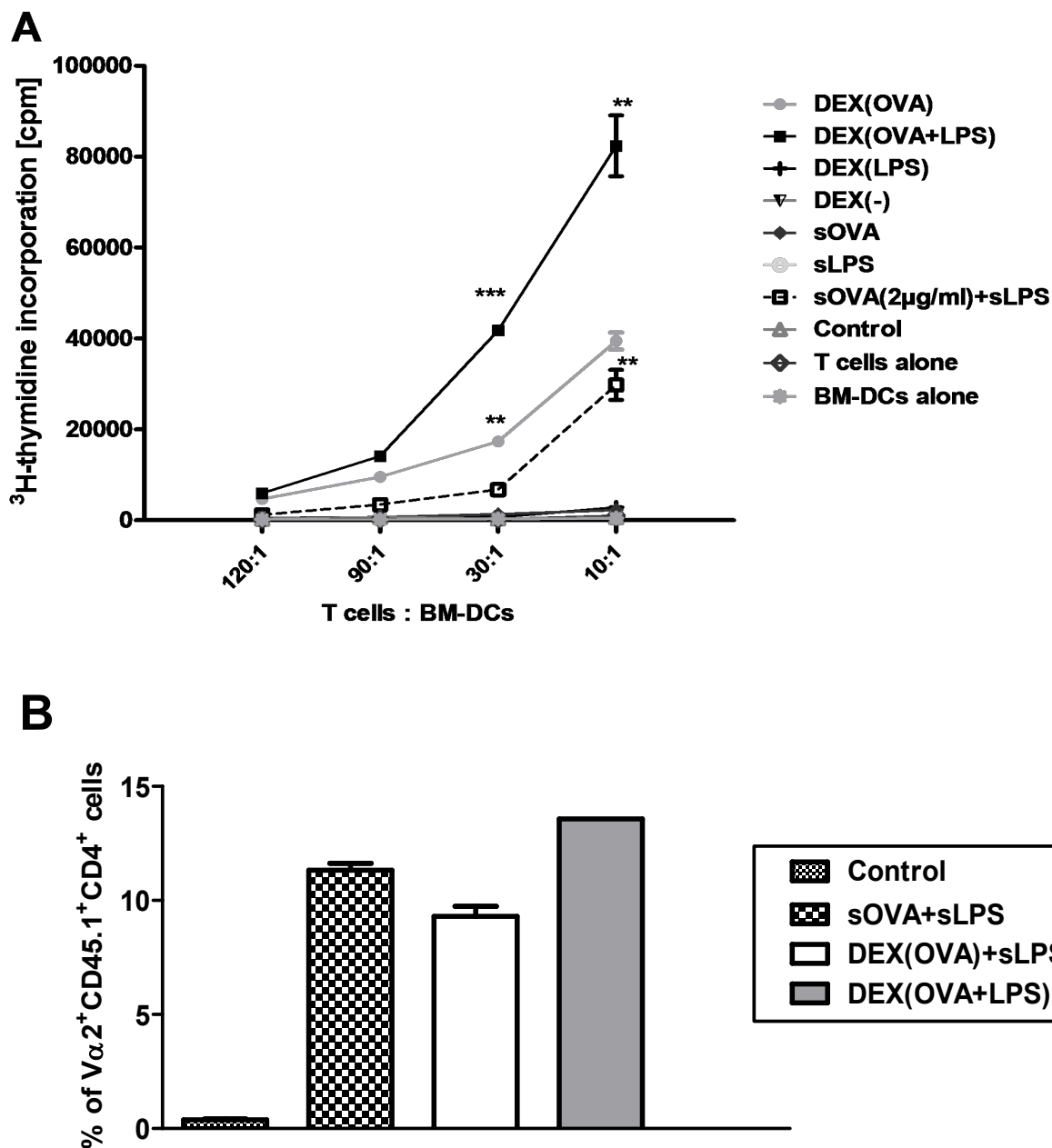


**Fig. 27: BMDC are strongly activated by LPS-containing DEX particle formulations, and codelivery of OVA results in robust antigen-specific  $CD4^+$  T cell activation. (A)** Unstimulated day 6 BMDC ( $10^6$  cells; C57BL/6) were treated with soluble OVA (2  $\mu\text{g}$ ) and soluble LPS for 24 hr. Titrated numbers of BMDC were cocultured with sorted  $CD4^+$  OT-II T cells in triplicates for 3 days at the indicated ratios. T cell proliferation was assessed as incorporation of  $^3\text{H}$ -thymidine added for the last 16-18h of culture. Data represent mean $\pm$ SEM of triplicates and are representative of three independent experiments. **(B)** Mice (BALB/c) received CFSE-labeled OVA-specific OT-II T cells ( $10^7$ ) *i.v.* Two days later, mice (three animals per group) were immunized *i.v.* with OVA (4  $\mu\text{g}$  per mouse), LPS (0.4  $\mu\text{g}$ ), and DEX particle formulations (200  $\mu\text{l}$ ) as indicated. After another three days, frequencies of  $CD4^+CD45.1^+V\alpha 2^+$  OT-II T cells in spleen cell suspensions were analyzed by flow cytometry. Data represent mean $\pm$ SEM of 5 mice per group of one from 3 independent experiments. The frequency of proliferating  $CD4^+$  OT II T cells in either treated group was significantly higher than in the non-immunized control group.

### 3.2.4. DEX-based nanovaccines induce strong CD8<sup>+</sup> T cell activation and strong cytotoxic activity of CD8<sup>+</sup> T cells *in vivo*

To assess the suitability of DEX-based nanovaccines to evoke robust CD8<sup>+</sup> T cell responses, splenocytes derived from OT-I mice bearing OVA peptide-specific CD8<sup>+</sup> T cells were labeled with CFSE and injected i.v. into syngeneic C57BL/6 mice. After two days, groups of mice were cotreated with LPS plus either OVA or DEX[OVA], or with DEX[OVA+LPS]. All groups received equimolar amounts of OVA. Four days later, the *in vivo* proliferation of CFSE<sup>+</sup> OT-I T cells was assessed in spleen cell suspensions.

In all groups immunized with OVA, OT-I T cell proliferation was significantly higher than in the untreated control group (Fig. 28A). In comparison, coapplication of soluble OVA and LPS mounted low T cell proliferation only, which was significantly enhanced upon prior immunization with OVA as a particulate formulation (DEX[OVA]), coadministered with soluble LPS. DEX particles loaded with OVA plus LPS (DEX[OVA+LPS]) evoked the strongest OVA-specific CD8<sup>+</sup> T cell proliferation of all groups compared. Similar to the extent of OT-I proliferation, the frequency of OT-I T cells producing the TH1 cytokine INF $\gamma$  was lowest in mice treated with sOVA plus sLPS, intermediate when DEX(OVA) plus sLPS had been coapplied, and highest in the group pretreated with the DEX-based nanovaccine containing OVA and LPS in combination (Fig. 28B).

These findings suggest that DEX-based nanovaccines applied *in vivo* were engulfed by DC, solely capable to mediate cross-presentation of processed OVA peptides. Moreover, the adjuvant LPS exerted higher bioactivity when applied in its particulate state in mediating APC stimulation than when injected in a soluble form.

The finding of robust CD8<sup>+</sup> T cell proliferation and INF $\gamma$  production as induced by DEX-based nanovaccines *in vivo* prompted us to assess the functional activity of OT-I T cells, as reflected by their cytotoxic activity. Splenocytes derived from OT-I mice were injected i.v. into C57BL/6 mice. Two days later, groups of mice were treated with OVA, LPS, and DEX-based nanovaccines as indicated at equivalent OVA doses. After 5 days, splenocytes from syngeneic Ly5.1 mice were labeled with CFSE at low or high dose, and the latter were pulsed with OVA<sub>257-264</sub> peptide as recognized by OT-

I CD8<sup>+</sup> T cells. Four hours later, spleen cell suspensions were analyzed for the frequency of CFSE<sup>high</sup> OVA peptide-presenting target cells.

In this *in vivo* killing assay target cell lysis occurred only in groups of mice pretreated with OVA and LPS (Fig. 28C, D). Coadministration of soluble OVA and LPS resulted in considerable target cell lysis, which was somewhat elevated in the group which had received OVA as a DEX-based formulation plus LPS. However, the strongest CTL response was obtained in mice pretreated with the DEX-based nanovaccine that codelivered OVA and LPS. These findings indicate that the nanovaccine DEX[OVA+LPS] constitutes a potent inducer of antigen-specific cytotoxic T cells.

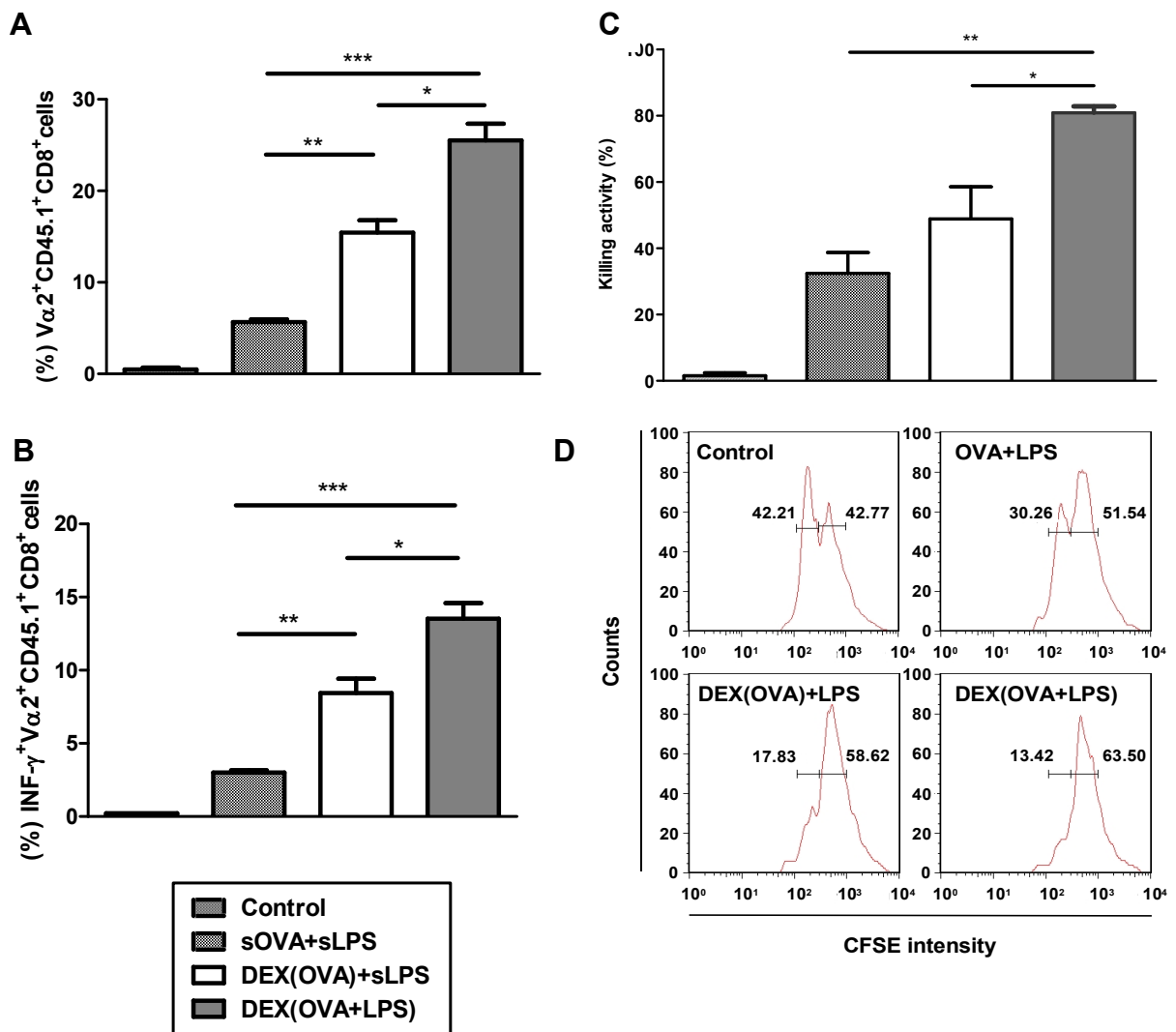


**Fig. 28: The nanovaccine DEX(OVA+LPS) induces profound activation of antigen-specific CD8<sup>+</sup> T cells *in vivo*.** C57BL/6 mice received CFSE-labeled, OVA-specific OT-I T cells ( $10^7$ ) *i.v.* Two days later, groups of mice (each five animals) were either left untreated or were immunized with OVA (4  $\mu$ g per mouse), LPS (4  $\mu$ g), and DEX particle formulations (each 200  $\mu$ l) as indicated. **(A)** On day 3, the frequency of CD8<sup>+</sup>CD45.1<sup>+</sup>V $\alpha$ 2<sup>+</sup> OT-I cells was determined in spleen cell suspensions by flow

cytometry. **(B)** In the same experiments, the frequencies of IFN $\gamma$ <sup>+</sup> OT-I T cells were assessed by flow cytometry. **(A, B)** Data represent mean $\pm$ SEM of two independent experiments. The frequencies of proliferating and IFN- $\gamma$  producing CD8<sup>+</sup> OT-I T cells in either group were significantly higher than in the non-immunized control group. Other statistically significant differences between groups are indicated (\* p<0.05, \*\* p<0.01, \*\*\* p<0.001). **(C)** On day 4 after immunization, mice were injected with CFSE<sup>low</sup> target cells (loaded with OVA<sub>257-264</sub>) and CFSE<sup>high</sup> control cells (each 10<sup>7</sup> cells) derived from syngeneic Ly-5.1<sup>+</sup> mice. 4h later, splenocytes were isolated and frequencies of CFSE-labeled cell populations were assessed by flow cytometry. **(D)** Upper panel: Data represent mean $\pm$ SEM of two independent experiments. Statistically significant differences between groups are indicated (\* p<0.05, \*\* p<0.01). Lower panel: Frequencies of Ly-5.1<sup>+</sup> target cells (CFSE<sup>low</sup>) and control cells (CFSE<sup>high</sup>) in spleen cell suspensions derived from one mouse of either group. Graphs are representative of two independent experiments.

### 3.2.5. DEX particles which codeliver OVA and LPS induce a Th2-biased humoral response

As demonstrated, DEX-based nanovaccines induce APC-dependent T cell mediated immune responses. With regard to the essential role of humoral immune responses for pathogen clearance and their contribution to anti-tumor responses, we asked for the potential of DEX-based nanovaccines to mount production of OVA-specific antibodies. For this, naive mice were injected i.v. with the different DEX formulations, and sera derived from mice either one or two weeks later was assayed for OVA-specific IgG titers. At either time point, OVA-specific IgG1 and IgG2a were detected in sera obtained from mice injected with OVA-containing DEX only, thereby confirming antigen-dependency of antibody production (Fig. 29). As expected, OVA-specific antibody titers were higher when OVA plus LPS was codelivered than mounted in response to OVA alone. In either case, more IgG1 than IgG2a was detected, reminiscent of a Th2-skewed IgG pattern. These findings show that DEX-based nanovaccines are capable to induce both a cellular and a humoral immune response *in vivo*.

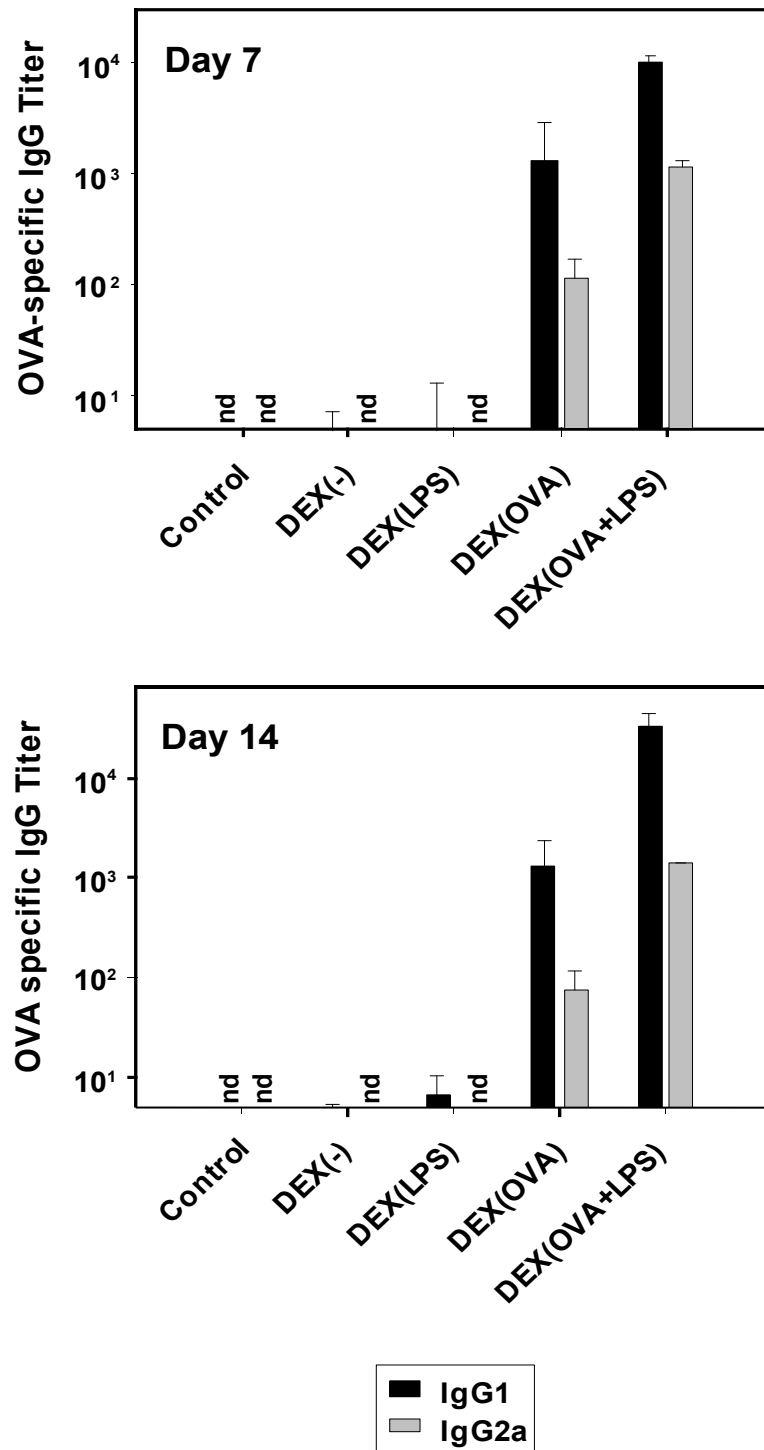


**Fig. 29: DEX formulations containing OVA elicit a specific Th2-biased humoral immune response, augmented upon codelivery of LPS.** Naive C57BL/6 mice (two mice per group) were immunized with DEX formulations as indicated. On days 7 (upper panel) and 14 (lower panel), mice were bled and derived sera were used for detection of OVA-specific IgG1 and IgG2a antibody titers. Data represent mean $\pm$ SEM of two sera per group.

### **3.3. Ferro-magnetic solid-core nanoparticles (NP) targeting DC induce antigen-specific cellular and humoral immune responses**

In this project, the suitability of solid core nanoparticles (NP) engineered to co-deliver a tumor model antigen and a DC adjuvant together with a DC-addressing antibody to induce potent antitumor immune responses in a therapeutic melanoma model was assessed.

#### **3.3.1. NP functionalized with a DC-targeting antibody are engulfed by BMDC**

In order to monitor binding of differentially functionalized NP to BMDC, unstimulated BMDC were coincubated with Cy5-labeled NP. In time kinetics assays the frequencies of Cy5<sup>+</sup>CD11<sup>+</sup>BMDC were determined by flow cytometry. NP formulations decorated with a control antibody (anti-human IL-5 antibody) showed moderate binding to BMDC over 24h of coincubation (Fig. 30A). In contrast, incubation of BMDC with NP functionalized with an anti-mouse DEC205-specific antibody (aDEC205), intended to specifically address this C-type lectin antigen uptake receptor, yielded a steadily increasing frequency of Cy5<sup>+</sup>CD11c<sup>+</sup>BMDC over the period of time monitored. Confocal microscopy confirmed a much stronger cellular binding of aDEC205 to BMDC (Fig. 30B, lower panel) than non-functionalized NP (Fig. 30B, upper panel) by BMDC as assessed 24h after the onset of coincubation. Based on this result, next the extent of binding of the different types of NP by CD8<sup>+</sup>CD11c<sup>+</sup>DC *in vivo* was analysed. For this, the different NP formulations were injected i.v into C57BL/6 mice. After 4 h, spleens were harvested, and the frequencies of Cy5<sup>+</sup>CD8<sup>+</sup>CD11c<sup>+</sup> were determined by flow cytometry. As depicted in Fig. 30C, primary CD8<sup>+</sup>CD11c<sup>+</sup>DC preferentially bound of NP formulations decorated with aDEC205.

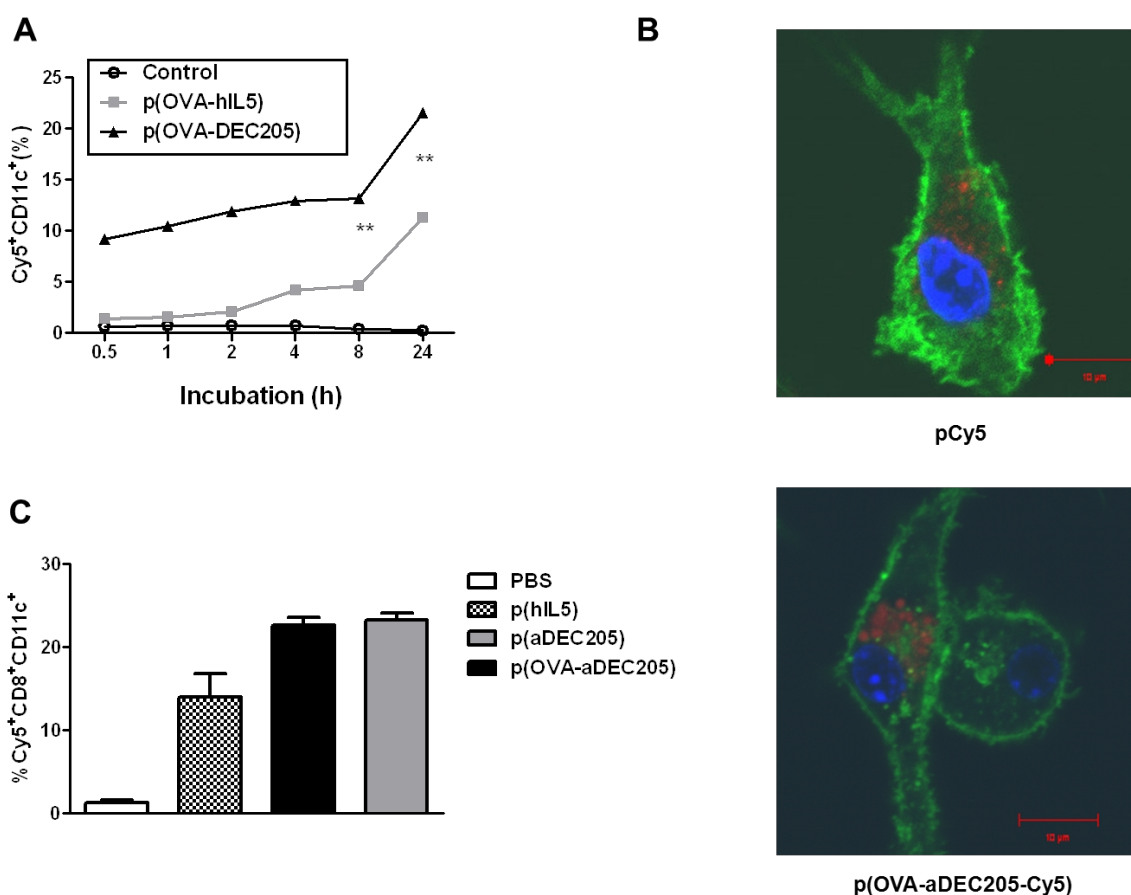


**Fig. 30: Functionalized NP are effectively engulfed by BMDC.** (A) Aliquots of unstimulated BMDC ( $0.75 \times 10^6$ ) were incubated in parallel settings in wells ( $500 \mu\text{l}$ ) of 24-well cell culture plates with each  $9.5 \times 10^9$  of either unloaded NP (p[-]) or with NP formulations coated with OVA plus either anti mouse DEC205 (p[OVA-aDEC205]) or anti human IL5 (p[OVA-anti-hIL5]) specific antibody, with the latter serving as a control for targeting specificity. All NP formulations were labeled with Cy-5. Aliquots of cells were removed after the indicated period of time, were stained with anti-CD11c antibody, and were analyzed by flow cytometry. Graphs denote the frequencies of Cy-5<sup>+</sup>CD11c<sup>+</sup> cells in the different groups for each time point. Data represent mean $\pm$ SEM of three independent experiments. Statistically significant differences between p(OVA-hIL5) and p(OVA-aDEC205) are indicated (\*\*  $p < 0.01$ ). (B) Cellular uptake of control NP (p[-]) (*upper panel*) and the DC-targeting NP formulation (p[OVA-aDEC205]) (*lower panel*) by BMDC as described in (A) was assessed by confocal laser scanning microscopy 24 h after the onset of coincubation. Cells were stained with anti-CD11c antibody (green) and DAPI (blue). Graphs are representative of 3 independent experiments (C). NP conjugated with aDEC205 antibody mediate efficient binding to primary CD11<sup>+</sup>CD8<sup>+</sup>DC *in vivo*. NP formulations conjugated either alone with the DC-targeting anti-DEC205 antibody (p[aDEC205]) or with OVA protein in addition (p[OVA-aDEC205]) were injected i.v. into mice (each  $3.7 \times 10^{12}$  nanoparticles). Control mice were injected with PBS. After 4 h, spleens were removed, CD8<sup>+</sup>CD11c<sup>+</sup>DC were isolated by immunomagnetic purification, and cells were subjected to analysis by flow cytometric analysis. Graphs denote the frequencies of Cy5<sup>+</sup>CD8<sup>+</sup>CD11c<sup>+</sup> cells in the different groups. Data represent mean $\pm$ SEM of 3 independent experiments.



### 3.3.2. DC-targeting NP coated with OVA protein induce robust antigen-specific T cell proliferation *in vitro*

Next, the capability of DC to process NP-delivered OVA protein (OVA) and to present derived antigenic peptides to antigen-specific T cells was analyzed. For this, unstimulated BMDC were incubated either with OVA protein or with equal amounts of NP-bound OVA (p[OVA-aDEC205], p[OVA-hIL5]). One day later, untreated or pretreated BMDC were cocultured with OVA-peptide specific CD8<sup>+</sup> (OT-I) and CD4<sup>+</sup> (OT-II) T cells, resp., and T cell proliferation was assessed after three days.

Unstimulated BMDC preincubated with soluble OVA protein or p(OVA-hIL5) induced no marked proliferation of antigen-specific CD8<sup>+</sup> (Fig. 31A) and CD4<sup>+</sup> (Fig. 31B) T cells. Only BMDC treated with the DC-targeting NP formulation p[OVA-aDEC205] induced considerable proliferation of either T cell population. To clarify whether DC targeting of aDEC205-conjugated NP was actually DEC205 receptor-dependent, BMDC were preincubated with a high concentration of anti-mouse DEC205 antibody prior to addition of the different NP formulations. This pretreatment affected only the proliferation of CD4<sup>+</sup> and CD8<sup>+</sup> T cells cocultured with the BMDC populations that were preincubated with the DEC205-targeting NP formulation. This clearly confirms that enhanced DC-specific endocytosis of particles is achievable through their conjugation with anti-DEC-205 mAbs, and that such NP are suitable for transfer of protein antigen.

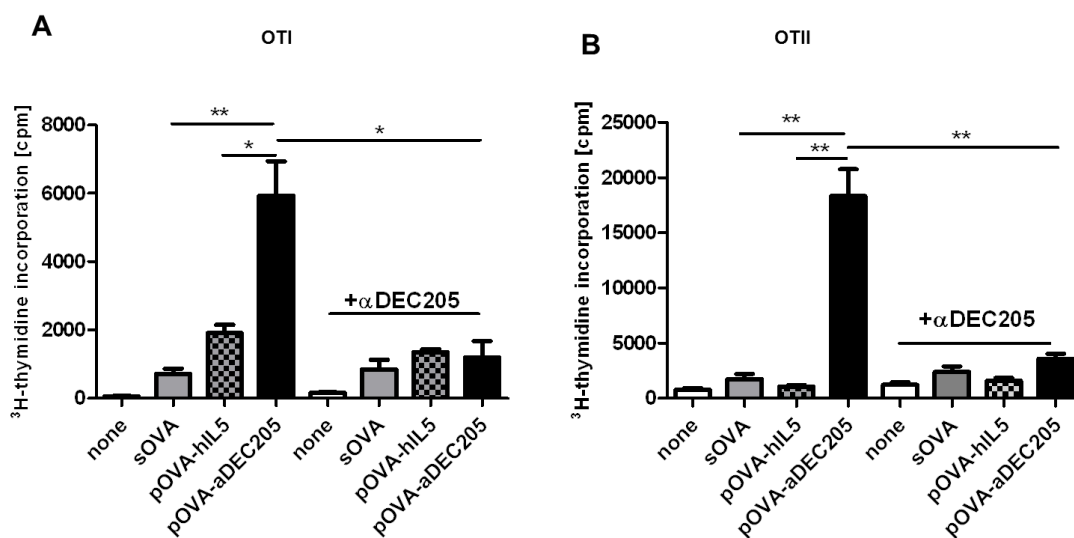


**Fig. 31: DC-targeting NP coated with OVA induce robust antigen-specific T cell proliferation *in vitro*.** Unstimulated BMDC ( $0.75 \times 10^6$ ) were incubated in parallel settings in wells (600  $\mu$ l) of 24-well cell culture plates with OVA protein (sOVA; 10  $\mu$ g/ml) or NP formulations coated with OVA plus either anti mouse DEC205 (p[OVA-aDEC205]) or anti human IL5 (p[OVA-anti-hIL5]) specific antibody (each 1  $\mu$ g/ml) for 24 h. In parallel assays unconjugated anti mouse DEC205 antibody was added at high concentration (100  $\mu$ g/ml) to block DEC205-dependent NP binding. After 24 h, titrated numbers of harvested BMDC were cocultured in parallel with OVA peptide-specific CD8<sup>+</sup> (OT-I) and CD4<sup>+</sup> (OT-II) T cells in triplicates for 72 h. T cell proliferation was assessed by uptake of <sup>3</sup>H-thymidine during the last 16 h of culture. Data represent mean  $\pm$  SEM of triplicates and are representative of two independent experiments. Statistically significant differences between groups are indicated (\*  $p < 0.05$ , \*\*  $p < 0.01$ ).

### 3.3.3. OVA-coated NP evoke stronger CD4<sup>+</sup> T cell proliferation *in vivo* when addressing DC via DEC205

Due to the stronger induction of T cell proliferation evoked by DEC205-targeting OVA-coated NP *in vitro*, next the suitability of these NP to mount an OVA-specific CD4<sup>+</sup> T cell response upon direct *in vivo* application was analyzed. To this end, OT-II T cells were labeled with CFSE and were injected i.v. into C57BL/6 mice. Two days later, groups of mice were treated with PBS, p(OVA-hIL5) and p(OVA-aDEC205), respectively, either alone or in combination with immunostimulatory CpG ODN. Four days later, the extent of OVA-dependent proliferation of CFSE-labeled OT-II T cells in spleen and LNs derived from treated mice was analyzed by flow cytometry. As shown in Fig. 32, application of OVA by DC-targeting NP resulted in somewhat higher T cell (OTI, OTII) proliferation as obtained after immunization with non-targeting NP. Codelivery of OVA-delivering NP plus soluble CpG ODN as an adjuvants mediated a significant increase in OTI and OT-II T cell proliferation, which was evidently higher when employing the DC-targeting NP formulation.

These data demonstrate that administration of particulate OVA resulted in antigen-specific T cell proliferation also when applied directly *in vivo*, which was elevated upon codelivery of CpG. In this combination, employment of OVA-delivering NP conjugated with the DC-targeting antibody aDEC205 was much more efficient than non-targeting NP. This finding suggests that the former NP formulations were engulfed at higher efficiency by myeloid APC due to interaction with the DEC205 receptor, predominantly expressed by DC.

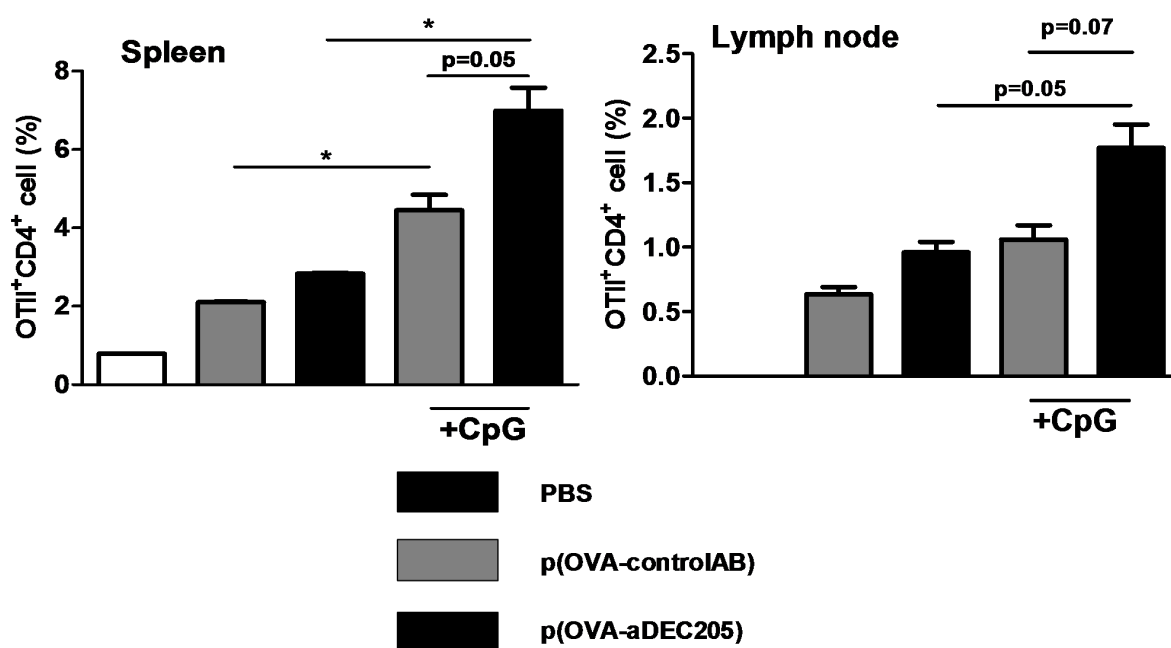


**Fig. 32:** Upon codelivery of DEC205, OVA-coated NP evoke stronger CD4<sup>+</sup> T cell proliferation *in vivo* when addressing DC. Splenocytes derived from OT-II transgenic mice were labeled with 0.5  $\mu$ mol CFSE.  $10 \times 10^6$  OT-II cells were injected i.v. into syngenic C57BL/6 mice (each group 5 mice). After 2 days, recipients were immunized with OVA-coated NP coupled in addition either to anti human IL5 antibody (p[OVA-hIL5]) or anti mouse DEC205 (p[OVA-DEC205]) antibody at amounts equivalent to 10 $\mu$ g of OVA protein by i.v injection. In parallel assays, soluble CpG (5 $\mu$ g per mouse) was coapplied. Three days later, the frequencies of CFSE<sup>+</sup>CD4<sup>+</sup> CD45.1<sup>+</sup> V $\alpha$ 2<sup>+</sup> cells within the spleen (*left panel*) and LN (*right panel*) cell suspensions were assessed by flow cytometry. Data represent the mean $\pm$ SEM of 2 independent experiments. Statistically significant differences between p(OVA-hIL5) versus p(OVA-aDEC205) are indicated (\*  $p < 0.05$ ).

### 3.3.4. p(CpG) induce stronger DC activation than soluble CpG *in vitro*

Due to the impact of coapplication of CpG in combination with p(OVA) on T cell proliferation *in vivo*, we asked for the efficacy of particulate versus soluble CpG to activate DC. Fig. 33 shows that particulate CpG enhanced the maturation of BMDC at significantly higher extent than soluble CpG in terms of expression of costimulatory markers. To further support these findings, the production of CpG-induced proinflammatory cytokines in BMDC was studied. p(CpG) induced significantly higher levels of IL-12, TNF- $\alpha$  and IL-6 as compared with DC cultures stimulated with soluble CpG (data not shown).

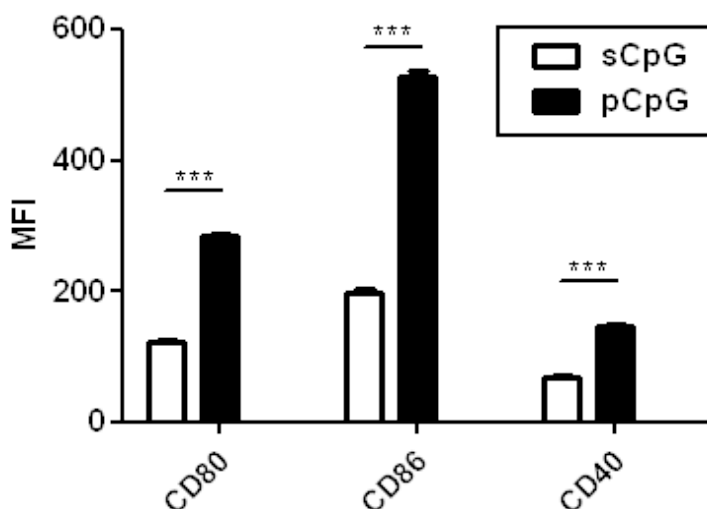


**Fig. 33: CpG mediates stronger BMDC activation when applied as a NP-coated formulation.** Unstimulated BMDC ( $10^6$ ) were stimulated in parallel settings in wells (200  $\mu$ l) of 96-well cell culture plates with CpG and NP coated with CpG (p[CpG]) at equivalent CpG doses as indicated. One day later, the expression of the activation markers CD40 CD80 and CD86, denoted as mean fluorescence intensities (MFI), was analyzed by flow cytometry. Data represent mean $\pm$ SEM of 3 independent experiments each. Statistically significant differences between p(OVA-hIL5) versus p(OVA-aDEC205) are indicated (\*\*\*)  $p < 0.001$ .

### 3.3.5. p(CpG) induce stronger CD4<sup>+</sup> and CD8<sup>+</sup> T cell proliferation *in vivo*

Based on these *in vitro* results, next the capacity of p(CpG) to induce T cell responses *in vivo* was evaluated. For this, splenocytes derived from transgenic mice bearing OVA peptide-specific T cells (OT-I: CD8<sup>+</sup>, OT-II: CD4<sup>+</sup>) were labeled with CFSE and injected i.v. into syngeneic C57BL/6 mice. After two days, all groups received equimolar amounts of p(OVA) and were cotreated with soluble CpG or NP-conjugated CpG (p[CpG]) at equimolar amounts. Four days later, the *in vivo* proliferation of CFSE<sup>+</sup> T cells was assessed in spleen cell suspensions derived from immunized mice. Either T cell population proliferated at significantly larger extent after pretreatment of mice with particulate than soluble CpG (Fig. 34A and B). Similar to the proliferation pattern, the frequency of both CD8<sup>+</sup> and CD4<sup>+</sup> T cells producing the Th1 cytokine INF- $\gamma$  was higher in mice treated with p(CpG) than soluble CpG (Fig. 34C and D), albeit statistically significant only in case of CD8<sup>+</sup> T cells.

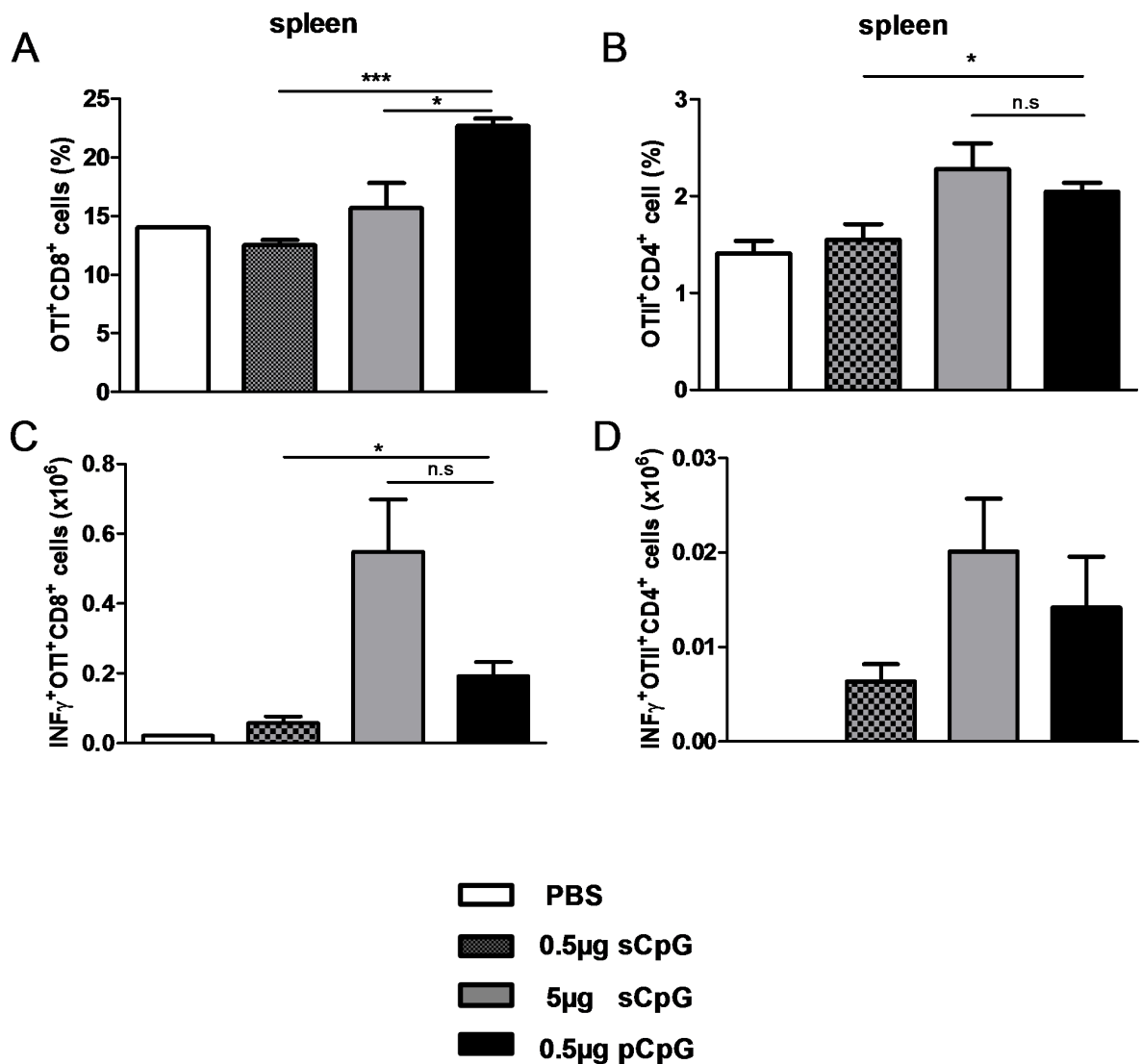
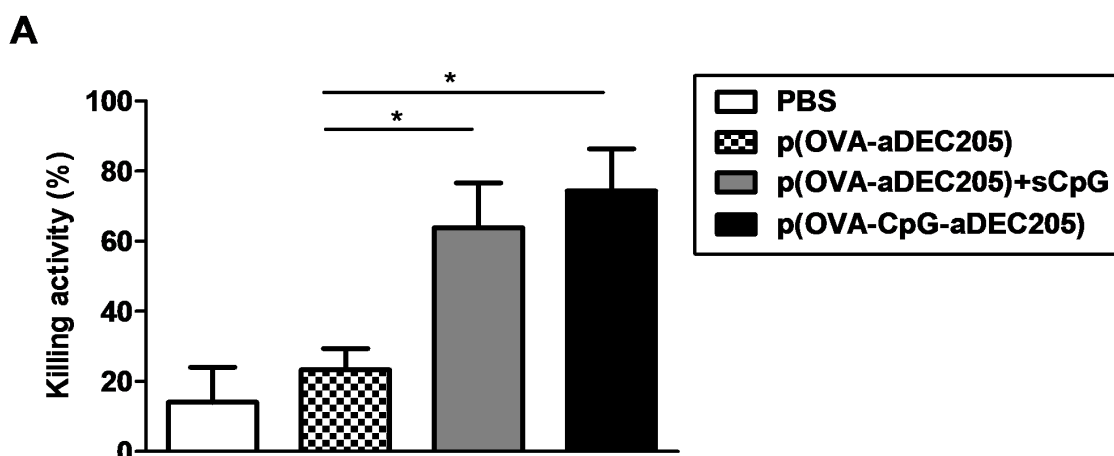


**Fig. 34: Coapplication of CpG as a NP-coated formulation induces enhanced Tc1/Th1 responses *in vivo*.** Splenocytes derived from transgenic mice (OT-IxCD45.1, OT-IIxCD45.1) were labeled with CFSE (0.5 µmol). CFSE-labeled spleen cells ( $10^7$  in 200 µl) were injected i.v. into syngenic C57BL/6 mice. After 2 days, recipients were immunized with p(OVA) equivalent to 0.1 µg of OVA plus either soluble CpG (sCpG) or p(CpG) at CpG doses indicated by injection into the right foot pad. Control mice received PBS instead. Three days later, the spleens were removed and derived splenocytes ( $0.5 \times 10^6$ ) were incubated in wells (200 µl) of 96-well cell culture plates with OVA<sub>257-264</sub> peptide (1 µg/ml) and OVA<sub>323-339</sub> peptide in the presence of Brefeldin A (1:2000) and IL-2 (1:2000) for 5 h. The frequency of IFN $\gamma$ <sup>+</sup> (A) CD8<sup>+</sup> CD45.1<sup>+</sup> V $\alpha$ 2<sup>+</sup> cells and (B) CD4<sup>+</sup> CD45.1<sup>+</sup> V $\alpha$ 2<sup>+</sup> cells was analyzed by FACS. (A,B) Data represent mean  $\pm$  SEM of two independent experiments with each 5 mice per group. Statistically significant differences between sCpG versus pCpG are indicated (\*  $p < 0.05$ , \*\*  $p < 0.01$ , \*\*\*  $p < 0.001$ ).

### 3.3.6. Efficient *in vivo* CTL activation by vaccination with a trifunctional NP, conjugated with OVA, CpG, and anti-DEC-205

Due to the superior activity of particulate OVA and CpG to induce T cell proliferation *in vivo*, next the capacities of DC-addressing NP formulations engineered to deliver OVA either alone or in combination with CpG to mediate T cell activation was analyzed. For this, CD8<sup>+</sup> OT-I T cells were transferred to mice, subsequently immunized with p(OVA-aDEC205), p(OVA-aDEC205) plus soluble CpG, and trifunctional NP (p[OVA-CpG-aDEC205]). To assess the cytotoxic activity of activated OT-I T cells, splenocytes of syngeneic Ly5.1 mice were labeled with CFSE at low or high dose, and the latter were pulsed with OVA<sub>257-264</sub> peptide as recognized by OT-I CD8<sup>+</sup> T cells. Four hours later, spleen cell suspensions were analyzed for the frequency of CFSE<sup>high</sup> OVA peptide-presenting target cells.

In this *in vivo* killing assay target cell lysis occurred only in groups of mice pretreated with either p(OVA-aDEC205) plus soluble CpG, or the trifunctional NP formulation (p[OVA-CpG-aDEC205]), which mediated largely comparable CTL induction (Fig. 35). These findings indicate that the NP formulation with triple function constitutes a potent inducer of antigen-specific CTLs.



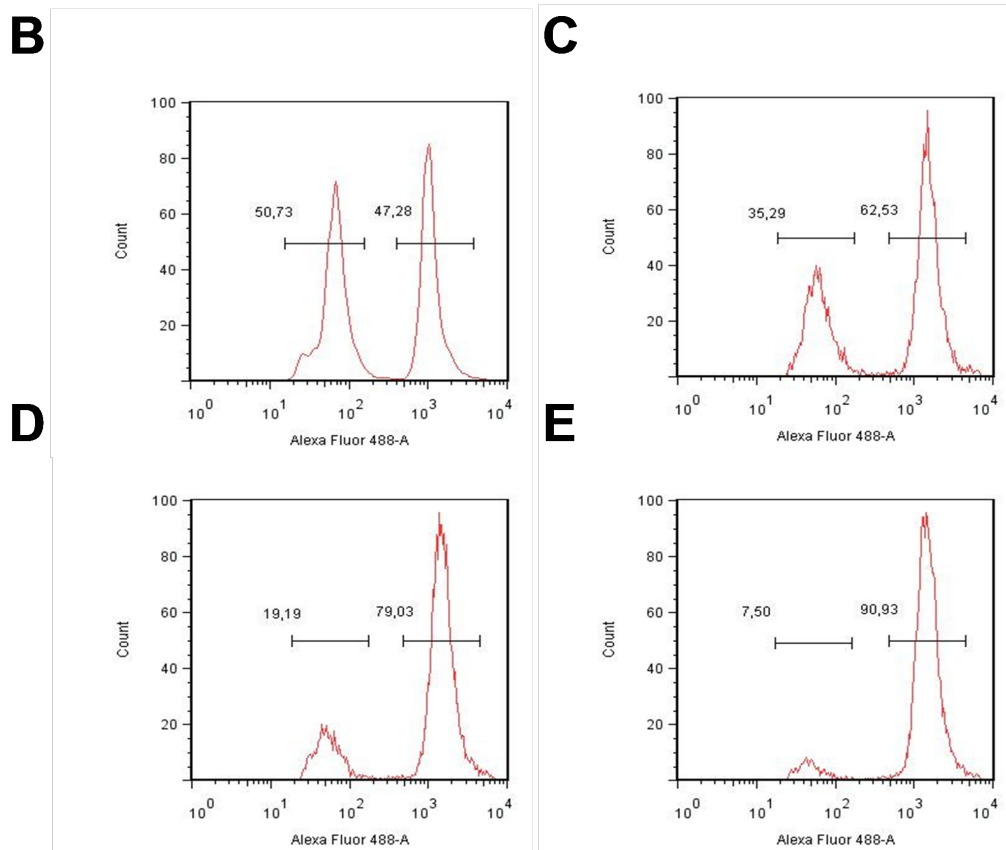


**Fig. 35: Coupled delivery of OVA by DC-targeting NP plus CpG results in elevated CTL activation *in vivo*.** Naive C57BL/6 mice (three mice per group) received OVA-specific CD8<sup>+</sup> OT-I T cells ( $10^7$ ) *i.v.* Two days later, mice were immunized *i.v.* with NP formulations and soluble CpG (sCpG) as indicated. On day 4, mice were injected with CFSE<sup>low</sup> target cells (loaded with OVA<sub>257-264</sub>) and CFSE<sup>high</sup> control cells (each  $10^7$ ) derived from syngeneic CD45.1<sup>+</sup> mice. 4 h later, splenocytes were isolated and frequencies of CFSE<sup>+</sup> cell populations were assessed by flow cytometry. (A) Data represent mean $\pm$ SEM of one of three independent experiments and 5 mice per group. Statistically significant differences between groups are indicated (\*  $p < 0.05$ ). (B-E) Frequencies of CD45.1<sup>+</sup> target (CFSE<sup>low</sup>) and control (CFSE<sup>high</sup>) cells were detected by flow cytometry in spleen cell suspensions derived from one mouse of either group. Graphs are representative of three independent experiments.

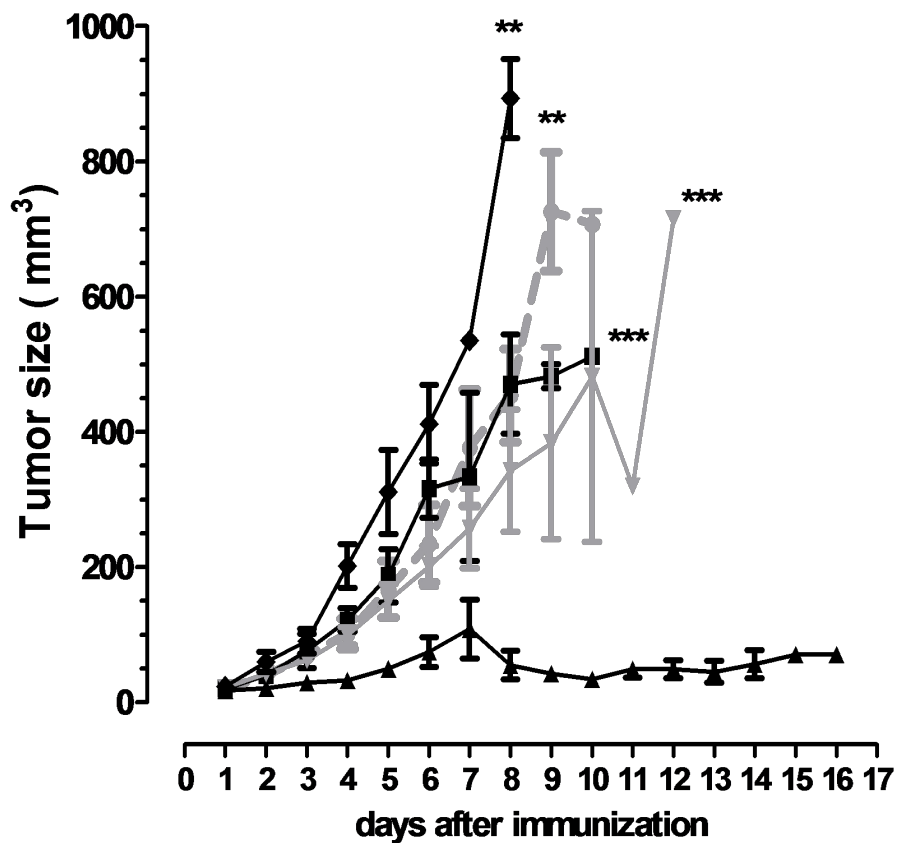
### 3.3.7. TrifunctionalNP inducepotent therapeutic anti-tumor immunity

#### 3.3.7.1. Tumor growth and size

Using the B16 melanoma tumor cell subline engineered to express OVA (B16-OVA), the ability of the different OVA-delivering types of NP to induce an effective anti-tumor response was analyzed. Mice were inoculated s.c. with B16-OVA tumor cells. At a tumor volume of about 15 mm<sup>3</sup>, groups of tumor-burdened mice were vaccinated i.v. with either NP formulation or PBS (Ctrl). Control mice showed fast tumor growth, which was attenuated in vaccinated mice in a NP type-dependent manner: Immunization with NP delivering OVA in a non-addressing (p[OVA]) or in a DC-addressing (p[OVA-aDEC205]) manner, resulted in a minor delayed tumor growth only (Fig. 36A) and a somewhat improved survival (Fig. 36B) as compared with the control group. Vaccination with NP that codelivered OVA and CpG (p[OVA+CpG]) slowed down tumor growth somewhat stronger. However, only vaccination with the trifunctional NP formulation, improved by the additional DC-targeting property, evoked a pronounced anti-tumor response as reflected by an arrested tumor growth and high survival rate as compared with the other groups.



A



B

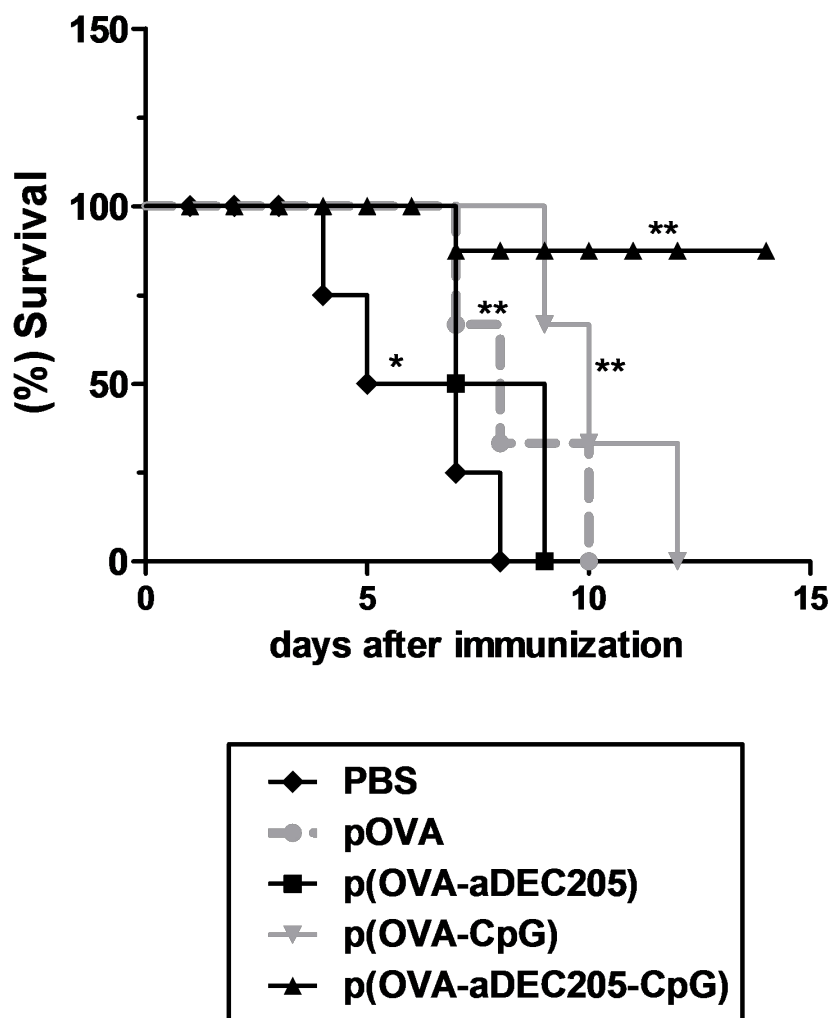


**Fig. 36: Trifunctional NP formulations that enable codelivery of OVA and CpG to DC effectively inhibit progressive growth of established tumors.** Mice were injected s.c. with 50,000 B16-OVA cells. Tumor growth was measured every day with a caliper. The tumor volume was recorded as the product of two orthogonal diameters (a: longest diameter, b: orthogonal width). When the tumor size exceeded 15 mm<sup>3</sup>, 6 mice per group were vaccinated with 5x10<sup>11</sup> nanoparticles of the different NP formulations as indicated, injected i.v every other day for a total of three times. Control mice received PBS only. Mice were sacrificed when the tumor size reached about 600 mm<sup>3</sup>. **(A)** Time course of tumor growth development as observed in one of 4 experiments. **(B)** Cumulative survival analysis of groups of mice treated as described derived from two independent experiments. Statistically significant differences between the control group versus any other are indicated (\* p<0.05, \*\* p<0.01, \*\*\* p<0.001).

### 3.3.7.2. Codelivery of CpG attenuates tumor-promoted MDSC frequencies

It is established by now that , tumor-derived mediators favor the expansion of a population of immature myeloid cells, termed myeloid-derived suppressor cells (MDSC), both in a wide range of murine tumor models and human cancers (Gabrilovich and Nagaraj, 2010). Gr1<sup>+</sup>CD11b<sup>+</sup>MDSC are present in low numbers in tumor-free mice (<4-6% of spleen cells). MDSC accumulate systemically due to a tumor-induced blockage of differentiation of myeloid precursor cells into APC and granulocytes. To examine the effect of *in vivo* immune stimulation of tumor-burdened mice with NP formulations on their MDSC frequency of spleen, spleens from the differentially treated B16-OVA tumor-bearing mice were harvested and the proportion of Gr1<sup>+</sup>CD11b<sup>+</sup>MDSC analyzed. Fig.37 shows a significant reduction of MDSC frequencies in mice immunized with NP formulations which codelivered CpG as compared with the frequency observed in tumor-burdened control mice.

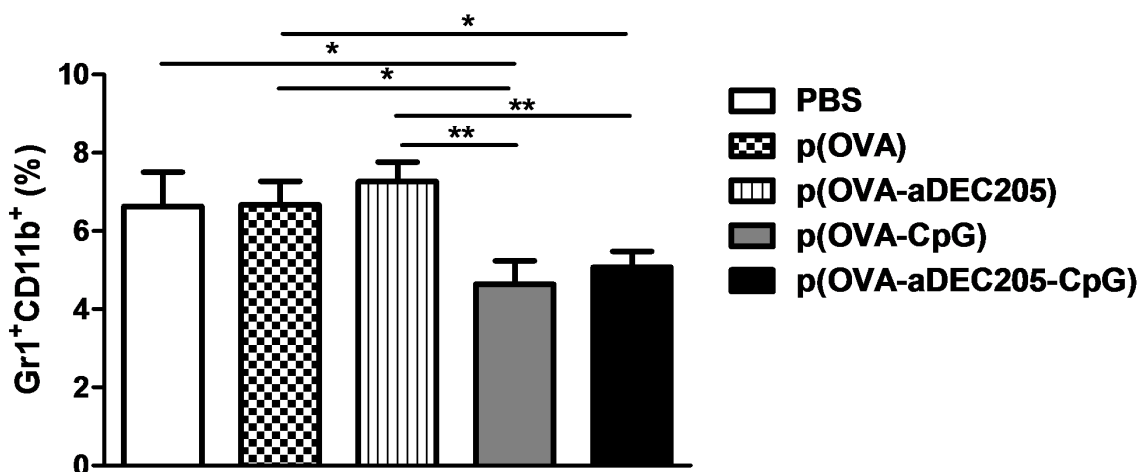


**Fig. 37: Trifunctional NP formulations that enable codelivery of CpG to DC effectively inhibit the expansion of MDSC in tumor bearing mice.** Mice were sacrificed when the tumor size reached about 600 mm<sup>3</sup>. The spleens were removed at the end of the experiment and the splenocytes were isolated and double stained with MDSC markers Gr1<sup>+</sup>CD11b<sup>+</sup>. Data present mean±SEM of 5 to 8 mice per group. Statistically significant differences between groups are indicated (\* p<0.05,\*\* p<0.01).

### 3.4. Nanoparticles induce an antigen-specific humoral response

#### 3.4.1. DEX-coated ferromagnetic NP colocalize with CD19<sup>+</sup> B cells irrespective of their targeting moiety

After the analysis of the cellular binding of different types of NP by immune cells *in vitro*, their *in vivo* uptake properties were assessed. For this, NP formulations were injected intravenously into mice, and after 4h and 24h the spleen was harvested and prepared for immunohistochemistry staining. Interestingly, all types of NP localized predominantly in the B cells zones (Fig. 38 and other data not shown).

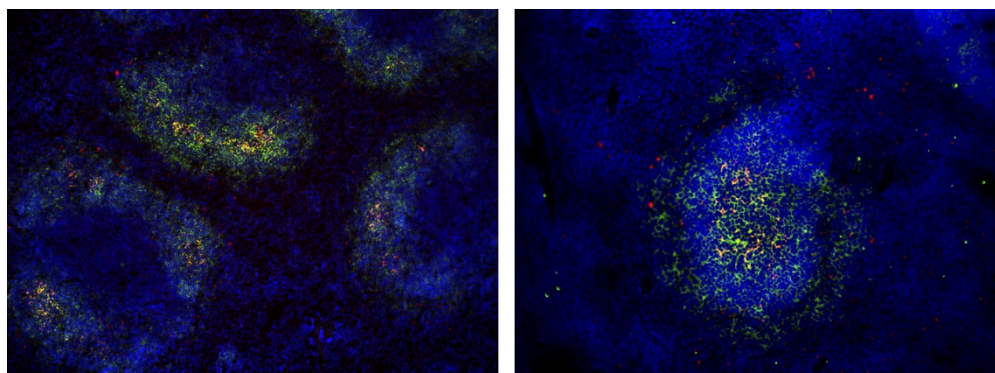


**Fig. 38: Immunohistochemical detection of NP *ex vivo*.** The control NP (p[Cy5]) was injected into C57BL/6 mice intravenously. After 4h, mice were sacrificed and the spleen were harvested and used for immunohistochemical staining. The pictures showed at 20 (left) and 40 (right) magnifications by microscopy (green: CD19, red: pCy5 nanoparticles, blue: Dapi).

#### 3.4.2. Binding of DEX-coated ferromagnetic NP to B cells *in vitro* requires serum

Due to the discrepancy of the differential NP binding properties, which *in vivo* predominantly colocalized with B cells, but upon *in vitro* coincubation of splenic cells preferably colocalized with macrophages and DC, we asked for a potential role of serum components in mediating these striking differences. In order to mimic the *in*

*in vivo* situation more closely, aliquots of control NP (p[*Cy5*]) were preincubated with native mouse serum prior to coincubation with isolated spleen cell suspensions for 4h and 24h. As shown in Fig.3 9, FACS analysis revealed no binding of untreated NP to the CD19<sup>+</sup> B cell population. In contrast, when preincubated with native serum for 1h, p(-) efficiently bound to B cells, at maximal extent within 1h of coincubation.

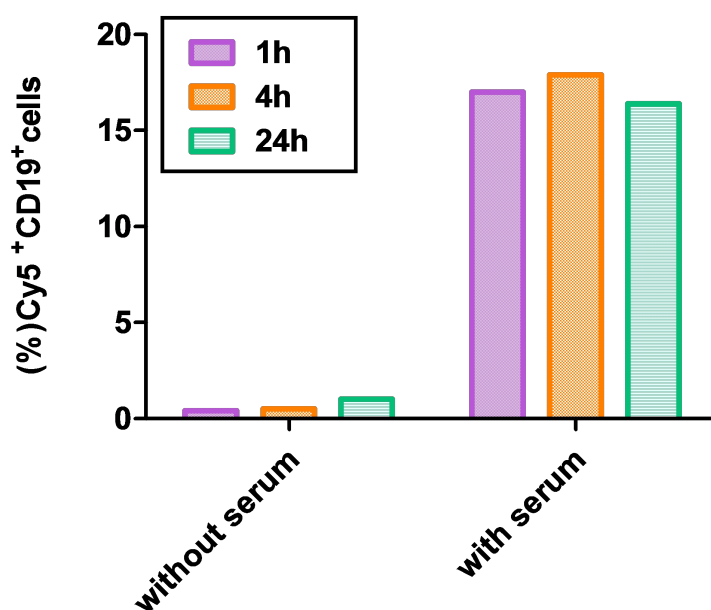


**Fig. 39: Binding of control NP by B cells requires serum.** B cells were isolated from spleen and aliquots of B cells ( $0.75 \times 10^6$ ) were incubated in parallel settings in wells (200  $\mu$ l) of 96-well cell culture plates with each  $5 \times 10^{11}$  p*Cy5* nanoparticles either left untreated (w/o) or preincubated with naïve autologous mouse serum together. All NP formulations were labeled with *Cy-5*. Aliquots of cells were removed after the indicated period of time, were stained with anti-CD19 antibody, and were analyzed by flow cytometry. Data represent one of 3 independent experiments.

### 3.4.3. Preincubation of DEX-coated ferromagnetic NP with heat labile serum components is necessary for B cell-specific binding

As shown in 3.4.2, binding of NP by B cells is mediated by serum components. Subsequently, I sought to identify more specifically, which serum components were responsible for this effect. When control NP were preincubated with albumin as the most abundant serum protein, no enhanced B cell binding was noted (Fig. 40). Since B cells are well equipped to bind immune-complexes via CD16/CD32 Fc receptors,

the potential of non-specific mouse IgG antibodies to opsonize NP, and thereby mediate B cell binding via interaction with Fc receptors was assessed. However, antibody-preincubated NP showed no elevated B cell binding. Congruently, blockade of the CD16/CD32 receptor by applying neutralizing antibodies had no effect on the B cell binding properties of serum-preincubated NP. Complement factors are part of the innate immune system and are able to bind to a variety of non-self surfaces. To analyze potential involvement of heat-labile complement factors, serum was heated at 56°C prior to preincubation with NP. In fact, NP pretreated in this manner showed no enhanced B cell binding, which indicates that complement factors may play an essential role in this process.

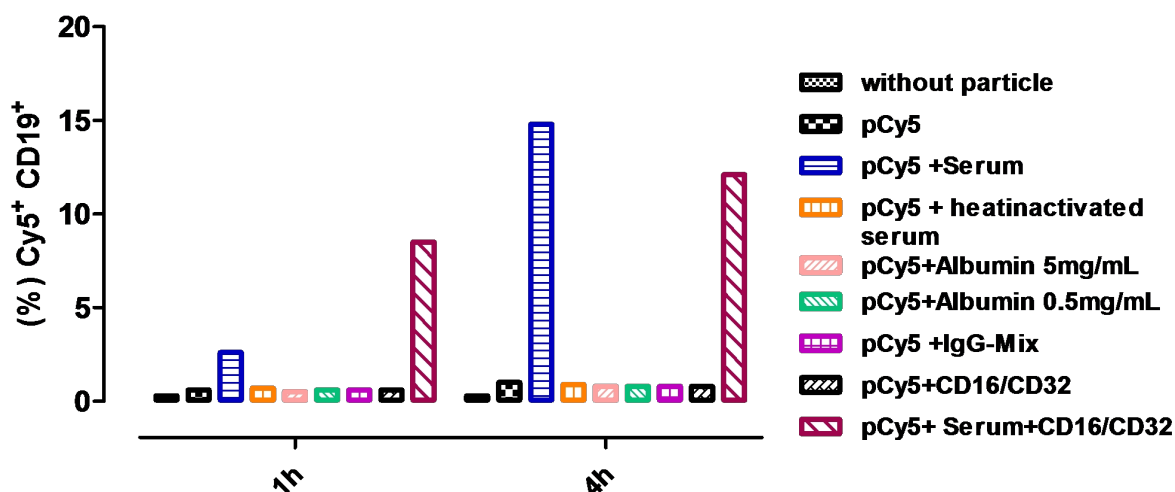


**Fig. 40: NP uptake by B cells required serum.** B cells were isolated from spleen and Aliquots of B cells ( $0.75 \times 10^6$ ) were incubated for 4h and 24h in parallel settings in wells (200  $\mu$ l) of 96-well cell culture plates with each  $5 \times 10^{11}$  nanoparticles of pCy5 preincubated with the indicated compounds( heatinactivated serum , differently concentration of albumin). In one group, B cell were preincubated with blocking anti-CD16/32 antibody (5 $\mu$ g/ml). All NP formulations were labeled with Cy5. Aliquots of cells were removed after the indicated period of time, were stained with anti-CD19 antibody, and were analyzed by flow cytometry. The data shown results of 3 independent experiments.

#### 3.4.4. Serum-coated NP bind to the B cell complement receptor (CD21/CD35)

The finding of complement-dependent binding of NP to B cells suggested involvement of the the B cell complement receptor (CD21/CD35). To test this

hypothesis, spleen cell suspensions were preincubated with a CD21/35 neutralizing antibody prior to coincubation with p(Cy5). Indeed, inhibition of CD21/35 binding activity strongly diminished B cell binding of complement-coated NP to B cells (Fig. 41).

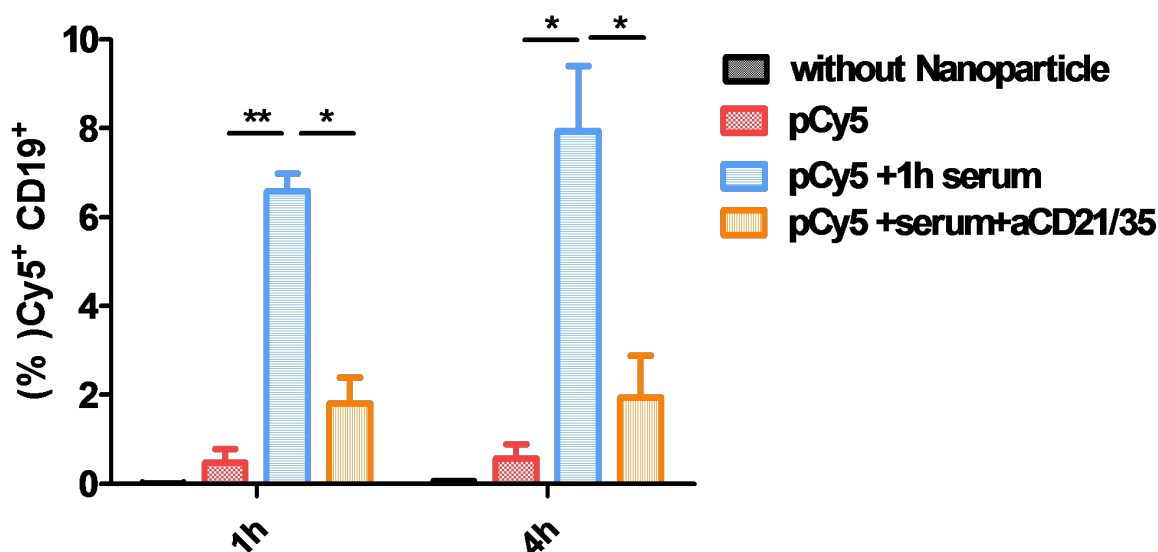


**Fig. 41: Control NP bind to B cells through complement receptor.** B cells were isolated from spleen and aliquots of B cells ( $0.75 \times 10^6$ ) were incubated in parallel settings in wells (200  $\mu$ l) of 96-well cell culture plates with anti-CD21/35 for 1h. Control NP (p[Cy5]) were preincubated with naïve serum or not, and then added into B cell cultures. Aliquots of cells were removed after the indicated period of time, stained with anti-CD19 antibody, and were analyzed by flow cytometry. Data represent mean  $\pm$  SEM of 3 independent experiments. Statistically significant differences between groups are indicated (\*  $p < 0.05$ , \*\*  $p < 0.01$ ).

### 3.4.5. NP contained with CpG are engulfed by B cell *in vitro* and in a serum-independent manner

In order to evaluate intracellular uptake of different types of NP by B cells, CD19<sup>+</sup> B cells isolated from spleen were coincubated with Cy5-labeled types of NP for 4h and 24h. After incubation, the cells were stained with DAPI (nuclei) and cell mask orange (membrane), and were analysed by confocal microscopy. By this, only uptake of NP, which contain CpG by B cells (Fig. 42) as assessed at 24h after the onset of

coincubation was observed (Fig. 42 A). The significant higher binding of CpG coated NP were also observed *in vivo* (Fig. 42B).

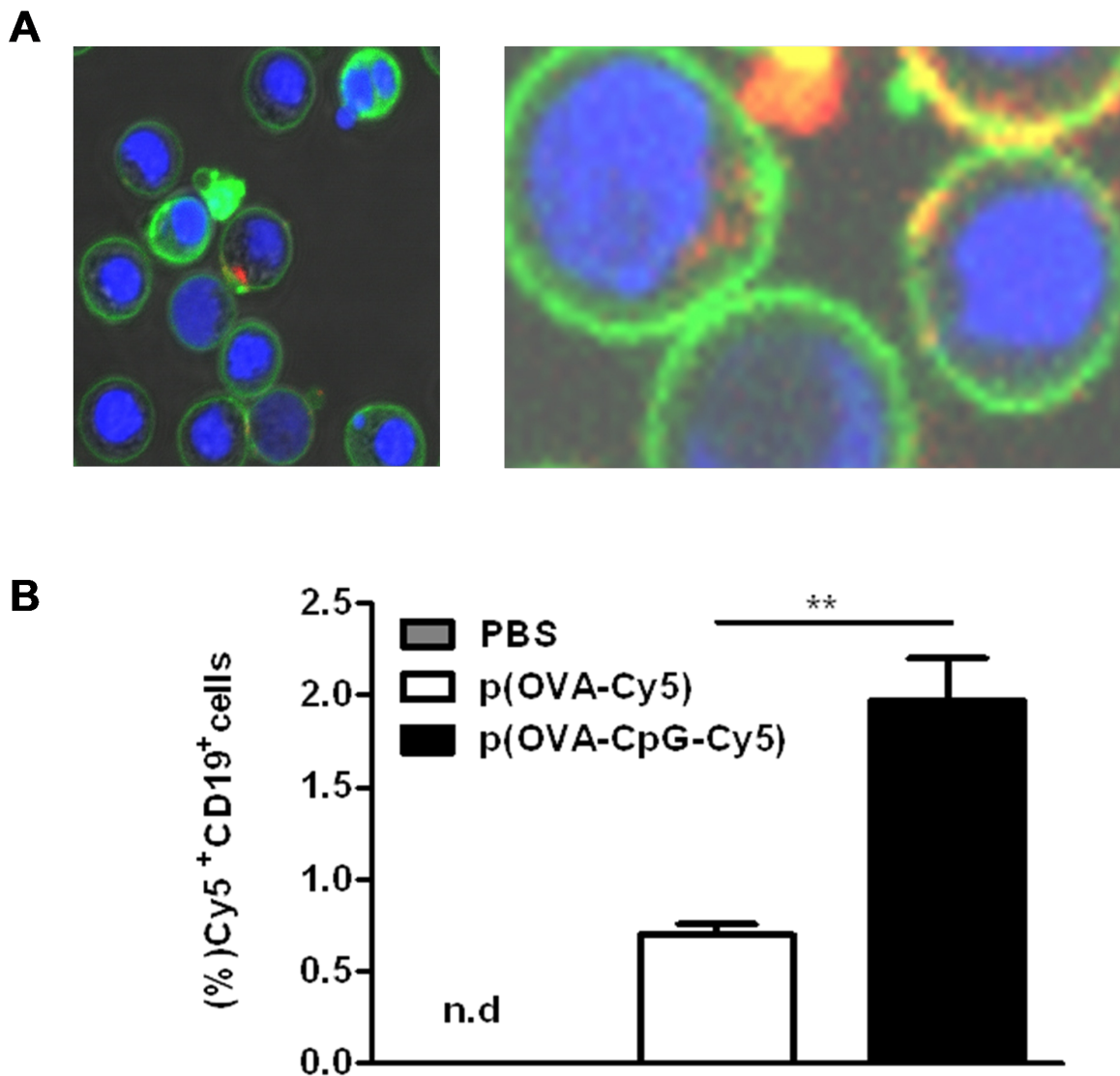


**Fig. 42: NP conjugated with CpG were engulfed by B cells. (A)** B cells were isolated from spleen and incubated with NP formulations as indicated. Cellular uptake of Cy5-labeled NP by B cells stained with cell mask orange (green) and DAPI (blue) was assessed by confocal laser scanning microscopy. **(B)** The NP formulations with CpG and without CpG were *i.v.* injected into mice, after 4h, the spleen cells were harvested and NP the binding to CD19<sup>+</sup> cells *ex vivo* was analysed by FACS. Data represent mean $\pm$ SEM of 2 independent experiments. Statistically significant differences between two groups are indicated (\*\*  $p < 0.01$ ).



### 3.4.6. Functionalized NP induce an antigen-specific Th1-biased humoral response

So far, it has been shown that functionalized NP induced T cell mediated immune responses. Based on the finding of serum-dependent B cell binding of NP, their potential to mount production of OVA-specific antibodies was evaluated. For this, naive mice were injected i.v. with the different NP formulations, and sera derived either one or two weeks later were assayed for OVA-specific IgG titers. At either time point, OVA-specific IgG1 and IgG2a was detected in sera obtained from mice injected with OVA-containing types of NP (p[OVA+CpG], p[OVA+CpG+aDEC205]) only, thereby confirming antigen-dependency of antibody production (Fig. 43). As expected, OVA-specific antibody titers were significantly higher when OVA and CpG were codelivered in a DEC205-targeting manner (p[OVA+CpG+aDEC205]). In general, more IgG2a than IgG1 was detected, reminiscent of a Th1-skewed IgG pattern, which was most probably due to usage of CpG as a well-known inducer of Th1-biased immune responses. Taken together, these findings demonstrate that NP-based nanovaccines are capable to induce both a cellular and a humoral immune response *in vivo*.

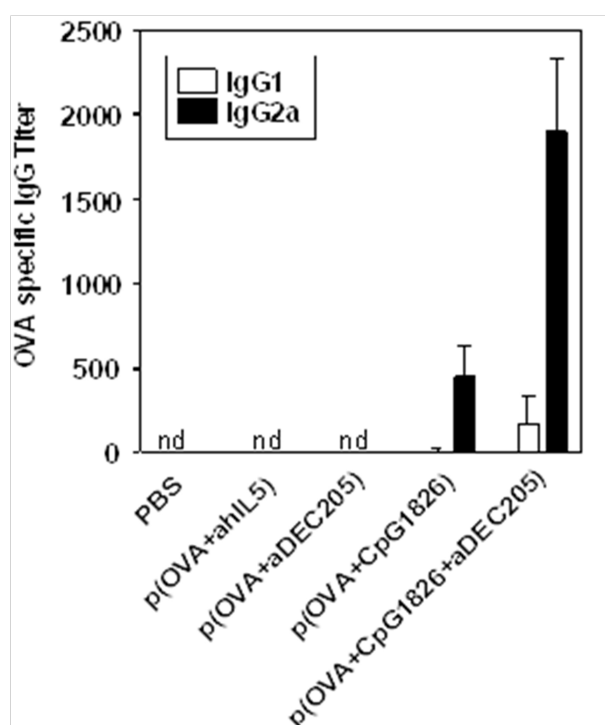


**Fig. 43: NP induced OVA specific antibody response.** NP formulations containing OVA elicit a specific Th1-biased humoral immune response. Naive C57BL/6 mice (three mice per group) were immunized with NP formulations as indicated. On day 14, mice were bled and OVA-specific IgG1 and IgG2a antibody titers were detected in derived sera. Data represent mean $\pm$ SEM of three sera per group.

### 3.4.7. Complement-dependent binding of NP to B cells is conserved between mouse and human

In light of the potential of NP-mediated B cell targeting for immunotherapeutic applications, and based on the high degree of evolutionary conservation of the complement system, the applicability of complement-mediated NP binding to human B cells was tested. For this, peripheral blood-derived mononuclear cells (PBMCs) were prepared and coincubated with control NP left untreated or preincubated with human autologous serum. In contrast to the studies involving mouse target cells, no marked binding of NP to B cells was noted after 4h of coincubation. However, after 24h of culture, efficient binding of serum-preincubated NP was observed. The binding of the NP formulation coated with OVA as a model antigen to B cells was also observed. These findings indicate that functionalized NP formulations may serve as a platform for B cell specific targeting *in vivo* in order to evoke antigen-specific humoral immune responses.

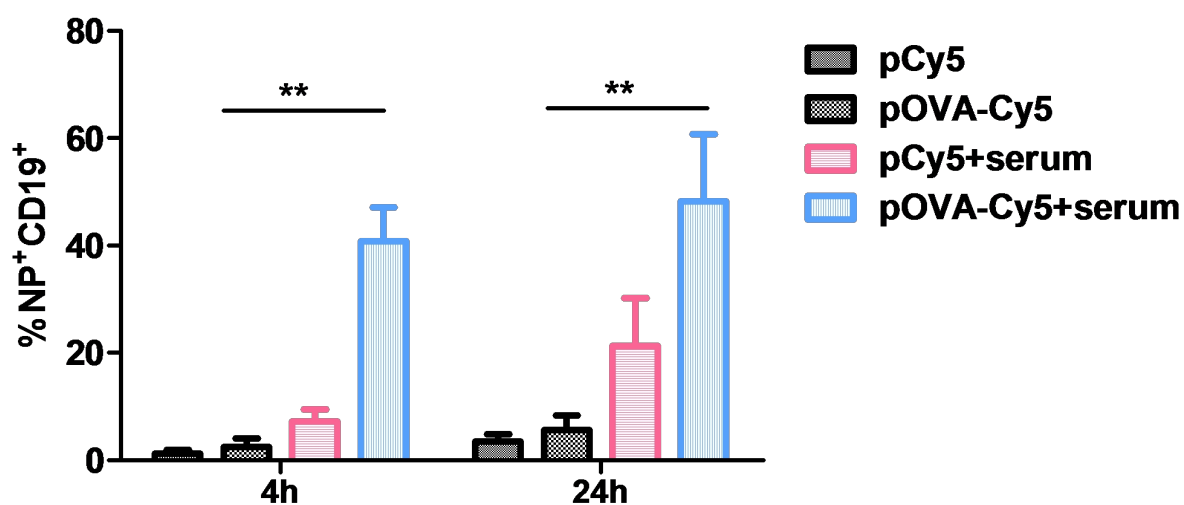


**Fig. 44: NP binding to B cells requires serum in human system.**  $1 \times 10^6$  PBMCs were isolated and reseeded in wells (200  $\mu$ l) of 96-well cell culture plates. PBMCs were coincubated with each  $5 \times 10^{11}$  nanoparticles left untreated or preincubated with native autologous serum. All NP formulations were labeled with Cy-5. Aliquots of cells were removed after the indicated period of time, stained with anti-CD19 antibody, and analyzed by flow cytometry. Results from one out of five independent experiments are shown. Data represent mean  $\pm$  SEM of triplicates. Statistically significant differences between groups are indicated (\*\*  $p < 0.01$ ).

### 3.5. B cell-based immunotherapy with nanoparticles

#### 3.5.1. Anaphylaxis model

##### 3.5.1.1. Codelivery of OVA and CpG suppresses induction of OVA-specific IgE in a therapeutic model of anaphylaxis

It is well established that IgE initiates immediate hypersensitivity reactions by triggering mast cell degranulation via  $Fc\epsilon RI$ . Thus, we asked for contents of antigen

specific IgE in mice sensitized with OVA, and subsequently immunized with distinct NP formulations. The serum levels of OVA-specific IgE elicited in BALB/c mice after sensitization with soluble OVA protein (10  $\mu$ g/c) are depicted in Fig. 45 (left panel). IgE antibody titers in the different groups were comparable prior to vaccination with the different types of NP. After the last vaccination, sera obtained from mice treated with NP formulations that contained OVA and CpG (p[OVA+CpG], p[OVA+CpG+aDEC205]) showed largely unaltered IgE titers, while IgE contents in the other groups were significantly elevated (Fig. 45, right panel). These results demonstrated that NP conjugated with OVA and CpG suppress production of OVA-specific IgE level in serum.

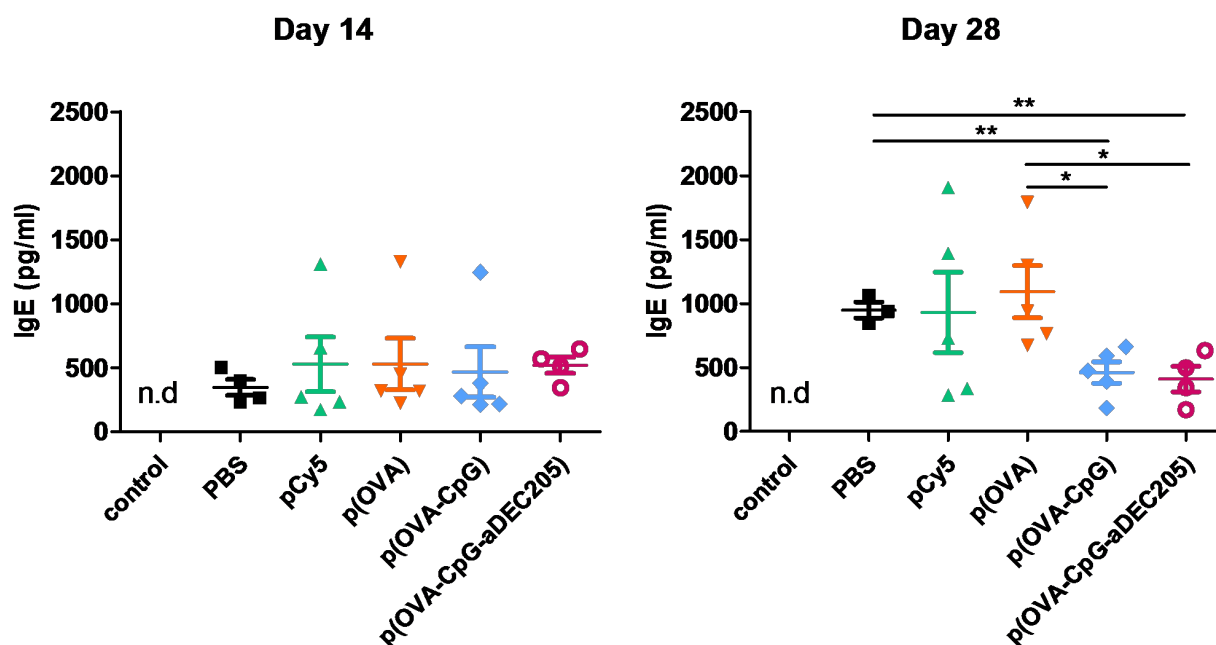
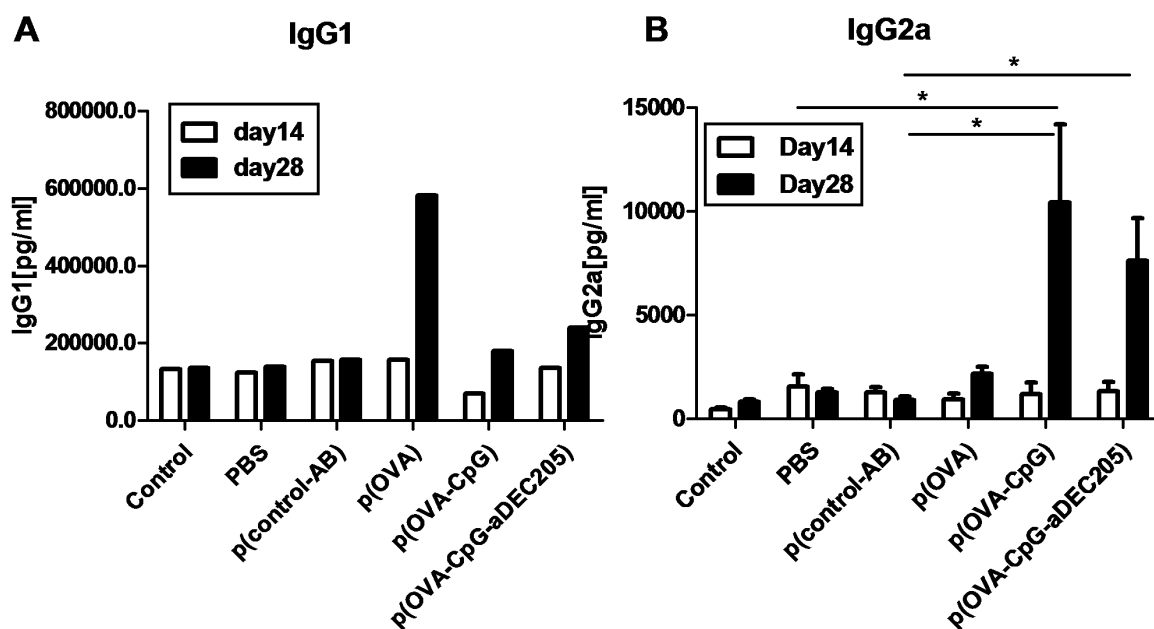


**Fig. 45: Vaccination of OVA-sensitized mice with OVA/CpG-codelivering NP prevents upregulation of IgE expression.** Mice were sensitized s.c. three times at days 0, 7 and 14 with OVA (10  $\mu$ g/mouse). 7 days after the last sensitization, mice were intravenously immunized three times at days 14, 21 and 28 with different NP formulations as indicated. On days 14 (prior to 1st immunization with NP) and 28 (after last immunization) blood samples were collected, and OVA-specific antibody titers were measured by ELISA as described. Results from one out of five independent experiments are shown. Data represent mean  $\pm$  SEM of 5 mice per group. Statistically significant differences between groups are indicated (\*  $p < 0.05$ , \*\*  $p < 0.01$ ).

### 3.5.1.2. NP which codeliver OVA and CpG induce a Th1-skewed humoral response in a therapeutic model of anaphylaxis

The serum levels of OVA-specific IgG subtypes elicited in BALB/c mice after immunization with 10  $\mu$ g OVA protein prior to (day 14) and after three rounds of vaccination with different NP formulations (day 28) are depicted in Fig. 46. Sera of mice sensitized with OVA contained comparable concentrations of IgG1 (Fig. 46A) and IgG2a (Fig. 46B) antibodies, while untreated mice lacked OVA-specific antibodies. Furthermore, sera derived from groups of mice vaccinated with OVA plus

CpG-functionalized types of NP contained elevated concentrations of IgG2a OVA-specific antibodies after the last round of vaccination (day 28). Coapplication of immunostimulatory CpG ODN diminished the IgG1 content. Consequently, the IgG2a/IgG1 ratio was strongly elevated in sera derived from mice vaccinated with OVA plus CpG ODN NP formulations codelivering as compared with sera from control mice and mice vaccinated with NP containing OVA alone (Fig. 46C). This result confirms the Th1-promoting character of CpG-containing NP. Importantly, no difference of the IgG2a content between DC targeting and non-targeting was observed. This suggests that, only B cell targeting by nanoparticle is sufficient to induce a Th1-skewed humoral response.



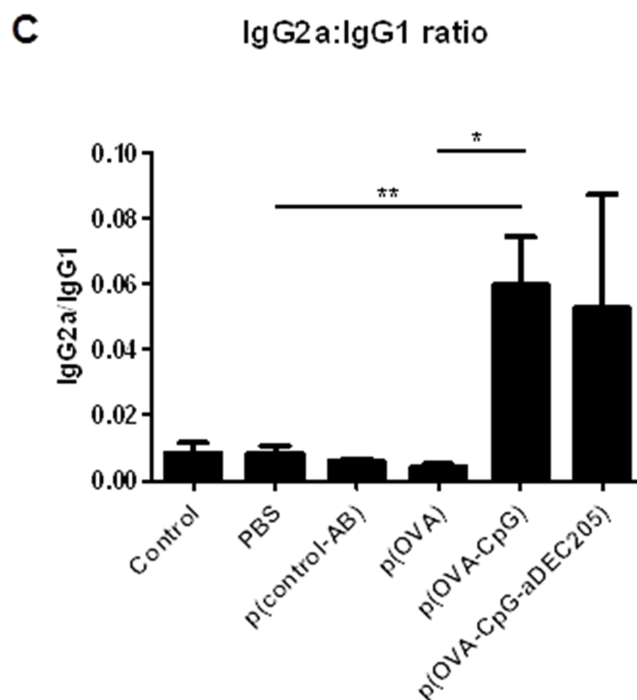


**Fig. 46: Vaccination of OVA-sensitized mice with OVA/CpG-codelivering NP formulations promotes a Th1-biased IgG pattern.** Female BALB/c mice were s.c. sensitized three times (days 0, 7, and 14) with OVA (10  $\mu$ g/mouse). After the last sensitization, groups of mice were immunized i.v. three times (days 14, 21 and 28) with different NP formulations as indicated. At days 14 (prior to 1st vaccination) and 28 (after 3rd vaccination), blood samples were collected, and OVA-specific antibody titers were measured by ELISA as described. OVA specific (A) IgG1, and (B) IgG2a contents were detected, and (C) the ratio of IgG1/IgG2a was determined. Results from one out of five independent experiments are shown with 5 mice per group in each experiment. Data represent mean $\pm$ SEM of 5 mice per group. Statistically significant differences between groups are indicated (\*  $p < 0.05$ , \*\*  $p < 0.01$ ).

### 3.5.1.3. Body temperature after the passive systemic anaphylaxis reaction

During anaphylactic shock, a dramatic drop in body temperature is commonly observed and is a very important parameter to determine its intensity (Makabe-Kobayashi *et al.*, 2002). In this study, BALB/c mice were immunized three times with each 10  $\mu$ g OVA protein, and were subsequently vaccinated with different NP formulations for three times. 7 days after the 3<sup>rd</sup> vaccination, mice were challenged with OVA by i.v injection to induce a passive systemic anaphylaxis reaction. The body rectal temperature was monitored every 15 min. As shown in Fig. 47, in the PBS, p(Cy5-control AB), and p(OVA) groups an immediate and increasing decline in body temperature throughout the period of time assessed was observed. In case of the p(OVA-CpG) and p(OVA-CpG-aDEC205) groups, this decrease in temperature

was less intense. Moreover, body temperatures of mice of the latter two groups remained steady (p[OVA-CpG-aDEC205]) or even increased (p[OVA-CpG]) between 30 to 60 min after challenge, . At the end time point, the differences in body temperatures between mice of the p(OVA+CpG) and control groups was significant.

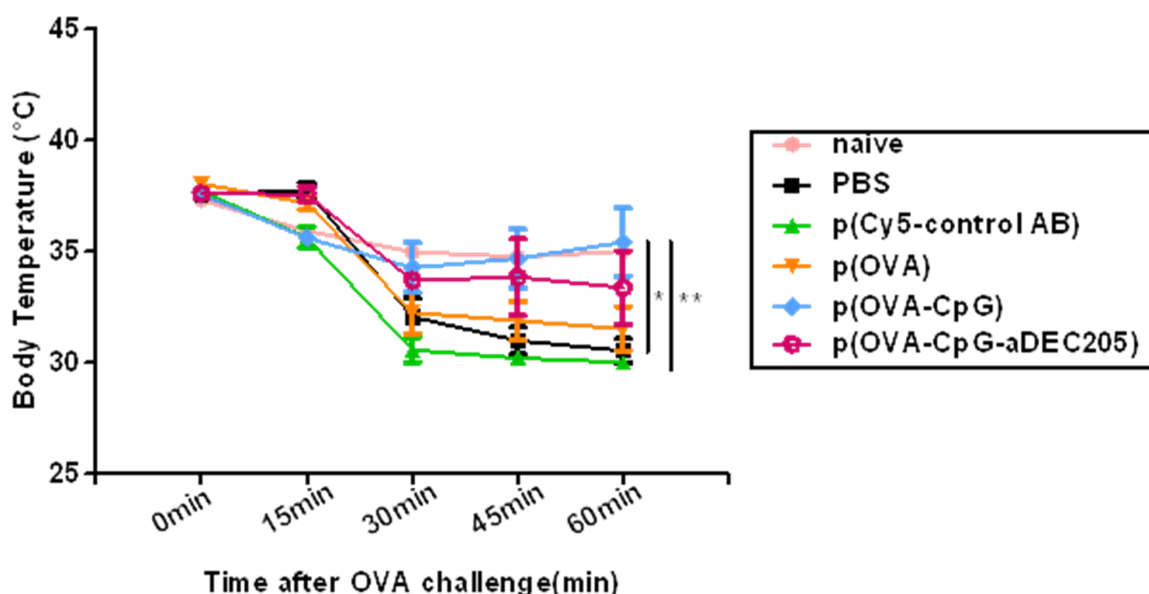


**Fig. 47: Changes in body temperature in mice after induction of a passive systemic anaphylaxis reaction.** Female BALB/c mice were s.c. sensitized three times (days 0, 7, and 14) with OVA (10  $\mu\text{g}/\text{mouse}$ ). After the last sensitization, each 5 mice per group were immunized i.v. three times (days 14, 21 and 28) with either of the different NP formulations as indicated. 7 days after the last immunization, mice were challenged with OVA (25  $\mu\text{g}/\text{mouse}$ ) by i.v. injection and the temperature was monitored every 15 mins. Data represent mean $\pm$ SEM of 5 mice per group. Statistically significant differences between PBS versus NP-vaccinated groups are indicated (\*  $p < 0.05$ , \*\*  $p < 0.01$ ).

### 3.5.2. Acute asthma model

#### 3.5.2.1. Airway hyperreactivity (AHR)

Based on the therapeutic efficacy of NP formulations that codelivered OVA and CpG in a model of anaphylactic shock, we tested for the curative potential of these nanovaccines also in a mouse model of OVA-dependent asthma. AHR is one of the important characteristic features of asthma (Kumar *et al.*, 2008). To determine whether NP could attenuate AHR, lung function parameters of mice sensitized with

OVA, and subsequently treated with NP formulations were measured in response to increasing concentrations of the broncho-constrictant methacholine. As shown in Fig. 48, compared with naïve mice, all other groups of mice showed increasing bronchial hyper-responsiveness in response to increasing methacholine concentrations. However, the airway response of the groups immunized with OVA plus CpG (p[p(OVA-CpG) and p[OVA-CpG-aDEC205]) delivering NP formulations was much lower than in the positive control group. Mice treated with p(Cy5-control AB) and p(OVA) rather augmented AHR. These results indicate that administration of NP conjugated with OVA plus CpG was effective to attenuate bronchial hyper-responsiveness. DC targeting exerted no additional benefit in AHR.

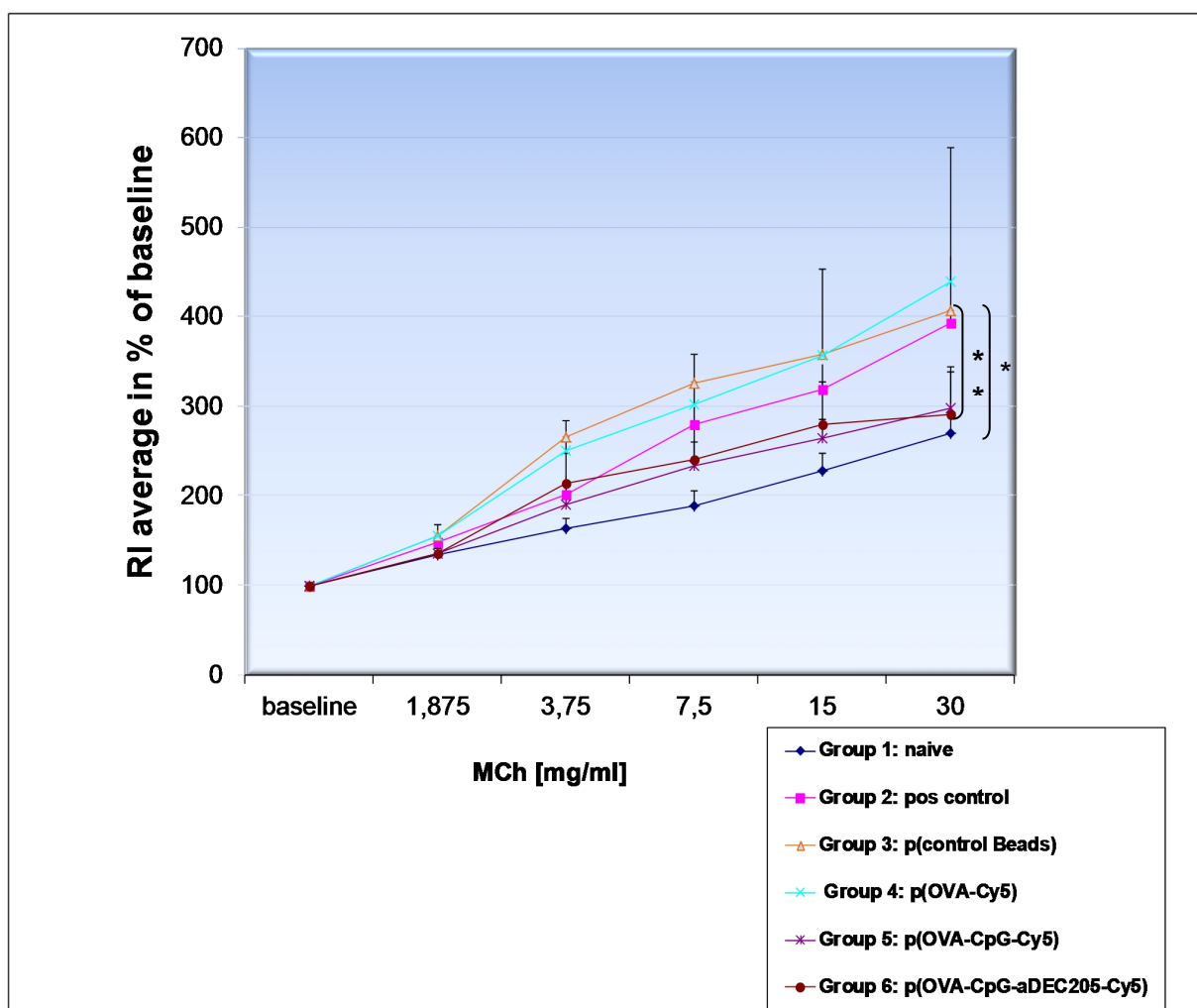


**Fig. 48: Effect of different types of nanoparticles on airway hyperresponsiveness to inhaled methacholine in OVA-sensitized and OVA-challenged mice.** 24h after the last challenge with OVA, the mice were administered serially increasing doses of methacholine at the indicated concentration every 20 mins, and airway hyperresponsiveness was measured. Values are expressed as the means  $\pm$



SEM of 11-12 mice per group. Statistically significant differences between groups are indicated (\*  $p < 0.05$ , \*\*  $p < 0.01$ , \*\*\*).

### 3.5.2.2. NP conjugated with OVA and CpG suppress the induction of OVA-specific IgE in a model of acute asthma

Asthma is a multifactorial disease in which both allergic factors and non-allergic triggers interact and subsequently result in airway-hyperactivity and lung inflammation. Allergic responses are induced by allergen/IgE immunocomplexes that bind and cross-link mast cell surface IgE receptors, which trigger mast cell activation. Given the IgE suppressing activity of NP formulations that codelivered OVA and adjuvant in anaphylaxis, their effect on IgE production in asthma was monitored: OVA-sensitized mice, subsequently treated with NP formulations that contained OVA and CpG (p[OVA+CpG], p[OVA+CpG+aDEC205]) showed largely reduced IgE titers after the 2<sup>nd</sup> vaccination as compare with control group, while IgE contents in the other groups were significantly elevated (Fig. 49).

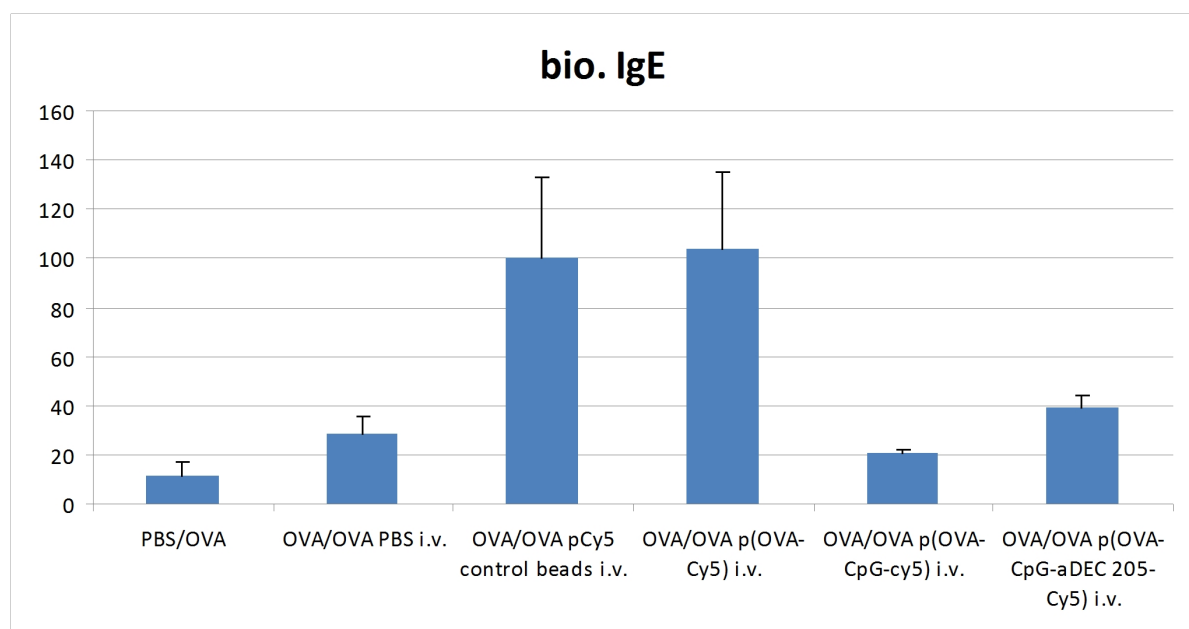


**Fig. 49: Vaccination of OVA-sensitized mice with OVA/CpG-codelivering NP prevents upregulation of IgE expression.** After measurement of *in vivo* airway responsiveness, mice were sacrificed and bled by cardiac puncture. Subsequently, serum was collected and stored at  $-80^{\circ}\text{C}$  until analysis. OVA-specific IgE in serum was measured as described. Values are expressed as mean  $\pm$  SEM (n = 12).

### 3.5.2.3. NP which codeliver OVA and CpG induce a Th1-skewed humoral response in a model of acute asthma

The serum levels of OVA-specific IgG subtypes in the different groups of mice as assessed after measurement of *in vivo* airway responsiveness are depicted in Fig. 50. Sera of mice immunized with OVA contained comparable concentrations of IgG1 (Fig. 50A) antibodies, while untreated mice (naïve) lacked OVA-specific antibodies. Only codelivery of OVA plus immunostimulatory CpG ODN irrespective of DEC205 targeting resulted in enhanced OVA-specific IgG2a titers as compared with sera derived from control mice and those vaccinated with NP containing OVA alone (Fig. 50B). This finding confirms the Th1-promoting character of CpG.

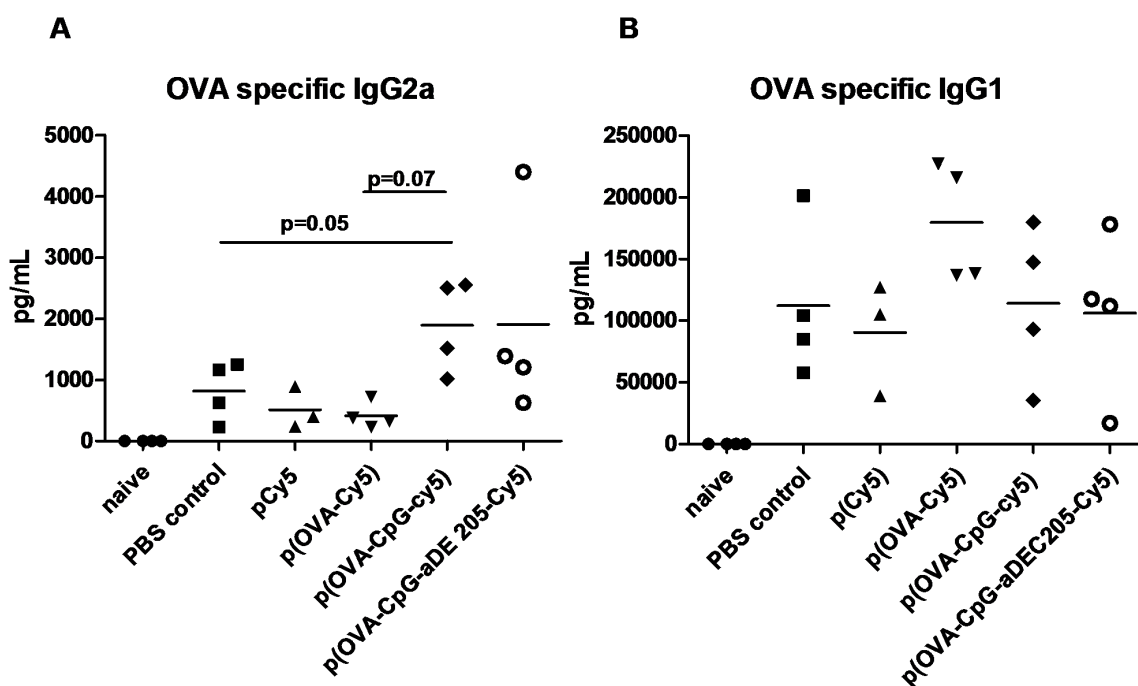
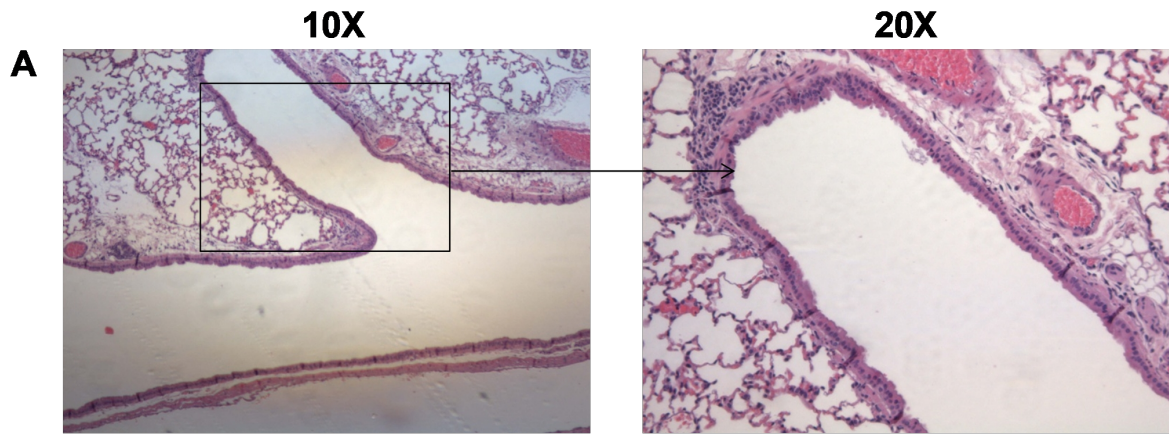


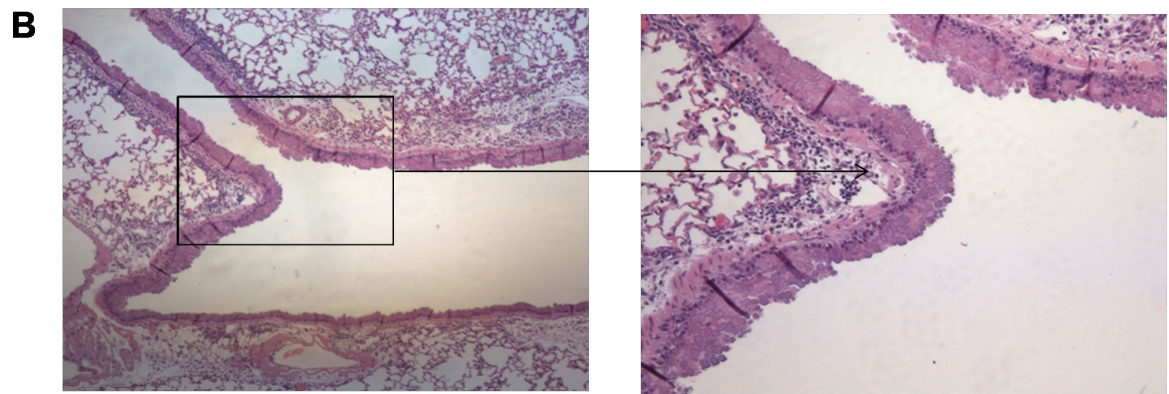
**Fig. 50: Vaccination of OVA-sensitized mice with OVA/CpG-codelivering NP formulations promotes a Th1-biased IgG pattern.** After measurement of airway responsiveness, mice were sacrificed and bled by cardiac puncture. Subsequently, serum was collected and OVA-specific IgG isotype levels were measured as described. Values are expressed as the means  $\pm$  SEMs with 4 mice in each group. Data represent of 3 independent experiments.

#### **3.5.2.4. Histological analysis of lung inflammation parameters in OVA-immunized mice vaccinated with different NP formulations**

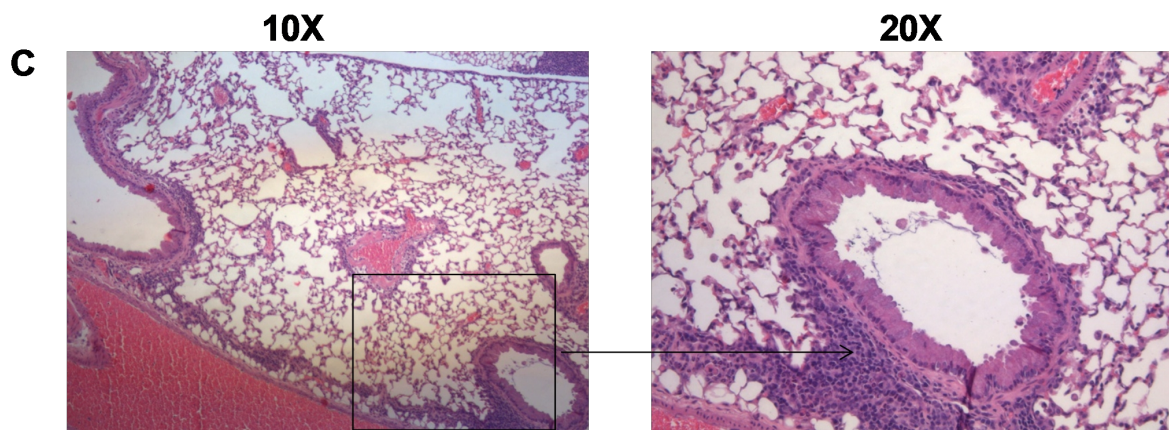
Airway inflammation, hyperplastic goblet cells, and collagen deposition are typical features of asthma. The histological sections of lung tissue from mice showed increased number of inflammatory cells and hyperplastic goblet cells. Therefore, haematoxylin and eosin (H&E) staining was performed in this study to analyze the inflammation of lung in this asthma model after AHR measurement. As shown in Fig. 51A, the lungs of naïve mice were devoid of inflammatory cells in the airways, whereas the positive control mice (PBS, no vaccination), and mice vaccinated with p(Cy5) or p(OVA) showed a marked infiltration with inflammatory cells (Fig. 51B-D). Accordingly, the scores for total lung inflammation were significantly increased after OVA inhalation as compared with the score in the naïve group (Fig. 51G). OVA-immunized mice treated with p(OVA-CpG) and p(OVA-CpG-aDEC205) prior to OVA challenge (Fig. 50E,F) showed a significantly lower frequency of inflammatory cells in lung tissue as compared to the other experimental groups (Fig. 51 B-D). The scores for total lung inflammation in mice vaccinated with p(OVA-CpG) and p(OVA-CpG-aDEC205) were significantly lower as compared with the scores in the other two groups vaccinated (Fig. 51G).



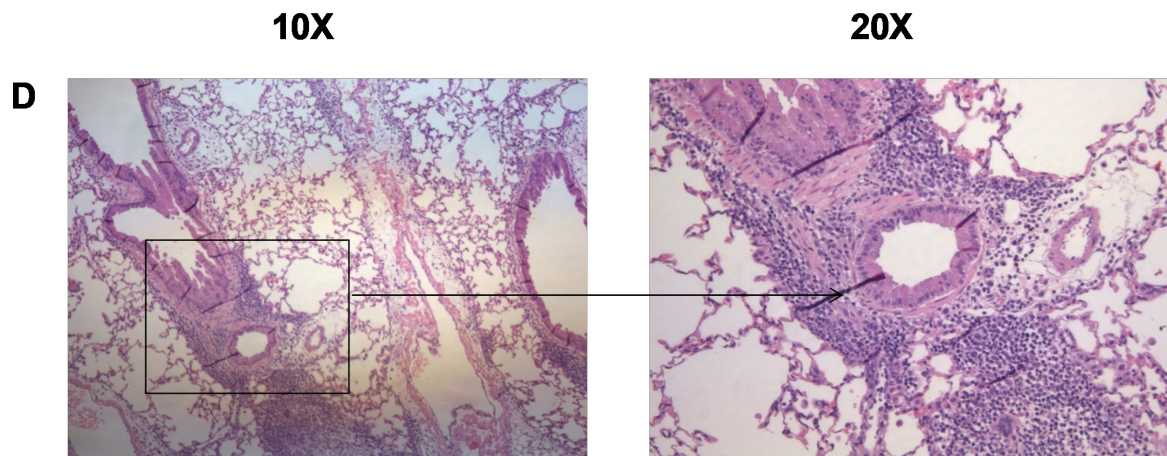
Naive



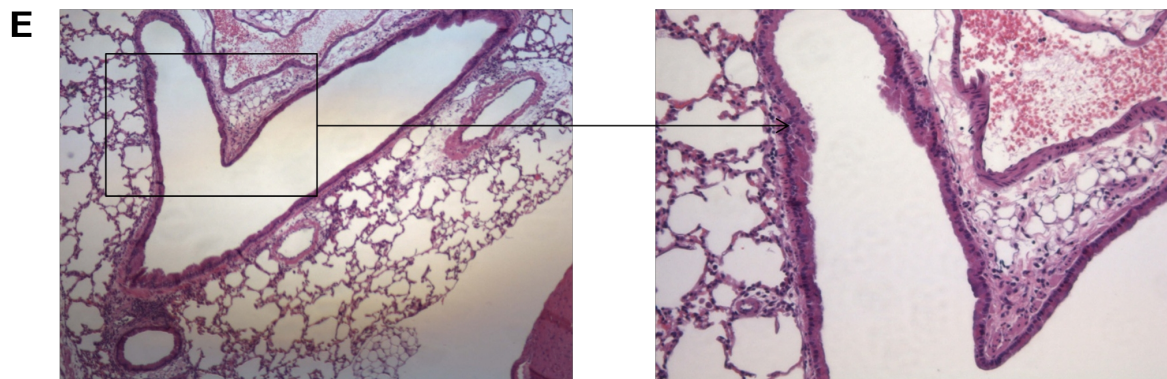
Positive



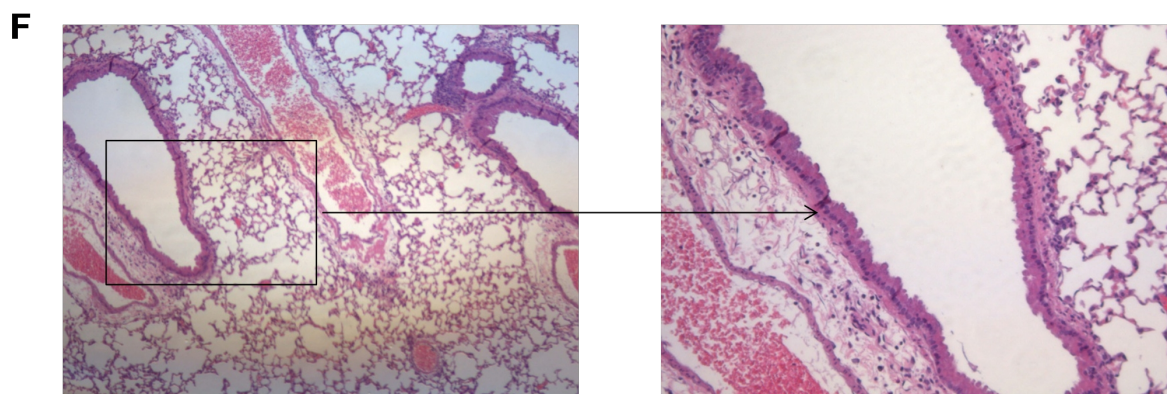
P(control-beads)



pOVA



p(OVA-CpG)



p(OVA-CpG-aDEC205)

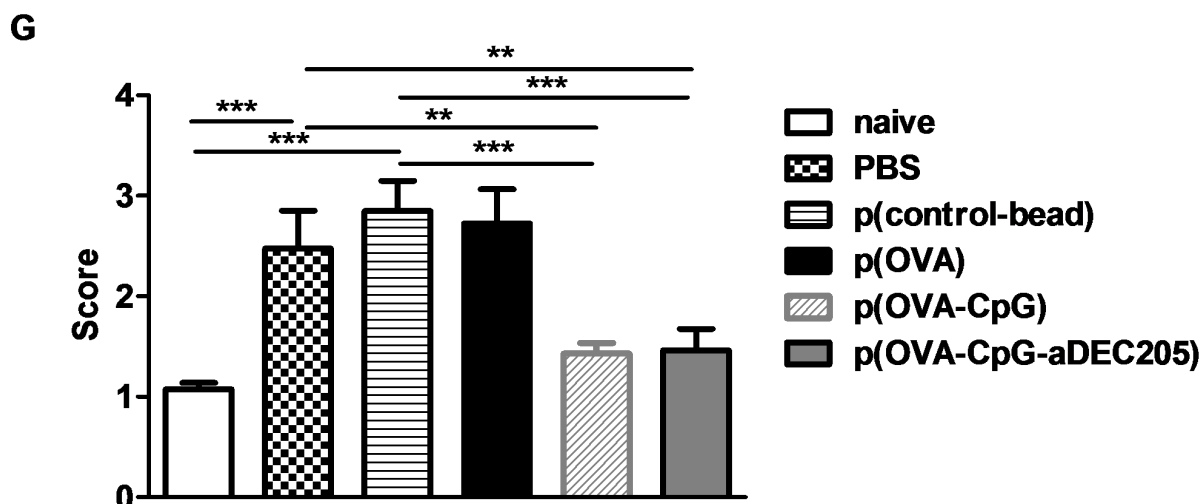


**Fig. 51: Lung inflammation of mice immunized with OVA, and vaccinated with different NP formulations prior to inhalative challenge with OVA.**(A-F) Representative haematoxylin and eosin (H&E) stained lung histology sections of OVA-Alum-sensitized mice, immunized with different NP formulations prior to challenge are shown at 10X (left), and sections of these at 20x (right) magnification. (A) Naïve control, (B) PBS, (C-F) vaccinated with different NP formulations: pCpG (C), p(OVA) (D), p(OVA-CpG) (E), p(OVA-CpG-aDEC205) (F). (G) Quantification of lung inflammation. Inflammatory cells in the lungs were determined by histology from H&E-stained longitudinal cross-sections and graded as no change (score = 0), mild (score = 1), moderate (score = 2), or severe (score = 3) as described (Buchweitz *et al.*, 2007). To assess lung inflammation scores, 40 lung sections of each group were scored. Data show total lung inflammation scores (mean±SEM) of 11-12 mice per group treated as described derived from two independent experiments. Statistically significant differences between groups are indicated (\*\*  $p < 0.01$ , \*\*\*  $p < 0.001$ ).

Taken together, the results of the anaphylaxis and acute asthma model indicated that nanoparticles functionalized with OVA and CpG can shift the balance between Th2 and Th1 responses in the allergic response towards Th1 response. The consequences are an increased Th1 antibodies production and a reduction in Th2-associated antibodies, and a suppression of antigen specific IgE. The results suggest that co-delivery of the model allergen OVA and the adjuvant CpG may have important benefits for the application of allergen-specific immunotherapy (SIT). In this regard, DC targeting has no additional benefits.

## 4. Discussion

### 4.1. The impact of FV-infection on DC phenotype and functions

#### 4.1.1. Alterations of the phenotype of BMDC induced by FV infection occur both in a genotype-dependent and -independent manner

Understanding the basic immunological mechanisms that facilitate resistance to retroviral infections is vital for the rational development of preventive and therapeutic treatments against retrovirus-induced diseases (Dittmer *et al.*, 2004). In the FV model, numerous antiviral activities of CD4<sup>+</sup> T cells, CTL responses (Zelinsky *et al.*, 2006) and B cell induced antibody responses (Poluquin *et al.*, 2011) have been described, but how FV infection affects DC required to evoke antiviral responses are not clear. As a central part of the immune system, DC are crucial for the induction of protective antiviral immunity. The most important functional properties of stimulated DC are T cell engagement and subsequent activation of antigen-specific T cells, which is the critical step for the induction of adaptive immunity after infection. Therefore, one focus of this project was to identify differentially regulated molecules in DC derived from FV-infected progenitor cells of a FV-susceptible (BALB/c) versus -resistant (C57BL/6) genotype (Hasenkrug *et al.*, 1997 & Marrison *et al.*, 1987), and to assess their role in inducing an antiviral response. pDC as described in the introduction have been shown to constitute an important cell population that produces large amounts of type I interferons in response to viral infection (Colonna *et al.*, 2004). Our group started this project with a focus on cDC. Therefore, the FV-dependent effects on pDC in FV infection will be analysed in the future.

Due to the low susceptibility of C57BL/6 mice against FV infection, in order to obtain enough infected DC, these mice were inoculated with rather high doses of FV. Nonetheless, in FV-resistant C57BL/6 mice, after inoculation only an average of 6.2% of CD11c<sup>+</sup> splenic DC were FV-infected, while 25.29 % of splenic DC derived from FV-inoculated susceptible BALB/c mice were FV-Gag protein positive. Likewise, as shown Fig. 2, about 8% of BMDC derived from bone marrow of FV-infected C57BL/6 mice were virus-positive compared to about 24% of FV-Gag<sup>+</sup> BMDC differentiated from FV-infected BALB/c BM cells. To my knowledge, the effect of FV

infection on genotype dependent DC has been analyzed in detail in any other studies.

Usually, upon viral infection of the host, DC receive activation signals (such as virus ssRNA, which triggers TLR3), subsequently become mature, and induce anti-viral T cells responses. Due to direct infection of their progenitor cells, BMDC derived from FV-infected BM cells from both strains showed reduced expression of co-stimulatory molecules CD80, CD86, CD40, and of MHC II, both at unstimulated state and after stimulation with LPS, as compared with the corresponding control DC population (Fig. 11). These data confirmed the results from Balkow *et al.*, (2007), who showed that FV infection impaired the maturation of BALB/c DC. In accordance, FV-infected BMDC from susceptible and resistant strains maintained their capacity for endocytosis (Fig. 18), which is normally downregulated during DC maturation. Thus, FV infection prevents full DC maturation and thereby may impair the host's capacity to mount effective T cell-mediated FV-specific immune responses. It has been demonstrated for other virus infections that virus induced immunosuppression was associated with an inhibition of DC activation as well, such as shown for measles virus or human immunodeficiency virus type 1 (HIV-1) (Schneider-Schaulies *et al.*, 2006).

IL-12 and IL-10 are important cytokines produced by DC to affect activation and differentiation of T cells upon DC-T-cell contact. Usually, when DC are immature, they are not efficient in producing IL-12 and IL-10. However, as shown in Fig. 18, FV-infected DC were immature, but upon stimulation secretion of IL-12 and IL-10 were similar to uninfected DC in a genotype-independent manner. This is very surprising, because usually other virus infections like human cytomegalovirus (HCMV), infection impairs maturation of DC, and therefore impairs production of IL-12 (Moutaftis *et al.*, 2002). It has been also shown that HIV-1 infection inhibited IL-12 production but upregulated IL-10 in DC (Fantuzzi *et al.*, 2004). In my study, IL-10 production was unaltered in FV-DC. It will be interesting to analyse other cytokines like IL-35, a cytokine belongs to the IL-12 family as well, but suppresses T cell proliferation, and plays a role in immunosuppression (Collison *et al.*, 2012).



#### 4.1.2. FV infected BMDC induce alteration of T cell response in genotype independent manner

Preliminary studies from our lab group have indicated that FV infection of DC induced a maturation-resistant immature state (Balkow *et al.*, 2007). Analysis of the interactions between DC and T cells by time lapse microscopy revealed that FV-infected DC (FV-DC) showed a higher frequency of prolonged contacts with T cells (median contact duration of 38 min) as compared with uninfected DC (Balkow *et al.* 2007). In this PhD study, the contacts between FV-infected DC and CD4<sup>+</sup> T cells were also assessed. Similar to the results of Balkow *et al.*, (2007), DC/T cell contacts were prolonged, when DC were derived from FV-infected progenitors from FV-susceptible BALB/c mice, whereas no significant difference was observed between FV-infected and uninfected C57BL/6 BMDC. It still remains to be determined which molecules are involved in stabilizing the long contacts of FV-DC. As shown in Tab. 5, FV infection induces differently regulation of some cytoskeletal proteins. These proteins are important for DC migration and adhesion. Potential effects of these proteins on DC-T cell contacts will be analysed in the future.

In BALB/c mice, during the long DC/T cell contacts, T cells become activated by FV-infected DC, but this activation does not result in profound antigen-specific T cell proliferation. In contrast, these prolonged contacts induced the expansion of Tregs (Balkow *et al.*, 2007). Since some mouse strains are susceptible towards FV infection (e.g. BALB/c), while others (e.g. C57BL/6) are resistant (Hasenkrug *et al.*, 1997 & Marrison *et al.*, 1987), strain-dependent differences in FV-induced T cell responses and the associated changes of the function of DC were analyzed in the course of this project.

An antiviral immune response is a complex orchestration of components of both the innate and adaptive immune system (Wu and Kewal Ramani, 2006). The innate immune response is a rapid, non-specific response to infection that provides an early line of defense, prior to the induction of highly specific adaptive responses, that include a cellular and a humoral component. The results of my study show that upon FV infection the DC activation state is impaired in a genotype-independent manner in FV-susceptible BALB/c mice as well as in FV-resistant C57BL/6 mice. In general, as a result of activation, DC are able to present antigens through MHC I and MHC II to T

cells, and provide both costimulatory and T cell polarizing signals to induce antigen specific T cells responses. Figs. 13 and 16 A,B show that CD4<sup>+</sup> T cell proliferation and IFN $\gamma$  production was reduced when FV-infected, LPS-stimulated DC of BALB/c or C57BL/6 genotype were used as stimulators *in vitro* and *vivo*. A lack of antiviral IFN $\gamma$  production by CD4<sup>+</sup> T cells, as well as loss of direct CD4<sup>+</sup> T cell cytotoxic activity against virus-infected cells has been shown to contribute to immunodeficiency (e.g HIV) (Norris *et al.*,2001). However, the loss of CD4<sup>+</sup> T cell helper activity may effect on CTL activation (Iwashiro and Hasenkrug, 2001) and the establishment of long-term CD8<sup>+</sup> T cell memory, as well as the development of efficient antibody production and memory B cell induction, both of which are deficient in HIV-1 retroviral infections (Altfeld and Rosenberg , 2000).

Some previous studies have shown that CD4<sup>+</sup> T cells may exert direct antiviral effects during the persistent phase of infection, rather than providing classical helper functions for CD8<sup>+</sup> CTLs or antibody-producing B cells only (Hasenkrug & Dittmer, 2000). However cytotoxic CD8<sup>+</sup> T lymphocytes (CTL) are necessary for the control of viral infections, and are critical for recovery from the acute phase of FV infection (Hasenkrug *et al.*, 1995). Due to the reduced level of activated antigen-specific CD4<sup>+</sup> T cells proliferation and reduced IFN $\gamma$  production by these CD4<sup>+</sup> T cells as induced by FV-DC of either genotype was detected in this study, the *in vivo* proliferation of antigen-specific CD8<sup>+</sup> T cells stimulated by FV-DC in C57BL/6 mice was analyzed in addition. Similar to the results concerning CD4<sup>+</sup> T cells, the proliferation of CD8<sup>+</sup> T cells was reduced, and the frequency of IFN $\gamma$  producing CD8<sup>+</sup> T cells was lower in mice immunized with FV-infected BMDC than uninfected BMDC. IFN $\gamma$  plays an important role in resistance against FV infection, and is likely to be critical also to induce more effective and long-lasting anti-tumor immunity (Iwashiro *et al.*,2001 & Kennedy, 2008). Taken together, the results of this PhD thesis demonstrate that FV-infected DC cannot induce effective Th1/Tc1 cell responses.

At the onset of this study, it was assumed that the differential susceptibility of BALB/c and C57BL/6 mouse strains towards FV may be analogous to the strain-specific susceptibility to *Leishmania major* infections, for which BALB/c mice are susceptible because of a Th2 bias, in contrast to C57BL/6 mice (Launois *et al.*,1995). Interestingly, in FV infection the results concerning the character of the CD4<sup>+</sup> T cell responses in DC/T cell cocultures demonstrated that DC of either mouse strain

favored a Th2 response. Congruently, the Th1 and Th17 responses evoked by FV-infected DC were impaired in a genotype-independent manner (Fig. 14, 15). Taken together, FV infection induced poor total CD4<sup>+</sup> T cell proliferation in a genotype independent manner, while Th2 responses was significantly enhanced by DC of either strains. To my best knowledge, this PhD study was the first in which the T cell stimulatory and polarizing properties of FV-infected vs. uninfected DC of different genotype have been assessed.

#### **4.1.3. FV-induced alterations in protein expression in DC in genotype dependent manner**

##### **4.1.3.1. Expression of cytoskeletal proteins in BMDC were altered in genotype dependent manner**

It is interesting that although BALB/c mice are FV-susceptible and C57BL/6 mice are rather FV-resistant, the CD4<sup>+</sup> and CD8<sup>+</sup> T cell responses and their cytokine secretion patterns as induced by FV-infected DC of either mouse strain were largely comparable. In order to determine whether FV-infected DC of either genotype may differentially contribute to resolve a FV infection, the proteome of uninfected and FV-infected BMDC of FV-susceptible BALB/c and C57BL/6 -resistant mice was comparatively analyzed by protein mass fingerprinting. By this, more than 300 differentially expressed proteins were identified. Among these, many cytoskeletal proteins and molecules known to be involved in DC-T cell interaction (e.g Myosin 10, Filamin A, Tubulin) were identified as differentially regulated (Tab. 3). Differentially regulated cytoskeletal proteins may contribute to the prolonged contact duration in BALB/c DC-T cell. In accordance, the expression of F-actin in FV-infected BALB/c DC was clearly increased as compared with FV-infected C57BL/6 DC, which displayed unaltered Dc-T cell contact characteristics (Fig. 19). On the other hand, the mobility of FV-infected DC of both mouse strains was also changed, since C57BL/6 FV-infected DC showed an enhanced spontaneous migratory activity in collagen gels, albeit not statistically significant. In future experiments, the mobility of FV-DC will be analyzed in more detail, for example, in terms of chemokine-dependent migration.

#### 4.1.3.2 Expression of S100A9 was differently regulated in FV-infected BMDC in a genotype dependent manner

One of the most interesting results of the comparative protein-mass fingerprinting analysis was that S100A9 was differently regulated in DC derived from FV-infected BM cells of BALB/c and C57BL/6 mice: In FV-infected BALB/c-DC, S100A9 was significantly downregulated as compared with control DC, but in FV-infected C57BL/6-DC this protein was upregulated in expression. S100A9, also referred to as myeloid-related protein 14 (MRP14), calprotectin or calgranulin B, is a member of the large family of S100 proteins (Heizmann, 2002 & Roth, 1992). S100A9 heterodimerizes with S100A8 (MRP8 or calgranulin A), and is predominantly expressed in circulating neutrophils and monocytes, but not in resting tissue macrophages (Ehrchen, 2009). S100A8/9 complexes have been identified as endogenous activators of TLR4, and have been shown to promote lethal, endotoxin-induced septic shock (Vogl, 2007). S100A8/9 is not only involved in promoting an inflammatory response in infections, but has also been identified as a potent amplifier of inflammation in autoimmunity as well as in cancer development and tumor spread (Ghavami, 2009). Many studies have demonstrated the high level expression of S100A8/9 in macrophages, monocytes and neutrophils in inflammation conditions (Ryckman *et al.*, 2003 & Roth *et al.*, 2003). However, the role of S100A9 in DC has scarcely been analyzed so far.

To investigate the role of S100A8/9 in FV infection, S100A8/9 knockout mice on C57BL/6 background, kindly provided by Prof. J. Roth (Institute of Immunology, University of Münster), were infected with FV. Due to the fact that splenomegaly is an important symptom of FV infection, first the weight of spleens from FV-infected WT and KO mice was compared, but no difference was noted (data not shown).

However, S100A8/9 mice were more susceptible to FV-infection as compared with wild type (WT) mice, since the frequency of FV-infected BM cells was significantly higher than in case of BM cells derived from infected WT mice (see Fig. 21). In addition, 7 days after BM cell culture in the presence of GM-CSF, the frequency of FV-infected S100A9<sup>-/-</sup>-BMDC was significantly higher than in WT controls. This result indicates that S100A9 may be involved in the innate anti-FV response.

A couple of studies have shown that S100A8/9 is able to interact with components of the cytoskeleton in a calcium-dependent manner (Dirk, 2007). In human neutrophils, S100A9 was found associated with cortical F-actin and *in vitro* studies have demonstrated a direct association of S100A8/9 with F-actin (Lominadze *et al.*, 2005). Functionally, the S100A8/9 complex was shown to modulate the tubulin-dependent cytoskeleton during the migration of phagocytes (Vogl and Ludwig, 2004). In this PhD study, DC derived from FV-infected S100A9<sup>-/-</sup> BM cells mice also showed a reduced migratory velocity compare with the FV-infected WT BMDC(Fig. 22). However, due to limited availability of KO mice, the difference between FV-infected versus uninfected KO DC was not significant yet. Additional experiments are intended to clarify the potential role of S100A9 on the migratory acitivity of (FV-)DC.

Ongoing work is focussed on the analysis of type I interferon (IFN- $\alpha$  and IFN- $\beta$ ) production after FV infection in S100A9 KO versus wild type mice, and of FV-antigen specific IgE, as well as of other parameters of disease progression which may be modulated by S100A8/9. As described in the introduction, mouse APOBEC3 (mA3) is a key factor in FV infection: mA3 family members are potent restriction factors of viruses and retrotransposable elements (Hakata, 2006 & Harris, 2003), and several mechanisms have been proposed to contribute to the antiviral activity of APOBEC3. For example, when a retroviral nucleocapsid penetrates the target cells and subsequently initiatsthe reverse transcription of the RNA genome into DNA, APOBEC enzymes can induce the conversion of cytosine to uracil in the minus strand viral DNA, this process leading to a failure in reverse transcription and to a high number of G-to-A mutations in the integrated proviral genome, whichmay impair viral replication (Zhang *et al.*, 2003).

Virl and his colleagues (Virl, 2009) showed that treatment of BMDC of mice with lipopolysaccharide (LPS) caused increased levels of mA3 expression and rendered them resistant to MMTV infection (Virl, 2009 & Okeoma *et al.*, 2009). Several A3 proteins are also expressed at higher levels in cells that restrict HIV-1infection, such as monocytes and mDC (Peng *et al.*, 2007). S100A8/9 is an endogenous TLR4 ligand (Vogl *et al.*, 2007), and therefore may have an effect on mA3 expression. Therefore, the expression of mA3 in S100A9 KO DC wasinvestigated in my study too.As shown in Fig. 23, the expression of mA3 was decreased in S100A9<sup>-/-</sup>BMDC as compared with WT BMDC.Fortunately, it was provided with recombinant S100A8/9

from Prof. J. Roth, and effects of S100A8/9 and S100A9 homo-heterodimer on mA3 in wild type BMDC were analyzed by qPCR. Only S100A8/9 significantly enhanced the expression of mA3 in BMDC (Fig. 24). Altogether, these results indicate that S100A8/9 may contribute to restrict FV infection by inducing mA3. Ongoing work is dedicated to further delineate the role of S100A9. In this regard, the content of S100A9 in serum of FV-infected mice of either genotype (BALB/c, C57BL/6) will be measured in a time kinetics study after the onset of infection. In many studies Vogl and his colleagues have shown that S100A9 as a proinflammatory marker (Foell *et al.*, 2004) was released at the beginning of inflammation and then downregulated. In my study, the expression of S100A9 was found highly expressed in unstimulated BMDC derived from FV-infected BM cells. Therefore, it will be of interest to analyze time- and differentiation-dependent production of S100A9 by FV-infected BM cells and derived BMDC in a time kinetics assay in the course of DC differentiation. Some studies have demonstrated that in BALB/c mice, the lack of APOBEC3 expression and lower APOBEC3  $\delta 5$  exon isoform expression may be the reason for the susceptible of FV infection. In this PhD thesis showed that S100A8/9 can upregulate expression of APOBEC3. Therefore, with regard to a potential therapeutic usage, it will be interesting to investigate, whether injection of S100A8/9 into FV-susceptible BALB/c mice prior to FV infection will alter the otherwise lethal course of disease.

The S100A9 deficient mice used for this study were conditional KO. It will be interesting to use S100A9 DC-specific KO mice to understand how retroviral infection alters the phenotype and function of DC, whether these effects are important for retrovirus-induced immunosuppression and deviation, and how suppression of antigen presentation and formation of erythroleukemia are related. Since the immunological features of FV infection are analogous in many ways to infections with human pathogenic retrovirus (Dittmer, 2001), this mouse disease model may provide an opportunity to develop new concepts in vaccine development against retroviruses. For example, using functional nanoparticles as vaccines carrying FV antigen(s) plus adjuvant that address DC subsets with high cross presenting activity may constitute a worthwhile strategy in future studies to induce an effective anti-retroviral response.

## 4.2. Dextran nanoparticles

DC constitute an attractive target for immunotherapeutic strategies based on their versatile functional properties, namely to maintain peripheral tolerance under steady state conditions (Morel *et al.*, 2011), but to induce potent immune responses when activated by pathogen-associated or endogenous danger signals (Joffre *et al.*, 2009). In conventional vaccination strategies protein antigen(s) and APC-activating adjuvant(s) are coinjected. However, it is well established by now, that antigen in combination with an adjuvant induces a stronger immune response when codelivered as a particulate formulation.

Although a number of nanoparticulate formulations have been developed by now, but major restrictions arise on one hand from their laborious synthesis and functionalization, and other hand from the limited biodegradability, cytotoxicity, and intrinsic immune-modulatory properties of such formulations (Liu *et al.*, 2011). As an alternative in this part of the PhD study, usage of dextran based-nanoparticles (DEX) as a simple to produce, biodegradable and non-cytotoxic carrier system for APC-focussed delivery of cargo was assessed. DEX-based nanovaccines have been introduced 30 years ago by Schröder and his colleagues (1983), and were shown to release entrapped compounds *in vivo* (Schröder 1983). In that study, DEX particle-entrapped proteins with signaling function constituted enzymes and antibodies were shown to retain their biological activity after release. Accordingly, in this PhD study DEX particles were demonstrated to serve as antigen carriers which elicited antigen-specific humoral responses *in vivo* after s.c. immunization of mice, enhanced upon codelivery of immunomodulators at much higher extent than direct immunization with soluble antigen.

The DEX preparations used in this study appeared as spherical nanoparticles of 50nm in diameter, devoid of cytotoxic or direct immunoactivating effects, important prerequisites for their intended use as a nanovaccine platform.

The rationale of using OVA as a model protein antigen was based in part on its mannosylated state (Mao *et al.*, 2003), reported to confer efficient binding to the mannose receptor (MR) and subsequent cellular uptake by DC (Burgdorf *et al.*, 2006). The MR is a CLR receptor, which belongs to a group of antigen sensing surface

receptors with endocytotic activities, largely confined to DC and macrophages (Robinson *et al.*, 2006). Hence, the MR is involved in the clearance of endogenous proteins (Gazi *et al.*, 2009), but binds mannosylated pathogen-derived antigens (Gazi *et al.*, 2009) and mannosylated allergens (Royer *et al.*, 2010) as well. In this project the intrinsic APC targeting property of OVA, which by itself constitutes an important model antigen frequently employed to study adaptive immune responses, was to be exploited in order to facilitate APC-focussed particle delivery. In agreement with the well-established MR-targeting properties of OVA, DEX particles that contained OVA were efficiently engulfed by murine BMDC in an OVA- and MR-dependent manner (Fig. 26B). Likewise, OVA-containing DEX particles efficiently bound primary splenic DC and macrophages that also express the MR, but not MR-deficient B cells and T cells (Fig. 26 D).

These results suggest that mannosylation of a given protein antigen may suffice to mediate binding and cellular uptake of a conjugated nanovaccine by MR-expressing APC. Accordingly, OVA protein may serve both as a source of antigen, and as an APC-targeting molecule. The finding that BMDC incubated with DEX(OVA) remained in an immature state (data not shown) indicates that MR engagement as such is not sufficient to mediate DC activation. Many studies have demonstrated that nanoparticles may exert immunomodulatory activity (Coffman *et al.*, 2010). The intrinsic immunomodulatory property of nanovaccines may determine the character of an immune response in an unwanted manner, e.g. uncontrolled T cell polarization (Peck *et al.*, 2010). On the other hand, the lack of immunomodulatory activity of DEX particles on BMDC clearly broadens their range of application because it may allow shaping the nanovaccine-mediated immune response solely according to the properties of codelivered adjuvants (Tacke *et al.*, 2011). In this PhD study, LPS was employed as a TLR4 ligand, well known to activate DC, which in turn evoke Th1-biased immune responses (Agrawal, 2003). Indeed, LPS-containing DEX particles readily activated BMDC to similar extent as LPS when applied directly, as reflected by comparable upregulation of costimulatory markers. Interestingly, DEX particles that contained LPS alone were not engulfed by BMDC at higher degree than empty DEX (Fig. 26A). Interestingly, a study from Demento and his colleague (2009) showed that PGLA-based nanoparticles were engulfed by murine DC at higher efficiency when conjugated with LPS, which suggested that TLR4 engagement may be sufficient for subsequent uptake of TLR4 ligand-coated nanovaccines. The



discrepancy between the observations of Demento (2009) and the results of this study may be explained at least in part by differences in particle-surface LPS densities (Demento *et al.*, 2009).

BMDC coincubated with DEX(OVA) subsequently induced robust CD4<sup>+</sup> T cell proliferation to a higher extent than pretreatment at DC with soluble OVA protein (Fig. 27A). This observation is in full agreement with previous studies which reported on strongly enhanced bioactivity of antigen when delivered in a particulate formulation (Bolhassani *et al.*, 2011). In accordance with the finding of specific targeting of primary myeloid APC via the MR by OVA-containing DEX, codelivery of LPS *in vivo* induced a robust OVA-specific CD4<sup>+</sup> T cell proliferation. In addition, DEX particles loaded with OVA plus LPS (DEX[OVA+LPS]) evoked the strongest OVA-specific CD8<sup>+</sup> T cell proliferation and IFN $\gamma$  production of all groups assessed (Fig. 28 A, B). These observations are in full agreement with previous studies which reported on strongly enhanced bioactivity of antigen when delivered in a particulate formulation (Bolhassani *et al.*, 2011). The strongest CTL response was obtained in mice vaccinated with the DEX-based nanovaccine that codelivered OVA and LPS. Therefore, DEX-based nanovaccines also served to mediate cross presentation of OVA-derived peptides entrapped by APC after *in vivo* application (Amigorena *et al.*, 2010). These results demonstrate that DEX-based nanovaccines may constitute a suitable platform for the development of vaccines against tumors and intracellular pathogens, when CTL-mediated cell killing and CD4<sup>+</sup> T helper cells are essential to resolve the disease.

Besides mounting potent T cell responses, in line with the results obtained by Schröder *et al.*, (1984), DEX-based nanovaccines also induced a humoral response: In this regard, vaccination with DEX(OVA) induced a Th2-biased OVA-specific IgG isotype pattern (IgG1>IgG2a). Coapplication of the adjuvant LPS (DEX[OVA+LPS]) resulted in enhanced antibody production (Fig. 29), while the Th2-biased character of humoral response was retained. This finding suggests that in context with DEX-derived nanovaccines other adjuvants than LPS are required to induce a pronounced Th1-skewed pattern of antibody production.

As described above, the method of DEX-based particle preparation as adopted in this PhD thesis was described more than 30 years ago. However, both the exact structure of this type of nanoparticle and the character of particle binding of OVA and

LPS are still unclear. Concerning the usability of dextran for the synthesis of nanoparticles in general, it has been shown that acetalated dextran capsules loaded with OVA can induce a stronger MHC I presentation than mediated by soluble OVA protein (Broaders *et al.*, 2009 & Bachelder *et al.*, 2008).

Taken together, in this part of my Ph.D thesis it was shown that DEX-based nanoparticles are biocompatible, biodegradable and rather simple to prepare. Due to these favorable attributes, such nanoparticles may have significant advantages over other more complex polymers or microparticles currently tested for their suitability to mediate APC-specific delivery of antigen and adjuvant *in vivo*.

### 4.3. Solid core nanoparticles induce an effective antitumor response

Due to their potent APC activity, DC are a natural focus for the development of immunotherapeutic strategies. In clinical settings, for anti-tumor therapy, DC differentiated from cancer patient-derived progenitor cells have been expanded in culture, loaded with tumor antigens and re-administered into the patient (Tacke *et al.*, 2007). Such immunization strategies have produced some limited successes, but so far have not emerged as an effective means of cancer treatment. In the last decade, the use of nanoparticles as vaccine and adjuvants delivery systems has been reviewed extensively: As a principal finding, a stronger immune response is elicited when an antigen (Petros, 2010) and an adjuvant (Nembrini, 2011) are co-delivered by nanoparticles as compared with direct application of soluble antigen and adjuvant directly delivery.

In this part of this PhD study, supramagnetic solid core nanoparticles coated with a biocompatible polysaccharide shell (Fe-NP) were used as carriers for antigen, adjuvant, and a DC-targeting antibody. Compared with DEX particle, the exact structure of this type of nanoparticle and the character of binding of antigen and adjuvants are better defined. Therefore, these supramagnetic solid core nanoparticles were employed for a tumor immunotherapeutic model. In order to determine the best strategy to enhance immune responses by delivering antigen plus adjuvant rather specifically to DC *in vivo*, three issues were considered: The first was the choice of the DC subset to be targeted. In this regard, CD8<sup>+</sup> DC were favored as the most potent DC subset to induce of effective CTL responses, because of its inherent ability to cross-present antigen of exogenous origin to effectively prime CD8<sup>+</sup> T cells. As described in 2.2.4.2, by now several CLRs has been explored as target receptors for antibody-mediated antigen delivery, including DEC205 (CD205) (Bonifaz, 2002), DCIR2 (Meyer-Wentrup, 2008), Dectin-1 (Carter *et al.*, 2006), MR (Tacke, 2005), and DC-SIGN (Tacke, 2005). To specifically target CD8<sup>+</sup> DC, DEC205 predominantly expressed by this DC subset (Jiang *et al.*, 1995), was chosen as an adequate target receptor. Targeted delivery of antigens to CLR was demonstrated to lead to efficient induction of humoral and anti-viral as well as anti-tumor immune responses (Robinson, 2006 & Tacke *et al.*, 2007). However, while

antibody-mediated delivery of antigens to DC may ensure antigen presentation and tolerance (Singhet *et al.*, 2009), the presence of suitable adjuvants is required to ensure appropriate activation of DC. Some studies have also proven that targeting DEC205 on DC in the absence of maturation signals results in T-cell tolerance (Bonifaz *et al.*, 2002), but when targeting DEC205 and coapplying maturation signals like anti-CD40mAb T cell immunity was improved (Bonifaz *et al.*, 2004). Based on our finding that DEC205-addressing NP were internalized by DC by receptor-mediated endocytosis, indicative of endo/lysosomal localization, it was conceivable that NP-released material may have direct access to TLRs 7/8, and 9 localized in this compartment to recognize (pathogen-derived) nucleic acids (Takeda *et al.*, 2003). To prevent the induction of tolerance, as a third property, Fe-NP were engineered to carry immunostimulatory CpG oligonucleotides as an effective ligand of endo/lysosomal TLR 9 receptor, aimed to induce a Th1-promoting capacity in DC after NP engulfment (Takeshita, 2001 & Diwan, 2002). Consequently, antigen-delivering NP engineered to target DC via DEC205 engagement were functionalized with CpG ODN to ensure coupled delivery of antigen and adjuvants specifically to the same DC, and thereby avoid unspecific APC activation.

By confocal laser microscopy, it was shown that engulfment of Fe-NP by BMDC was enhanced when these NP were conjugated with a DEC205-targeting antibody (Fig. 30 A,B). In correspondence, splenic CD8<sup>+</sup>CD11c<sup>+</sup> DC of NP-immunized mice displayed an enhanced binding and uptake of aDEC205-antibody conjugated NP as compared with control NP (Fig. 30C). In order to determine the qualitative advantage of DEC205-mediated cellular binding of NP, blocking experiments employing soluble DEC205-specific antibody were performed. Blocking of aDEC205-mediated binding of p(OVA-aDEC205) to BMDC prevented acquisition of CD4<sup>+</sup> (OT-II) and CD8<sup>+</sup> (OT-I) T cell proliferation *in vitro* (Fig. 31) as exerted by the differentially pretreated BMDC. The finding of efficient proliferation of CD4<sup>+</sup> (OT-II) and CD8<sup>+</sup> (OT-I) T cells *in vivo* verified that OVA targeted to DEC205 was efficiently presented to either T cell population. These results confirm that enhanced DC-specific endocytosis of particles can be achieved through their conjugation with anti-DEC-205 antibody. Such NP are suitable for the transfer of protein antigen and DC-activating adjuvant.

As shown in this PhD study, particulate OVA which may be engulfed by DC via the mannose receptor (Mao *et al.*, 2003), induced much stronger CD4<sup>+</sup> T cell proliferation *in vitro* than direct application of the same amount of soluble OVA. Similarly, Fe-NP which contained CpG evoked stronger DC activation *in vitro* than soluble CpG applied at the same concentration, as assessed by expression of MHCII and costimulatory markers (Fig. 33). Anyway, also *in vivo* codelivery of antigen plus CpG as a particulate formulation yielded stronger proliferation of OT-I and OT-II T cells than soluble CpG (Fig. 34).

Although various types of APC can cross-present model antigens *in vivo*, most studies indicate that murine CD8<sup>+</sup> DC are the main cross-presenting APC population *in vivo* (Jung, 2002 & Oliver, 2012). Cross-presentation is defined by the ability of certain types of DC to engulf exogenous antigens and to deliver derived peptides to MHC class I molecules to be presented to CD8<sup>+</sup> T cells. This process ensures that DC can develop CTL immunity against tumor cells and virus-infected cells other than the APC themselves (Kurts, 2000 & Heath, 2001). The results of the *in vivo* cytotoxic killing assay (Fig. 35) show that trifunctional NP induced a stronger antigen-specific CTL response as compared with NP conjugated only with antigen and DEC205-specific antibody. In accordance with the CTL effect of the trifunctional NP formulation, only mice immunized with this nanovaccine showed a sustained production of the Th1/Tc1 cytokines IFN $\gamma$ . To my best knowledge, the NP used in this study that codeliver a DC targeting antibody, a DC activation signal and a model antigen are the first trifunctional formulation designed and evaluated for immunotherapeutic use.

Based on the profound DC-activating and T cell stimulatory properties of this trifunctional NP formulation, a further aim of this study was to investigate whether these NP were suitable to induce a sustained antitumor response. For this, a therapeutic melanoma model was established. C57BL/6 mice were injected with cells of the B16-OVA tumor subline, and when the tumor was measurable (about 15mm<sup>3</sup>), mice were vaccinated in parallel with various NP formulations.

Mice immunized with the trifunctional NP formulation developed a pronounced anti-tumor response as reflected by an arrested tumor growth and a significantly higher

survival rate as compared with the other groups (Fig. 36). In a number of other studies efficient cross-presentation and induction of potent antitumor responses by employing NP formulations that contain antigen and adjuvant has been demonstrated as well, but in virtually all of these studies a preventive experimental setting was employed (Davis *et al.*, 2008 & Klippstein *et al.*, 2010, Haiyan *et al.*, 2011), or mice were immunized directly after tumor cell injection (Cho *et al.*, 2011). Therefore, based on their therapeutic efficacy, trifunctional NP formulations as evaluated in this work may serve as a base for the development of therapeutically suitable cancer vaccines.

Closer analysis of the spleen cell populations of the differentially vaccinated mice revealed that mice immunized with trifunctional NP formulations induced a significant reduction of the frequency of tumor-expanded MDSC. On first sight, this finding may be interpreted as a consequence of halted tumor growth and therefore impaired tumor-mediated expansion of MDSC. However, the MDSC frequency was also reduced in case of vaccination with the non-addressing NP formulation that codelivered OVA and CpG. Since the latter NP formulation exerted no major anti-tumor activity, another CpG-dependent mechanism may contribute to inhibition of MDSC expansion, uncoupled from DC-dependently induced anti-tumor T cell responses. In this regard, Shirota and coworkers (2012) have recently demonstrated TLR9 expression by monocytic MDSC, which in response to soluble CpG differentiated to macrophages that exerted anti-tumor activity. Therefore, further studies are required to assess potential uptake of NP by MDSC, which may promote MDSC differentiation. In this regard, most recently we have confirmed that NP conjugated with CpG were taken up by MDSC *in vivo* and *ex vivo* (data not shown). It is planned to analyze the effect of cpG-conjugated NP on the differentiation of MDSC *in vitro*.

#### 4.4. Fe-NP that codeliver antigen and a TLR9 ligand induce a potent humoral response

The aforementioned results suggest that DC-targeting NP are well suited to target vaccine components to DC *in vivo* with high efficacy. As shown in this PhD thesis, DC targeting *in vivo* is necessary to induce an efficient antitumor response.

As shown in this PhD study, DEC205-targeting Fe-NP that codelivered antigen and adjuvant were engulfed by DC *in vitro*, and only this trifunctional NP formulation induced a potent anti-tumor response. This finding suggested an essential role of DC targeting *in vivo* to induce therapeutic effects. Surprisingly, however, NP of either formulation which localized in spleen were apparent predominantly within the B cell zone (Fig. 38). In accordance, control NP bound primary B cells *in vitro* in a serum-dependent manner (Fig. 39), mediated by opsonization of complement factors and subsequent binding to the B cell complement receptor CD21/CD35 (Fig. 41). Confocal laser microscopy confirmed binding of NP to B cells, but not their cellular engulfment. Immunohistochemical staining of spleen sections showed that many NP colocalized with CD19<sup>+</sup> B cells (Fig. 38), but FACS analysis of splenic cells derived from NP-injected mice demonstrated that only 3% CD19<sup>+</sup> cells were Cy-5<sup>+</sup> due to binding of NP. These results suggest that binding of NP to B cells *in vivo* is not quite strong, and it is possible that most of the cargo may be released in close vicinity of the B cells rather than intracellularly.

In light of the intrinsic property of Fe-NP to specifically target B cells *in vivo*, their potential to induce an antigen-specific antibody response was evaluated. The finding of a lack of antibody production in response to immunization with control NP suggests that *in vivo* these NP exerted no profound AB production. Marked levels of OVA-specific IgG2a antibodies were produced only in response to immunization with NP functionalized with a TLR9 ligand, known to activate APC including B cells, but also DC. NP conjugated with CpG and aDEC205 in addition in order to address DC, elicited a markedly higher IgG2a antibody response (Fig. 43), which confirms the essential role of activated DC to boost antibody production by "generating" T cell help for B cells (San Román *et al.*, 2009).

Due to the detection of a higher IgG2a/IgG1 antibody ratio, which suggested a Th1-biased humoral response as induced by NP functionalized with CpG (Kline, 2007), we investigated the suitability of Fe-NP to suppress Th2/IgE-driven allergic symptoms in an anaphylactic shock model. In a therapeutic setting, OVA was administered prior to vaccination with NP formulations, and subsequently mice were challenged with OVA. NP-mediated codelivery of CpG and OVA resulted in a strongly enhanced IgG2a/IgG1 ratio (0.03) as compared with the injection of PBS or the NP formulation that contained OVA alone (each 0.0003). Since IgG1 production is driven by IL-4 (Th2), and IgG2a is induced by IFN $\gamma$  (Th1) (Tourney, 2002), an increase of the IgG2a/IgG1 ratio after vaccination with appropriate NP formulations is indicative of a Th1-biased humoral response. In accordance, NP formulations that contained CpG prevented the upregulation of IgE, which initiates immediate hypersensitivity reactions by triggering mast cell degranulation via Fc $\epsilon$ RI (Yssel *et al.*, 1998).

It is hypothesized that IgE have evolved in asthma development (Larché *et al.*, 2006). Increased IgE production initiates the activation of mast cells and subsequently induces an allergy response (Maddox *et al.*, 2002). In this study, in the group of p(OVA-CpG), a suppressed IgE production was observed. In accordance, the challenge induced decrease of body temperature was temporary and returned to the baseline. According to these results, nanoparticles functionalized with OVA and CpG appeared to exert a therapeutic function in the anaphylactic reaction in mice. For this, but DC targeting via aDEC205 is not necessary. To my knowledge this is the first study to show that functionalized nanoparticles directly target B cells in a therapeutic anaphylaxis model.

To confirm the therapeutic efficacy of functionalized Fe-NP in allergic diseases due to their pronounced Th1 skewing and IgE suppressive potential, the therapeutic suitability of these particles also in a model of acute asthma was assessed. As observed in the anaphylaxis model, NP functionalized with CpG induced higher IgG2a antibody production (Fig. 50A), a higher IgG2a/IgG1 ratio and lower IgE



production (Fig. 49). Consequently, on functional level this group of mice showed less bronchial hyper-responsiveness (Fig. 48) than control group. Asthma is a chronic inflammatory disease in which several inflammatory cells and mediators contribute to pathogenesis (Kikkawa *et al.*, 2012). Eosinophils are the major cell type associated with airway inflammation (van Oosterhout *et al.*, 2000 & Luet *et al.*, 2010). In this study, in lung lavage from the group immunized with NP that codelivered OVA and CpG either in a non-addressing or DC-addressing manner the number of eosinophils was significantly decreased as compared with no vaccinated group. This result confirmed that NP functionalized with CpG are able to reduce asthma-associated inflammation in lung. Besides eosinophils, neutrophils can also induce asthma, due to the release of diverse mediators (Monteseirín, 2009), like leukotriene B4 (LTB4), and platelet-activating factor (PAF), myeloperoxidase and matrix metalloproteinases (MMP-9) (Hampton *et al.*, 1998). However, vaccination with the NP formulations employed in this study exerted no increase in the number of neutrophils in lung lavage (data not shown). In correspondence, hematoxylin and eosin (HE) staining of lung showed significant lower inflammation scores (Fig. 50). Soluble CpG ODN have been used in many studies for treatment of asthma and allergic disease (Fonseca *et al.*, 2009 & Gupta *et al.*, 2010 & Kline, 2007). These studies showed that CpG ODN efficiently suppressed Th2 cytokine production and reduced airway eosinophilia and systemic levels of IgE in preventive and therapeutic asthma models. The study of Martínez Gómez and his coworkers (2007) showed in a preventive asthma model that a microparticle mediated codelivery of allergen and CpG is an available strategy to improve the safety of conventional SIT. To my knowledge, our study was the first to demonstrate that *in vivo* NP directly targeted on B cells to induce a therapeutic immune response in therapeutic asthma model.

NP that contained no specific targeting molecule preferentially accumulated in the B cell zone of lymphatic organs, and NP conjugated with CpG were indeed engulfed by B cells *in vitro*, as evidenced by confocal laser microscopy. Moreover, mice immunized with Ag plus CpG-containing NP produced less IgE and significantly lower disease scores in therapeutics models of anaphylactic shock and acute asthma. Therefore, we investigated what might be the reason for this spontaneous B cell affinity of the NP used here and whether these NP can be used for the allergy immunotherapy. Concerning the data obtained in both anaphylaxis and acute asthma

model, we observed no enhanced effect of NP functionalized with OVA, CpG and aDEC205 as compared with NP conjugate with OVA and CpG only. These results propose that there was no benefit when DC were targeted with aDEC205 in these allergic disease models. The question whether DC play an important role in NP-induced immune responses against allergic inflammation remains to be answered. Anyway, the NP formulations used in this study may open the field for direct modulation of B cells in terms of activation and switch of isotype, mediated by single or combinations of adjuvants coupled to the Fe-NP.

#### 4.5. Scavenger receptor mediated nanoparticle uptake

As shown in Fig. 34, we noted that *in vivo* particulate CpG induced stronger activation of DC than soluble CpG. Likewise, DC incubated with particulate CpG secreted the proinflammatory cytokines IL-6 and IL-12 at higher levels than induced by soluble CpG *in vitro* (Fig. 33). However, these *in vitro* results may be compromised in part by the fact that scavenger receptors (SR) may be responsible at least in part for the preferential uptake of oligonucleotide-coated Fe-NP, as shown for gold nanoparticles coated in a similar manner (Yi *et al.*, 2012). SR are expressed primarily on phagocytic cells of the immune system, including DC. DC use a repertoire of pattern recognition receptors (PRRs), e.g., toll-like receptors (TLRs) and SR, to constantly sample or sense their surroundings for the presence of stress or “danger” signals, e.g., pathogens and cellular debris (Guo *et al.*, 2012). Some studies showed that the polysaccharide fucoidan and autologous serum can block binding of ODN to the SRs (Thelen *et al.*, 2010). In our study, when DC were preincubated with serum or fucoidan, the upregulated expression of costimulatory molecules as induced by coincubation with p(CpG) was reduced, and cytokine production was decreased (data not shown). These results demonstrate that p(CpG) may be engulfed by DC through the SR activity.

As described in 4.4, the binding of control NP (p[Cy5]) by B cells was serum dependent and mediated by the complement receptor. However, when NP conjugated with CpG were used, the NP binding to B cells *in vitro* was not serum-dependent. By confocal laser microscopy it was shown that p(CpG) was exactly internalized into B cells in contrast to p(Cy5) (Fig. 42A). Therefore, SR mediated NP

uptake by B cells *in vitro* was analyzed too. In fact, both fucoidan and excess of serum blocked uptake of p(CpG) by B cells can be detected *in vitro*.

Taken together, the Fe-NP formulations used in this study showed differentially binding activities *in vivo* and *in vitro* in a cargo-dependent manner. *In vitro*, NP conjugated with aDEC205, preferentially bound to DC as intended. However, NP decorated with OVA engaged the MR as well (data not shown). Moreover, CpG-conjugated NP formulations were readily bound and engulfed by any cell type tested via SR activity. The latter mechanism is blocked most probably *in vivo* due to the presence of serum proteins binding to SR at higher affinity. aDEC-conjugated NP engaged DC at low frequency, nonetheless decisive for the induction of a sustained anti-tumor response. Rather unexpected, any NP formulation colocalized predominately with B cells via binding of complement factors, which facilitated interaction with the B cell CD21/CD35 complement receptor. On functional level, interaction of CpG-decorated types of NP with B cells was important to skew immune responses towards Th1, which largely inhibited allergic reactions.

Altogether, these findings underscore the necessity to assess the characteristics of nanoparticles both *in vitro* and *in vivo*, which may display altered binding characteristics dependent both on the interaction of cargo components with soluble mediators and surface receptors in a serum-dependent manner. Thorough testing of such nanovaccines is an important prerequisite to determine their actual properties with regard to their therapeutic suitability.

## 5. Materials and Equipments

### 5.1. Expendable materials

<b>Material</b>	<b>Manufacture</b>
Canula, 23Gx1¼, 0.6x30 B.	Braun, Melsungen
Canula, 26Gx1½, 0.45x12	Braun, Melsungen
Canula, 23Gx1½, 0.3x13	BD, Heidelberg
Cell culture bottle, 25 cm <sup>2</sup>	Greiner Bio-One, Frickenhausen
Cell culture bottle, 75 cm <sup>2</sup>	Greiner Bio-One, Frickenhausen
Cell culture plate 6 well, flat bottom	Greiner Bio-One, Frickenhausen
Cell culture plate 24 well, flat bottom	Greiner Bio-One, Frickenhausen
Cell culture plate 48 well, flat bottom	Greiner Bio-One, Frickenhausen
Cell culture plate 96 well, flat bottom	Greiner Bio-One, Frickenhausen
Cell culture plate 96 well, U bottom	Greiner Bio-One, Frickenhausen
Cell strainer, 40 µm	Falcon, Fisher Scientific, Schwerte
Greiner Tubes, 15 ml	Greiner-One, Frickenhausen
Greiner Tubes, 50 ml	Greiner-One, Frickenhausen
MACS Cell separation column MS	Miltenyi Biotec, Berg. Gladbach
MACS Cell separation column LS	Miltenyi Biotec, Berg. Gladbach
Petridishes	Greiner Bio-One, Frickenhausen
Pipett-Tips, 0.1 – 10 µl	Carl Roth, Karlsruhe
Pipett-Tips, 10 – 200 µl	Carl Roth, Karlsruhe
Pipett-Tips, 100 – 1000 µl	Carl Roth, Karlsruhe
Plastic Pipett 5ml,10ml,25ml	Cellstar, Germany
Syringe, 0.5 ml	Braun, Melsungen
Syringe, 1 ml	Braun, Melsungen

## 5.2. Buffers and Solution

### 5.2.1. Cell Culture Medium for Mouse Experiment

#### RPMI (complete Medium)

10% FCS  
100U/mL Penicilin/streptomycin  
2mM Glutamine  
10mM HEPES  
1mM sodiumpyruvate  
50 $\mu$ M  $\beta$ -mercaptoethanol  
Ad 500 ml RPMI 1640

#### RPMI (DC Medium)

5% FCS  
2mM Glutamine  
50 $\mu$ M  $\beta$ -mercaptoethanol  
1X Non Essential Amino Acids (NEAA)  
4ng/mL GM-CSF  
Ad 500 ml RPMI 1640

#### Collagenase-Buffer

1% Penicilline /Streptomycine  
0.1% Collagenase A  
in sterile DMEM

### 5.2.2 Cell Culture Medium for Human PBMC Experiments

#### IMDM Medium

5% FCS  
1% Glutamine  
25 mM HEPES  
1% Non Essential Amino Acids  
0.1%  $\beta$ -mercaptoethanol  
Ad 500 ml RPMI 1640

### 5.2.3. Buffers

#### FACS-buffer

1% FCS  
2mmol EDTA  
in sterile PBS

#### Cell lysis buffer for subsequent mass spectrometric analysis

7 M Urea  
2 M Thiourea  
5 mM DTT  
In 1X PBS Buffer

#### ACK-lysis Buffer

NH<sub>4</sub>CL 4.145g  
KHCO<sub>3</sub> 0.5g  
EDTA 18.6mg  
PH 7.27  
Ad 500mL H<sub>2</sub>O  
Sterile

### 5.2.4. Reagents and chemicals

Substance	Manufacture
Ethanol (70%)	Brüggemann, Heilbronn, Germany
Acetone	Sigma-Aldrich, Taufkirchen, Germany
Collagenase, Clostridiopeptidase A	Sigma-Aldrich, Taufkirchen, Germany
CpG 1826	Sigma-Aldrich, Taufkirchen, Germany
DMEM w/o pyruvate	Merck, Darmstadt, Germany
Dextran 500	Pharmacosmos A/S, Holbaek, Denmark
EDTA (Ethylendiamintetraacetat	Sigma-Aldrich, Taufkirchen, Germany
FACS Clean Solution	BD Pharmingen, Heidelberg, Germany
FACS Flow Sheath fluid	BD Pharmingen, Heidelberg, Germany
FACS Rinse Solution	BD Pharmingen, Heidelberg, Germany
Ficoll 400	Sigma.-Aldrich, Taufkirchen, Germany

---

FCS, fetal calf serum	PAA Laboratories, Cölbe, Germany
Forene (Isoflurane)	Abbott, Wiesbaden, Germany
GM-CSF	R&D, Wiesbaden, Germany
L-Glutamin	Gibco, Life Technologies, Germany
LPS	Sigma-Aldrich, Taufkirchen, Germany
HEPES Pufferan, 99.5%	Gibco Life Technologies , Germany
Hydrochloride acid (HCl)	Merck, Darmstadt, Germany
Isopropanol	Hedinger, Stuttgart, Germany
β-mercaptoethanol, 99% p.a.	Carl Roth, Karlsruhe, Germany
Ovalbumin	Sigma-Aldrich, Taufkirchen, Germany
Paraformaldehyde	Sigma-Aldrich, Taufkirchen, Germany
Recombinant murine GM-CSF	Natutec, Germany
RPMI 1640 medium Biochrome, Berlin	Life Technologies , Germany
Sodium azide (NaN <sub>3</sub> )	Sigma-Aldrich, Taufkirchen, Germany
Sodiumchlorid (NaCl)	Sigma-Aldrich, Taufkirchen, Germany
Trypanblau solution	Sigma-Aldrich, Taufkirchen, Germany
Tween 80	Sigma-Aldrich, Taufkirchen, Germany
Tris-Base	Sigma-Aldrich, Taufkirchen, Germany

---

### 5.3. Antibodies

<b>Antibody specificity(clone)</b>	<b>Fluorescence label</b>	<b>Manufacture</b>
CD 4 (GK1.5)	FITC, APC-Cy7,e-Flour450	eBioscience, USA, Biolegend
CD 8 (53.6.7)	APC-Cy7,e-Flour450	eBioscience, USA
CD11c (N418)	PE-Cy7	eBioscience, USA
CD11b (M1/70)	PE-Cy7	Biolegend, USA
CD19 (1D3)	APC-Cy7	Becton Dickinson,USA
CD25 (IL-2 receptor $\alpha$ chain,p55 PC61)	PE	Becton Dickinson,USA
CD40 (1C10)	APC	eBioscience, USA
CD45.1 (A20)	PE-Cy5	eBioscience, USA
CD45R(B220)	Horizon450	eBioscience, USA
CD68 (FA-11)	FITC	Biolegend, USA
CD80 (B7-1)	PE	Becton Dickinson,USA
CD86 (GL1)	FITC	eBioscience, USA
MHCII (M5/114.15.2)	e-Flour450	eBioscience, USA
F4/80 (BM8)	e-Flour450	eBioscience, USA
Foxp3 <sup>+</sup> (FJK-16a)	APC	eBioscience, USA
Gr1 (RB6-8C5)	PE	eBioscience, USA
Ly6-C (AL-21)	APC	Becton Dickinson,USA
Ly6-G	e-Flour450	Becton Dickinson,USA
V $\alpha$ -2 (B20.1)	PE	eBioscience, USA
INF- $\gamma$ (XMG1.2)	APC	eBioscience, USA



#### 5.4. Friend retrovirus

Friend virus (FV) is a retroviral complex comprised of 2 components: a replication-competent helper virus called Friend murine leukemia virus (F-MuLV), which is nonpathogenic in adult mice; and a replication-defective but pathogenic component called spleen focus-forming virus (SFFV). The complex of Friend retrovirus are kind of gift from Prof. Dr. Dittmer. In this study for the acute infection, the susceptible mice model (BALB/c) was infected with 3000 spleen focus forming units (SFFU)/mouse, for resistant mice model (C57BL/6) 12500 SFFU/mouse.

#### 5.5. Cell culture

All tissue/cell culture reagents were from Gibco/BRL (Gaithersburg, Md.). All cells (BMDC, PBMCs, T-lymphocytes and B-lymphocytes) were cultured at 37°C and 5% CO<sub>2</sub> in RPMI media containing heat-inactivated fetal calf serum and supplemented with 2 mM glutamine, 100 µg/ml streptomycin sulfate, 0.025 µg/ml amphotericin B, 0.5 MEM nonessential amino acids, 1 mM sodium pyruvate and 50 µM 2-mercaptoethanol (RPMI Complete media).

#### 5.6. B16-OVA melanoma cell line

B16-OVA is a B16 melanoma cell subline (H2b), that has been stably transfected with an expression construct encoding chicken OVA as a model antigen (Kedl et al., 2001). This cell line has been kindly provided by Prof. Sahin, University Medical Center Mainz. B16-OVA cells were grown *in vitro* as described above (6.2); for injection into mice, the cells were trypsinized with 5 ml trypsin/EDTA. After 5 mins, the cells were collected and washed three times in PBS before counting and dilution to the appropriate concentration in sterile PBS.

## 5.7. Animals

Mouse strain	Source
C57BL/6	Zentrale Versuchstiereinrichtung, Johannes Gutenberg University, Mainz
BALB/c	Zentrale Versuchstiereinrichtung, Johannes Gutenberg University, Mainz
OT-IxLy5.1	Zentrale Versuchstiereinrichtung, Johannes Gutenberg University, Mainz
OT-IIxLy5.1	Zentrale Versuchstiereinrichtung, Johannes Gutenberg University, Mainz
DO11.10	Zentrale Versuchstiereinrichtung, Johannes Gutenberg University, Mainz

All mouse strains used (C57BL/6, BALB/c, OT-IxLy5.1, OT-IIxLy5.1, DO11.10) were bred and maintained in the Central Animal Facilities of the University of Mainz under specific pathogen-free conditions on a standard diet. The "Principles of Laboratory Animal Care" (NIH publication no. 85-23, revised 1985) were followed. DO11.10 mice on a BALB/c background expressing a transgenic T-cell receptor (TCR), which recognizes ovalbumin peptide 323-339 (ISQAVHAAHAEINEAGR) in the context of I-Ad. CD4<sup>+</sup> T cells of OT-II (C57BL/6 background) are transgenic for a  $\alpha\beta$ TCR specific for OVA323-339 peptide in context of H-2 I-Ab, respectively. CD8<sup>+</sup> T cells of OT-I (C57BL/6) mice are transgenic for a  $\alpha\beta$ TCR specific for OVA257-264 peptide in the context of H-2Kb. OT-I and OT-II mice were crossed with CD45.1<sup>+</sup> C57BL/6J congenic mice.

The S100A9 knockout mice were a gift from Dr. Thomas Vogl of the Institute of immunology, Westfälische Wilhelms-Universität, Münster. The TLR4 and TLR9 knockout mice were nice gifts from Prof. Dr. Hansjörg Schild of the Institute of immunology, University of Mainz Medical Center.

## 5.8. Electronic Equipments

<b>Divice</b>	<b>Manufacture</b>
Calliper, digital, 150 mm	Rheinwerkzeuge, Mainz, Germany
Centrifuge Biofuge pico	Electron Coporation, Germany
Centrifuge Mutlifuge 3 L-R	Electron Coporation, Germany
CO <sub>2</sub> -Incubator	Electron Coporation, Germany
FACS LSR II, Flow Cytometer	BD, Heidelberg, Germany
Laser scanning microscopy	Zeiss, Germany
Realtime PCR 7300	Applied Biosystems, CA,USA
Robsep	STEM CELL Technologie <sup>R</sup> , Germany
Shandon Cytospin centrifuge	Thermo Electron, Langenselbold,
Vortex	Merck Eurolab, Darmstadt, Germany
Water bath, type GFL-1003, 14 l	Gesellschaft für Labortechnik, Germany

## **6. Experimental procedures**

### **6.1 Cell biology methods**

#### **6.1.1 Generation of murine bone marrow-derived dendritic cells**

Bone marrow (BM)-derived dendritic cells (DC) were generated as previously described (Sandra Balkowet.al/2007) with some modifications. In brief, BM cells were collected from murine tibias and femurs. In case BM cells were derived from mice inoculated with FV, FV-infected BM cells were positively sorted (see 6.1.3.1). BM cells were resuspended in RPMI 1640 medium (PAA Laboratories, Pasing, Austria), supplemented with 5% FCS, 2 mM L-Glutamine, 0.1 mM nonessential amino acids, 50 µg/ml gentamycin (all from PAA), 50 µM β-mercaptoethanol (Sigma), 4 ng/ml recombinant murine GM-CSF (R&D, Wiesbaden, Germany), and seeded into 6 well cell culture plates (BD, NJ) ( $3 \times 10^6$  cells/4ml). On day 3, 4 ml fresh DC culture medium was added. After a total of 6 or 7 days of culture, non-adherent and loosely adherent BMDC were collected and used in subsequent experiments. For coculture experiments with T cells, DC were stimulated on day 7 for 24h with an appropriate stimulus (LPS: 100ng/ml, CpG: 0.5µg/ml).

#### **6.1.2 Isolation of human PBMCs from whole blood**

25 ml whole blood was transferred carefully from heparin syringe (or tube) to a 50mL falcon tube which was added 20ml Ficoll Hypaque solution. The sample was spun down at 2000g for 20 min at RT without brake. Collect PBMCs were collected from interphase of sera/ Ficoll with a transfer pipette and transferred to a new 50mL tube.

#### **6.1.3. Detection of Friend virus infected murine BMDC**

##### **6.1.3.1. Infection of mice with FV**

Mice were injected i.v. with Friend murine leukemia virus (F-MuLV) and spleen focus-forming virus (SFFV). In susceptible mice model (BALB/c), 3000SFFU FV

complex were inoculated, whereas in resistant mice model (C57BL/J), 12500 SFFU were inoculated.

#### **6.1.3.2. Detection of Friend virus infected cells**

To detect FV-infected cells, either BM cells from FV-infected mice one week after inoculation or or cultured BMDC were stained with tissue culture supernatant containing monoclonal antibody (mAb) 34, which is specific for F-MuLV glycosylated Gag protein that is expressed on the surface of infected cells. (Dittmer U, J Virol. 2001.) mAb 34 binding was detected with a goat anti-mouse IgG2b-PE antibody(BD Pharmingen).

#### **6.1.3.3. Enrichment of FV-infected DC**

BM cells from FV-infected mice were isolated on day 7 after infection and stained with anti-mAb 34 and a PE-conjugated secondary antibody. Infected cells were isolated using anti-PE microbeads and magnetic-activated cell sorter (Stem cell) sorting (Stemcell Technologies Köln, Germany. EasySep mouse cell isolation kits). Cells were cultured to generate BMDC as described above, and were used for experiments.

#### **6.1.4. DC isolation from the spleen**

Splenic DC were obtained using a variation of the method described by Vremec et al., Briefly, spleens from mice were perfused with RPMI-FCS supplemented with 0.5 M EDTA, 5 mg/mL collagenase (Typ III; Worthington Biochemical, CellSystems, St. Katharinen, Germany), and DNase I (1 mg/mL; AppliChem, Darmstadt, Germany). Spleens were digested for 30 minutes at 37°C. After centrifugation at 1,100 U/min for 10 minutes, erythrocytes were removed by incubation with a hypotonic lysis buffer. Then, DC were further enriched to greater than 90% purity by magnetic cell sorting as recommended by the manufacturer (MACs Miltenyi Biotec GmbH, Germany).

### **6.1.5. Endocytosis Assay *in vitro***

Quantitative analysis of macropinocytosis and mannose receptor-mediated endocytosis was performed using FITC-labeled dextran, and phagocytosis was analyzed using FITC-OVA. Day 6 BMDC were harvested and washed with FACS buffer (PBS1% FCS, 0.5 mM EDTA).  $5 \times 10^5$  BMDC were first equilibrated for 10 min in 50  $\mu$ l DHB medium (DMEM, 25 mM HEPES, pH 7.4, 0.5% BSA) and subsequently incubated with 1 mg/ml FITC-dextran (Molecular Probes, Invitrogen, Life Technologies, Frankfurt, Germany) or FITC-OVA at either 37°C or 4°C as a control. Endocytosis was stopped at the indicated time points by rapidcooling of the cells on ice, followed by 3 washes with ice-cold PBS. Cells were labeled on ice with an APC-labeled anti-CD11c-antibody (BD Pharmingen™, Heidelberg, Germany) and examined by flow cytometry.

### **6.1.6. BMDC migration within 3D collagen Gels**

To prepare 100  $\mu$ l of cell-loaded collagen matrices, first 5  $\mu$ l of 7.5%  $\text{Na}_2\text{CO}_3$  and 10  $\mu$ l of 10XMEM (Invitrogen) were mixed and then added to 75  $\mu$ l Purecol® bovine collagen I (Vitrogen, Life Technologies, Frankfurt, Germany). 67  $\mu$ l of the mixture was further mixed with 33  $\mu$ l cell suspension ( $1.5 \times 10^7$  cells/ml) and placed into a humidified incubator (37 °C) for 45 min to induce gelation.

Migration of BMDC was monitored in 3D collagen gels by time-lapse microscopy using an Olympus BX61 microscope with an UAPO lens (Olympus, Frankenthal, Germany) (20X/340, NA 0.75). Differential interference contrast (DIC) images were capture every 1.5 min by a FView camera controlled by Cell^P software (SIS).

### **6.1.7. Isolation and proliferation of T-lymphocytes**

#### **6.1.7.1. Isolation of T-lymphocytes**

Spleens and LN of naïve mice were harvested and resuspended by squeezing with the hilt of a sterile syringe. The cell suspension was filtered through a 40 µm cell strainer and washed with RPMI Complete Medium and centrifuged at 1,400 rpm for 5 min. The pellet was resuspended in 5 ml ACK buffer to lyse erythrocytes and incubated for 1 min. Afterwards, 10 ml RPMI complete were added, the cell suspension was centrifuged again at 1,400 rpm for 5 min and the cells were counted. CD4<sup>+</sup> and CD8<sup>+</sup>T cells were enriched to greater than 96% purity by magnetic cell sorting as recommended by the manufacturer (Stemcell Technologies, Köln, Germany. EasySep mouse cell isolation kits).

#### **6.1.7.2. Antigen specific T cell proliferation *in vitro* (<sup>3</sup>H-Thymidin)**

Metabolic incorporation of tritium-labeled thymidine (<sup>3</sup>H-TdR) into cellular DNA is a widely used protocol to monitor rates of DNA synthesis and thereby cell proliferation. Cell suspensions containing DC and T cell subsets (CD4<sup>+</sup> or CD8<sup>+</sup>) were cultured in wells of round-bottom 96-well plates, and <sup>3</sup>H-Thymidin was added in excess after 48 h, and cells were cultured for 16 hrs at 37°C. Afterwards, cellular DNA was transferred onto a filter membrane that enriched solely intact genomic DNA. The filter membrane was dried and the amount of membrane-bound radioactivity was counted in a liquid scintillation counter.

#### **6.1.7.3. Antigen specific T cell proliferation *in vivo***

The carboxyfluorescein diacetate succinimidyl ester (CFSE) is an amine-reactive reagent which can diffuse through cell membrane easily. The non-fluorescent nature of CFSE turns into that of a fluorescent one upon cleavage of its acetate groups by esterases in the cytoplasm. Due to its amine-reactivity, the succinimidyl ester group can bind to amine-containing residues of intracellular proteins, thereby retaining the product in cells even when they divided. As CFSE is halved between daughter cells during cellular division, CFSE labeling can be used to follow proliferation of lymphocytes *in vitro* and *in vivo* by FACs. (Lyons, 2000).

To assess T cell proliferation *in vivo*, splenocytes derived from mice with transgenic T cell receptor (OT-IxCD45.1, OT-IIxCD45.1) were labeled with CFSE

(0.5  $\mu$ M, CFSE) (Life Technologies) for 5 min at 37°C, and then placed on ice for 5 min. The cells were washed twice with PBS. Afterwards, the spleen cells were incubated with PBS+1% FCS at 37°C for 15mins. CFSE-labeled splenocytes ( $10^7$  in 200  $\mu$ l PBS) were transferred i.v. into mice. After 48h, 4  $\mu$ g of OVA protein or NP formulations at equivalent OVA dosage were injected i.v. into according groups of mice. In some experiments, LPS (4 $\mu$ g/mouse or CpG (0.5 $\mu$ g/mouse) were coapplied. Four days later, spleens and peripheral LNs were removed and cell suspensions were analyzed for proliferation of CFSE-labeled T cells by flow cytometry.

#### 6.1.8. *In vivo* killing assay

Spleen cells derived from OT-IxLy-5.1 mice were resuspended in PBS ( $5 \times 10^7$  /ml) and injected  $10^7$  (200 $\mu$ L i.v.) into mice via the tail vein. Two days later, groups of mice were immunized with the model antigen OVA either as soluble protein or as particulate formulation (each 4  $\mu$ g OVA/mouse), with an adjuvant in soluble or particulate form (LPS: 4  $\mu$ g/mouse or CpG: 0.5  $\mu$ g/mouse). After 5 days, spleen cells were isolated from Ly-5.1 mice. One fraction was pulsed with 1  $\mu$ g/ml OVA<sub>257-264</sub> peptide (1 h, 37°C) to serve as the target cell population. Target cells were labeled at a high concentration of CFSE (0.5  $\mu$ M, CFSE<sup>high</sup> cells). The other fraction was left unpulsed and was labeled at lower CFSE concentration (0.05  $\mu$ M, CFSE<sup>low</sup> cells) to serve as an internal control. Equal numbers of cells from both spleen cell populations were mixed, and a total of  $10^7$  cells in 200  $\mu$ l of PBS was injected i.v. per mouse. 4 h after injection, splenocytes were derived from treated mice, and the frequencies of CFSE<sup>+</sup> Ly-5.1<sup>+</sup> cells were assessed by FACS analysis to determine the extent of *in vivo* killing. The level of specific cytotoxicity was calculated according to the following calculation:

$$100\% - \text{CFSE}_{\text{low}} / \text{CFSE}_{\text{high}} * 100\%.$$

#### 6.1.9. Isolation of B-lymphocytes

Spleens from naïve mice were harvested and suspended by squeezing with the hilt of a sterile syringe. The suspension was filtered through a 40  $\mu$ m cell strainer,



the resulting cell suspension was washed with RPMI Complete Medium and centrifuged at 1,400 rpm for 5 min. The pellet was resuspended in 5 ml ACK buffer to lyse erythrocytes and incubated for 1 min. Afterwards, 10 ml RPMI complete were added; the cell suspension was centrifuged again at 1,400 rpm for 5 min. The cells were counted and ready for following purification. B cells were enriched to greater than 96% purity by magnetic cell sorting as recommended by the manufacturer (Stemcell Technologies, Köln, Germany, EasySep mouse cell isolation kits).

#### **6.1.10. Cytospins**

In order to quantify protein expression single cell level, cells were spun down on a glass microscope slide using a cyto-centrifuge.  $5 \times 10^5$  cells in 100  $\mu$ l PBS were added to each slide and centrifuged for 5 min at 500 rpm. After centrifuge, the slides were dry at room temperature for 2 hours, subsequently, were stained with immunofluorescence antibodies

#### **6.1.11. Laser Scanning Microscopy (LSM)**

Day 6 BMDC were harvested and washed with FACS buffer (PBS1% FCS, 0.5 mM EDTA). Subsequently, the cells were transferred onto chamber slides (IBIDI, Germany). Cells were incubated with antibodies (e.g. CD11c, CD19) as described above, and nuclei were stained with DAPI (Life Technologies). Immunofluorescence was analyzed by confocal laser scanning microscopy (LSM510-UV, Zeiss, Germany) in core facility for confocal scanning laser microscopy in medical centre of Johannes Gutenberg University, Mainz.

### **6.2. Immunological methods**

#### **6.2.1. Magnetic cell sorting (MACS)**

Specific target cells can be isolated from a mixture of different cell populations by immunomagnetic sorting, using the MACS technique. For this, target cells are incubated with ferromagnetic microbeads, labeled with antibodies specific for molecules on the surface of the cells. The heterogeneous cell suspension is loaded onto a magnetic column, and all cells, which had not bound any microbeads were washed off. After removing the column from the magnetic field, the purified fraction of target cells was eluted. The MACS method was used in accordance with the manufacturer's guidelines for isolation of CD4<sup>+</sup> and CD8<sup>+</sup> T cells, and of B cells.

### 6.2.2. Fluorescence Activated Cell Sorting (FACS)

Flow cytometry is a technique to count and characterize single cells within a cell suspension in a stream of fluid, passing the cells by an electronic detection unit. A beam of laser light of a single wavelength is directed onto the hydrodynamically-focussed stream of the cell suspension, which is stained with fluorescence-labeled antibodies. Each cell with a diameter of 0.2-150  $\mu\text{m}$  passes through the beam and scatters the light. Fluorescent dyes attached to the cell due to detection of proteins with fluorescence-labeled antibodies may be excited to emit light at a longer wavelength than the original light source. The combination of scattered and fluorescent light is analysed by detectors. The forward scatter correlates with the cell volume and the SSC with the granularity of the cell.

For FACS analysis, cells were washed twice with FACS buffer, and free Fc-receptors were blocked by incubation with Fc-blocking antibody (1:200) for 15 min at RT. Further, cells were incubated in a 100  $\mu\text{l}$  solution with fluorescent-labelled antibodies (1:500) for an additional 15 min at RT. If more than one fluorescent dye was used, cells were washed after the first incubation step twice with FACS buffer before staining with the second antibody.

For intracellular detection of IFN $\gamma$ , cells were costained with anti-CD8, PE-conjugated anti-V $\alpha$ 2, and PE-Cy5-conjugated CD45.1, and fixed with 4% paraformaldehyde. Fixed cells were permeabilized and stained with APC-conjugated anti-IFN- $\gamma$ . For intracellular detection of Foxp3<sup>+</sup>, spleen cells were first stained with e-Fluor450-conjugated CD8, FITC-conjugated CD4, PE-conjugated CD25, and the cells were fixed and permeabilized with fixation / permeabilization

buffer. (eBioscience, San Diego, USA). After that, the cells were stained with APC-conjugated anti-Foxp3.

### 6.2.3. Cytokine measurement

The cytokine production by BMDC was determined in cell culture supernatants from CD11c<sup>+</sup>DC or cocultures of BMDC and CD4<sup>+</sup> T cells using a cytometric bead array (CBA Inflammation; BD Pharmingen). In a bead assay, one or more bead populations (bead) with discrete and distinct fluorescence intensities are used to simultaneously detect multiple cytokines in a small sample volume. The beads capture and quantify cytokines through a sandwich schema. Each capture bead in the array has a unique fluorescence intensity and is coated with a capture antibody specific for a single cytokine. A combination of different beads is mixed with a sample or standard and afterwards with detection antibodies that are conjugated to a reporter molecule (PE). Following incubation and subsequent washing, the samples are acquired on a flow cytometer.

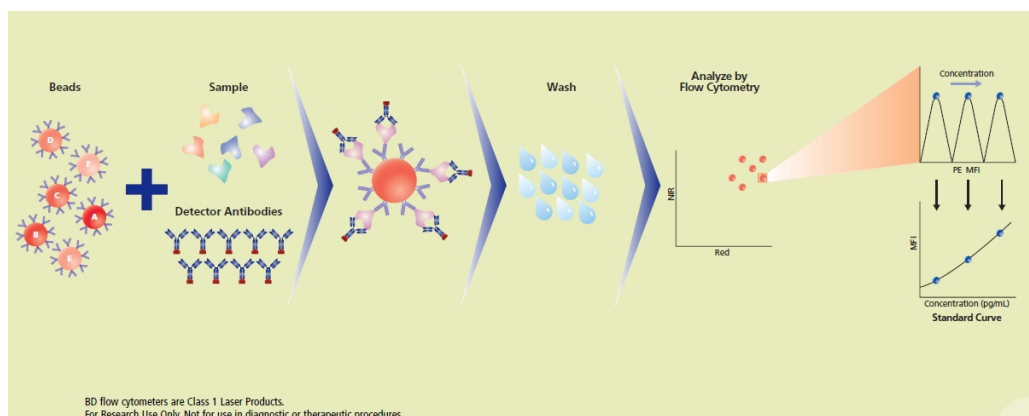


**Fig. 52: Overview of BD™ CBA assay principle.** Every capture bead in this array has fluorescence intensity and is coated with a capture AB specific for a single analyte. A combination of different beads is mixed with a sample or standard and a mixture of detection ABs that are conjugated to detection molecule (PE). Following incubation and subsequent washing, the samples are acquired on a flow cytometer. (from BD bioscience)

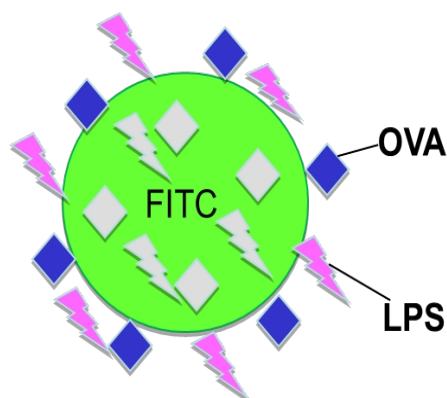
### 6.2.4. Bicinchoninic Acid (BCA) Protein Assay

To determine protein concentrations, the BCA Assay was used, which combines the protein-induced biuret reaction with the highly sensitive and selective colorimetric detection of the resulting cuprous cation ( $\text{Cu}^{1+}$ ) by bicinchoninic acid (BCA).  $\text{Cu}^{2+}$  is reduced to  $\text{Cu}^{+}$  due to proteins in alkaline solutions. Two BCA molecules bind one  $\text{Cu}^{+}$ -ion and a chelate complex is formed, which can be detected at 562 nm. Herein, we used the BCA Protein Assay Reagent Kit to determine protein concentrations of BMDC cells for Mass Spectrometry and Western blot analysis. The assay was performed in accordance to the manufacturer's guidelines.

### 6.3. Nanoparticle Experiments

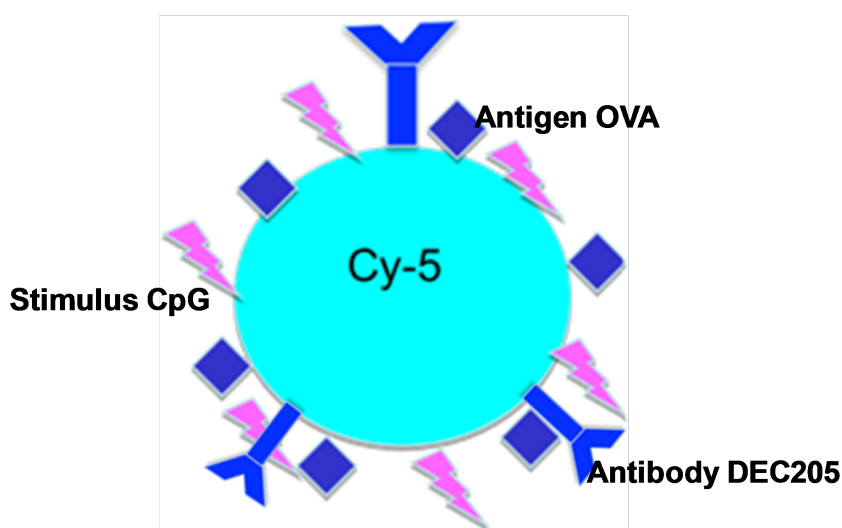
#### 6.3.1. Preparation of dextran nanospheres

Dextran nanospheres (DN) were prepared as described by Schröder [12] with some modifications. Briefly, 7.69 g Dextran 500 (Pharmacosmos A/S, Holbaek, Denmark) was dissolved in distilled water (26% w/v). In some preparations, 20 mg of chicken ovalbumine (OVA) protein (Sigma-Aldrich, Deisenhofen, Germany), and 125  $\mu\text{g}$  lipopolysaccharide (LPS, Sigma) were dissolved in 400  $\mu\text{l}$  of PBS, and were subsequently added to the dextran solution respectively. Then, 30 ml of customary vegetable oil pre-cooled to 4°C was added, and the mixture was emulsified by magnetic stirring for 20 min at 4 °C, followed by sonification (Bandelin electronic: BM70, Berlin, Germany) in an ice-bath for 40 s. The resulting emulsion was slowly poured into 200 ml of 0.1 % (w/v) solution of Tween 80 (STRVA, Feinbiochemica, Heidelberg/New York) in acetone under constant stirring to precipitate DN at room temperature. After 6 hr, DNs were filtered through a cell strainer (40  $\mu\text{m}$  diameter) to remove aggregates. DN were washed 3 times with 0.1 % Tween 80 in acetone solution and collected by centrifugation at 3,000 g for 5 min. DNs were resuspended in 2 ml of 1% (w/v) Tween 80-acetone solution and air dried at room temperature. To prepare FITC-labeled DN, FITC-conjugated dextran 500 (Sigma-Aldrich) was mixed with unlabeled dextran 500 at a ratio of 1:1,000 (w/w) during the initial solubilization step.



### 6.3.2. Iron oxide solid core nanoparticle

Iron particles coated with OVA, CpG-ODN, and anti-DEC205, either alone or in combinations thereof, were provided by Miltenyi.



### 6.3.4. BMDC viability

To assess potential cytotoxic effects of nanoparticles (NP), day 6 BMDC ( $2.5 \times 10^5$ ) were reseeded into wells of 96 well cell culture plates in a volume of 100  $\mu$ l, and NP were added at different concentrations as indicated. To assay cell viability, tetrazolium substrate was added which is reduced to a chromogenic formazan product by mitochondrial succinate dehydrogenase, correlating with the number of metabolically active cells. The reaction was stopped by addition of an organic

solvent, and the concentration of solubilized formazan was detected spectrophotometrically in an ELISA reader according to the protocol provided by manufacturer (Promega, Madison, WI, USA).

### 6.3.5. Cellular uptake of Nanoparticles by BMDC *in vitro*

BMDC ( $5 \times 10^5$  cells) or spleen cell suspensions ( $2 \times 10^6$  cells) derived from C57BL/6 mice were incubated with fluorescence-labelled nanoparticles ( $6 \times 10^{10}$  nanoparticle) in a volume of 200  $\mu$ l at 37°C in 96 wells of a cell culture plate for the indicated periods of time. To assess for MR-dependent endocytosis of OVA-containing DEX by BMDC, cells ( $5 \times 10^5$  in 200  $\mu$ l) were preincubated with mannan (200  $\mu$ g/ml; Sigma) for 30 min at 37°C. After incubation, cells were harvested and stained for surface lineage marker expression (e.g. CD11c<sup>+</sup>) as indicated for subsequent flow cytometry analysis as described.

### 6.4. Tumor therapeutic models (Melanoma model)

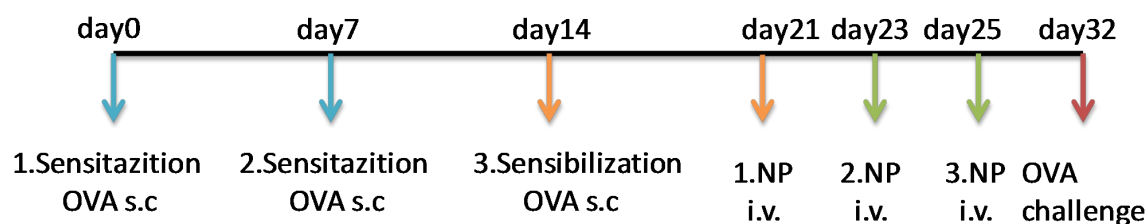
B16 OVA cells were grown in RPMI medium with 10% FCS, 100U/mL Penicillin/streptomycin, 2mM Glutamine, 10mM HEPES, 1mM sodium pyruvate 50 $\mu$ M  $\beta$ -mercaptoethanol and G418. OVA expression was analyzed by FACS analysis before injection.

Naïve C57BL/6 mice were injected s.c. with  $10^5$  B16-OVA cells. The mice were observed every day. Palpable tumors started to appear between days 10 to 14. The tumor size was measured with vernier caliper and when the tumors were palpable (15 mm<sup>3</sup>), mice were assigned in 5 groups (8-10 mice per group). Mice were vaccinated with different types of NP by i.v. application. Mice were administered booster immunizations with the same formulations every two days for a total of three times. The tumor volume was recorded as the product of two orthogonal diameters (a: longest diameter, b: orthogonal with mm<sup>3</sup>). Animals were observed every day, and were euthanized when the tumor size exceeded 600

mm<sup>3</sup> or when ulceration of the tumors was observed. The animals were sacrificed, sera, spleens and tumors were isolated for further analysis.

## 6.5. Anaphylaxis model

A therapeutic disease model of anaphylaxis was established as described (Roy, 1999). Briefly, mice were given s.c. administrations of 10 µg OVA at a weekly interval (days 0, 7, and 14). After the last sensitization, mice were assigned in 5 groups and were injected i.v. with different types of NP. Mice were given booster immunization with the same formulations every two days for a total of three times (days 21, 23, and 25). On day 32, 25 µg OVA was administered i.v. into the mice (challenge). The anaphylactic score was evaluated as described (Finkelman, 2007). The sera were collected on days 7, 14, 21 and 28 for detection of OVA-specific immunoglobulins.

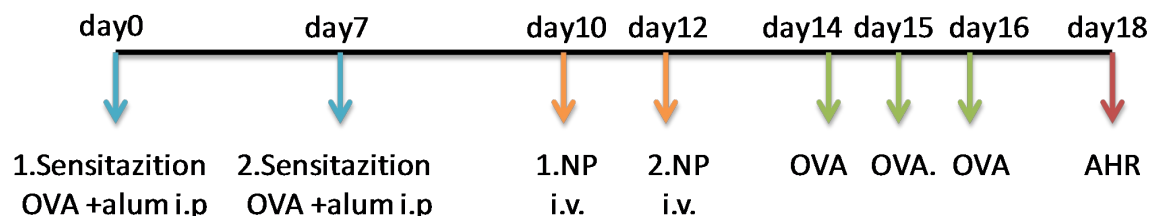


Tab. 6: Experimental design of anaphylaxis schock model.

## 6.6. Acute Asthma model

Asthma is a chronic respiratory disease characterized by bronchial inflammation and airway hyperresponsiveness. To help researchers evaluate experimental therapies, we offer the mouse ovalbumin (OVA) plus alu sensitization model of acute asthma. Six to eight weeks female BALB/c mice were sensitized i.p with 10 mg OVA (grade VI) emulsified in 1.5mg alum (Pierce, Rockford, IL, USA) in 200 mL phosphate-buffered saline (PBS) on days 0 and 7. 3 days after sensitization, the mice were immunized with NP by i.v. injection on day 10 and 12, followed by 20min 1% OVA (grade V) aerosol treatments on days 14, 15 and 16.

S.c. injection was performed at the scruff of the neck and was verified by the observation of a fluid bubble forming under the skin during injection. I.p. injection was performed in the lower right quadrant of the abdomen.



Tab. 7: Experimental design of acute asthma model.

Group	Sensitization	Challenge	Immunization
Naive	PBS	OVA	PBS
PBS	OVA+Alum	OVA	PBS
pCy5	OVA+Alum	OVA	pCy5
pOVA	OVA+Alum	OVA	pOVA
p(OVA-CpG)	OVA+Alum	OVA	p(OVA-CpG)
p(OVA-CpG-aDEC205)	OVA+Alum	OVA	p(OVA-CpG-aDEC205)

Tab. 8: Group of acute asthma model.

### 6.6.1. Invasive measurement of AHR to MCh in mice.

In this PhD study, AHR is determined by invasive method directly measuring lung resistance and dynamic compliance. The invasive measurement of the lung function is a very sensitive and effective method, characterized by controlled ventilation, bypassing the upper airways and a local delivery of the aerosolized bronchoconstrictor via a tracheal tube. Four chambers of RC system were calibrated and 50mg/ml stock solution of methacholine were prepared in PBS and serially diluted in 25, 12.5, 6.25, 3.125 mg/mL. The mice were injected an appropriate volume of Narcoren ® working solution intraperitoneally (75mg/kg



body weight). Skin and muscle tissue covering the trachea were removed and a medical yarn under the trachea were inderted, which will subsequently be used to tie the trachea to the tracheal tube. 18 gauge tracheal tube was placed into the cut and carefully pushes it in the airways. The mouse was aubsequently placed into the chamber of the RC system. Record the baseline resistance and compliance for 60 s, aerosolized methacholine at the lowest concentration (3.125 mg/mL) were delivered for 30 s. The change of resistance and compliance were measured for 5 min. Finally, the raw data were analyzed with the BioSystem XA Software. Calculate the fold increase of resistance and compliance measured for each concentration of methacholine in relation to baseline resistance and compliance.

### **6.6.2. Serum collection and detection of OVA specific IgE**

Blood was collected by cardiac puncture immediately after the thoracic cavity was opened and before BAL was performed. Blood was allowed to clot, then was centrifuged, and aliquots of serum were stored at -80°C before analysis. OVA specific IgE, IgG2a and IgG1 antibody concentration were measured by ELISA as previously described.

### **6.6.3. Bronchoalveolar lavage (BAL)**

Immediately after the administration of a fatal dose of avertin, the thoracic cavity was opened by careful dissection. The trachea was then exposed, and a small transverse incision made just below the level of the larynx. BAL was then performed using two doses of 0.5 ml of PBS, ensuring that both lungs inflated during the lavage process and that there was no leakage of lavage fluid from the trachea. The lavage samples from each mouse were pooled and kept on ice until processing. BAL was centrifuged at 400g for 5 min, and the supernatant was removed.

### **6.6.4. Lung histology**

After BAL sampling had been collected, the lungs were removed from the thoracic cavity. The lungs were inflated with 1 ml of 10% neutral-buffered Formalin and

then fixed in 10% neutral-buffered Formalin. After fixation, the lung was dissected free and embedded in paraffin, and 6 $\mu$ m sections were cut. Sections were then stained with H&E in histology corfacility in Department of Dermatology.

## **6.7. Statistical analysis and software**

Statistical significance was determined using the unpaired Students-*t*-test using StatView® for Windows. Results are expressed as mean $\pm$ SEM; statistically significant differences are designated as \* $p\leq 0.05$ , \*\* $p\leq 0.005$ , and \*\*\* $p\leq 0.001$ .

All flow cytometry results were obtained by using a LSR II (BD Bioscience) and FlowJo® software. The cytokine quantification results were analyzed by using FCAP Array Software (BD Bioscience).

## 7. Reference

1. **Abudu A Takaori-Kondo A, Izumi T, Shirakawa K, Kobayashi M, Sasada A, Fukunaga K, Uchiyama T.** Murine retrovirus escapes from murine APOBEC3 via two distinct novel mechanisms. *Curr Biol.* 16(15):1565-70., 2006 Aug 8.
2. **Adler HS Steinbrink K.** Tolerogenic dendritic cells in health and disease: friend and foe. *Eur J Dermatol.* 2007 Nov-Dec; 17(6):476-91. Epub 2007 Oct 19.
3. **AE Morelli** The immune regulatory effect of apoptotic cells and exosomes on dendritic cells: its impact on transplantation. *Am J Transplant.* 2006 Feb;. 6(2):254-61.
4. **Agrawal S Agrawal A, Doughty B, Gerwitz A, Blenis J, Van Dyke T, Pulendran B.** Cutting edge: different Toll-like receptor agonists instruct dendritic cells to induce distinct Th responses via differential modulation of extracellular signal-regulated kinase-mitogen-activated protein kinase and c-Fos. *J Immunol.* 2003. 171(10):4984-9.
5. **Ahmad-Nejad P Häcker H, Rutz M, Bauer S, Vabulas RM, Wagner H.** Bacterial CpG-DNA and lipopolysaccharides activate Toll-like receptors at distinct cellular compartments. *Eur J Immunol.* 2002. 32(7):1958-68.
6. **Akira S Takeda K, Kaisho T.** Toll-like receptors: critical proteins linking innate and acquired immunity. *Nat Immunol.* 20012(8):675-80.
7. **Akira S Takeda K.** Toll-like receptor signalling. *Nat Rev Immunol.* 2004. 4(7):499-511.
8. **Alberts B Johnson A, Lewis J, et al** Activation, Helper T Cells and Lymphocyte . *Molecular Biology of the Cell.* 4th edition. Garland Science, 2002.
9. **Allan RS Smith CM, Belz GT, van Lint AL, Wakim LM, Heath WR, Carbone FR.** Epidermal viral immunity induced by CD8alpha+ dendritic cells but not by Langerhans cells . *Science.* 2003 Sep 26; 301(5641):1925-8.
10. **Almand B Clark JI, Nikitina E, van Beynen J, English NR, Knight SC, Carbone DP, Gaborilovich DI.** Increased production of immature myeloid cells in cancer patients: a mechanism of immunosuppression in cancer. *J Immunol.* 166(1):678-89., 2001 Jan 1.

11. **Altfeld M Rosenberg ES.** The role of CD4(+) T helper cells in the cytotoxic T lymphocyte response to HIV-1. *Curr Opin Immunol.* 2000 12(4):375-80.
12. **AM Krieg** Antitumor applications of stimulating toll-like receptor 9 with CpG oligodeoxynucleotides. *Curr Oncol Rep.* 2004. 6(2):88-95.
13. **AM. Krieg** CpG motifs in bacterial DNA and their immune effects. *Annu Rev Immunol.* 2002;. 20:709-60. Epub 2001 Oct 4.
14. **Amigorena S Savina A.** Intracellular mechanisms of antigen cross presentation in dendritic cells . *Curr Opin Immunol.* 2010. 22(1):109-17. Epub 2010 Feb 18.
15. **Antunes I Tolaini M, Kissenpfennig A, Iwashiro M, Kuribayashi K, Malissen B, Hasenkrug K, Kassiotis G.** Retrovirus-specificity of regulatory T cells is neither present nor required in preventing retrovirus-induced bone marrow immune pathology. *Immunity.* 2008. 29(5):782-94.
16. **Arai K Takano S, Teratani T, Ito Y, Yamada T, Nozawa R.** S100A8 and S100A9 overexpression is associated with poor pathological parameters in invasive ductal carcinoma of the breast. *Curr Cancer Drug Targets.* 2008 Jun;. 8(4):243-52.
17. **Ardavín C Amigorena S, Reis e Sousa C.** Dendritic cells: immunobiology and cancer immunotherapy . *Immunity.* 2004. 20(1):17-23.
18. **Ardavín C.** Origin, precursors and differentiation of mouse dendritic cells. *Nat Rev Immunol.* 2003. 3(7):582-90..
19. **Aspard C Pedroza-Gonzalez A, Gallegos M, Tindle S, Burton EC, Su D, Marches F, Banchereau J, Palucka AK.** Breast cancer instructs dendritic cells to prime interleukin 13-secreting CD4+ T cells that facilitate tumor development. *J Exp Med.* 2007 May 14; 204(5):1037-47. Epub 2007 Apr 16.
20. **Auffray C Sieweke MH, Geissmann F.** Blood monocytes: development, heterogeneity, and relationship with dendritic cells. *Annu Rev Immunol.* 2009. 27:669-92.
21. **Auffray C Sieweke MH, Geissmann F.** Blood monocytes: development, heterogeneity, and relationship with dendritic cells. *Annu Rev Immunol.* 27:669-92. doi: 10.1146/annurev.immunol.021908.132557., 2009.
22. **Bachelder EM Beaudette TT, Broaders KE, Dashe J, Fréchet JM.** Acetal-derivatized dextran: an acid-responsive biodegradable material for therapeutic applications . *J Am Chem Soc.* 2008 Aug 13;. 130(32):10494-5. Epub 2008 Jul 17.

23. **Banchereau J Palucka AK.** Dendritic cells as therapeutic vaccines against cancer. *Nat Rev Immunol.* 2005. 5(4):296-306.
24. **Banchereau J Steinman RM.** Dendritic cells and the control of immunity..*Nature.* 1998. 392(6673):245-52.
25. **Bánki Z Posch W, Ejaz A, Oberhauser V, Willey S, Gassner C, Stoiber H, Dittmer U, Dierich MP, Hasenkrug KJ, Wilflingseder D.** Complement as an endogenous adjuvant for dendritic cell-mediated induction of retrovirus-specific CTLs. *PLoS Pathog.* 2010. 6(4):e1000891.
26. **Batista FD Harwood NE.** The who, how and where of antigen presentation to B cells. *Nat Rev Immunol.* 2009. 9(1):15-27.
27. **Batista FD Harwood NE.** The who, how and where of antigen presentation to B cells. *Nat Rev Immunol.* 9(1):15-27. doi: 10.1038/nri2454., 2009 Jan.
28. **Bedoui S Whitney PG, Waithman J, Eidsmo L, Wakim L, Caminschi I, Allan RS, Wojtasiak M, Shortman K, Carbone FR, Brooks AG, Heath WR** Cross-presentation of viral and self antigens by skin-derived CD103+ dendritic cells. *Nat Immunol.* 2009 May; 10(5):488-95. doi: 10.1038/ni.1724. Epub 2009 Apr 6.
29. **Bedoui S Whitney PG, Waithman J, Eidsmo L, Wakim L, Caminschi I, Allan RS, Wojtasiak M, Shortman K, Carbone FR, Brooks AG, Heath WR.** Cross-presentation of viral and self antigens by skin-derived CD103+ dendritic cells. *Nat Immunol.* 2009 May;10(5):488-95. doi: 10.1038/ni.1724. Epub 2009 Apr 6 10(5):488-95. doi: 10.1038/ni.1724. Epub 2009 Apr 6., 2009 May.
30. **Bell D Young JW, Banchereau J** Dendritic cells. *Adv Immunol.* 1999; 72:255-324.
31. **Belz GT Nutt SL** Transcriptional programming of the dendritic cell network *Nat Rev Immunol.* 2012 Jan 25. 12(2):101-13. doi: 10.1038/nri3149.
32. **Ben-David Y Bernstein A.** Friend virus-induced erythroleukemia and the multistage nature of cancer. *Cell.* 66(5):831-4., 1991 Sep 6.
33. **Bennett SR Carbone FR, Karamalis F, Flavell RA, Miller JF, Heath WR** Help for cytotoxic-T-cell responses is mediated by CD40 signalling. *Nature.* 1998 Jun 4;. 393(6684):478-80.
34. **Bettelli E Oukka M, Kuchroo VK** T(H)-17 cells in the circle of immunity and autoimmunity. *Nat Immunol.* 2007 Apr;. 8(4):345-50.
35. **Bevan MJ.** Helping the CD8(+) T-cell response. *Nat Rev Immunol.* 4(8):595-602., 2004 Aug.

36. **Bochner BS Udem BJ, Lichtenstein LM** Immunological aspects of allergic asthma. *Annu Rev Immunol.* 1994;. 12:295-335.
37. **Bogdan C.** Nitric oxide and the immune response. *Nat Immunol.* 2001 Oct;. 2(10):907-16.
38. **Bogunovic M Ginhoux F, Helft J, Shang L, Hashimoto D, Greter M, Liu K, Jakubzick C, Ingersoll MA, Leboeuf M, Stanley ER, Nussenzweig M, Lira SA, Randolph GJ, Merad M.** Origin of the lamina propria dendritic cell network. *Immunity.* 2009 Sep 18;.31(3):513-25 .
39. **Bokoch GM.** Regulation of innate immunity by Rho GTPases. *Trends Cell Biol.* - [s.l.] ;15(3):163-71., 2005 Mar.
40. **Bolhassani A Safaiyan S, Rafati S.** Improvement of different vaccine delivery systems for cancer therapy . *Mol Cancer.* 2011. 10:3.
41. **Bolhassani A Safaiyan S, Rafati S.** Improvement of different vaccine delivery systems for cancer therapy. *Mol Cancer.* [s.n.], 2011 Jan 7;10:3. doi: 10.1186/1476-4598-10-3.
42. **Bonifaz LC Bonnyay DP, Charalambous A, Darguste DI, Fujii S, Soares H, Brimnes MK, Moltedo B, Moran TM, Steinman RM.** In vivo targeting of antigens to maturing dendritic cells via the DEC-205 receptor improves T cell vaccination. *J Exp Med.* 2004. 199(6):815-24.
43. **Boonstra A Asselin-Paturel C, Gilliet M, Crain C, Trinchieri G, Liu YJ, O'Garra A.** Flexibility of mouse classical and plasmacytoid-derived dendritic cells in directing T helper type 1 and 2 cell development: dependency on antigen dose and differential toll-like receptor ligation .*J Exp Med.* 2003. 197(1):101-9.
44. **Brannon-Peppas L Blanchette JO.** Nanoparticle and targeted systems for cancer therapy. *Adv Drug Deliv Rev.* 2004. 56(11):1649-59.
45. **Broaders KE Cohen JA, Beaudette TT, Bachelder EM, Fréchet JM.** Acetalated dextran is a chemically and biologically tunable material for particulate immunotherapy. *Proc Natl Acad Sci U S A.* 2009 Apr 7;. 106(14):5497-502. Epub 2009 Mar 24.
46. **Buchweitz JP Karmaus PW, Harkema JR, Williams KJ, Kaminski NE.** Modulation of airway responses to influenza A/PR/8/34 by Delta9-tetrahydrocannabinol in C57BL/6 mice. *J Pharmacol Exp Ther.* 323(2):675-83. Epub 2007 Aug 28., 2007 Nov.
47. **Bunt SK Yang L, Sinha P, Clements VK, Leips J, Ostrand-Rosenberg S.** Reduced inflammation in the tumor microenvironment delays the

- accumulation of myeloid-derived suppressor cells and limits tumor progression. *Cancer Res.* 2007 Oct 15;. 67(20):10019-26.
48. **Burgdorf S Lukacs-Kornek V, Kurts C.** The mannose receptor mediates uptake of soluble but not of cell-associated antigen for cross-presentation. *J Immunol.* 2006. 176(11):6770-6.
  49. **Carmody RJ Chen YH.** Nuclear factor-kappaB: activation and regulation during toll-like receptor signaling. *Cell Mol Immunol.* 2007. 4(1):31-41.
  50. **Carotta S Dakic A, D'Amico A, Pang SH, Greig KT, Nutt SL, Wu L.** The transcription factor PU.1 controls dendritic cell development and Flt3 cytokine receptor expression in a dose-dependent manner. *Immunity.* 32(5):628-41. doi: 10.1016/j.immuni.2010.05.005., 2010 May 28;.
  51. **Carter RW Thompson C, Reid DM, Wong SY, Tough DF** Preferential induction of CD4+ T cell responses through in vivo targeting of antigen to dendritic cell-associated C-type lectin-1. *J Immunol.* 177(4):2276-84., 2006 Aug 15.
  52. **Chesebro B Miyazawa M, Britt WJ.** Host genetic control of spontaneous and induced immunity to Friend murine retrovirus infection. *Annu Rev Immunol.* 1990. 8:477-99.
  53. **Cho NH Cheong TC, Min JH, Wu JH, Lee SJ, Kim D, Yang JS, Kim S, Kim YK, Seong SY.** A multifunctional core-shell nanoparticle for dendritic cell-based cancer immunotherapy. *Nat Nanotechnol.* 6(10):675-82. doi: 10.1038/nnano.2011.149., 2011 Sep 11.
  54. **Cho NH Cheong TC, Min JH, Wu JH, Lee SJ, Kim D, Yang JS, Kim S, Kim YK, Seong SY.** A multifunctional core-shell nanoparticle for dendritic cell-based cancer immunotherapy. *Nat Nanotechnol.* 2011. 6(10):675-8..
  55. **Chomarat P Banchereau J, Davoust J, Palucka AK.** IL-6 switches the differentiation of monocytes from dendritic cells to macrophages. *Nat Immunol.* 2000 Dec;. 1(6):510-4.
  56. **Chung DR Kasper DL, Panzo RJ, Chitnis T, Grusby MJ, Sayegh MH, Tzianabos AO.** CD4+ T cells mediate abscess formation in intra-abdominal sepsis by an IL-17-dependent mechanism. *J Immunol.* 2003 Feb 15;. 170(4):1958-63.
  57. **Coffman RL Sher A, Seder RA.** Vaccine adjuvants: putting innate immunity to work. *Immunity.* 2010 Oct 29 33(4):492-503. doi: 10.1016/j.immuni.2010.10.002.
  58. **Collison LW Delgoffe GM, Guy CS, Vignali KM, Chaturvedi V, Fairweather D, Satoskar AR, Garcia KC, Hunter CA, Drake CG, Murray**

- PJ, Vignali DA** The composition and signaling of the IL-35 receptor are unconventional. *Nat Immunol.* 13(3):290-9. doi: 10.1038/ni.2227., 2012 Feb 5.
59. **Colonna M Samaridis J, Angman L.** Molecular characterization of two novel C-type lectin-like receptors, one of which is selectively expressed in human dendritic cells. *Eur J Immunol.* 2000. 30(2):697-704.
60. **Colonna M Trinchieri G, Liu YJ** Plasmacytoid dendritic cells in immunity. *Nat Immunol.* 2004. 5(12):1219-26.
61. **Corcoran L Ferrero I, Vremec D, Lucas K, Waithman J, O'Keeffe M, Wu L, Wilson A, Shortman K.** The lymphoid past of mouse plasmacytoid cells and thymic dendritic cells. *J Immunol.* 2003 May 15;. 170(10):4926-32.
62. **Crawford A Macleod M, Schumacher T, Corlett L, Gray D.** Primary T cell expansion and differentiation in vivo requires antigen presentation by B cells. *J Immunol.* 2006 Mar 15;. 176(6):3498-506.
63. **Curtsinger JM Mescher MF.** Inflammatory cytokines as a third signal for T cell activation. *Curr Opin Immunol.* 2010 Jun; 22(3):333-40. doi: 10.1016/j.coi.2010.02.013. Epub 2010 Apr 2.
64. **D. Kabat** Molecular biology of Friend viral erythroleukemia. *Curr Top Microbiol Immunol.* . 1989;. 148:1-42.
65. **Davis ME Chen ZG, Shin DM.** Nanoparticle therapeutics: an emerging treatment modality for cancer. *Nat Rev Drug Discov.* 2008. 7(9):771-82.
66. **Davis ME Chen ZG, Shin DM.** Nanoparticle therapeutics: an emerging treatment modality for cancer. *Nat Rev Drug Discov.* [s.l.] 7(9):771-82. doi: 10.1038/nrd2614, 2008 Sep.
67. **de Bie JJ Kneepkens M, Kraneveld AD, Jonker EH, Henricks PA, Nijkamp FP, van Oosterhout AJ.** Absence of late airway response despite increased airway responsiveness and eosinophilia in a murine model of asthma. *Exp Lung Res.* 2000 Oct-Nov;. 26(7):491-507.
68. **del Rio ML Rodriguez-Barbosa JI, Kremmer E, Förster R.** CD103- and CD103+ bronchial lymph node dendritic cells are specialized in presenting and cross-presenting innocuous antigen to CD4+ and CD8+ T cells. *J Immunol.* 2007 Jun 1;. 178(11):6861-6.
69. **Delebecque F Suspène R, Calattini S, Casartelli N, Saïb A, Froment A, Wain-Hobson S, Gessain A, Vartanian JP, Schwartz O** Restriction of foamy viruses by APOBEC cytidine deaminases. *J Virol.* 80(2):605-14., 2006 Jan.



70. **Demento SL Eisenbarth SC, Foellmer HG, Platt C, Caplan MJ, Mark Saltzman W, Mellman I, Ledizet M, Fikrig E, Flavell RA, Fahmy TM** Inflammasome-activating nanoparticles as modular systems for optimizing vaccine efficacy. *Vaccine*. [s.n.], 2009 May 18; Bde. 27(23):3013-21. doi: 10.1016/j.vaccine.2009.03.034. Epub 2009 Apr 3.
71. **den Brok MH Nierkens S, Figdor CG, Ruers TJ, Adema GJ.** Dendritic cells: tools and targets for antitumor vaccination. *Expert Rev Vaccines*. 2005. 4(5):699-710.
72. **Depoil D Fleire S, Treanor BL, Weber M, Harwood NE, Marchbank KL, Tybulewicz VL, Batista FD.** CD19 is essential for B cell activation by promoting B cell receptor-antigen microcluster formation in response to membrane-bound ligand. *Nat Immunol*. 2008. 9(1):63-72. Epub 2007 Dec 2.
73. **Diamond MS Kinder M, Matsushita H, Mashayekhi M, Dunn GP, Archambault JM, Lee H, Arthur CD, White JM, Kalinke U, Murphy KM, Schreiber RD** Type I interferon is selectively required by dendritic cells for immune rejection of tumors . *J Exp Med*. 2011. 208(10):1989-2003.
74. **Dittmer U Hasenkrug KJ.** Cellular and molecular mechanisms of vaccine-induced protection against retroviral infections. *Curr Mol Med*.. 2001. 1(4):431-6.
75. **Dittmer U He H, Messer RJ, Schimmer S, Olbrich AR, Ohlen C, Greenberg PD, Stromnes IM, Iwashiro M, Sakaguchi S, Evans LH, Peterson KE, Yang G, Hasenkrug KJ** Functional impairment of CD8(+) T cells by regulatory T cells during persistent retroviral infection. *Immunity*. 20(3):293-303, 2004 Mar.
76. **Dittmer U He H, Messer RJ, Schimmer S, Olbrich AR, Ohlen C, Greenberg PD, Stromnes IM, Iwashiro M, Sakaguchi S, Evans LH, Peterson KE, Yang G, Hasenkrug KJ** Functional impairment of CD8(+) T cells by regulatory T cells during persistent retroviral infection. *Immunity*. .2004 Mar;. 20(3):293-303.
77. **Dittmer U Peterson KE, Messer R, Stromnes IM, Race B, Hasenkrug KJ.** Role of interleukin-4 (IL-4), IL-12, and gamma interferon in primary and vaccine-primed immune responses to Friend retrovirus infection. *J Virol*. 2001 Jan. 75(2):654-60.
78. **DM. Klinman** Immunotherapeutic uses of CpG oligodeoxynucleotides. *Nat Rev Immunol*. 2004 Apr;. 4(4):249-58.
79. **Doitsh G Cavois M, Lassen KG, Zepeda O, Yang Z, Santiago ML, Hebbeler AM, Greene WC.** Abortive HIV infection mediates CD4 T cell

- depletion and inflammation in human lymphoid tissue. *Cell*. 2010 Nov 24;. 143(5):789-801.
80. **Donaghy H Wilkinson J, Cunningham AL.** HIV interactions with dendritic cells: has our focus been too narrow? *J Leukoc Biol.* 2006 80(5):1001-12. Epub 2006 Aug 21.
81. **Ehrchen JM Sunderkötter C, Foell D, Vogl T, Roth J.** The endogenous Toll-like receptor 4 agonist S100A8/S100A9 (calprotectin) as innate amplifier of infection, autoimmunity, and cancer. *J Leukoc Biol.* 2009 Sep;. 86(3):557-66. doi: 10.1189/jlb.1008647. Epub 2009 May 18.
82. **Eri Takeda 1 Sachiyo Tsuji-Kawahara,1 Mayumi Sakamoto,1 Marc-Andre´ Langlois,2** Mouse APOBEC3 Restricts Friend Leukemia Virus Infection and Pathogenesis In vivo. *J Virol.* 2009 Apr;. 83(7):3029-38. Epub 2009 Jan 19.
83. **F Geissmann** The origin of dendritic cells. *Nat Immunol.* 2007 Jun;. 8(6):558-60.
84. **Fantuzzi L Purificato C, Donato K, Belardelli F, Gessani S** Human immunodeficiency virus type 1 gp120 induces abnormal maturation and functional alterations of dendritic cells: a novel mechanism for AIDS pathogenesis. *J Virol.* 78(18):9763-72, 2004 Sep.
85. **FD. Finkelman** Anaphylaxis: lessons from mouse models. *J Allergy Clin Immunol.* 2007 Sep;. 120(3):506-15; quiz 516-7.
86. **Figdor CG de Vries IJ, Lesterhuis WJ, Melief CJ.** Dendritic cell immunotherapy: mapping the way. *Nat Med.* [s.l.] 10(5):475-80., 2004 May.
87. **Figdor CG van Kooyk Y, Adema GJ.** C-type lectin receptors on dendritic cells and Langerhans cells. *Nat Rev Immunol.* 2002. 2(2):77-84.
88. **Finberg RW Wang JP, Kurt-Jones EA.** Toll like receptors and viruses. *Rev Med Virol.* 2007. 17(1):35-43.
89. **Fiorentino DF Zlotnik A, Vieira P, Mosmann TR, Howard M, Moore KW, O'Garra A.** IL-10 acts on the antigen-presenting cell to inhibit cytokine production by Th1 cells. *J Immunol.* 1991 May 15;. 146(10):3444-51.
90. **Foell D Frosch M, Sorg C, Roth J.** Phagocyte-specific calcium-binding S100 proteins as clinical laboratory markers of inflammation. *Clin Chim Acta.* 344(1-2):37-51., 2004 Jun.
91. **Foell D Wittkowski H, Vogl T, Roth J.** S100 proteins expressed in phagocytes: a novel group of damage-associated molecular pattern molecules. *J Leukoc Biol.* 2007 Jan;. 81(1):28-37. Epub 2006 Aug 30.

92. **Fonseca DE Kline JN.** Use of CpG oligonucleotides in treatment of asthma and allergic disease. *Adv Drug Deliv Rev.* 2009 Mar 28;. 61(3):256-62. doi: 10.1016/j.addr.2008.12.007. Epub 2009 Jan 9.
93. **FRIEND C.** Cell-free transmission in adult Swiss mice of a disease having the character of a leukemia . *J Exp Med.* 1957. 105(4):307-18.
94. **Gabrilovich DI Nagaraj S.** Myeloid-derived suppressor cells as regulators of the immune system . *Nat Rev Immunol.* 2009 Mar;. 9(3):162-74.
95. **Gabrilovich DI Nagaraj S.** Myeloid-derived suppressor cells as regulators of the immune system. *Nat Rev Immunol.* 9(3):162-74. doi: 10.1038/nri2506., 2009 Mar.
96. **Gazi U Martinez-Pomares L.** Influence of the mannose receptor in host immune responses. *Immunobiology.* 2009. 214(7):554-61. Epub 2009 Jan 21.
97. **Gebhardt C Németh J, Angel P, Hess J.** S100A8 and S100A9 in inflammation and cancer. *Biochem Pharmacol.* 2006 Nov 30;. 72(11):1622-31. Epub 2006 Jul 17.
98. **Gerondakis S Grumont RJ, Banerjee A.** Regulating B-cell activation and survival in response to TLR signals. *Immunol Cell Biol.* 2007 85(6):471-5. Epub 2007 Jul 17.
99. **Ghavami S Chitayat S, Hashemi M, Eshraghi M, Chazin WJ, Halayko AJ, Kerkhoff C.** S100A8/A9: a Janus-faced molecule in cancer therapy and tumorigenesis. *Eur J Pharmacol.* 2009 Dec 25; 625(1-3):73-83. Epub 2009 Oct 14.
100. **Ginhoux F Tacke F, Angeli V, Bogunovic M, Loubreau M, Dai XM, Stanley ER, Randolph GJ, Merad M** Langerhans cells arise from monocytes in vivo. *Nat Immunol.* 2006 Mar; 7(3):265-73. Epub 2006 Jan 29.
101. **Glimcher LH Murphy KM.** Lineage commitment in the immune system: the T helper lymphocyte grows up. *Genes Dev.* 2000 Jul 15;. - 14(14):1693-711.
102. **Gough PJ Gordon S.** The role of scavenger receptors in the innate immune system. *Microbes Infect.* 2(3):305-11., 2000 Mar.
103. **Gould HJ Sutton BJ, Beavil AJ, Beavil RL, McCloskey N, Coker HA, Fear D, Smurthwaite L.** The biology of IGE and the basis of allergic disease. *Annu Rev Immunol.* 2003;. 21:579-628. Epub 2001 Dec 19.
104. **Guermontprez P Saveanu L, Kleijmeer M, Davoust J, Van Endert P, Amigorena S.** ER-phagosome fusion defines an MHC class I cross-

- presentation compartment in dendritic cells. *Nature*. 2003. 425(6956):397-402.
105. **Guerriero A Langmuir PB, Spain LM, Scott EW.** PU.1 is required for myeloid-derived but not lymphoid-derived dendritic cells. *Blood*. 2000 Feb 1;. 95(3):879-85.
106. **Guo C Yi H, Yu X, Hu F, Zuo D, Subject JR, Wang XY.** Absence of scavenger receptor A promotes dendritic cell-mediated cross-presentation of cell-associated antigen and antitumor immune response. *Immunol Cell Biol*. 2012 Jan;. 90(1):101-8. doi: 10.1038/icb.2011.10. Epub 2011 Mar 8.
107. **Gupta GK Agrawal DK.** CpG oligodeoxynucleotides as TLR9 agonists: therapeutic application in allergy and asthma. *BioDrugs*. 2010 Aug 1;. 24(4):225-35. doi: 10.2165/11536140-000000000-00000.
108. **Hacker C Kirsch RD, Ju XS, Hieronymus T, Gust TC, Kuhl C, Jorgas T, Kurz SM, Rose-John S, Yokota Y, Zenke M.** Transcriptional profiling identifies Id2 function in dendritic cell development. *Nat Immunol*. 2003 Apr; 4(4):380-6. Epub 2003 Feb 24.
109. **Hakata Y Landau NR.** Reversed functional organization of mouse and human APOBEC3 cytidine deaminase domains. *J Biol Chem*. 2006 Dec 1. 281(48):36624-31. Epub 2006 Oct 4.
110. **Hamid Q Tulic M.** Immunobiology of asthma. *Annu Rev Physiol*. 2009;. 71:489-507. doi: 10.1146/annurev.physiol.010908.163200.
111. **Hampton MB Kettle AJ, Winterbourn CC** Inside the neutrophil phagosome: oxidants, myeloperoxidase, and bacterial killing. *Blood*. 92(9):3007-17., 1998 Nov 1.
112. **Haniffa M Shin A, Bigley V, McGovern N, Teo P, See P, Wasan PS, Wang XN, Malinarich F, Malleret B, Larbi A, Tan P, Zhao H, Poidinger M, Pagan S, Cookson S, Dickinson R, Dimmick I, Jarrett RF, Renia L, Tam J, Song C, Connolly J, Chan JK, Gehring A, Bertol** Human tissues contain CD141hi cross-presenting dendritic cells with functional homology to mouse CD103+ nonlymphoid dendritic cells. *Immunity*. 2012 Jul 27;. 37(1):60-73. doi: 10.1016/j.immuni.2012.04.012. Epub 2012 Jul 12.
113. **Haniffa M Shin A, Bigley V, McGovern N, Teo P, See P, Wasan PS, Wang XN, Malinarich F, Malleret B, Larbi A, Tan P, Zhao H, Poidinger M, Pagan S, Cookson S, Dickinson R, Dimmick I, Jarrett RF, Renia L, Tam J, Song C, Connolly J, Chan JK, Gehring A, Bertol** Human tissues contain CD141hi cross-presenting dendritic cells with functional homology to mouse CD103+ nonlymphoid dendritic cells. *Immunity*. 37(1):60-73. doi: 10.1016/j.immuni.2012.04.012. Epub 2012 Jul 12., 2012 Jul 27.

114. **Harris RS Bishop KN, Sheehy AM, Craig HM, Petersen-Mahrt SK, Watt IN, Neuberger MS, Malim MH.** DNA deamination mediates innate immunity to retroviral infection. *Cell*. [s.l.] 113(6):803-9., 2003 Jun 13.
115. **Harris RS Sheehy AM, Craig HM, Malim MH, Neuberger MS.** DNA deamination: not just a trigger for antibody diversification but also a mechanism for defense against retroviruses. *Nat Immunol*. 2003 Jul; 4(7):641-3.
116. **Hasenkrug KJ Brooks DM, Chesebro B.** Passive immunotherapy for retroviral disease: influence of major histocompatibility complex type and T-cell responsiveness. *Proc Natl Acad Sci U S A*. 1995 . 92(23):10492-5.
117. **Hasenkrug KJ Brooks DM, Dittmer U.** Critical role for CD4(+) T cells in controlling retrovirus replication and spread in persistently infected mice. *J Virol*. 1998 Aug; 72(8):6559-64.
118. **Hasenkrug KJ Chesebro B.** Immunity to retroviral infection: the Friend virus model. *Proc Natl Acad Sci U S A*. 1997. 94(15):7811-6.
119. **Hashimoto D Miller J, Merad M.** Dendritic cell and macrophage heterogeneity in vivo. *Immunity*.. 2011. 35(3):323-35.
120. **He LZ Crocker A, Lee J, Mendoza-Ramirez J, Wang XT, Vitale LA, O'Neill T, Petromilli C, Zhang HF, Lopez J, Rohrer D, Keler T, Clynes R.** Antigenic Targeting of the Human Mannose Receptor Induces Tumor Immunity . *J Immunol*. 2007. 178(10):6259-67.
121. **Heath WR Belz GT, Behrens GM, Smith CM, Forehan SP, Parish IA, Davey GM, Wilson NS, Carbone FR, Villadangos JA.** Cross-presentation, dendritic cell subsets, and the generation of immunity to cellular antigens. *Immunol Rev*. 2004 Jun; 199:9-26.
122. **Heath WR Carbone FR.** Dendritic cell subsets in primary and secondary T cell responses at body surfaces. *Nat Immunol*. 2009. 10(12):1237-44. Epub 2009 Nov 16.
123. **Heizmann CW Fritz G, Schäfer BW.** S100 proteins: structure, functions and pathology. *Front Biosci*. 2002 May 1; 7:d1356-68.
124. **Hemmi H Takeuchi O, Kawai T, Kaisho T, Sato S, Sanjo H, Matsumoto M, Hoshino K, Wagner H, Takeda K, Akira S.** A Toll-like receptor recognizes bacterial DNA. *Nature*. 2000 Dec 7; 408(6813):740-5.
125. **Hildner K Edelson BT, Purtha WE, Diamond M, Matsushita H, Kohyama M, Calderon B, Schraml BU, Unanue ER, Diamond MS, Schreiber RD, Murphy TL, Murphy KM.** Batf3 deficiency reveals a critical

- role for CD8alpha+ dendritic cells in cytotoxic T cell immunity. *Science*. 322(5904):1097-100. doi: 10.1126/science.1164206., 2008 Nov 14.
126. **Hiltbold EM Vlad AM, Ciborowski P, Watkins SC, Finn OJ.** The mechanism of unresponsiveness to circulating tumor antigen MUC1 is a block in intracellular sorting and processing by dendritic cells. *J Immunol*. 2000. 165(7):3730-41.
127. **Hou B Reizis B, DeFranco AL** Toll-like receptors activate innate and adaptive immunity by using dendritic cell-intrinsic and -extrinsic mechanisms. *Immunity*. 29(2):272-82. doi: 10.1016/j.immuni.2008.05.016. Epub 2008 Jul 24.
128. **Houde M Bertholet S, Gagnon E, Brunet S, Goyette G, Laplante A, Princiotta MF, Thibault P, Sacks D, Desjardins M.** Phagosomes are competent organelles for antigen cross-presentation. *Nature*. 2003. 425(6956):402-6.
129. **Huang W Na L, Fidel PL, Schwarzenberger P.** Requirement of interleukin-17A for systemic anti-*Candida albicans* host defense in mice . *J Infect Dis*. 2004 Aug 1;. 190(3):624-31. Epub 2004 Jun 22.
130. **Hung K Hayashi R, Lafond-Walker A, Lowenstein C, Pardoll D, Levitsky H.** The central role of CD4(+) T cells in the antitumor immune response. *J Exp Med*. 1998 Dec 21;. 188(12):2357-68.
131. **Iijima N Linehan MM, Zamora M, Butkus D, Dunn R, Kehry MR, Laufer TM, Iwasaki A.** Dendritic cells and B cells maximize mucosal Th1 memory response to herpes simplex virus. *J Exp Med*. 2008 Dec 22;. 205(13):3041-52. Epub 2008 Dec 1.
132. **Iwasaki A Medzhitov R.** Regulation of adaptive immunity by the innate immune system. *Science*.. 2010. 327(5963):291-5.
133. **Iwasaki A Medzhitov R.** Toll-like receptor control of the adaptive immune responses. *Nat Immunol*.. 2004. 5(10):987-95.
134. **J. Monteseirín** Neutrophils and asthma. *J Investig Allergol Clin Immunol*. 2009;. 19(5):340-54.
135. **Jarrossay D Napolitani G, Colonna M, Sallusto F, Lanzavecchia A.** Specialization and complementarity in microbial molecule recognition by human myeloid and plasmacytoid dendritic cells. *Eur J Immunol*. 2001. 31(11):3388-93.
136. **Jiang W Swiggard WJ, Heufler C, Peng M, Mirza A, Steinman RM, Nussenzweig MC** The receptor DEC-205 expressed by dendritic cells and

- thymic epithelial cells is involved in antigen processing. *Nature*. 375(6527):151-5., 1995 May 11.
137. **JN. Kline** Immunotherapy of asthma using CpG oligodeoxynucleotides. *Immunol Res*. 39(1-3):279-86., 2007.
138. **JN. Kline** Immunotherapy of asthma using CpG oligodeoxynucleotides. *Immunol Res*. 2007;. 39(1-3):279-86.
139. **Joffre O Nolte MA, Spörri R, Reis e Sousa C.** Inflammatory signals in dendritic cell activation and the induction of adaptive immunity. *Immunol Rev*. 2009 Jan;. 227(1):234-47. doi: 10.1111/j.1600-065X.2008.00718.x.
140. **Joffre OP Segura E, Savina A, Amigorena S.** Cross-presentation by dendritic cells. *Nat Rev Immunol*. 2012 Jul 13;. 12(8):557-69. doi: 10.1038/nri3254.
141. **Jonuleit H Kühn U, Müller G, Steinbrink K, Paragnik L, Schmitt E, Knop J, Enk AH** Pro-inflammatory cytokines and prostaglandins induce maturation of potent immunostimulatory dendritic cells under fetal calf serum-free conditions. *Eur J Immunol*. 1997 Dec 27(12):3135-42.
142. **Jordö ED Wermeling F, Chen Y, Karlsson MC.** Scavenger receptors as regulators of natural antibody responses and B cell activation in autoimmunity. *Mol Immunol*. 48(11):1307-18. doi: 10.1016/j.molimm.2011.01.010. Epub 2011 Feb 17., 2011 Jun.
143. **Jr. Janeway CA** Approaching the asymptote? Evolution and revolution in immunology. *Cold Spring Harb Symp Quant Biol*. 1989;. 54 Pt 1:1-13.
144. **Jung S Unutmaz D, Wong P, Sano G, De los Santos K, Sparwasser T, Wu S, Vuthoori S, Ko K, Zavala F, Pamer EG, Littman DR, Lang RA.** In vivo depletion of CD11c+ dendritic cells abrogates priming of CD8+ T cells by exogenous cell-associated antigens. *Immunity*. 2002 Aug;. 17(2):211-20.
145. **Kabat D** Molecular biology of Friend viral erythroleukemia. *Curr Top Microbiol Immunol*. 1989. 148:1—42.
146. **Kalinski P Muthuswamy R, Urban J.** Dendritic cells in cancer immunotherapy: vaccines and combination immunotherapies. *Expert Rev Vaccines*. 2013 Mar;. 12(3):285-95. doi: 10.1586/erv.13.22.
147. **Kasturi SP Skountzou I, Albrecht RA, Koutsonanos D, Hua T, Nakaya HI, Ravindran R, Stewart S, Alam M, Kwissa M, Villinger F, Murthy N, Steel J, Jacob J, Hogan RJ, García-Sastre A, Compans R, Pulendran B.** Programming the magnitude and persistence of antibody responses with innate immunity. *Nature*. 2011 Feb 24;. 470(7335):543-7.

148. **Keene JA Forman J.** Helper activity is required for the in vivo generation of cytotoxic T lymphocytes. *J Exp Med.* 1982 Mar 1; 155(3):768-82.
149. **Kelli McKenna Anne-Sophie Beignon, and Nina Bhardwaj\*** Plasmacytoid dendritic cells: linking innate and adaptive immunity . *J Virol.* 2005. 79(1): 17–27.
150. **Kennedy R Celis E.** Multiple roles for CD4+ T cells in anti-tumor immune responses . *Immunol Rev.* 2008 Apr;. 222:129-44.
151. **Klippstein R Pozo D.** Nanotechnology-based manipulation of dendritic cells for enhanced immunotherapy strategies. *Nanomedicine.* 2010 Aug. 6(4):523-9. Epub 2010 Jan 18.
152. **Korn T Bettelli E, Oukka M, Kuchroo VK.** IL-17 and Th17 Cells. *Annu Rev Immunol.* 2009; 27:485-517. doi:10.1146/annurev.immunol.021908.132710.
153. **Korn T Bettelli E, Oukka M, Kuchroo VK.** L-17 and Th17 Cells. *Annu Rev Immunol.* 27:485-517. doi:10.1146/annurev.immunol.021908.132710., 2009.
154. **Kripke ML Munn CG, Jeevan A, Tang JM, Bucana C.** Evidence that cutaneous antigen-presenting cells migrate to regional lymph nodes during contact sensitization. *J Immunol.* 1990 Nov 1;. 145(9):2833-8.
155. **Krug A Rothenfusser S, Hornung V, Jahrsdörfer B, Blackwell S, Ballas ZK, Endres S, Krieg AM, Hartmann G** Identification of CpG oligonucleotide sequences with high induction of IFN-alpha/beta in plasmacytoid dendritic cells. *Eur J Immunol.* 2001 Jul;. 31(7):2154-63..
156. **KS Ravichandran** Beginnings of a good apoptotic meal: the find-me and eat-me signaling pathways . *Immunity.* 2011 Oct 28; 35(4):445-55. doi: 10.1016/j.immuni.2011.09.004.
157. **Kumar RK Herbert C, Foster PS.** The "classical" ovalbumin challenge model of asthma in mice. *Curr Drug Targets.* 2008 Jun;. 9(6):485-94.
158. **Larché M Akdis CA, Valenta R.** Immunological mechanisms of allergen-specific immunotherapy. *Nat Rev Immunol.* 2006 Oct;. 6(10):761-71.
159. **Latz E Schoenemeyer A, Visintin A, Fitzgerald KA, Monks BG, Knetter CF, Lien E, Nilsen NJ, Espevik T, Golenbock DT.** TLR9 signals after translocating from the ER to CpG DNA in the lysosome. *Nat Immunol.* 2004. 5(2):190-8. Epub 2004 Jan 11.
160. **Launois P Ohteki T, Swihart K, MacDonald HR, Louis JA.** In susceptible mice, *Leishmania major* induce very rapid interleukin-4 production by



- CD4+ T cells which are NK1.1-. *Eur J Immunol.* 1995 Dec;. 25(12):3298-307.
161. **Le Bon A Schiavoni G, D'Agostino G, Gresser I, Belardelli F, Tough DF.** Type I interferons potently enhance humoral immunity and can promote isotype switching by stimulating dendritic cells in vivo. *Immunity.* 14(4):461-70., 2001 Apr.
162. **Lewis KL Reizis B.** Dendritic cells: arbiters of immunity and immunological tolerance. *Cold Spring Harb Perspect Biol.* 4(8):a007401. doi: 10.1101/cshperspect.a007401., 2012 Aug 1.
163. **Li H Li Y, Jiao J, Hu HM.** Alpha-alumina nanoparticles induce efficient autophagy-dependent cross-presentation and potent antitumour response. *Nat Nanotechnol.* 2011. 6(10):645-50.
164. **Liu C Zhang N.** Nanoparticles in gene therapy principles, prospects, and challenges. *Prog Mol Biol Transl Sci.* 2011;. 104:509-62. doi: 10.1016/B978-0-12-416020-0.00013-9.
165. **Liu K Nussenzweig MC.** Origin and development of dendritic cells. *Immunol Rev.* 2010. 234(1):45-54..
166. **Liu K Waskow C, Liu X, Yao K, Hoh J, Nussenzweig M** Origin of dendritic cells in peripheral lymphoid organs of mice. *Nat Immunol.* 2007 Jun; 8(6):578-83. .
167. **Lominadze G Rane MJ, Merchant M, Cai J, Ward RA, McLeish KR.** Myeloid-related protein-14 is a p38 MAPK substrate in human neutrophils . *J Immunol.* 2005. 174(11):7257-67.
168. **London CA Abbas AK, Kelso A** Helper T cell subsets: heterogeneity, functions and development. *Vet Immunol Immunopathol.* 63(1-2):37-44., 1998 May 15.
169. **Lu Y Sjöstrand M, Malmhäll C, Rådinger M, Jeurink P, Lötvall J, Bossios A.** New production of eosinophils and the corresponding TH1/TH2 balance in the lungs after allergen exposure in BALB/c and C57BL/6 mice. *Scand J Immunol.* 2010 Mar; 71(3):176-85. doi: 10.1111/j.1365-3083.2009.02363.x..
170. **Lund FE Randall TD.** Effector and regulatory B cells: modulators of CD4(+) T cell immunity. *Nat Rev Immunol.* 2010 Apr;. 10(4):236-47 .
171. **M Moser** Dendritic cells in immunity and tolerance-do they display opposite functions? *Immunity.* . 2003 Jul;. 19(1):5-8.
172. **Ma W Chen M, Kaushal S, McElroy M, Zhang Y, Ozkan C, Bouvet M, Kruse C, Grotjahn D, Ichim T, Minev B.** PLGA nanoparticle-mediated

- delivery of tumor antigenic peptides elicits effective immune responses. *Int J Nanomedicine*. 2012. 7:1475-87. Epub 2012 Mar 15.
173. **Maddox L Schwartz DA**. The pathophysiology of asthma. *Annu Rev Med*. . 2002;. 53:477-98.
174. **Mahnke K Schmitt E, Bonifaz L, Enk AH, Jonuleit H**. Immature, but not inactive: the tolerogenic function of immature dendritic cells. *Immunol Cell Biol*. 2002 Oct;. 80(5):477-83.
175. **Makabe-Kobayashi Y Hori Y, Adachi T, Ishigaki-Suzuki S, Kikuchi Y, Kagaya Y, Shirato K, Nagy A, Ujike A, Takai T, Watanabe T, Ohtsu H**. The control effect of histamine on body temperature and respiratory function in IgE-dependent systemic anaphylaxis. *J Allergy Clin Immunol*. 110(2):298-303., 2002 Aug.
176. **Mao X Wang K, Du Y, Lin B**. Analysis of chicken and turkey ovalbumins by microchip electrophoresis combined with exoglycosidase digestion . *Electrophoresis*. 2003 Sep;. 24(18):3273-8.
177. **Maraskovsky E Brasel K, Teepe M, Roux ER, Lyman SD, Shortman K, McKenna HJ**. Dramatic increase in the numbers of functionally mature dendritic cells in Flt3 ligand-treated mice: multiple dendritic cell subpopulations identified. *J Exp Med*. 1996 Nov 1;. 184(5):1953-62.
178. **Maraskovsky E Daro E, Roux E, Teepe M, Maliszewski CR, Hoek J, Caron D, Lebsack ME, McKenna HJ**. In vivo generation of human dendritic cell subsets by Flt3 ligand. *Blood*. 2000 Aug 1; 96(3):878-84.
179. **Marigo I Dolcetti L, Serafini P, Zanovello P, Bronte V**. Tumor-induced tolerance and immune suppression by myeloid derived suppressor cells. *Immunol Rev*.. 2008. 222:162-79.
180. **Mark E. Davis Zhuo (Georgia) Chen & Dong M. Shin** Nanoparticle therapeutics: an emerging treatment modality for cancer. *Nat Rev Drug Discov*. 2008. 7(9):771-82.
181. **Martínez Gómez JM Fischer S, Csaba N, Kündig TM, Merkle HP, Gander B, Johansen P**. A protective allergy vaccine based on CpG- and protamine-containing PLGA microparticles. *Pharm Res*. 24(10):1927-35. Epub 2007 May 31., 2007 Oct.

182. **Masaaki Miyazawa\* Sachiyo Tsuji-Kawahara, Yasuyoshi Kanari** Host genetic factors that control immune responses to retrovirus infections . *Vaccine*. 2008. 26(24):2981-96. Epub 2008 Jan 22.
183. **Medzhitov Akiko Iwasaki & Ruslan** Toll-like receptor control of the adaptive immune responses. *Nat Immunol.* 2004. 5(10):987-95.
184. **Melief CJ Finn OJ.** Cancer immunology. *Curr Opin Immunol.* 2011 Apr; 23(2):234-6. doi: 10.1016/j.coi.2011.01.003. Epub 2011 Feb 1.
185. **Melief CJ.** Cancer immunotherapy by dendritic cells. *Immunity*. 2008. 29(3):372-83.
186. **Mellman I Coukos G, Dranoff G.** Cancer immunotherapy comes of age. *Nature*. 2011 Dec 21; 480(7378):480-9. doi: 10.1038/nature10673.
187. **Merad M Ginhoux F, Collin M.** Origin, homeostasis and function of Langerhans cells and other langerin-expressing dendritic cells. *Nat Rev Immunol.* 8(12):935-47. doi: 10.1038/nri2455., 2008 Dec.
188. **Mercedes B. Fuertes 1 Aalok K. Kacha,1 Justin Kline,1 Seng-Ryong Woo,1 David M. Kranz,2 Kenneth M. Murphy,3 and Thomas F. Gajewski**corresponding author1 Host type I IFN signals are required for antitumor CD8+ T cell responses through CD8α+ dendritic cells. *J Exp Med.* 2011. 208(10): 2005–2016.
189. **Meyer-Wentrup F Benitez-Ribas D, Tacke PJ, Punt CJ, Figdor CG, de Vries IJ, Adema GJ.** Targeting DCIR on human plasmacytoid dendritic cells results in antigen presentation and inhibits IFN-α production. *Blood*. 2008 Apr 15; 111(8):4245-53. Epub 2008 Feb 7.
190. **Morel PA Turner MS.** Dendritic cells and the maintenance of self-tolerance. *Immunol Res.* 2011 Aug;. 50(2-3):124-9. doi: 10.1007/s12026-011-8217-y.
191. **Morrison RP Earl PL, Nishio J, Lodmell DL, Moss B, Chesebro B.** Different H-2 subregions influence immunization against retrovirus and immunosuppression. *Nature*. 1987 Oct 22-28;329(6141):729-32.
192. **Moutaftsi M Mehl AM, Borysiewicz LK, Tabi Z.** Human cytomegalovirus inhibits maturation and impairs function of monocyte-derived dendritic cells *Blood*. 99(8):2913-21., 2002 Apr 15.
193. **Mukhopadhyay S Gordon S.** The role of scavenger receptors in pathogen recognition and innate immunity. *Immunobiology*. 2004;. 209(1-2):39-49.

194. **Naik SH Metcalf D, van Nieuwenhuijze A, Wicks I, Wu L, O'Keeffe M, Shortman K.** Intrasplenic steady-state dendritic cell precursors that are distinct from monocytes. *Nat Rev Immunol.* 2007. 7(7):543-55..
195. **Naik SH Proietto AI, Wilson NS, Dakic A, Schnorrer P, Fuchsberger M, Lahoud MH, O'Keeffe M, Shao QX, Chen WF, Villadangos JA, Shortman K, Wu L.** Cutting edge: generation of splenic CD8+ and CD8-dendritic cell equivalents in Fms-like tyrosine kinase 3 ligand bone marrow cultures. *J Immunol.* 174(11):6592-7., 2005 Jun 1.
196. **Naik SH Sathe P, Park HY, Metcalf D, Proietto AI, Dakic A, Carotta S, O'Keeffe M, Bahlo M, Papenfuss A, Kwak JY, Wu L, Shortman K.** Development of plasmacytoid and conventional dendritic cell subtypes from single precursor cells derived in vitro and in vivo. *Nat Immunol.* 2007. 8(11):1217-26. Epub 2007 Oct 7.
197. **Naik SH Shortman K.** Intrasplenic steady-state dendritic cell precursors that are distinct from monocytes. *Nat Immunol.* 2006. 7(6):663-71. Epub 2006 May 7.
198. **Nemazee D Gavin A, Hoebe K, Beutler B.** Immunology: Toll-like receptors and antibody responses. *Nature.* 2006. 441(7091):E4.
199. **Nembrini C Stano A, Dane KY, Ballester M, van der Vlies AJ, Marsland BJ, Swartz MA, Hubbell JA.** Nanoparticle conjugation of antigen enhances cytotoxic T-cell responses in pulmonary vaccination. *Proc Natl Acad Sci U S A.* 2011. 108(44):E989-97. Epub 2011 Oct 3..
200. **Norris PJ Sumaroka M, Brander C, Moffett HF, Boswell SL, Nguyen T, Sykulev Y, Walker BD, Rosenberg ES.** Multiple effector functions mediated by human immunodeficiency virus-specific CD4(+) T-cell clones. *J Virol.* 2001. 75(20):9771-9.
201. **Obermajer N Wong JL, Edwards RP, Odunsi K, Moysich K, Kalinski P.** PGE(2)-driven induction and maintenance of cancer-associated myeloid-derived suppressor cells. *Immunol Invest.* 41(6-7):635-57. doi: 10.3109/08820139.2012.695417., 2012.
202. **Ochoa AC Zea AH, Hernandez C, Rodriguez PC.** Arginase, prostaglandins, and myeloid-derived suppressor cells in renal cell carcinoma. *Clin Cancer Res.* 13(2 Pt 2):721s-726s., 2007 Jan 15.
203. **O'Garra A.** Cytokines induce the development of functionally heterogeneous T helper cell subsets . *Immunity*8(3):275-83., 1998 Mar.
204. **Okeoma CM Low A, Bailis W, Fan HY, Peterlin BM, Ross SR.** Induction of APOBEC3 in vivo causes increased restriction of retrovirus infection . *J Virol.* . 2009 Apr;. 83(8):3486-95. Epub 2009 Jan 19.

205. **Onai N Manz MG.** The STATs on dendritic cell development. *Immunity*. 28(4):490-2. doi: 10.1016/j.immuni.2008.03.006., 2008 Apr.
206. **Palucka AK Ueno H, Fay JW, Banchereau J.** Taming cancer by inducing immunity via dendritic cells. *Immunol Rev.* 2007. 220:129-50.
207. **Palucka K Banchereau J** Cancer immunotherapy via dendritic cells. *Nat Rev Cancer.* 12(4):265-77. doi: 10.1038/nrc3258., 2012 Mar 22.
208. **Pasare C Medzhitov R.** Control of B-cell responses by Toll-like receptors . *Nature.* 2005. 438(7066):364-8.
209. **Peck A Mellins ED.** Plasticity of T-cell phenotype and function: the T helper type 17 example. *Immunology.* 2010 129(2):147-53. Epub 2009 Nov 17.
210. **Peer D Karp JM, Hong S, Farokhzad OC, Margalit R, Langer R.** Nanocarriers as an emerging platform for cancer therapy. *Nat Nanotechnol.* [s.l.] 2(12):751-60. doi: 10.1038/nnano.2007.387., 2007 Dec.
211. **Peng G Greenwell-Wild T, Nares S, Jin W, Lei KJ, Rangel ZG, Munson PJ, Wahl SM.** Myeloid differentiation and susceptibility to HIV-1 are linked to APOBEC3 expression. *Blood.* 2007 Jul 1;. 110(1):393-400. Epub 2007 Mar 19.
212. **Peranzoni E Zilio S, Marigo I, Dolcetti L, Zanovello P, Mandruzzato S, Bronte V.** Myeloid-derived suppressor cell heterogeneity and subset definition. *Curr Opin Immunol.* 2010. 22(2):238-44. Epub 2010 Feb 17.
213. **Petros RA DeSimone JM.** Strategies in the design of nanoparticles for therapeutic applications. *Nat Rev Drug Discov.* 2010. 9(8):615-27. Epub 2010 Jul 9.
214. **Petros RA DeSimone JM.** Strategies in the design of nanoparticles for therapeutic applications. *Nat Rev Drug Discov.* 9(8):615-27. doi: 10.1038/nrd2591. Epub 2010 Jul 9., 2010 Aug.
215. **Ploquin MJ Eksmond U, Kassiotis G.** B cells and TCR avidity determine distinct functions of CD4+ T cells in retroviral infection. *J Immunol.* 187(6):3321-30. doi: 10.4049/jimmunol.1101006. Epub 2011 Aug 12., 2011 Sep 15.
216. **Pollara G Kwan A, Newton PJ, Handley ME, Chain BM, Katz DR.** Dendritic cells in viral pathogenesis: protective or defective. *Int J Exp Pathol.* 2005. 86(4):187-204.
217. **R. Medzhitov** Toll-like receptors and innate immunity. *Nat Rev Immunol.* 2001. 1(2):135-45.

218. **Rakoff-Nahoum S Medzhitov R.** Toll-like receptors and cancer. *Nat Rev Cancer*.. 2009. 9(1):57-63. Epub 2008 Dec 4.
219. **Randall Frances E. Lund and Troy D.** Effector and regulatory B cells: modulators of CD4+ T cell immunity . *Nat Rev Immunol*. 2010 April; 10(4): 236–247. 2010 April; 10(4): 236–247.
220. **Randolph GJ Ochando J, Partida-Sánchez S.** Migration of dendritic cell subsets and their precursors. *Annu Rev Immunol*.. 2008. 26:293-316.
221. **Reddy ST Rehor A, Schmoekel HG, Hubbell JA, Swartz MA.** In vivo targeting of dendritic cells in lymph nodes with poly(propylene sulfide) nanoparticles. *J Control Release*.. 2006. 112(1):26-34. Epub 2006 Mar 10.
222. **Reis e Sousa C Hieny S, Scharon-Kersten T, Jankovic D, Charest H, Germain RN, Sher A.** In vivo microbial stimulation induces rapid CD40 ligand-independent production of interleukin 12 by dendritic cells and their redistribution to T cell areas. *J Exp Med*. 1997 Dec 1;. 186(11):1819-29.
223. **Ribechini E Greifenberg V, Sandwick S, Lutz MB.** Myeloid-derived suppressor cell heterogeneity and subset definition. *Curr Opin Immunol*. 22(2):238-44. doi: 10.1016/j.coi.2010.01.021. Epub 2010 Feb 17., 2010 Apr.
224. **Rietschel E Hutegger I, Lange L, Urbanek R.** [Anaphylaxis : Diagnostic and therapeutic management.. *Med Klin Intensivmed Notfmed*. 2013 Apr; 108(3):239-251.
225. **RJ. Ulevitch** Therapeutics targeting the innate immune system. *Nat Rev Immunol*. 2004. 4(7):512-20..
226. **RM. Steinman** DC-SIGN: a guide to some mysteries of dendritic cells. *Cell*. 2000 Mar 3; 100(5):491-4.
227. **Robinson MJ Sancho D, Slack EC, LeibundGut-Landmann S, Reis e Sousa C** Myeloid C-type lectins in innate immunity. *Nat Immunol*. 2006. 2006 Dec; 7(12):1258-65..
228. **Rodriguez A Regnault A, Kleijmeer M, Ricciardi-Castagnoli P, Amigorena S.** Selective transport of internalized antigens to the cytosol for MHC class I presentation in dendritic cells. *Nat Cell Biol*. 1999. 1999 Oct;. 1(6):362-8.
229. **Rosenberg SA Yang JC, Restifo NP.** Cancer immunotherapy: moving beyond current vaccines. *Nat Med*.. 2004. 10(9):909-15.
230. **Roth J Vogl T, Sorg C, Sunderkötter C.** Phagocyte-specific S100 proteins: a novel group of proinflammatory molecules. *Trends Immunol*. : 24(4):155-8., 2003 Apr.

231. **Rothenfusser S, Hornung V, Ayyoub M, Britsch S, Towarowski A, Krug A, Sarris A, Lubenow N, Speiser D, Endres S, Hartmann G.** CpG-A and CpG-B oligonucleotides differentially enhance human peptide-specific primary and memory CD8+ T-cell responses in vitro. *Blood*. 2004 Mar 15; 103(6):2162-9. Epub 2003 Nov 20.
232. **Roy K, Mao HQ, Huang SK, Leong KW.** Oral gene delivery with chitosan--DNA nanoparticles generates immunologic protection in a murine model of peanut allergy. *Nat Med*. 1999 Apr; 5(4):387-91.
233. **Royer PJ, Emara M, Yang C, Al-Ghouleh A, Tighe P, Jones N, Sewell HF, Shakib F, Martinez-Pomares L, Ghaemmaghami AM.** The mannose receptor mediates the uptake of diverse native allergens by dendritic cells and determines allergen-induced T cell polarization through modulation of IDO activity. *J Immunol*. 2010. 185(3):1522-31. Epub 2010 Jul 7.
234. **Ryckman C, Vandal K, Rouleau P, Talbot M, Tessier PA.** Proinflammatory activities of S100: proteins S100A8, S100A9, and S100A8/A9 induce neutrophil chemotaxis and adhesion. *J Immunol*. 170(6):3233-42., 2003 Mar 15.
235. **SA. Rosenberg** Progress in human tumour immunology and immunotherapy. *Nature*. 2001. 411(6835):380-4.
236. **Salem ML, Kadima AN, Cole DJ, Gillanders WE.** Defining the antigen-specific T-cell response to vaccination and poly(I:C)/TLR3 signaling: evidence of enhanced primary and memory CD8 T-cell responses and antitumor immunity. *J Immunother*. 2005. 28(3):220-8..
237. **San Román B, Irache JM, Gómez S, Gamazo C, Espuelas S.** Co-delivery of ovalbumin and CpG motifs into microparticles protected sensitized mice from anaphylaxis. *Int Arch Allergy Immunol*. 149(2):111-8. doi: 10.1159/000189193. Epub 2009 Jan 6., 2009.
238. **Sancho D, Mourão-Sá D, Joffre OP, Schulz O, Rogers NC, Pennington DJ, Carlyle JR, Reis e Sousa C.** Tumor therapy in mice via antigen targeting to a novel, DC-restricted C-type lectin. *J Clin Invest*. 118(6):2098-110. doi: 10.1172/JCI34584., 2008 Jun;.
239. **Satpathy AT, Murphy KM, KC W.** Transcription factor networks in dendritic cell development. *Semin Immunol*. 23(5):388-97. doi: 10.1016/j.smim.2011.08.009. Epub 2011 Sep 15., 2011 Oct.
240. **Schiavoni G, Mattei F, Sestili P, Borghi P, Venditti M, Morse HC 3rd, Belardelli F, Gabriele L.** ICSBP is essential for the development of mouse type I interferon-producing cells and for the generation and activation of CD8alpha(+) dendritic cells. *J Exp Med*. 2002 Dec 2; 196(11):1415-25.

241. **Schnorrer P Behrens GM, Wilson NS, Shortman K, Heath WR, Villadangos JA.** The dominant role of CD8+ dendritic cells in cross-presentation is not dictated by antigen capture .Proc Natl Acad Sci U S A. 2006. 103(28):10729-34. Epub 2006 Jun 28.
242. **Schröder U Ståhl A.** Crystallized dextran nanospheres with entrapped antigen and their use as adjuvants. J Immunol Methods..1984. 70(1):127-32.
243. **Scott AM Wolchok JD, Old LJ.** Antibody therapy of cancer. Nat Rev Cancer. [s.l.] 12(4):278-87. doi: 10.1038/nrc3236., 2012 Mar 22.
244. **Seder RA Ahmed R.** Similarities and differences in CD4+ and CD8+ effector and memory T cell generation.Nat Immunol. 4(9):835-42., 2003 Sep.
245. **Serafini P Carbley R, Noonan KA, Tan G, Bronte V, Borrello I.** High-dose granulocyte-macrophage colony-stimulating factor-producing vaccines impair the immune response through the recruitment of myeloid suppressor cells. Cancer Res. 2004 Sep 1;. 64(17):6337-43.
246. **Shortman K Caux C.** Dendritic cell development: multiple pathways to nature's adjuvants. Stem Cells.. [s.l.] 15(6):409-19., 1997.
247. **Shortman K Heath WR.** The CD8+ dendritic cell subset. Immunol Rev.. 2010.234(1):18-31.
248. **Shortman K Liu YJ.** Mouse and human dendritic cell subtypes. Nat Rev Immunol.. 2002. 2(3):151-61.
249. **Shortman K Naik SH** Steady-state and inflammatory dendritic-cell development. Nat Rev Immunol.. 2007. 7(1):19-30. Epub 2006 Dec 15.
250. **Singh SK Stephani J, Schaefer M, Kalay H, García-Vallejo JJ, den Haan J, Saeland E, Sparwasser T, van Kooyk Y.** Targeting glycan modified OVA to murine DC-SIGN transgenic dendritic cells enhances MHC class I and II presentation. Mol Immunol. 47(2-3):164-74. doi: 10.1016/j.molimm.2009.09.026. Epub 2009 Oct 8., 2009 Dec.
251. **Sinha P Clements VK, Fulton AM, Ostrand-Rosenberg S.** Prostaglandin E2 promotes tumor progression by inducing myeloid-derived suppressor cells. Cancer Res. 2007 May 1;. 67(9):4507-13.
252. **Song E Zhu P, Lee SK, Chowdhury D, Kussman S, Dykxhoorn DM, Feng Y, Palliser D, Weiner DB, Shankar P, Marasco WA, Lieberman J.** Antibody mediated in vivo delivery of small interfering RNAs via cell-surface receptors. Nat Biotechnol.. 2005. 23(6):709-17. Epub 2005 May 22.



253. **Steinman RM Cohn ZA.** Identification of a novel cell type in peripheral lymphoid organs of mice. I. Morphology, quantitation, tissue distribution. *J Exp Med.* . 1973 May 1;. 137(5):1142-62.
254. **Steinman RM Cohn ZA.** Pillars Article: Identification of a novel cell type in peripheral lymphoid organs of mice. I. Morphology, quantitation, tissue distribution. *J Immunol.* 2007. 178(1):5-25.
255. **Steinman RM Hawiger D, Nussenzweig MC.** Tolerogenic dendritic cells. *Annu Rev Immunol.* 2003. 21:685-711. Epub 2001 Dec 19.
256. **Steven A Rosenberg James C Yang & Nicholas P Restifo** Cancer immunotherapy: moving beyond current vaccines. *Nat Med.* 2004. 10(9):909-15.
257. **Suzuki S Honma K, Matsuyama T, Suzuki K, Toriyama K, Akitoyo I, Yamamoto K, Suematsu T, Nakamura M, Yui K, Kumatori A.** Critical roles of interferon regulatory factor 4 in CD11b<sup>high</sup>CD8 $\alpha$ <sup>-</sup> dendritic cell development. *Proc Natl Acad Sci USA.* 2004 Jun 15; 101(24):8981-6. Epub 2004 Jun 7.
258. **Tacke PJ de Vries IJ, Gijzen K, Joosten B, Wu D, Rother RP, Faas SJ, Punt CJ, Torensma R, Adema GJ, Figdor CG.** Effective induction of naive and recall T-cell responses by targeting antigen to human dendritic cells via a humanized anti-DC-SIGN antibody. *Blood.* 2005 Aug 15;. 106(4):1278-85. Epub 2005 May 5.
259. **Tacke PJ de Vries IJ, Torensma R, Figdor CG.** Dendritic-cell immunotherapy: from ex vivo loading to in vivo targeting. *Nat Rev Immunol.* 2007. 7(10):790-802..
260. **Tacke PJ Zeelenberg IS, Cruz LJ, van Hout-Kuijter MA, van de Glind G, Fokkink RG, Lambeck AJ, Figdor CG.** Targeted delivery of TLR ligands to human and mouse dendritic cells strongly enhances adjuvant activity. *Blood.* 2011. 118(26):6836-44. Epub 2011 Oct 3.
261. **Takeda E Tsuji-Kawahara S, Sakamoto M, Langlois MA, Neuberger MS, Rada C, Miyazawa M.** Mouse APOBEC3 restricts friend leukemia virus infection and pathogenesis in vivo. *J Virol.* 2008. 82(22):10998-1008. Epub 2008 Sep 10.
262. **Takeda K Kaisho T, Akira S.** Toll-like receptors. *Annu Rev Immunol.* 2003. 21:335-76. Epub 2001 Dec 19.
263. **Takeshita F Leifer CA, Gursel I, Ishii KJ, Takeshita S, Gursel M, Klinman DM.** Cutting edge: Role of Toll-like receptor 9 in CpG DNA-induced activation of human cells. *J Immunol.* 2001 Oct 167(7):3555-8..

264. **Thelen T Hao Y, Medeiros AI, Curtis JL, Serezani CH, Kobzik L, Harris LH, Aronoff DM** The class A scavenger receptor, macrophage receptor with collagenous structure, is the major phagocytic receptor for *Clostridium sordellii* expressed by human decidual macrophages. *J Immunol.* 185(7):4328-35. doi: 10.4049/jimmunol.1000989. Epub 2010 Sep 1., 2010 Oct 1;.
265. **Tsujimura H Tamura T, Ozato K.** IFN consensus sequence binding protein/IFN regulatory factor 8 drives the development of type I IFN-producing plasmacytoid dendritic cells. *J Immunol.* 2003 Feb 1;. 170(3):1131-5.
266. **Ueno H Klechevsky E, Morita R, Aspod C, Cao T, Matsui T, Di Pucchio T, Connolly J, Fay JW, Pascual V, Palucka AK, Banchereau J.** Dendritic cell subsets in health and disease. *Immunol Rev.* 2007. 219:118-42.
267. **Valladeau J Ravel O, Dezutter-Dambuyant C, Moore K, Kleijmeer M, Liu Y, Duvert-Frances V, Vincent C, Schmitt D, Davoust J, Caux C, Lebecque S, Saeland S** Langerin, a novel C-type lectin specific to Langerhans cells, is an endocytic receptor that induces the formation of Birbeck granules. *Immunity.* 2000. 12(1):71-81.
268. **van Broekhoven CL Parish CR, Demangel C, Britton WJ, Altin JG.** Targeting dendritic cells with antigen-containing liposomes: a highly effective procedure for induction of antitumor immunity and for tumor immunotherapy. *Cancer Res.* . 2004 Jun 15;. 64(12):4357-65.
269. **van Broekhoven CL Parish CR, Demangel C, Britton WJ, Altin JG.** Targeting dendritic cells with antigen-containing liposomes: a highly effective procedure for induction of antitumor immunity and for tumor immunotherapy. *Cancer Res.* 2004 Jun 15;. 64(12):4357-65.
270. **van Kooyk Y Geijtenbeek TB.** DC-SIGN: escape mechanism for pathogens. *Nat Rev Immunol.* 2003. 3(9):697-709.
271. **Varol C Landsman L, Fogg DK, Greenshtein L, Gildor B, Margalit R, Kalchenko V, Geissmann F, Jung S** Monocytes give rise to mucosal, but not splenic, conventional dendritic cells. *J Exp Med.* 2007 Jan 22; 204(1):171-80. Epub 2006 Dec 26.
272. **Verthelyi D Ishii KJ, Gursel M, Takeshita F, Klinman DM.** Human peripheral blood cells differentially recognize and respond to two distinct CPG motifs. *J Immunol.* 2001 Feb 15. 166(4):2372-7.
273. **Villadangos JA Schnorrer P.** Intrinsic and cooperative antigen-presenting functions of dendritic-cell subsets in vivo *Nat Rev Immunol.* 2007. 7(7):543-55..

274. **Vinay DS Kwon BS.** CD11c+CD8+ T cells: two-faced adaptive immune regulators *Cell Immunol.* 2010. 264(1):18-22. Epub 2010 May 27.
275. **Vogl T Ludwig S, Goebeler M, Strey A, Thorey IS, Reichelt R, Foell D, Gerke V, Manitz MP, Nacken W, Werner S, Sorg C, Roth J.** MRP8 and MRP14 control microtubule reorganization during transendothelial migration of phagocytes *Blood.* 2004. 104(13):4260-8. Epub 2004 Aug 26.
276. **Vogl T Tenbrock K, Ludwig S, Leukert N, Ehrhardt C, van Zoelen MA, Nacken W, Foell D, van der Poll T, Sorg C, Roth J.** Mrp8 and Mrp14 are endogenous activators of Toll-like receptor 4, promoting lethal, endotoxin-induced shock. *Nat Med.* 2007. 13(9):1042-9. Epub 2007 Sep 2.
277. **West MA Wallin RP, Matthews SP, Svensson HG, Zaru R, Ljunggren HG, Prescott AR, Watts C.** Enhanced dendritic cell antigen capture via toll-like receptor-induced actin remodeling. *Science.* 2004 305(5687):1153-7.
278. **Wojciechowski W Harris DP, Sprague F, Mousseau B, Makris M, Kusser K, Honjo T, Mohrs K, Mohrs M, Randall T, Lund FE.** Cytokine-producing effector B cells regulate type 2 immunity to *H. polygyrus*. *Immunity.* 2009 Mar 20;. 30(3):421-33. Epub 2009 Feb 26.
279. **Wu L Dakic A.** Development of dendritic cell system. *Cell Mol Immunol.* 2001. 1(2):112-8..
280. **Wu L D'Amico A, Winkel KD, Suter M, Lo D, Shortman K** RelB is essential for the development of myeloid-related CD8alpha- dendritic cells but not of lymphoid-related CD8alpha+ dendritic cells. *Immunity.* . 1998 Dec;. 9(6):839-47..
281. **Wu L KewalRamani VN.** Dendritic-cell interactions with HIV: infection and viral dissemination. *Nat Rev Immunol.* 6(11):859-68, 2006 Nov.
282. **Wu L Liu YJ.** Development of dendritic-cell lineages. *Immunity.* 2007. 26(6):741-50.
283. **Yi H Zuo D, Yu X, Hu F, Manjili MH, Chen Z, Subject JR, Wang XY.** Suppression of antigen-specific CD4+ T cell activation by SRA/CD204 through reducing the immunostimulatory capability of antigen-presenting cell *J Mol Med (Berl).* . 2012 Apr;. - 90(4):413-26. Epub 2011 Nov 15.
284. **Zelinskyy G Kraft AR, Schimmer S, Arndt T, Dittmer U.** Kinetics of CD8+ effector T cell responses and induced CD4+ regulatory T cell responses during Friend retrovirus infection. *Eur J Immunol.* 36(10):2658-70., 2006 Oct.

285. **Zhang H Yang B, Pomerantz RJ, Zhang C, Arunachalam SC, Gao L.** The cytidine deaminase CEM15 induces hypermutation in newly synthesized HIV-1 DNA. *Nature*. 424(6944):94-8. Epub 2003 May 28., 2003 Jul 3.
286. **Zoglmeier C Bauer H, Nörenberg D, Wedekind G, Bittner P, Sandholzer N, Rapp M, Anz D, Endres S, Bourquin C.** CpG blocks immunosuppression by myeloid-derived suppressor cells in tumor-bearing mice. *Clin Cancer Res.* 2011. 17(7):1765-75. Epub 2011 Jan 13.

